Table of Contents

List of Figures

Chapter 1

Chapter 2

Chapter 3

Chapter 4

List of Tables

Chapter 1

Chapter 2

Chapter 4

Abbreviations

ac	acetylation
ACN	acetonitrile
AGC	automatic gain control
APAD	3-acetylpyridine adenine dinucleotide
ApiAP2	Apicomplexan AP2
ATP	adenosine triphosphate
BDP	bromodomain protein
CID	collision induce dissociation
clag3	cytoadherence-linked asexual gene 3
CVGE	clonally variant gene expression
DDA	data-dependent acquisition
DDT	dichlorodiphenyltrichloroethane
DNDM	DNA demethylase
DNMT	DNA methyltransferase
DNMTi	DNA methyltransferase inhibitors
epi-drugs	epigenetic drugs
FDR	false discovery rate
FWHM	full width at half maximum
G6PD	Glucose-6-phosphate dehydrogenase
GO	Gene Ontology
H3Cen	H3 centromeric
HAT	histone acetyltransferase
HCD	Higher Energy Collision Dissociation
HDAC	histone deacetylase
HDACi	histone deacetylase inhibitors
HDM	histone demethylase
HKMT	histone lysine methyltransferase
HKMTi	histone lysine methyltransferase inhibitors
HP1	Heterochromatin protein 1
Hpi	hours post invasion
iBAQ	Intensity-based absolute quantification
IC_{50}	half maximal inhibitory concentration
IDC	Intra-erythrocytic developmental cycle
IRS	indoor residual spraying
ITNs	insecticide treated nets
JHDM	jumonji histone demethylase
LAMP	Loop-mediated isothermal amplification
lncRNAs	long non-coding RNAs
LSD	lysine-specific demethylase
lysoPC	lysophosphatidylcholine
me1	monomethylation
me2	dimethylation
me3	trimethylation
MS	Mass spectrometry
MudPIT	multidimensional protein identification technology
nanoLC	nano liquid chromatography
NBT	nitro blue tetrazoliumchloride
PBS	phosphate buffered saline
PCA	Principle Component Analysis

PES	phenazine ethosulphate
P. falciparum	*Plasmodium falciparum*
PfEMP1	*P. falciparum* erythrocyte membrane proteins 1
PfNAP	*P. falciparum* nucleosome assembly proteins
pfmc-2tm	*P. falciparum* Maurer's cleft 2 transmembrane gene family
ph	phosphorylation
pLDH	parasite lactate dehydrogenase
PRMT	protein arginine methyltransferase
PTMs	post-translational modifications
Puf	Pumilio and FEM3 binding factor
RBC	red blood cell
RDTs	rapid diagnostic tests
RI	resistance index
rif	repetitive interspersed gene family
RNA	Ribonucleic acid
RNAi	RNA interference machinery
SAH	*S*-adenosyl-L-homocysteine
SAHA	Suberoylanilide hydroxamic acid
SAM	*S*-adenosyl-L-methionine
SI	selectivity index
StageTip	STop And Go Extraction Tip
stevor	subtelomeric variable open reading frame gene family
SUMO	Small Ubiquitin-like MOdifier
TCA	tricarboxylic acid
TFA	trifluoroacetic acid
TSA	Trichostatin A
Ub	ubiquitination
var	variant gene family

Chapter 1: Introduction

1.1 Malaria in general

Malaria is still the deadliest parasitic disease in Africa, even though it is an entirely preventable and treatable mosquito-borne illness. However, an estimated 3.4 billion people are at risk of contracting the disease annually, and 212 million malaria cases and 429 000 deaths were reported in 2015 [1]. The symptoms of malaria include normal flu-like symptoms, e.g. fever, headache, nausea, vomiting, fatigue, diarrhoea and, in some cases, anaemia and jaundice. Should the infected patient remain untreated, the blood supply to vital organs would be limited, leading to severe symptoms such as kidney failure, seizures, mental confusion and ultimately death [1].

Malaria is still endemic in 91 countries in tropical and subtropical regions although malaria incidence rates decreased substantially over the last five years (21% decrease globally) and several countries have achieved, or are approaching, elimination status (Figure 1.1). Populations residing in the African region are severely affected, with 90% of the malaria cases and 92% of the deaths due to malaria still occurring on the continent (Figure 1.1) [1]. Pregnant women and children below the age of five years remain the most vulnerable populations [1]. Three main factors contribute to the severity of the disease on the African continent: 1) the presence of the most effective of *Anopheles* mosquito vectors; 2) the prevalence of *Plasmodium falciparum* as the most lethal form of the parasite; and 3) poor socioeconomic conditions resulting in substandard public health facilities for early detection and treatment of the disease.

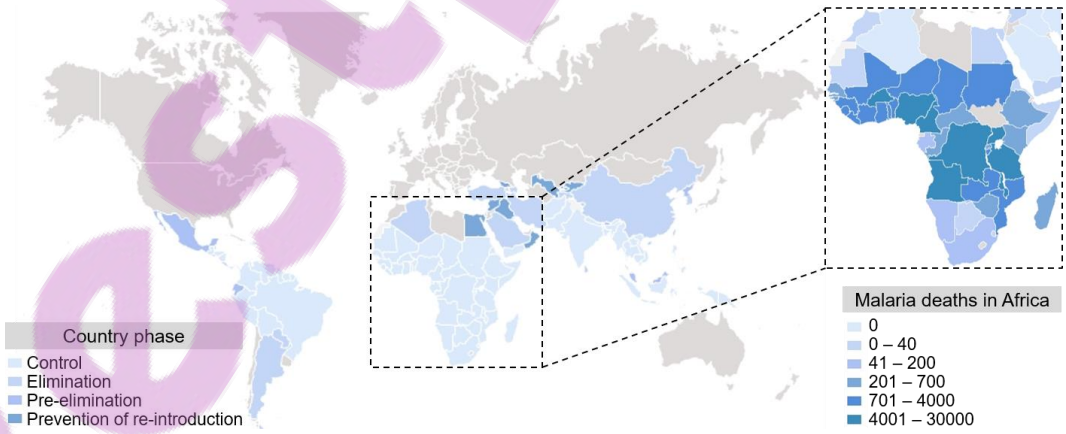

Figure 1.1: Global distribution of malaria control and elimination strategies. Several countries are in the pre-elimination phase, or have already achieved elimination status and focus their efforts on the prevention of malaria re-introduction. The African region remains endemic for malaria and has the highest number of reported malaria deaths yearly, despite global malaria control strategies. Image created using the freely accessible online Global Malaria Mapper platform (World Malaria Report Map Tool; http://www.worldmalariareport.org/home) provided by the World Health Organisation [1].

Malaria control requires an interdisciplinary, multipronged approach including controlling the insect vectors, parasite control through chemoprophylaxis and treatment, early disease diagnosis, accurate surveillance mechanisms and primary health education (Figure 1.2) [2].

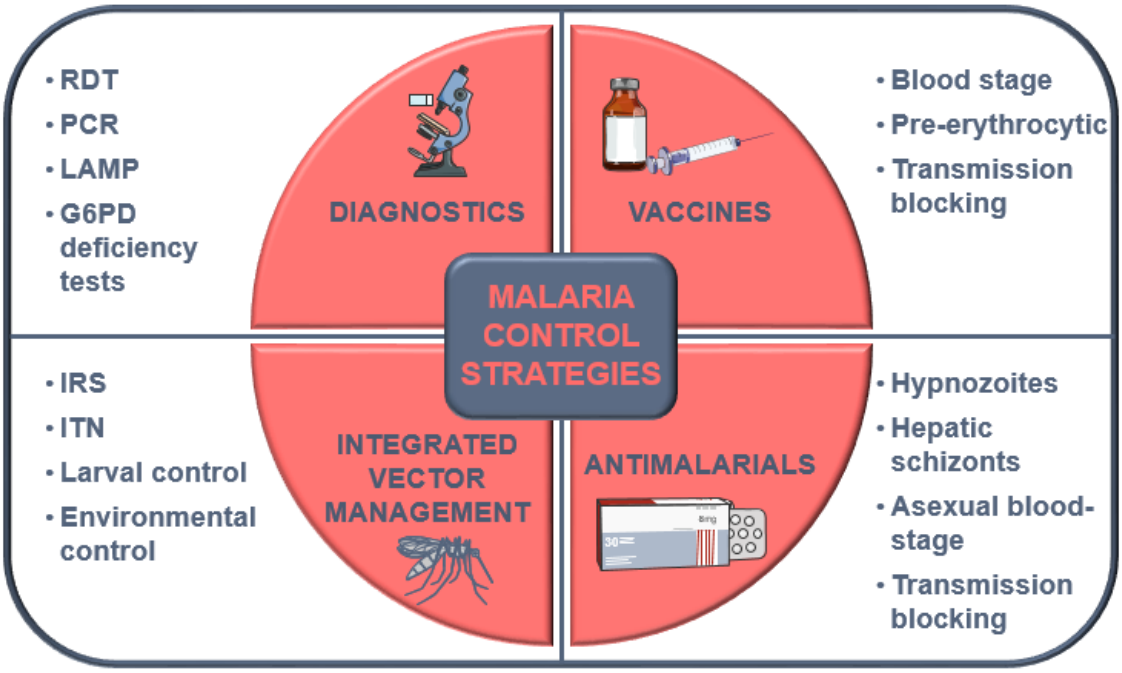

Figure 1.2: Worldwide malaria control strategies. Malaria control consists of diagnostics [rapid diagnostic tests (RDTs); PCR; Loop-mediated isothermal amplification (LAMP); Glucose-6-phosphate dehydrogenase (G6PD) deficiency tests], vaccines, antimalarials and integrated vector management [IRS; ITNs; Larval control; Environmental control], each with a myriad of strategies to combat multiple aspects of the disease. Vaccines and antimalarial control strategies are aimed at various parasite life cycle stages. Images were adapted from Servier Medical Art (URL link to the license: https://creativecommons.org/licenses/by/3.0/) and changes were made in terms of colour and size.

Vector control strategies focus on targeting the female *Anopheles* mosquitoes that transmit *Plasmodium* parasites to human hosts. *Anopheles* mosquitoes can be classified into ~430 species, of which only 30-40 are vectors of major importance for malaria transmission including *An. arabiensis*, *An. gambiae* and *An. funestus,* the latter of which is the main malaria vector species in South Africa [3-5]. Integrated vector management comprise of indoor residual spraying (IRS) of insecticides, personal protection measures (e.g. insecticide treated nets, ITNs), larval control and environmental control [6]. IRS, specifically by means of dichlorodiphenyltrichloroethane (DDT), involves the spraying of insecticides on the inside walls of rural dwellings and has long been used to reduce malaria incidence [7, 8], and is the main means of control of *An. funestus* in South Africa [9].

Malaria vaccine development has been extremely challenging due to a wide array of effective defences employed by the parasite. This includes the extensive use of antigenic

variation mechanisms, complicated by a poor understanding of the interaction between *P. falciparum* parasites and the human immune system [10]. Recent advances in malaria vaccine development led to the identification of two leading pre-erythrocytic stage vaccine candidates, RTS,S/AS01 (GlaxoSmithKline in partnership with the PATH Malaria Vaccine Initiative) and PfSPZ (Sanaria Inc.). There are currently 25 ongoing malaria vaccine projects globally, where four are in Phase IIb or III clinical trials and can potentially lead to the development of a vaccine that successfully prevents malaria infection and/or transmission.

Parasite control is still fully reliant on chemical intervention strategies and this has to be individualised to target the complexity associated with different parasite populations. Besides *P. falciparum* parasites, there are four additional species within the Apicomplexa phylum of parasitic protozoa that affect humans namely *P. vivax*, *P. ovale*, *P. malariae* and *P. knowlesi*. *P. falciparum* causes the most severe cases of malaria, due to its ability to cytoadhere to microvasculature and evade clearance by the immune system (reviewed in [11]), resulting in the highest mortality rates (99% of malaria deaths in 2015) [1]. The second most prevalent species is *P. vivax,* which is commonly found in most of Asia and the Eastern Mediterranean. *P. vivax* parasites have the ability to survive in the *Anopheles* mosquito vector at lower temperatures and higher altitudes, and form dormant hypnozoites in the human host's liver, leading to recrudescence of the disease [12]. *P. ovale* and *P. malariae* cause measurably fewer malaria cases worldwide, after which *P. knowlesi*, the zoonotic malaria species, is the least widespread [1].

Antimalarial drugs serve multiple purposes and target product profiles for case management (chemotherapeutics) and chemoprotection is prioritised globally by partnerships such as the Medicines for Malaria Venture (mmv.org; [13]). *Plasmodium* parasites are unicellular eukaryotes that undergo a series of phenotypic transformations during the course of their multistage life cycle and this multistage development complicates drug discovery [14, 15]. Sexual reproduction of the parasites occur in the mosquito vectors, while asexual development occurs in the human host [15]. Both of these developmental processes can be divided into two phases. Asexual replication involves exo-erythrocytic development in the liver of the human host and an intra-erythrocytic developmental cycle (IDC) in the bloodstream of the human host. Sexual reproduction involves intra-erythrocytic gametocyte development in the human host and sporogonic development in the mosquito [16]. This multistage development of *P. falciparum* parasites requires parasite control strategies to be aimed at every stage of the

parasite's life cycle in order to relieve the disease burden and limit parasite transmission. New antimalarials therefore has to meet the challenges above and be useful in the context of the aim of global malaria elimination. As such, target candidate profiles for antimalarials therefore include 1) molecules that clear asexual blood-stage parasites; 2) molecules that have activity against *P. vivax* hypnozoites; 3) molecules against liver stage schizonts for prophylaxis; 4) molecules able to block transmission by targeting gametocytes; and 5) molecules blocking transmission by targeting the insect vector [13].

However, the development of novel antimalarials is a continuous process due to the persistent development of resistance in *P. falciparum* parasites (reviewed in [17]). These parasites are extremely adaptive and has developed resistance to all chemotypes clinically used thus far including three major classes namely the quinolones, antifolates and artemisinins (summarised in Table 1.1) [18-20].

Table 1.1: The history of antimalarial drug resistance. Three major compound classes have historically been used to treat malaria, each with a unique mechanism of action and a different mechanism of resistance development that rendered them unusable.

COMPOUND CLASS	EXAMPLE DRUGS	MECHANISM OF ACTION	RESISTANCE MUTATIONS
Quinolines 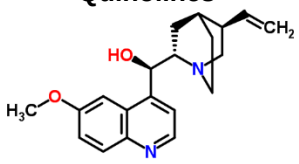	Chloroquine, quinine, amodiaquine, piperaquine, primaquine, mefloquine, etc.	Targets haem polymerisation	Single-point mutation in the transporter gene *Pfcrt* and the multidrug resistance gene *Pfmdr1*
Antifolates 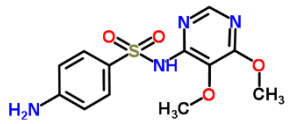	Pyrimethamine, proguanil, sulfadoxine, dapsone, etc.	Targets folate metabolism	Point mutations in the dihydrofolate reductase and dihydropteroate synthase genes
Artemisinins 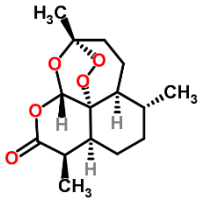	Artemisinin, artemether, artesunate, dihydroartemisinin, etc.	Production of reactive oxygen species, haem polymerisation, targets various proteins and the mitochondria	Kelch13 propeller mutations

For any new entity to be considered as antimalarial candidate, it therefore needs to be able to 1) target various stages of parasite development including gametocytes to block malaria parasite transmission to be useful in an elimination strategy; and 2) be able to target parasites with diverse resistance backgrounds to delay resistance development. The latter implies that novel chemotypes need to be discovered that target essential

biochemical activities not previously targeted. This, however, highlights the caveat in antimalarial drug discovery, since several biological processes of the parasite is still poorly understood. Only once we have a better understanding of essential activities, will we be able to define novel druggable targets.

1.2 *P. falciparum* development

1.2.1 Asexual development

An infection is initiated when mature sporozoites (present in saliva) are transmitted to an uninfected human host via the bite of a female *Anopheles* mosquito (Figure 1.3). These sporozoites enter the circulatory system and are rapidly transported to the liver (15 min to a few hours) [21], where exo-erythrocytic schizogony within hepatocytes is initiated and thousands of merozoites are released in the bloodstream to initiate the 48 h IDC [22-24]. Erythrocyte invasion by merozoites leads to the formation of ring stage parasites. These parasites subsequently undergo cell growth and round up to form trophozoites, the highly metabolically active form of the parasite that consumes host cytoplasm and breaks down haemoglobin to amino acids [15]. Once enlarged, sequential rounds of nuclear division occur through asexual intra-erythrocytic schizogony and schizonts are formed that each consist of 16-32 individual merozoites [25]. These are released into the bloodstream when the schizonts rupture, where they are free to invade new erythrocytes [26]. This IDC of the *P. falciparum* parasite repeats every 48 h whereby the continuous infection, rupturing and re-infection of erythrocytes result in the clinical manifestations and pathogenicity of malaria.

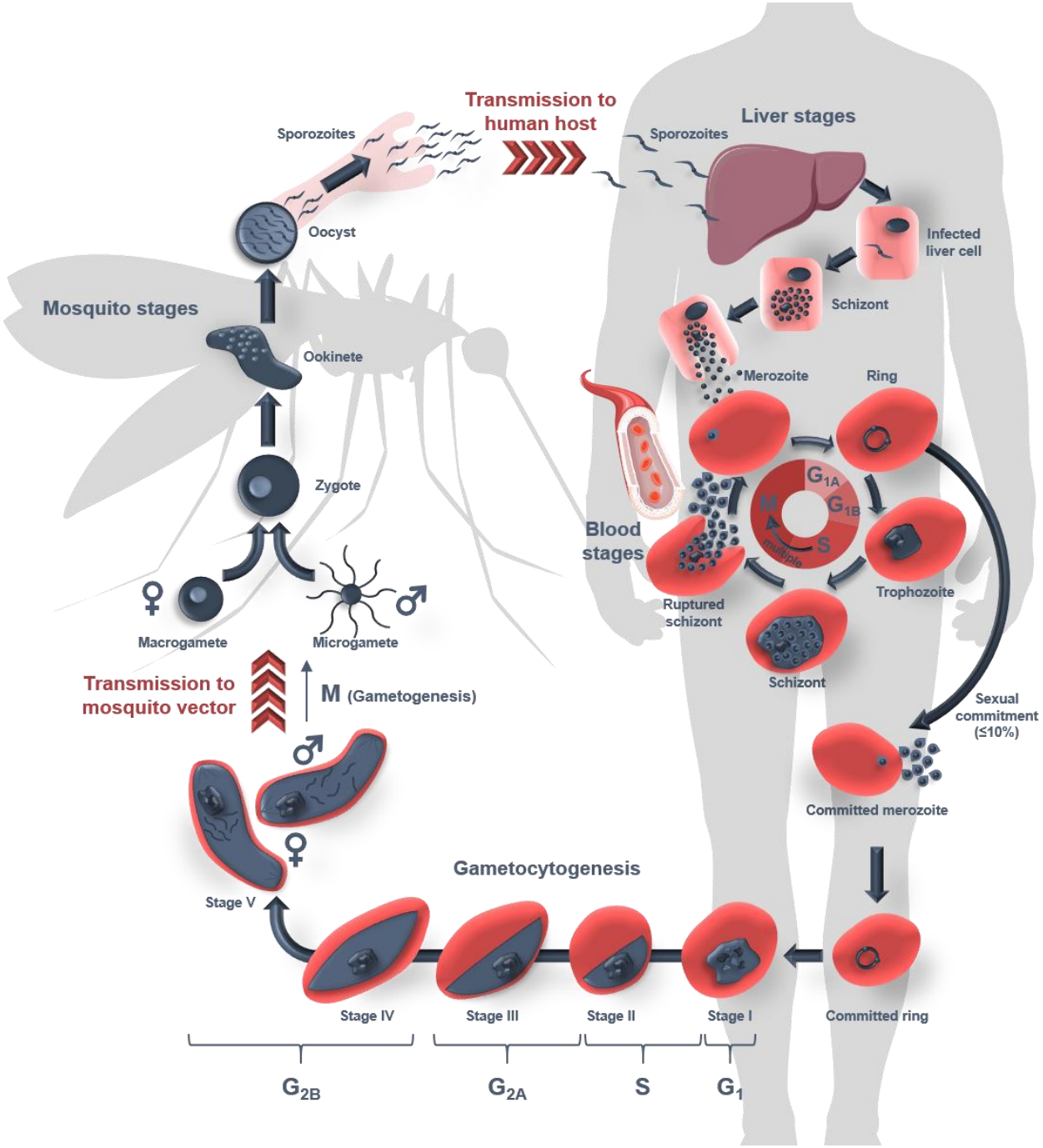

Figure 1.3: The *P. falciparum* parasite life cycle. The life cycle includes three separate stages namely the exo-erythrocytic stage inside hepatocytes, the IDC inside erythrocytes and the sporogonic stage inside the mosquito vector. Briefly, sporozoites invade hepatocytes that ultimately rupture to release merozoites into the human bloodstream. These merozoites infect erythrocytes and develop into rings, trophozoites and schizonts that will again rupture to release multiple merozoites. During each round of asexual development, a proportion (≤10%) of the schizonts commit to sexual development to initiate gametocytogenesis. These schizonts produce committed merozoites that induces the production of stage I-V gametocytes during the course of ~10-12 days. Gametocytogenesis follows a different cell cycle than during asexual development, where the G_1–phase occurs during the first few hours of stage I development, S-phase in stage I-II, G_{2A} in stage II/III, G_{2B} in stage IV-V and finally the M-phase as gametogenesis occurs within the mosquito vector. Upon transmission, macro- and microgametes fuse in the mosquito midgut to form a zygote, ookinete and an oocyst that will eventually rupture, releasing sporozoites that are able to be transmitted to the human host, thus completing the cycle. Images were adapted from Servier Medical Art (URL link to the license: https://creativecommons.org/licenses/by/3.0/) and changes were made in terms of colour and size.

Asexual development of *P. falciparum* parasites do not mimic typical eukaryotic cell cycle development and the association to specific cell cycle compartments is still disputed [15, 27, 28]. When the rings develop into early trophozoites, the chromatin is condensed as the parasites seemingly undergo the G_{1A} to G_{1B} transition of the cell cycle (Figure 1.3). DNA synthesis is initiated as mature trophozoites are formed and the cell cycle progresses from the G_1 to S-phase where chromatin decondensation occurs [29, 30]. During schizogony, asynchronous nuclear division occurs as mitosis is initiated in the M-phase [30, 31]. Numerous rounds of DNA synthesis and nuclear division occurs interchangeably during S- and M-phase progression where ~5 nuclear divisions take place [30, 31]. No evidence for the presence of the G_2 phase of cell cycle development has been found in *P. falciparum* [31].

1.2.2 Sexual development

P. falciparum parasites undergo a binary decision to ensure transmission to the mosquito vector and this requires specialised cell differentiation known as gametocytogenesis. A certain proportion parasites (≤10%) cease asexual multiplication by committing to sexual differentiation [32]. Unique to *P. falciparum*, commitment to gametocytogenesis precedes schizogony, yielding merozoites from a single schizont committed to either asexual or sexual development [33]. Male and female gametocytes each develop from a single committed schizont that determines the sex specificity of all resulting gametocytes, with a female-biased ratio of 5:1 [34, 35].

The parasite is environmentally sensitive and a wide array of exogenous induction triggers have been associated with gametocyte commitment *in vitro.* This includes parasite stress responses, increased parasitaemia, nutrient-deficient culture medium, drug treatment (e.g. chloroquine) and extracellular vesicles released by infected erythrocytes [36-41]. One factor that was recently indicated to play a critical role in sexual commitment is human serum factor lysophosphatidylcholine (lysoPC), where its depletion leads to induction of commitment *in vitro* (Nicholas Brancucci & Matthias Marti; GRC Malaria, Switzerland, 2017). In response to parasites being unable to maintain phospholipid metabolism, the Kennedy pathway enzymes are activated as compensatory metabolic responses. Although these factors influence the probability of commitment for a specific parasite, the ultimate decision to commit or continue in asexual development remains arbitrary [42] and the precise timing and triggers involved remain unclear [34, 43, 44].

During gametocytogenesis, the parasites undergo a series of essential morphological, physiological and biochemical transformations to develop into five distinct stages [37]. *P. falciparum* gametocytogenesis is evolutionarily distinct from other *Plasmodium* species specifically in maturation time (~10-12 days *in vitro*) and morphology (five stages; characteristic crescent shape) [37, 45-47]. For the other four human malaria species, the gametocytes mature within 24-48 h, depending on the species, and have a mononucleic enlarged round shape occupying most of the host erythrocyte [48-50].

The first stage of gametocyte development resembles an asexual trophozoite with a round compact shape (Figure 1.3) [45]. As these parasites further progress into mononucleic spherical stage II and subsequent stage III gametocytes, they adopt a D-shape where the gametocytes elongate with rounded edges [32]. Stage IV gametocytes develop after further elongation of the parasite occurs with sharpened edges [32, 51], where osmiophilic bodies and rough endoplasmic reticulum start to form in female gametocytes and the host erythrocyte is reduced to a flattened cytoplasmic edge as a result of adapting to the curved gametocyte shape (Laveran's bib) [52, 53]. Gametocyte maturation ultimately leads to the development of crescent-shaped stage V female (macro-) and male (micro-) gametocytes with rounded edges, where females are more elongated and curved than males [46].

Association of cell cycle compartments result in a brief G_1 phase during stage I development, directly followed by DNA synthesis during the S-phase in stage I-II gametocytes, confined to the first 48 h of gametocytogenesis (Figure 1.3). As stage II-III gametocytes are formed, the G_{2A} phase of the cell cycle is initiated where significant RNA and protein synthesis continue to occur. The late stage IV-V gametocytes develop during the G_{2B} phase of the cell cycle that is associated with increased transcriptional control mechanisms and decreased RNA and protein synthesis [54]. Mature stage V gametocytes remain in their terminally differentiated forms in the G_{2B} phase until they are transmitted to the mosquito vector to activate a series of molecular changes during gametogenesis (M-phase).

During gametocyte development, immature gametocytes (stages I-IV) avoid splenic clearance by preferentially sequestering in the host bone marrow, but upon maturation, terminally differentiated stage V gametocytes are released in the peripheral blood system, ready for transmission [55-57]. After the stage V macro- and microgametocytes are ingested by a mosquito, they round up and egress from the enveloping erythrocytes within

the mosquito midgut (Figure 1.3). This results due to specific environmental cues that induce the production of mature micro- and macrogametes including lowered temperature, increased pH and exposure to xanthurenic acid [58, 59]. *P. falciparum* gametocyte egress is mediated by the expression of two specific proteins, Pfg377 and PfMDV-1/Peg3, which are pivotal for gametocyte-specific secretory organelle (osmiophilic body) formation [60, 61]. As macrogametocytes round up and haploid round-shaped gametes exit from erythrocytes, microgametocytes undergo three rounds of DNA replication within ~20 min post-activation to form an octoploid nucleus [62], resulting in eight motile microgametes after exflagellation [63]. Upon transmission, the M-phase of the cell cycle is initiated to induce *de novo* protein synthesis crucial for exflagellation of microgametes [54]. Sexual reproduction occurs as a diploid zygote is produced by fertilisation, followed by zygote maturation into infective motile ookinetes that can enter mosquito midgut epithelial cells to develop into oocysts [51, 64]. Asexual replication occurs continuously within an oocyst to produce a number of haploid sporozoites during sporogony that are released and transported to the salivary glands of the mosquito to ensure continued transmission [65].

The complicated life cycle and associated cell cycle of *P. falciparum* parasites evidently requires tight control to ensure optimal survival. However, the parasite seems to rely on atypical regulatory mechanisms to accomplish this feature. Over the past decade, various systems-wide studies gave us a better understanding of the molecular aspects involved in asexual multiplication and sexual differentiation [66-78]. Ultimately, gene expression is facilitated by highly connected regulatory mechanisms on the transcriptional, post-transcriptional, translational and post-translational levels in response to a constantly changing host environment and shape-shifting life cycle progression [79-83].

1.3 Regulation of *P. falciparum* life cycle development

The *P. falciparum* genome consists of ~23 Mb distributed among 14 chromosomes and encodes for ~5300 genes (3D7 parasite strain) [70]. *P. falciparum* parasites employ a "just-in-time" transcriptional model that allows for specific transcripts to only be produced in particular life cycle compartments. This is subject to stringent regulation during development through the parasite's various life cycle stages [66, 84], particularly at the transcriptional level with ~80% of the *P. falciparum* parasite's genes expressed during the IDC [66, 74]. The IDC genes were shown to have a cyclic expression pattern, with >75% of transcripts reaching peak steady-state levels at a single time point during development

[66, 69, 74]. Association of co-expressed transcript sets that encode proteins involved in similar biological processes allowed for the derivatisation of the “just-in-time” transcriptional model [69]. Gametocytogenesis has been associated with differential expression of ~15% of genes [74], with 246 genes showing highly correlated gametocyte-specific expression patterns that may be involved in transcriptional control mechanisms during gametocytogenesis [78]. Sexual stage development in preparation for parasite entry into the mosquito midgut also triggers the stage-specific activation of ~20% of genes [68, 71, 74], including expression of various sexual stage specific surface antigens (e.g. *pfs*25, *pfs*28, *pfs*48/45, *pfs*47, *pfs*230, etc.; reviewed in [63]). Compared to cell cycle progression of model organisms like yeast (*Saccharomyces cerevisiae*) and humans, where only 15% of the total genome is periodically regulated, this suggests that *P. falciparum* gene expression is regulated primarily by unusual mechanisms [66]. Most strikingly, *P. falciparum* parasites rely on a single 27-member family of Apicomplexan-specific unique transcription factors belonging to the Apicomplexan apatela 2 (ApiAP2) family of proteins, thereby proposing altered regulatory mechanisms to facilitate coordination of the transcriptional cascade [70, 85, 86]. This supports evidence that post-transcriptional control is prevalent during *P. falciparum* development, as genes encoding RNA-binding and RNA-regulatory proteins are more abundant [87, 88].

Following transcription, a fine-tuned equilibrium results in steady-state protein levels associated with development through specific life cycle stages [89]. An 11-18 h delay is typically seen in *P. falciparum* between peak mRNA and protein levels [73], indicating immediacy in translation of protein complexes necessary to develop into the next life cycle stage [90]. Several families of RNA-binding proteins have been identified [85, 87, 88], including the Pumilio and FEM3 binding factor (Puf; PfPuf1&2) family that was extensively shown to be differentially expressed during gametocytogenesis and play a significant role in post-transcriptional regulation of specifically male gametocyte differentiation and translational repression [91, 92]. Translational repression of specific female transcripts has been observed during sexual differentiation as a means of post-transcriptional regulation, awaiting translation as gametogenesis is initiated upon transmission [72, 91, 92].

Life cycle progression and the cascade of gene expression is further accompanied by fluctuations in chromatin status of the parasite and post-translational regulatory mechanisms. Chromatin modifications are considered as key transcriptional regulators in eukaryotes, and the paucity of transcription factors present in Plasmodia leads to

speculations that these parasites may indeed also rely heavily on chromatin level regulation [93]. These modifications integrate specific environmental and developmental cues into a highly interconnected gene expression cascade [94]. In other protozoan parasites (e.g. *Toxoplasma gondii*), chromatin regulation is essential in gene expression during differentiation, specifically involving a fine-tuned cascade of histone acetylation, deacetylation and methylation [95]. Multiple chromatin-associated proteins, similar to those found in model eukaryotes, have been identified in *P. falciparum* and de-regulation of the transcriptional cascade was shown following perturbation of chromatin structure [96, 97]. Argumentatively, epigenetic gene regulation and in particular the chromatin remodelling landscape is of major importance to parasite biology [98].

1.4 A primer on epigenetic gene regulation

Epigenetic gene regulation comprise of heritable chemical alterations to a genome that changes gene expression without modifying the DNA sequence [99]. Epigenetic gene regulation is tightly regulated and fully reversible, and the total concerted contribution of the various chemical alterations to the overall epigenetic state of a cell (the resultant "epigenome") functionally results in the expression of certain gene sets needed for particular cellular processes [100].

Epigenetically guided differential gene expression varies between cell types and organisms, with different epigenetic mechanisms effective between model prokaryotes and eukaryotes (reviewed in [101]). Eukaryotic epigenetic gene regulation involves modifications at the DNA level (chemical modifications of the DNA bases by methylation), the nucleosome level (chromatin remodelling, histone post-translational modifications [PTMs] and/or the replacement of the core histones by variant histone proteins), the chromatin level (long non-coding RNAs; lncRNAs) and higher order organisation (Figure 1.4) [102, 103]. Regulation is mediated through changes in chromatin structure (i.e. euchromatin/heterochromatin observed in 11 or 30 nm fibers, respectively) and/or composition (nucleosomal changes in histone octamer [H3/H4 tetramer & two H2A/H2B dimers] including variant histone proteins and histone PTMs [104, 105]), altering the downstream functional outcome [90]. By contrast, epigenetic mechanisms are rather simplistic in prokaryotes [106, 107], where DNA adenine methylation is the only means of epigenetic regulation described to date to control transcription and facilitate DNA repair [108], as transcription and translation occurs simultaneously.

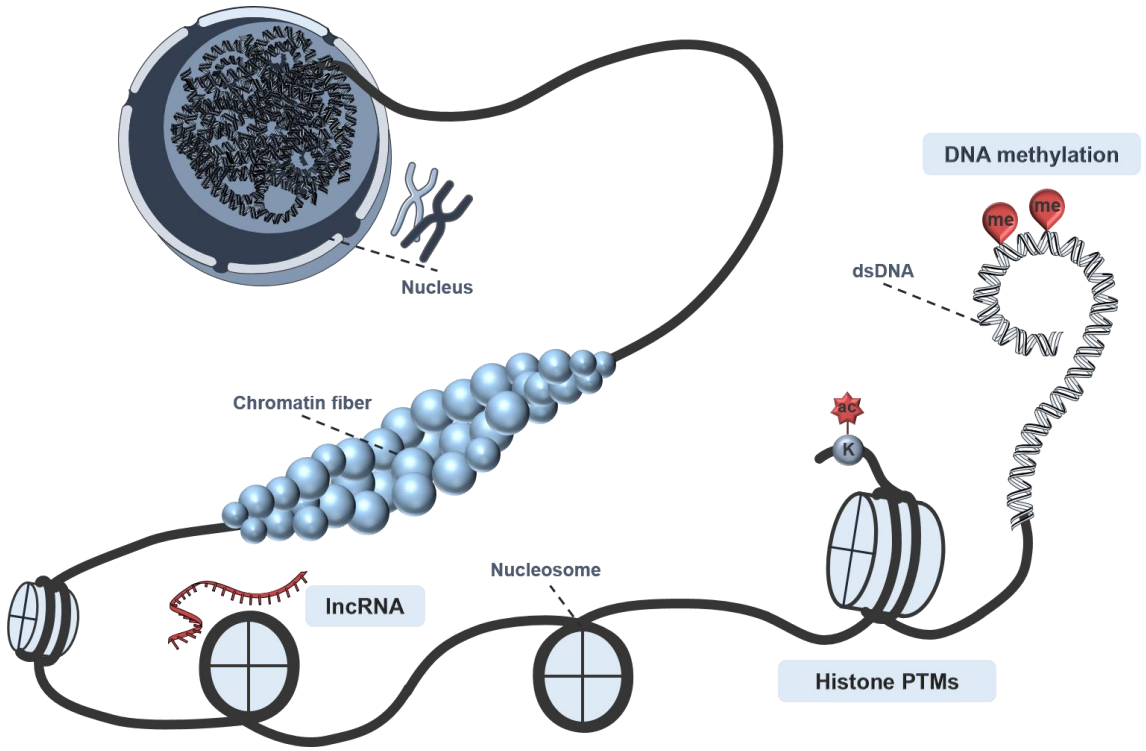

Figure 1.4: DNA packaging and epigenetic gene regulation. Chromosomal DNA is packaged in the cell nucleus into chromatin that consists of dsDNA wrapped around a histone octamer to form nucleosomes. Epigenetic regulation involves DNA methylation, histone PTMs and RNA mechanisms (lncRNA).

Epigenetic regulation at the DNA level occurs by the covalent methylation of cytosine by DNA methyltransferases (DNMT), resulting in 5-methylcytosine [109] most often found in CpG-rich regions [110]. These hydrophobic modifications project into the major groove of DNA and, when located in promoter regions, is generally associated with transcriptional silencing and condensation of chromatin into heterochromatin [103, 110]. DNA methylation has been recognised as an important target for epigenetic therapy in cancer cells [111]. Epigenetic regulation at the chromatin level via lncRNAs occurs by the latter forming a complex with chromatin-modifying proteins and recruiting their catalytic activity to specific genomic loci, thereby modifying chromatin states and influencing gene expression [112].

Epigenetic regulation at the nucleosome level involves the replacement of histones by variant histone proteins [103] and the chemical modification of particularly lysine and arginine residues on the N- or C-terminal histone tails (histone PTMs), altering chromatin structure and composition (Figure 1.5) [84, 90]. Upon chromatin remodelling or repositioning, the access of DNA-binding proteins (such as transcription factors and RNA polymerases) are affected and this alters the transcriptional state [103]. The replacement of canonical histones with histone variants regulates chromatin structure by influencing nucleosome stability [103]. Histone variants differ in a few amino acids from their

canonical counterparts and are generally expressed at much lower levels. This replacement requires ATP-dependent chromatin remodelers and results in the formation of functionally specialised chromatin domains [93]. Histone variants show species-specific genomic distribution patterns and confer novel structural and functional properties on the nucleosome, affecting chromatin remodelling and histone PTMs [113].

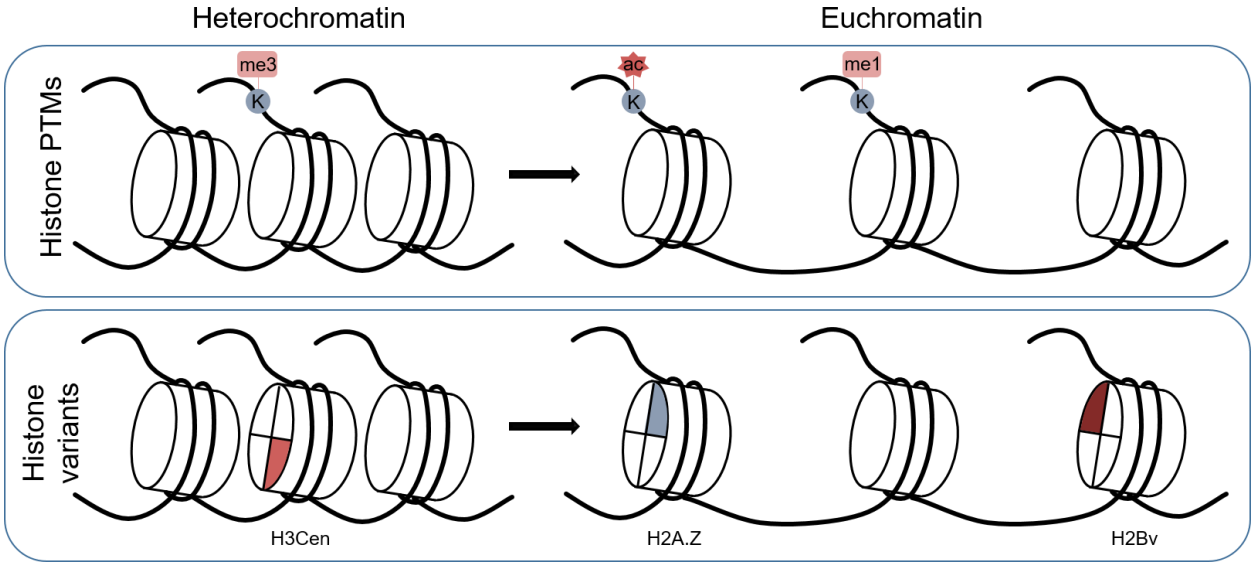

Figure 1.5: Epigenetic gene regulation at the nucleosome level. The mechanisms of nucleosome level epigenetic gene regulation include histone PTMs and the incorporation of variant histone proteins. These factors alter nucleosome stability and dynamics by facilitating the switch between euchromatin [typical histone PTMs: acetylation (ac), monomethylation (me1); H2A.Z and H2Bv histone variants] and heterochromatin [typical histone PTM: trimethylation (me3); H3Cen histone variant] formation.

1.4.1 Histone PTMs

Epigenetic writers, readers and erasers facilitate the establishment and function of histone PTMs; writers and erasers catalyse the addition or removal of histone PTMs, respectively, whilst readers use the modifications to result in a functional effect. The dynamic and reversible nature of histone PTMs result in either *cis* or *trans* effects on nucleosome stability, changing chromatin structure and ultimately promoting or inhibiting transcription and altering gene function [114, 115]. *Cis* effects directly reduce the strength of the histone-DNA interaction forming permissive euchromatin whereas *trans* effects influence the recruitment of specific effector proteins (readers such as cofactors, polymerases, etc.) [84, 103]. These reader proteins are recruited to specific histone PTMs by epigenetic writers and erasers, controlling their biological activity and influencing the altered downstream transcriptional response [84].

Histone PTMs include acetylation, methylation, phosphorylation, ubiquitination, SUMOylation, etc., with acetylation and methylation the most frequently observed. Lysine

acetylation occurs via the transfer of an acetyl group from acetyl-coenzyme A to the Ɛ-amino position on lysines, catalysed by histone acetyltransferase (HAT) (Figure 1.6) [116]. Acetylation weakens histone-DNA interaction by reducing the positive charge on histone tails [117] and resulting in decondensation of the chromatin structure, leaving the chromatin in a transcriptionally permissive state [93]. Deacetylation is catalysed by histone deacetylase (HDAC), resulting in heterochromatin formation [118]. Lysine methylation (mono-, di- and trimethylation) is catalysed by histone lysine methyltransferase (HKMT) and involves *S*-adenosyl-L-methionine as methyl donor (Figure 1.6) [119]. Lysine demethylases remove methyl groups and these proteins are either from the lysine-specific demethylase (LSD1) family or the jumonji histone demethylase (JHDM) family [117]. Lysine methylation is associated with transcriptional activation and repression and its effect is dependent on the position of the methylation site and the degree of methylation (mono-, di- and trimethylation). Both histone acetylation and methylation regulate cellular processes such as targeted gene silencing, cell cycle progression, cell type differentiation, DNA replication and repair.

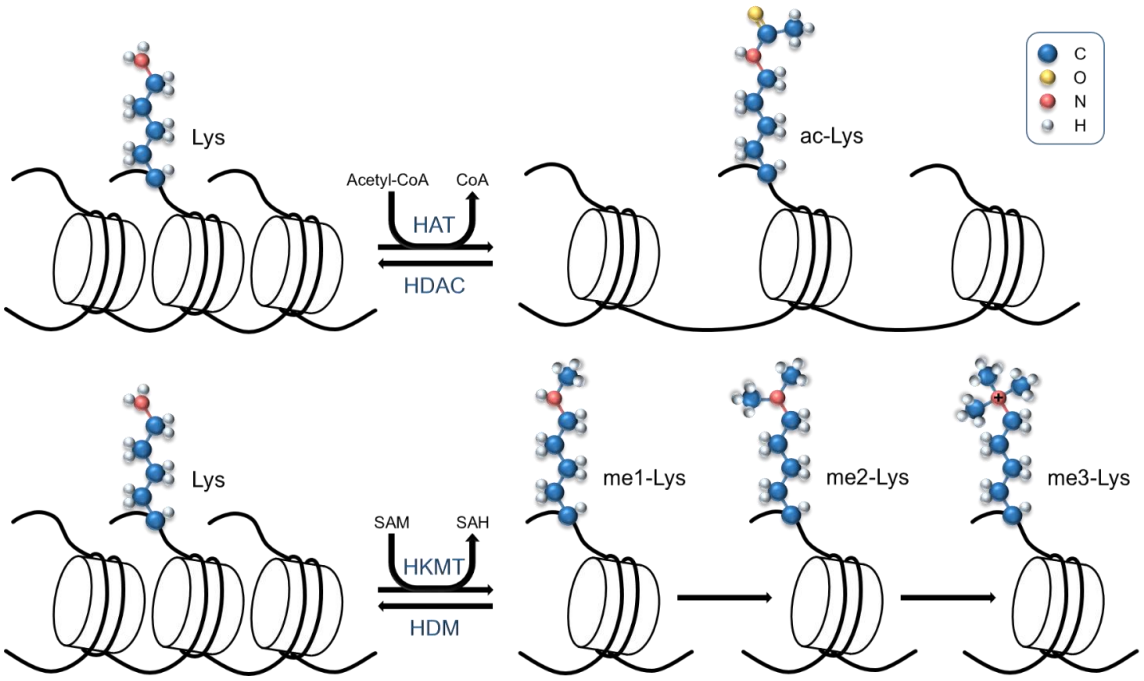

Figure 1.6: Mechanism of lysine acetylation and methylation. Lysine acetylation is catalysed by HAT that facilitates the transfer of an acetyl group from acetyl-coenzyme A to the Ɛ-amino group of the lysine residue. Lysine residues can also be mono-, di- or trimethylated (me1, me2 or me3) by HKMTs and occur by the transfer of a methyl group from *S*-adenosyl-L-methionine (SAM) that is converted to *S*-adenosyl-L-homocysteine (SAH).

Histone phosphorylation occurs on serine, threonine and tyrosine residues via the complementary action of kinases and phosphatases [120]. Similarly, lysine ubiquitination is affected by specific ubiquitin ligases and peptidases [121]. Both phosphorylation and

ubiquitination affects a variety of cellular processes including transcription, chromatin structure maintenance and DNA repair. Small Ubiquitin-like MOdifier (SUMO) proteins can be added to histones in an ATP-dependent process to alter their function. Histone SUMOylation facilitates gene silencing through the recruitment of HDAC and heterochromatin protein 1 (HP1) [122, 123] and is involved in various cellular processes such as transcriptional regulation, apoptosis, protein stability, stress response and cell cycle progression.

Multiple histone PTMs are hypothesised to act in combination to specify unique downstream functions and gene regulatory alterations [116]. This 'histone code' hypothesis implies that specific combinations or patterns of histone PTMs correlate with specific chromosomal states that regulate access to DNA, and influence histone-DNA and histone-histone interactions [124]. To give an idea of the potential complexity of a histone code, histone H3 contains 19 lysine residues known to be methylated. Each lysine can be un-, mono-, di- or trimethylated and allows a potential 4^{19} or 280 billion different lysine methylation patterns on H3, not including acetylation, phosphorylation, ubiquitination, or all the other histone PTMs [116]. However, only a few specific combinations have been validated to be functionally relevant and the full extent of the histone code is not fully understood [125]. In the human genome, a combination of 17 PTMs were found at 25% of promoters [126] with the co-regulation of H3K9me3 and H3S10ph validated to be involved in gene regulation. HP1 is recruited to heterochromatic regions marked by H3K9me3 resulting in transcriptional inactivation [127, 128]. However, if H3S10ph is present adjacent to H3K9me3, HP1 dissociates and transcriptional activation occurs, allowing mitotic progression. This serves as a clear indication of the importance of elucidating the histone code in specific organisms during particular life/cell cycle stages.

Although histone modifications and CpG DNA methylation are conserved mechanisms of epigenetic regulation in cell type differentiation and disease in a wide variety of eukaryotes, the complexity and effect of these epigenetic alterations were shown to differ amongst and between lower and higher eukaryotes. Histone proteins are mostly conserved amongst eukaryotes, but organism multicellularity and complexity necessitates an increased number of PTMs associated with these histone tails [129]. Malaria parasites have been shown to have an atypical repertoire of epigenetic regulatory mechanisms, where epigenetic regulation of chromatin structure was proposed to play a

key role in the parasite's stage-specific development, adaptation and survival [103]. These aspects are discussed in detail below in the context of the focus area of this thesis.

1.5 Epigenetic gene regulation in *P. falciparum*

Various aspects of *Plasmodium* biology are subject to alterations at the chromatin level, including tight transcriptional regulation for stage-specific parasite transitions, genome demarcation and antigenic variation [130]. These epigenetic mechanisms are known to be highly connected [103] and the epigenetic repertoire found in *P. falciparum* to date differs from typical epigenetic mechanisms in model eukaryotes (Figure 1.7) [131]. Gene activation/silencing in *P. falciparum* can be altered by heritable epigenetic mechanisms such as nucleosome, histone and chromatin modifications, ultimately affecting or directing the parasite's developmental switches [84]. Two distinct epigenetic features of *P. falciparum* are that RNAi machinery is apparently absent [132] and lncRNAs are mostly involved only in clonally variant gene expression (CVGE) [130]. DNA methylation [133] and a single characterised DNMT (PfDNMT) has been identified that may contribute to regulation of transcription and silencing of virulence genes [134].

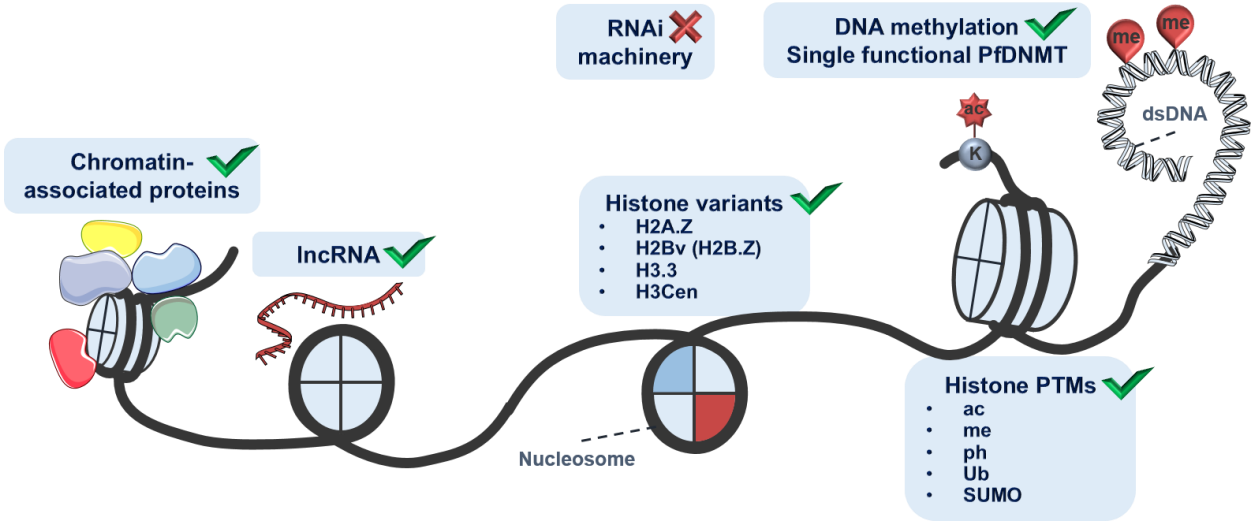

Figure 1.7: Epigenetic mechanisms of *P. falciparum* parasites. The epigenetic mechanisms of gene regulation in *Plasmodium* include DNA methylation by a single PfDNMT; histone PTMs [e.g. acetylation (ac), methylation (me), phosphorylation (ph), ubiquitination (Ub) and SUMOylation (SUMO)]; variant histone proteins (H2A.Z, H2Bv, H3.3 and H3Cen); association with lncRNAs; and the recruitment of chromatin-associated proteins to facilitate various biological outputs. The RNAi machinery is apparently absent. This figure was created based on [103].

1.5.1 The nucleosome & histone PTM landscape of *P. falciparum* parasites

P. falciparum nucleosomes consist of ~80% AT-rich DNA [70] wrapped around a histone octamer that contains the four eukaryotic core histones and four variant histones that

have been described specifically for *P. falciparum* [H2A.Z, H2Bv (or H2B.Z), H3.3 and H3Cen (H3 centromeric)] [100, 114], differing in amino acid composition from their core counterparts. Typically in *P. falciparum*, certain histone variants are associated with euchromatic (H2A.Z/H2Bv) or heterochromatic (H3Cen) domains. Linker histone H1 has not been identified in *P. falciparum* to date [100, 114] and this, to some extent, attributes to the transcriptionally active euchromatic state of the majority of the *P. falciparum* genome (~90%) [103]. The incorporation of histone variants and the full cascade of their associated histone PTMs await complete functional characterisation and can further expand the epigenetic regulatory potential of the malaria parasite [102].

Epigenetic gene regulation at the nucleosome level in *P. falciparum* parasites is generally mediated by reversible histone PTMs with homologues for histone modifying enzymes present in the parasite's genome [90, 135]. Of all the epigenetic gene regulatory processes in *P. falciparum*, histone PTMs are the most extensively studied, particularly so during asexual development. Various reports have qualitatively indicated the presence of acetylation, methylation, phosphorylation, ubiquitination and SUMOylation on the N-terminal tails of the canonical and variant histones (Figure 1.8) [100, 114, 136-143]. Higher levels of histone PTMs associated with chromatin activation are present, with the conserved eukaryotic marks H3K4me3, H3K9ac, H3K14ac, H4ac and H4K20me3 present in *P. falciparum* [98], similar to other unicellular eukaryotes [84]. In *P. falciparum* these marks have also been positively associated with transcription, exhibiting dynamic patterns in their association with the genome and across the IDC [141, 144]. Heterochromatic histone PTMs are less abundant in *P. falciparum* and are restricted to specific heterochromatic regions, typically involving H3K9me3, H3K27me3 and H3K36me2/me3 [100, 144, 145].

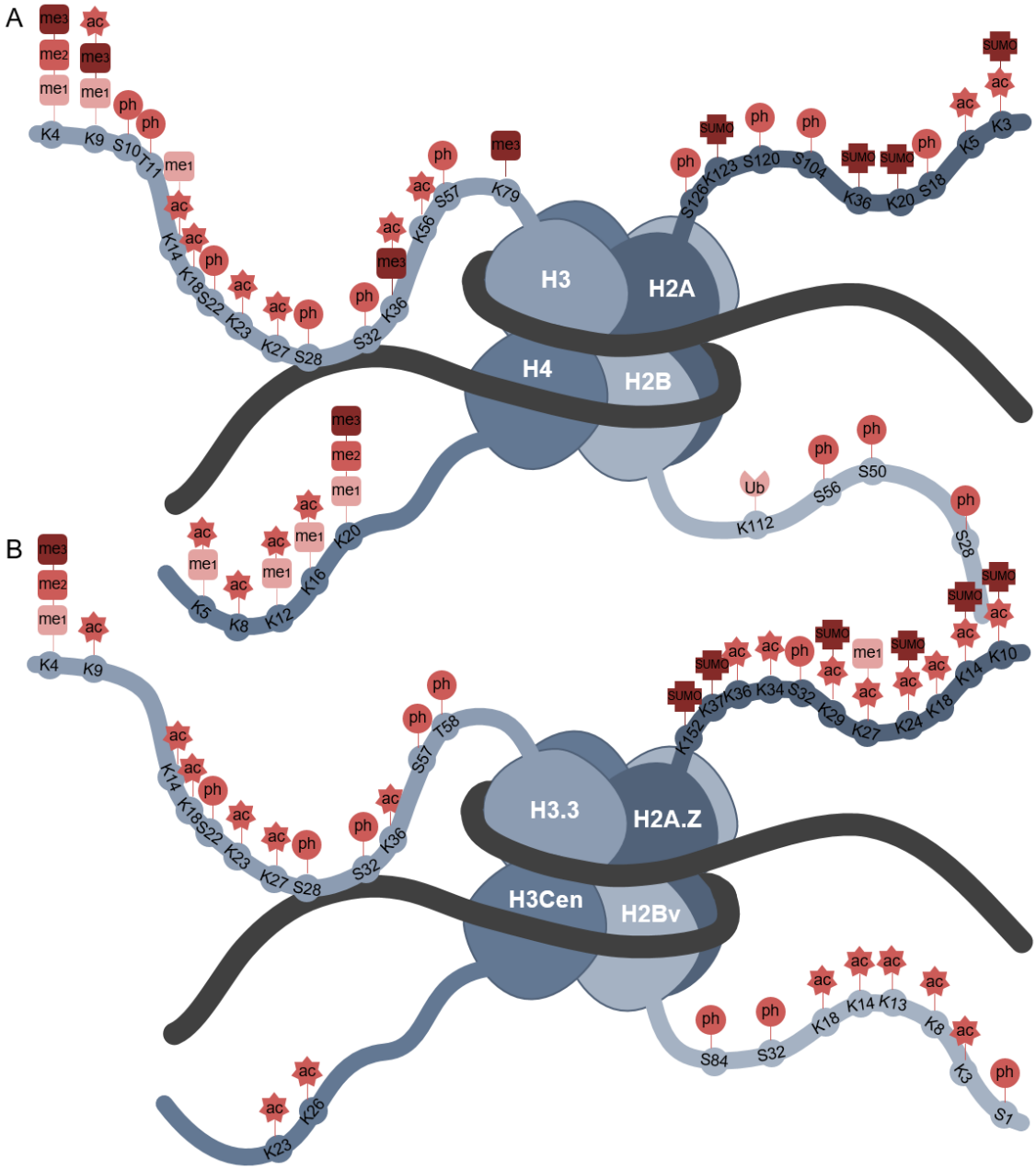

Figure 1.8: The current histone PTM landscape of *P. falciparum* parasites. Various histone PTMs have been identified on (A) the canonical and (B) variant histones, including lysine acetylation (ac), lysine methylation (me1, 2 and 3), serine and threonine phosphorylation (ph), lysine ubiquitination (Ub) and lysine SUMOylation (SUMO). Data obtained from various publications [100, 114, 136-143].

Two histone PTMs that have extensively been studied and thought to play a major role in *P. falciparum* epigenetic regulation are lysine acetylation and methylation. Four HATs (PfGCN5, PfMYST, PFL1345c and PFD0795w/PfHAT1), five HDACs (PfHDAC1, PfHDAC2, PfHDAC3, PfSir2A and PfSir2B), ten HKMTs (PfSET1-10) and three demethylases (PfLSD1, PfJmjc1 and PfJmjc2) have been identified in *P. falciparum* to date (Table 1.2) [84]. Collectively, these histone modifying enzymes work antagonistically (acetylation/methylation vs. deacetylation/demethylation) in a dynamic equilibrium to selectively maintain specific chromosomal states during parasite development [98]. The

P. falciparum effector protein repertoire can be divided into several groups including bromodomains, the Royal superfamily including chromodomains, plant homeodomain fingers, WD40 repeats and 14-3-3 proteins [84]. These readers are recruited to the histone PTM sites to interpret their functional outcomes, and in *P. falciparum* they are mostly conserved, with specific unique adjustments to the dynamic nature of the histone PTM landscape. The full complexity of the *P. falciparum* epigenome remains to be discovered, including the contribution of these effector proteins to the epigenetic gene regulation.

Table 1.2: Writers, erasers and effector proteins involved in epigenetic regulation in *P. falciparum.* Data taken from [146], except PfNAPS.

PROTEIN NAME	GENE ID	PROPOSED FUNCTION	REFERENCES
HISTONE METHYLTRANSFERASES			
PfSET1	PF3D7_0629700	H3K4me3	[143]
PfSET2 (PfSETvs)	PF3D7_1322100	H3K36me2/3, participates in *var* regulation	[138, 143, 147, 148]
PfSET3 (PfKMT1)	PF3D7_0827800	H3K9me2/3	[143, 145, 149]
PfSET4	PF3D7_0910000	H3K4me	[138, 143, 149]
PfSET5	PF3D7_1214200	Unknown PTMs	[138, 143, 149]
PfSET6	PF3D7_1355300	H3K4me	[143, 149]
PfSET7	PF3D7_1115200	H3K4me and H3K9me	[143, 150]
PfSET8	PF3D7_0403900	H4K20me1/2/3	[138, 143, 147]
PfSET9	PF3D7_0508100	Unknown PTMs	[143]
PfSET10	PF3D7_1221000	H3K4me3, localised to the *var* expression site	[151]
HISTONE DEMETHYLASES			
JmjC1	PF3D7_0809900	H3K9me and H3K36me removal	[138, 143]
JmjC2	PF3D7_0602800	Unknown PTMs removal	[138, 143]
LSD1	PF3D7_1211600	Unknown PTMs removal	[138, 149]
HISTONE ACETYLTRANSFERASES			
PfGCN5	PF3D7_0823300	H3K9ac and H3K14ac	[152, 153]
PfHAT1	PF3D7_0416400	Probable orthologue to HAT1 in higher eukaryotes	-
PfMYST	PF3D7_1118600	H4K5, K8, K12 and K16 ac	[154]
HISTONE DEACETYLASES			
PfSIR2A & PfSIR2B	PF3D7_1328800 & PF3D7_1451400	Telomere maintenance and regulation of *var* gene expression	[155-158]
PfHDAC1	PF3D7_0925700	Probable orthologue of Rpd3 from yeast	[159]
PfHDAC2	PF3D7_1008000	*var* gene silencing and sexual differentiation	[159, 160]
PfHDAC3	PF3D7_1472200	-	[159]
OTHER			
PfBDP1	PF3D7_1033700	Regulation of genes linked to erythrocyte invasion	[161]
PfHP1	PF3D7_1220900	Maintenance of silenced regions of the genome, *var* gene silencing and sexual differentiation	[162-164]
PfNAPS	PF3D7_0919000	Histone binding & nucleosome assembly	[165, 166]

1.5.2 Epigenetic regulation is involved in specific developmental processes during *P. falciparum* life cycle development

Epigenetic gene regulation plays a significant role in *P. falciparum* through various developmental stages, including erythrocyte invasion, nutrient uptake, control of clonally variant gene expression, stage-specific life cycle development and sexual commitment (summarised in Figure 1.9) [115]. These factors have mostly been studied in the IDC stages of the parasite's life cycle [103] and to some extent during gametocyte commitment, but crucial epigenetic factors that could be vital for malaria transmission, if not pathogenesis, may be present in other *P. falciparum* life cycle stages [115].

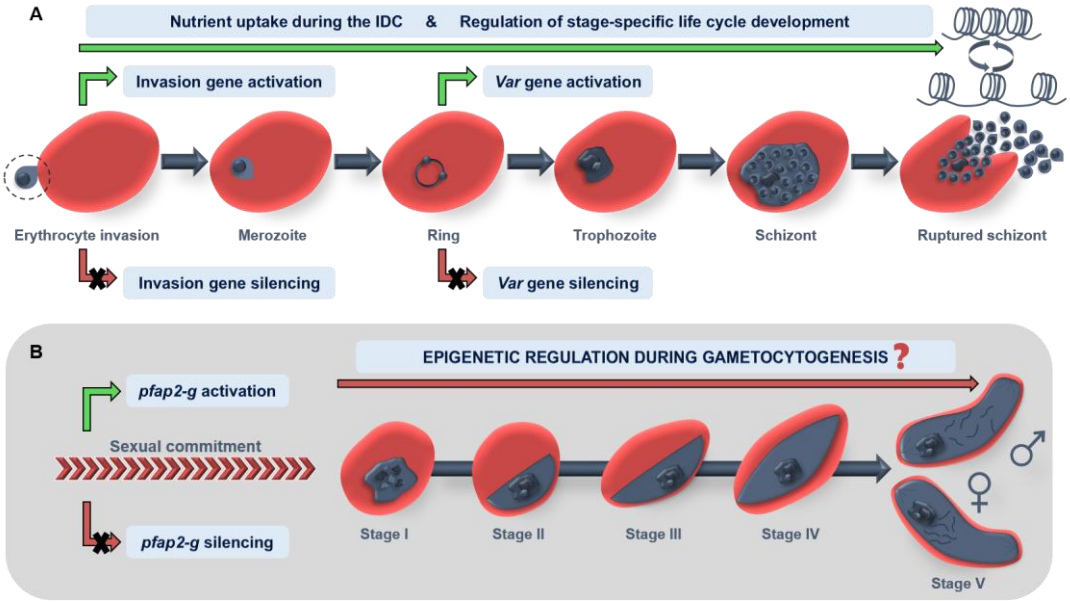

Figure 1.9: Involvement of epigenetic regulation in specific processes during *P. falciparum* life cycle development. Epigenetic regulation in *P. falciparum* is involved in various processes during life cycle development, including **(A)** erythrocyte invasion of merozoites; nutrient uptake during the IDC; control of clonally variant gene expression in ring stages and throughout the IDC; stage-specific life cycle development and **(B)** sexual commitment; mostly facilitating transcriptional activation (green arrow) or silencing (red arrow) by histone PTMs and a myriad of epigenetic modulators. The epigenetic factors associated with gametocytogenesis remains largely unknown.

1.5.2.1 Epigenetic regulation of clonally variant gene expression

P. falciparum parasites possess the ability to alter transcriptional states during development via CVGE, allowing single parasites in isogenic populations to express genes at varying levels to allow stochastic heterogeneity within parasite populations and guarantee optimal parasite survival in any given host environment (reviewed in [167]). This includes the variant (*var*), repetitive interspersed (*rif*), *P. falciparum* Maurer's cleft 2 transmembrane (*pfmc2tm*) and subtelomeric variable open reading frame (*stevor*) gene families [168-171]. CVGE has been studied in detail for the 60 member *var* gene family

encoding key virulence factors. Expression of single erythrocyte membrane proteins 1 (PfEMP1) from the *var* gene family mediates cytoadhesion and antigenic variation [172-174] and allows host immune evasion [155]. This process is mediated through bet-hedging which is the spontaneous transcriptional switching of genes [170], and is subject to epigenetic regulation. *Var* gene clusters are located at the nuclear periphery in heterochromatic regions, where the repressive modulators H3K9me3 and PfHP1 maintain the default inactive *var* gene states (Figure 1.10) [145, 156, 163, 164, 175, 176]. PfHP1 is a conserved eukaryotic transcriptional repressor known to recruit HKMTs and bind proteins that are involved in heterochromatin formation e.g. HDACs [177, 178]. These silencing events are accompanied by histone deacetylation by PfSIR2A, PfSIR2B and histone deacetylase 2 (PfHDAC2) that actively regulate these repressive clusters to maintain the H3K9me3 silencing cascade [145, 155, 158, 160]. Another epigenetic modulator that is involved is the HKMT PfSET2 (also known as PfSETvs) that selectively marks *var* genes with the silencing histone PTM H3K36me3 [138, 148]. All these modulators function together to maintain an inactive *var* gene state *in vitro*.

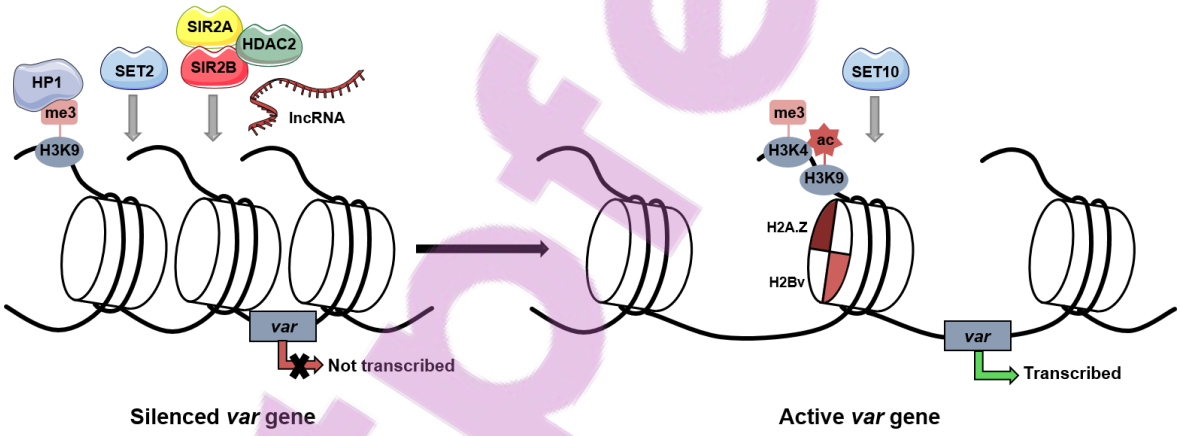

Figure 1.10: Mechanism of epigenetic gene regulation involved in *P. falciparum var* gene expression. CVGE is repressed by H3K9me3 and PfHP1 and associated with various epigenetic modulators that allows for selective silencing of *var* genes, including PfSET2, PfSIR2A, PfSIR2B, PfHDAC2 and lncRNAs. Activated *var* genes are marked by H3K4me3 and H3K9ac, facilitated by PfSET10 and histone variant incorporation (H2A.Z and H2Bv). Figure created based on Batugedara *et al*. [179].

Selective activation and transcription of a single *var* gene occurs during early ring stage development (~10-14 h) when the switch to enrichment in the H3K9ac and H3K4me3 euchromatic marks occurs (Figure 1.10) [145, 151, 155, 180]. Once activated, the HKMT PfSET10 maintains the *var* gene in a poised, activated state through the remainder of asexual development and facilitates epigenetic memory during schizogony for reactivation in the next IDC [151]. The incorporation of the variant histone H2A.Z and the double variant H2A.Z/H2Bv at active *var* gene promoters has also been implicated in *var* gene activation [181-183].

Although numerous epigenetic modulators have been implicated in *var* gene regulation in the parasite, the mechanisms of targeted genomic localisation in response to host cues remain unknown. Various reports have shown that lncRNAs are abundant in *P. falciparum* and are proposed to be essential for site-specific targeting of the histone modifying enzymes during *var* gene silencing, amongst other functions [184-194]. Two lncRNAs were identified that are both incorporated into chromatin, and may be involved in H3K36me3 positioning at *var* gene loci and ultimately *var* gene silencing [195, 196]. A recent study functionally characterised a GC-rich ncRNA gene and elucidated the first factor that associates with the active *var* expression site at a perinuclear position that is suggested to be involved in the gene counting process during CVGE [197].

1.5.2.2 Epigenetic regulation of erythrocyte invasion & permeability

Erythrocyte invasion by *P. falciparum* merozoites involves various gene families (*eba, rhoph1/clag, acbp, Pfrh,* etc.) that are also subject to bet-hedging via highly coordinated and epigenetically regulated CVGE [198]. H3K9me3 and PfHP1 have been linked to the selective repression of erythrocyte invasion genes, awaiting activation by the parasite-specific bromodomain protein (PfBDP1) that binds to H3K9ac and H3K14ac during schizogony (Figure 1.11) [161, 199]. PfBDP1 binds to chromatin at the promoter of invasion genes and directly coordinates their expression, essential for normal erythrocyte invasion [161]. Another essential aspect of the parasite's development that requires CVGE is the uptake of nutrients across the infected erythrocyte membrane by the plasmodial surface anion channel, where switching between expression of the cytoadherence-linked asexual gene 3 (*clag3.1* or *clag3.2*) is evidently epigenetically regulated, although the extent of this remains to be clarified [175, 199-202].

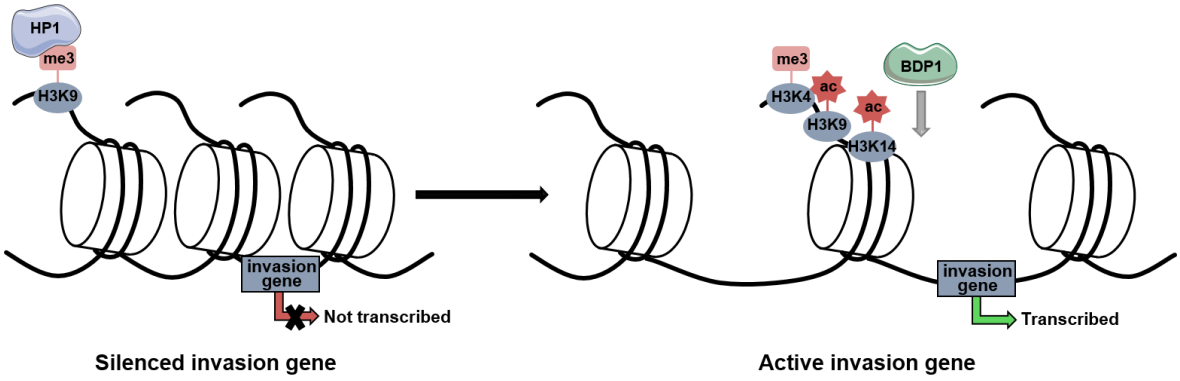

Figure 1.11: Mechanism of epigenetic gene regulation involved in *P. falciparum* erythrocyte invasion. Erythrocyte invasion genes are repressed by H3K9me3 and PfHP1, and activated by the binding of PfBDP1 to H3K9ac and H3K14ac, facilitating euchromatin formation and selective transcription of invasion genes. Figure created based on Batugedara *et al*. [179].

1.5.2.3 Epigenetic regulation of life cycle progression

Due to the “just-in-time” transcriptional nature of *P. falciparum* gene expression, tight epigenetic control of the gene expression cascades come in play during stage-specific developmental transitions and genome demarcation of functional transcriptional elements. This involves global variations in nucleosome occupancy (the density of nucleosomes on chromosomes), incorporation of histone variants and differential occupancy of certain histone PTMs [176, 203-205]. The rapid chromatin conformational changes during *P. falciparum* IDC development are hypothesised to contribute to the dynamic gene activation cascade between cell signalling pathways and the transcriptional machinery [94], rather than to induce these developmental signals [102, 130]. Nucleosome positioning has been shown to provide structure to the transcriptional unit by defining landmark positions at transcription start and end sites [206]. Nucleosome occupancy fluctuates across the 48 h IDC in a sequential manner, similar to what was observed for the transcriptome [207]. Additionally, some of the identified histone PTMs in *P. falciparum* have been mapped to their respective chromosomal occupation [141, 144]. Maximal nucleosome occupancy is obtained in schizonts and depleted in early trophozoites, parallel to the S-phase of the cell cycle, allowing access of transcription factors [204, 205]. These intergenic regions of transcribed genes in *P. falciparum* are euchromatic and typically characterised by H3K4me3 and H3K9ac, in parallel with the histone variant H2A.Z [176, 203]. Eight histone PTMs including H4K8ac, H4K16ac, H4ac4, H3K56ac, H3K9ac, H3K14ac, H3K4me3 and H4K20me1 could be positively correlated with transcription of genes associated with growth, metabolism and host-parasite interactions [141], although no preference for a specific IDC life cycle stage has been indicated.

Heterochromatic regions, enriched in nucleosomes mostly at telomeric and subtelomeric domains, maintain clusters of genes in a silenced state and are marked by increased nucleosome occupancy, histone deacetylation, H3K9me3 and PfHP1 and the histone variant H3Cen [145, 163]. Centromeres in *P. falciparum* are unique as specific sequence signatures can be associated with these regions, along with H3Cen, but pericentric heterochromatin is apparently absent [208, 209]. Dynamic expression was also observed for the *P. falciparum* histones, where all core histones showed peaked expression at the trophozoite-schizont transition [114]. The histone variants are constitutively expressed during the IDC with variance only seen in their reduced levels in trophozoites and increased during schizogony. A global repressive mark, H3K36me2, decrease as

activation marks H3K9ac and H3K4me3 increase and acts in a mutually exclusive manner with H3K9me3 [144]. This study suggested that even though the histone PTMs are present in all stages, the ratio between activating/repressive marks (quantitative levels of the "histone code") contribute to the control of gene expression in *P. falciparum*, particularly during stage-specific development.

Co-existing histone PTMs (as part of the parasite's histone code) include the prerequisite of H3K14ac for PfSET7 to extensively trimethylate H3K4 and H3K9 [150]. This implies that the combination of these three histone PTMs can potentially be important in stage-specific epigenetic gene regulation, linking to H3K9me3-controlled sexual commitment. H3K9ac also co-exists with H3K14ac through PfGCN5 activity [153]. Additionally, the acetylation of H4 at K5, K8, K12 and K16 has been shown to be co-existing and mediated simultaneously by PfMYST [154] to control schizogony. This all points to the potential and importance of co-existing histone PTMs in a coordinated histone code for the parasite. However, the lack of quantitative information on such co-existing histone PTMs throughout the different life cycle stages of *P. falciparum* parasites hampers our in-depth understanding of the impact of this epigenetic mechanism on parasite biology.

1.5.2.4 Epigenetic regulation during sexual differentiation

Recent studies in *P. falciparum* and *P. berghei* (a rodent malaria species) identified the transcription factor PfAP2-G as a master regulator of gametocyte commitment [210, 211]. PfAP2-G is a member of the ApiAP2 family of DNA-binding proteins that control several of the parasite's developmental switches including erythrocyte invasion and cell differentiation [212-216]. Disruption of the *pfap2-g* locus results in parasite strains that lost their ability to produce gametocytes with subsequent downregulation of genes associated with early stage gametocyte development, illustrating that PfAP2-G is involved in commitment and early gametocyte development [210, 211]. The *pfap2-g* locus is mostly heterochromatic and enriched in the silencing mark H3K9me3 [145]. In this state, PfHP1 protects H3K9me3 from demethylase activity and nucleosomal decondensation and silences *pfap2-g* expression (Figure 1.12) [217]. PfHP1 recruits PfHDAC2, which contributes to PfHP1-dependent PfAP2-G silencing in *P. falciparum* gametocyte commitment [160], although the exact mechanism of PfHDAC involvement is unclear. Selective PfHP1 removal, induced by yet unidentified regulatory factors, leads to depletion of H3K9me3 and the subsequent activation of *pfap2-g*, resulting in gametocyte commitment and development via selective activation of early gametocyte-associated

genes [162, 163]. Since gametocyte commitment and *var* gene expression use similar epigenetic regulatory systems, these processes have also been shown to be mutually exclusive [210, 218].

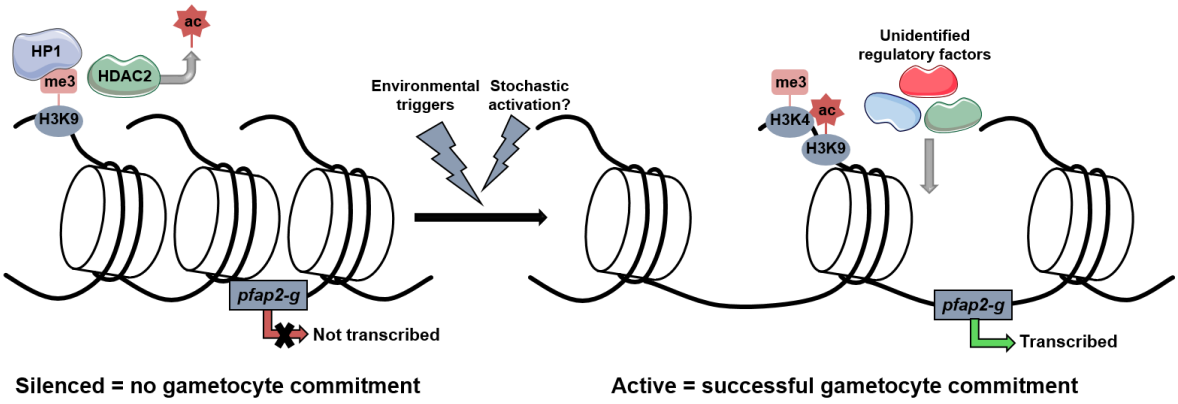

Figure 1.12: Mechanism of *P. falciparum* sexual commitment by PfAP2-G. Epigenetic silencing of *pfap2-g* occurs by H3K9me3, PfHP1 and PfHDAC2, leaving the locus in a heterochromatic state and parasites do not commit to gametocytogenesis. Upon activation by various environmental factors, H3K9me3 is removed (euchromatin formation = H3K9ac) in a subset of committed parasites that will transcribe *pfap2-g* and commence gametocytogenesis. Adapted from [42, 219].

In *P. falciparum,* PfHP1 is associated with ~40% of known gametocyte genes including PfAP2-G [160] and the clonally variant gene families [187, 220]. Similarly, PfHDAC2 removal upregulates early gametocyte genes, including ~70% of PfHP1-associated genes, resulting in increased gametocyte production [160]. It is proposed that PfHDAC2 is required before H3K9me3 and subsequent PfHP1 binding to selectively deacetylate H3K9 in preparation for heterochromatin formation and gametocyte commitment.

As the *P. falciparum* parasites progress into sexual development, information regarding the epigenetic regulation during these stages remains sparse. *P. falciparum* nucleosome assembly proteins (PfNAPS & PfNAPL) are the only other epigenetic factors associated with gametocytes but their function remains unknown [165]. In the asexual stages, these proteins are responsible for extraction and assembly of histones into nucleosomes, thus contributing to chromatin structure organisation [166, 221]. Association between sexual stage genes and CVGE, and the myriad of asexually silenced heterochromatin-associated genes that are transcribed during other developmental stages allows for conjecture that epigenetic mechanisms are at play during gametocyte differentiation [163, 170]. Additionally, gametocytes have been shown to be susceptible to therapeutic intervention using epigenetic inhibitors that target the histone PTM enzymes e.g. HDACs (TSA & SAHA) and HKMTs (BIX01294 & TM2-115) [222, 223]. Upon TSA treatment, hyper-acetylation was observed and gametocyte maturation was compromised,

emphasising the vital role of histone acetylation in gene regulation during gametocyte differentiation [97]. The susceptibility of these quiescent stages to epigenetic perturbations supports the notion that epigenetic gene regulation plays a significant role in gametocyte development [146].

Aside from gametocyte commitment, the differentiation of stage I-V gametocytes and the involvement of epigenetic mechanisms and other key regulatory factors during these stage-specific developmental processes have been poorly elucidated, specifically downstream of transcription. Importantly, the histone PTM landscape throughout gametocyte development remains unknown, and a clearer understanding thereof could contribute to our knowledgebase of the unique developmental processes required for *P. falciparum* sexual differentiation.

1.6 Parasite biology as a catalyst for intervention strategies

The above treatise attempted to outline some essential parasite-specific weaknesses that can be exploited in antimalarial drug discovery. However, certain knowledge gaps persist and is particularly associated with our lack of understanding basic biological processes guiding stage transition during both the asexual and sexual life cycle development phases. An integral component of malaria biology would therefore be to understand the molecular properties distinguishing one form of the parasite from another. This is best addressed on a global level by evaluating the functional consequence of differences in genome expression between parasite stages. Central to this are functional genomics approaches that collate gene expression information to allow comparative analyses and cross-correlation interpretations. Characterisation of the functional genome of the parasite has been limited to a high-content quantitative transcriptome of the complete IDC [66] and, comparatively, rather superficial analyses of gametocytogenesis [78]. Phenotype evaluation on the level of the parasite's proteome [68, 69, 71-73, 75, 76, 224-228] and metabolome [229-231] has also only been performed in depth for asexual development with no information available to provide an understanding of stage transition during gametocytogenesis. Also absent from the above is quantitative evaluation of the epigenome of the parasite in all its life cycle stages. There is, therefore, a need for the comprehensive profiling of stage transition of parasite development spanning both the asexual and sexual phases. A functional, quantitative and comparative description of the parasite's transcriptome, proteome and epigenome will provide a compendium of the parasite's functional genome that should shed light on the unique regulatory mechanisms

that the parasite employs during its atypical, multistage replication and reproduction development processes. This could identify processes for novel antimalarial discovery.

This thesis focused particularly on the contribution of epigenetic regulatory mechanisms to stage transition and life cycle development of the parasite and argues that this results in changes in gene expression (traced through global proteome evaluation), particularly guiding strategy-specific development of either asexual or sexual forms of the parasite. The innovation and significance of the thesis is imbedded in providing the most extensive, quantitative and comparative atlas of the parasite's proteome and histone PTM landscape during its complete life cycle development. This provides insight to the importance of an extensive framework of epigenetic regulatory mechanisms, and how this manifests functionally by influencing changes in protein levels, during both the asexual and sexual development of the parasite. Ultimately, the thesis translates these findings to prove that such unique features are essential to parasite development and survival and can be chemically targeted, providing novel strategies for malaria elimination endeavours.

1.7 Hypothesis and objectives

This study hypothesises that regulation of gene expression via histone PTMs and coordinated protein expression is involved in stage-specific sexual differentiation of *P. falciparum* gametocytes.

The main research aim of this study was to elucidate the regulatory involvement of histone PTMs in stage-specific *P. falciparum* sexual differentiation, to correlate the functional proteome as an end-point of gene expression during gametocytogenesis and to evaluate if the epigenetic regulatory machinery of the parasite can be exploited as a drug target in these stages.

Specific objectives of the study are described as:

Quantitative chromatin proteomics reveals a dynamic histone post-translational modification landscape that defines asexual and sexual *Plasmodium falciparum* parasites (Chapter 2). Here, the quantitative histone PTM landscape was characterised throughout the parasite's IDC and gametocyte differentiation by LC-MS/MS and quantified using EpiProfile. This was extrapolated to map various stage-specific histone PTM profiles and histone PTM combinations were quantified for the first time in *P. falciparum*, with additional histone PTMs validated using Western Blotting.

Stage-specific protein abundance drives gametocytogenesis of *Plasmodium falciparum* parasites (Chapter 3). The quantitative proteome throughout the parasite's IDC and gametocyte differentiation was described through LC-MS/MS and iBAQ quantification. Stage-specific protein abundance profiles were mapped to specific life cycle stages to investigate differential protein abundance throughout gametocytogenesis, and functional annotation of stage-specific protein sets was undertaken. The analysis included previously identified gametocyte sex-specific proteins and putative translationally repressed transcripts.

Multi-stage inhibition of *Plasmodium falciparum* by targeting the parasite's epigenetic gene regulation machinery (Chapter 4). A series of inhibitors were tested for their antiplasmodial activity against asexual parasites, early and late stage *P. falciparum* gametocytes. The inhibitory concentrations of the active compounds were

determined against the various *P. falciparum* life cycle stages *in vitro*, along with cross-resistance against three asexual parasite strains. Multi-stage targeting compounds were identified that show potential as novel chemical scaffolds which can be entered into the antimalarial drug discovery pipeline, specifically HDAC and HKMT inhibitors. These compounds have altered mechanisms of action compared to current antimalarials which is essential to combat drug resistance development.

1.8 Research outputs

Peer reviewed publications:

Coetzee, N., Sidoli, S., van Biljon, R., Painter, H., Llinas, M., Garcia, B. A., and Birkholtz, L. M. (2017) Quantitative chromatin proteomics reveals a dynamic histone post-translational modification landscape that defines asexual and sexual *Plasmodium falciparum* parasites, Sci Rep 7, 607 (impact factor 4.26).

Both Chapters 3 and 4 are being prepared as manuscripts for submission to the Journal of Proteome Research (impact factor 4.26) and the Journal of Antimicrobial Chemotherapy (impact factor 5.31).

Conference proceedings:

Poster presentations

Coetzee N., Ismail N., Verlinden BK., Birkholtz, L. Targeting epigenetic histone post-translational modifications in *Plasmodium falciparum* gametocytes. 6th Annual Multilateral Initiative for Malaria conference. Poster presentation. Durban, South Africa, 2013.

Coetzee N., Sidoli S., Llinas M., Garcia BA., Birkholtz, L. Qualitative delineation of the histone code of *Plasmodium falciparum* across the entire asexual and sexual life cycle reveals conserved and unique post-translational signatures. Gordon Research Conference (GRC): Malaria. Poster presentation. Girona, Spain, 2015.

Coetzee, N., Botha, M., Reader, J., Birkholtz, L. Epi-drugs: Inhibiting malaria parasite proliferation and transmission. 3rd H3D Symposium. Poster presentation. Rawsonville, South Africa, 2016.

Coetzee N., Sidoli S., Van Biljon RA., Painter H., Llinas M., Garcia BA., Birkholtz, L. Exploiting the epigenomic and proteomic complexity of *Plasmodium falciparum* gametocytogenesis. Gordon Research Conference (GRC): Malaria. Poster presentation. Les Diablerets, Switzerland, 2017.

Oral presentations

Coetzee N., Birkholtz, L. First comprehensive description of the complete histone code in *Plasmodium falciparum* asexual and gametocyte stages. SASBMB. Oral presentation. Western Cape, South Africa, 2014.

Coetzee N., Sidoli S., Garcia BA., Birkholtz, L. Qualitative delineation of the histone code of *Plasmodium falciparum* across the entire asexual and sexual life cycle reveals conserved and unique post-translational signatures. MRC Office of Malaria Research Conference. Oral presentation. Durban, South Africa, 2015.

Coetzee N., Sidoli S., Garcia BA., Birkholtz, L. Qualitative delineation of the histone code of *Plasmodium falciparum* across the entire asexual and sexual life cycle reveals conserved and unique post-translational signatures. Gordon Research Seminar (GRS): Malaria. Oral presentation. Girona, Spain, 2015.

Coetzee N., Sidoli S., Llinas M., Garcia BA., Birkholtz, L. Quantitative profiling of the *Plasmodium falciparum* parasite's histone posttranslational modification landscape during sexual differentiation. MRC Office of Malaria Research Conference. Oral presentation. Pretoria, South Africa, 2016.

Coetzee N., Sidoli S., Van Biljon RA., Painter H., Llinas M., Garcia BA., Birkholtz, L. Exploiting the epigenomic and proteomic complexity of *Plasmodium falciparum* gametocytogenesis. Gordon Research Seminar (GRS): Malaria. Oral presentation. Les Diablerets, Switzerland, 2017.

Chapter 2

Quantitative chromatin proteomics reveals a dynamic histone post-translational modification landscape that defines asexual and sexual *Plasmodium falciparum* parasites

The work in this chapter has been published as follows [67]:

Coetzee, N., Sidoli, S., van Biljon, R., Painter, H., Llinas, M., Garcia, B. A., and Birkholtz, L. M. (2017) Quantitative chromatin proteomics reveals a dynamic histone post-translational modification landscape that defines asexual and sexual *Plasmodium falciparum* parasites, Sci Rep 7, 607.

2.1 Introduction

Epigenetic heritage describes the ability of cells to transmit chromatin structural modifications during cell division and thereby maintaining differentiation status in eukaryotes. Histones proteins and their variants mediate this process and are modified through a myriad of PTMs such as acetylation, methylation, phosphorylation, SUMOylation and ubiquitination. Histone modifications impact DNA regulatory processes during normal cell cycle progression including transcriptional activation, DNA replication, DNA damage repair and chromosomal condensation [103]. The levels of histone PTMs are regulated by reader, writer and eraser proteins including families of HMTs, demethylases, HATs and HDACs. Histone acetylation is associated with gene activation in a transcriptionally permissive state, whereas methylation results in repression or activation, in a position-dependent manner [232]. Although histones and their modifying proteins are conserved between different organisms, they contain alternative sites for modification within early-branched Eukarya, mediated by divergence of the modifying proteins [233, 234]. This reveals evolutionary unique functions for these histone PTMs in gene expression regulation and other chromatin-mediated processes involved during development [15, 131, 132, 134, 135].

Within the Apicomplexans, malaria parasites still caused mortality in 438,000 individuals in 2015 [235]. These parasites have an extremely complex life cycle consisting of two distinct developmental phases including asexual proliferation and sexual progression. The characteristic pathogenesis associated with the disease is due to a massive increase in parasite numbers (e.g. *Plasmodium falciparum*) during their asexual amplification in

human erythrocytes. However, a minor portion (<10%) of these parasites are able to undergo sexual differentiation with every asexual cycle [64], forming male and female gametocytes that ensure continued parasite transmission to female Anopheline mosquitoes. Five distinct morphological forms of development are distinguishable during sexual maturation in humans. Gametocytogenesis is a non-replicative cellular differentiation process taking ~10-12 days [236] and resulting in a nearly quiescent phenotype, awaiting activation in the mosquito midgut [44]. Gametocyte maturation is characterised by transcriptional differentiation [78] and changes in energy and lipid metabolism [237]. Commitment to gametocytogenesis has recently been directly linked to epigenetic control, regulated by the PfAP2-G transcription factor [210, 211]. Disruptors of heterochromatin silencing have also been associated with gametocyte overproduction, leading to the identification of molecular players involved in epigenetics, including PfHP1 [162] and PfHDAC2 [160].

Developmental regulation in Plasmodia involves stringent transcriptional control through the expression of the majority of genes only at particular points during development [66, 78]. The parasite, therefore, relies on a complex program of regulation of gene expression [66, 141, 238], integrating post-transcriptional regulation with specific transcription factors, histone positioning, expression of histone variants and histone PTMs [90, 131]. During the asexual IDC, a large proportion of the Plasmodial genome is acetylated and found in a predominantly euchromatic, transcriptionally permissive chromatin state [176, 203, 239, 240]. The meticulous characterisation of the full cascade of histone PTMs (and the associated effector proteins) throughout the parasite's life cycle is a crucial first step towards identifying epigenomic 'check-points' in the cell cycle and sexual development in *P. falciparum* parasites [102]. For instance, HDACs and HMTs as effector proteins play critical roles in the parasite's maturation throughout the IDC [138, 151-154, 158, 164, 241]. Histone PTMs are associated with cell type-specific proteins in other organisms and have a high heritability during cell division [242]. This leads to the establishment of a global chromatin environment that contributes to the regulation of transcriptional expression [84, 103]. The type and position of a specific PTM, as well as the combination of PTMs, play a crucial role in determining its biological relevance in DNA-dependent biological processes [242].

The four core histones H2A, H2B, H3, and H4, as well as four *P. falciparum* variant histones H2A.Z, H2Bv, H3.3 and H3Cen , have previously been identified in *P. falciparum* parasites. Histone PTMs (including acetylation, methylation, etc.) have been qualitatively

identified for asexual stage parasites [93, 100, 103, 114, 115, 130, 136-143], with a single recent quantitative analyses during asexual replication using a mass spectrometry (MS)-based strategy that combines spectral counting and validation by targeted acquisition [77]. Only twelve modifications have been linked with the dynamic transcriptional pattern during asexual development through genome-wide localisation [141, 144]. However, information of the involvement of individual histone PTMs in progression through specific compartments throughout the entire asexual and sexual life cycle is still incomplete. Notably, information on histone PTMs in the sexual gametocyte forms of the parasite is limited to the identification of only two histone PTMs in inhibitor studies [223].

Given the relevance of histone PTMs to malaria parasite development and survival, profiling of the complete histone PTM landscape across the entire *P. falciparum* life cycle is, therefore, essential. Here, we report the first extensive and fully quantitative analysis of the complete histone PTM landscape across eight distinct life cycle stages of *P. falciparum* parasites, spanning the entire asexual and sexual development stages. To do so, we applied quantitative, high-resolution MS combined with nano liquid chromatography (nanoLC) and computational analysis using canonical database searching and our in-house developed software for accurate LC peak area extraction [243]. We demonstrate that histone PTM signatures differentiate the asexual (ring, trophozoite and schizont) from sexual (stage I-V gametocytes) developmental stages. Novel histone PTMs were identified, some of which are enriched in specific life cycle forms of the parasite. A proportion of the histone PTMs (e.g. H3K4ac, H3K9me3, H3K36me2, H3K122ac, H4ac and H4K20me3) show a marked dynamic nature within both asexual and sexual development. This work thus provides an enhanced understanding of the unique developmental cascade present in *P. falciparum* parasites, especially during the IDC, host-adaptation and sexual differentiation of these parasites.

2.2 Materials & Methods

2.2.1 Parasite production and isolation

P. falciparum 3D7 (drug sensitive) and *P. falciparum* NF54-PfS16-GFP-Luc (kindly provided by the Fidock lab, Columbia University, USA) [244] parasite cultures were maintained at 5% haematocrit in O^+ human erythrocytes and RPMI-1640 cell culture medium supplemented with 24 mM sodium bicarbonate, 0.024 mg/ml gentamicin, 25 mM HEPES, 0.2% v/v glucose, 0.2 mM hypoxanthine and 0.5% w/v AlbuMAX II Lipid Rich Bovine Serum Albumin. The parasite cultures were kept at 37ºC with moderate shaking at 60 rpm and gassed with a mixture of 5% O_2, 5% CO_2 and 90% N_2 [245]. Synchronous asexual parasites (>90%, Pf3D7) were obtained using 10% w/v D-sorbitol [246] and isolated as ring, trophozoite and schizont stages at 14, 32 and 42 hours post invasion (hpi), respectively. Gametocytes were induced from a >90% synchronised asexual *P. falciparum* NF54-PfS16-GFP-Luc culture (described previously [247], maintained in culture medium lacking glucose) at 0.5% parasitaemia (6% haematocrit) by enforcing environmental stress to asexual parasites [248]. Gametocyte cultures were maintained for 12 days, treated with 50 mM *N*-acetyl-D-glucosamine and the stage I, II, III, IV and V gametocytes were isolated on day 3, 5, 7, 9 and 12 of gametocytogenesis, respectively. The asexual and sexual parasites were released from the red blood cells (RBCs) using 0.06% w/v saponin in phosphate buffered saline (PBS), followed by several wash steps with PBS to eliminate the presence of any residual erythrocyte material.

2.2.2 Histone isolation and chemical derivatisation

Histones were isolated using a modified protocol from Trelle *et al.* (2009) [100]. Briefly, nuclei was released from the pure and isolated *P. falciparum* parasites using a hypotonic buffer containing 10 mM Tris-HCl, pH 8.0, 3 mM $MgCl_2$, 0.2% v/v Nonidet P40, 0.25 M sucrose in the presence of a protease inhibitor cocktail. The mixture was centrifuged at 500*g* and 4ºC for 10 min and this hypotonic buffer wash step was repeated twice. Subsequently, the chromatin pellet was homogenised in the hypotonic buffer lacking Nonidet P40, to which 10 mM Tris-HCl, pH 8.0, 0.8 M NaCl, 1 mM EDTA (including protease inhibitor cocktail) was added, followed by a 10 min incubation on ice. Histones were acid-extracted from the chromatin with 0.25 M HCl and rotation at 4ºC for 1 h. The histone-containing supernatant was mixed with an equal volume of 20% v/v trichloroacetic acid, incubated on ice for 15 min and pelleted. The histone-enriched pellet

was washed with acetone, air-dried and reconstituted using dddH_2O. All samples were dried using a SpeedVac concentrator (SC100, Savant) and reconstituted with 100 mM ammonium bicarbonate (pH 7-9). Histones were prepared for MS analysis via propionic anhydride chemical derivatisation and in-solution trypsin digestion as previously described [249]. Each of the eight stages was analysed in three independent biological experiments with three technical triplicates each. For the initial semi-quantitative study, the experimental procedures are outlined in Appendix III: Methods.

2.2.3 Quantitative nanoLC-MS/MS-based histone PTM identification

The MS analysis was performed at the Garcia Lab at the University of Pennsylvania (Philadelphia, USA) by Dr. Simone Sidoli. The ***candidate (Ms N. Coetzee)*** *was trained on the Orbitrap MS and* ***was able to do her own sample preparation and could observe the MS operating procedure. All data analysis was independently performed by the candidate.***

Samples were analysed by using a nanoLC-MS/MS setup. NanoLC was configured with a 75 µm ID x 17 cm Reprosil-Pur C18-AQ (3 µm; Dr. Maisch GmbH, Germany) nano-column using an EASY-nLC nanoHPLC (Thermo Scientific, San Jose, CA, USA). The HPLC gradient was 0-35% solvent B (A = 0.1% formic acid; B = 95% acetonitrile, 0.1% formic acid) over 40 min and from 34-100% solvent B in 30 min at a flow-rate of 300 nL/min. The LC was coupled with an LTQ-Orbitrap Velos Pro mass spectrometer (Thermo Scientific, San Jose, CA, USA). Full scan MS spectrum (*m/z* 290−1400) was performed in the Orbitrap with a resolution of 60,000 (at 400 m/z) with an automatic gain control (AGC) target of $1x10^6$. The 10 most intense ions at each cycle were selected for MS/MS performed with collision induced dissociation (CID) with normalised collision energy of 35, an AGC target of 10^4 and a maximum injection time of 100 ms. MS/MS data were collected in centroid mode in the ion trap. Precursor ion charge state screening was enabled and all unassigned charge states, as well as singly charged species, were rejected. The dynamic exclusion list was restricted to a maximum of 500 entries with a maximum retention period of 30 s. In selected time windows we included targeted scan events for isobarically modified peptides, in order to profile their fragment ions and discriminate their abundance, which cannot be performed with just the full MS chromatogram.

2.2.4 Data analysis

Modified histone peptides were identified by processing and searching MS/MS spectra and searching data-dependent acquisition (DDA) runs with Proteome Discoverer (v1.4, Thermo Scientific, Bremen, Germany). Mascot was used as the database searching engine, using PlasmoDB v24 (03/2015). Search parameters were as follows: MS tolerance: 10 ppm; MS/MS tolerance: 0.5 Da; enzyme: trypsin; static modifications: propionyl N-termini; dynamic modifications: methyl (+propionyl), dimethyl, trimethyl, acetyl, and propionyl (K). Peptides were filtered for high confidence (False Discovery Rate; FDR<1%) using Fixed Value validator. Quantification was performed using EpiProfile [243], which performs extracted ion chromatography of selected peptides. Once the peak area was extracted, the relative abundance of a given PTM was calculated by dividing its intensity by the sum of all modified and unmodified peptides sharing the same sequence. For trend analyses data were z-scored. Trend analysis and statistical regulations of PTMs across the developmental stages was assessed using multiple tests: (i) the Mann Kendall test was used to verify which marks have a significant monotonic trend (constantly increasing or decreasing); (ii) k-means clustering was used to group marks that have very similar trends between conditions; (iii) Co-expression correlation was used to compare every single modification with one another and by sorting such data, histone modifications that had the most similar and most different regulation, were verified; (iv) The Kolmogorov Smirnov test was used to verify whether a trend was random or with clear slopes in specific time points. Correlation of the histone yield with histone expression levels in *P. falciparum* were performed using full transcriptome data for asexual parasites (48 h IDC, H. Painter; unpublished data) and gametocytes (R. van Biljon; unpublished data); and proteomics data (N. Coetzee, see Chapter 3).

2.2.5 Western Blot validations

Isolated histones were separated on a 4-20% SDS-PAGE gel and transferred to a PVDF membrane (iBlot® 2 PVDF Mini stacks, Invitrogen) using the iBlot® 2 dry blotting system on program P0 for 7 min. Membranes were blocked in TBS-T (50 mM Tris-HCl, pH 7.5, 150 mM NaCl, 0.1% Tween-20) containing 5% milk powder and probed for H3K9ac (Abcam ab61231; 1:5000) or H4ac (K5+K8+K12+K16 acetyl; Abcam ab10807; 1:5000) primary antibodies diluted in TBS-T. This was followed by anti-rabbit HRP (Abcam ab97095; 1:5000) secondary antibody and visualisation using Pierce SuperSignal® West Pico chemiluminescent substrate.

2.3 Results

2.3.1 Histone abundance profile during development

To identify histone PTMs throughout asexual and sexual development of malaria parasites, we isolated histones from chromatin extracts of the parasites at eight life cycle stages: ring, trophozoite and schizont in asexual development (>90% synchronised) and stage I through V of gametocytogenesis (>60% stage I; >50% stage II; >80% stage III; >90% stage IV; and >85% stage V; see Figure 2.1).

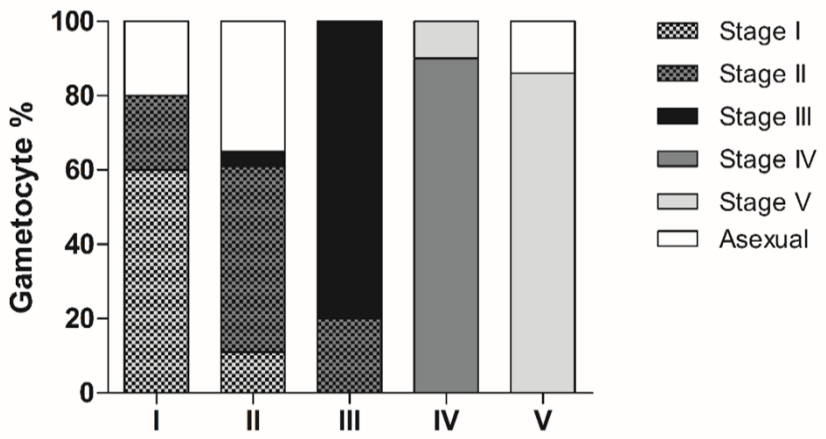

Figure 2.1: Gametocyte-stage composition. From the isolated parasites, the stage I, II, III, IV and V gametocytes were shown to have 60%, 50%, 80%, 90% and 86% synchronicity, respectively. The contaminating asexual stages were seen to be mostly earlier asexual stages, therefore contributing minimal to the histone prevalence. Synchronicity was determined by parasite counting.

This allowed for the identification of all core histones typically present in *P. falciparum* parasites, including their variants (Figure 2.2). The yields of the histone-enriched, acid-soluble nuclear protein fractions differed between the various life cycle stages (Figure 2.2A) with the lowest yield observed during early asexual development (rings at 0.015 ± 0.006 ng total histones/parasite; trophozoites at 0.017 ± 0.011 ng/parasite; $P>0.8$, n=3) and a significant increase observed in schizonts (0.36 ± 0.08 ng/parasite; $P<0.001$, n=3). This showed similar trends compared to histone gene expression, transcriptional activity and DNA synthesis during schizogony [15, 102, 114]. By comparison, the total yields of the histone-enriched fractions for gametocytes were significantly higher ($P<0.001$, n=3) than that of early asexual stage parasites (stage I at 0.208 ± 0.030 ng/parasite, stage II at 0.27 ± 0.05 ng/parasite, stage III at 0.19 ± 0.04 ng/parasite) and the yield of late gametocyte development (stage IV at 0.63 ± 0.09 ng/parasite and stage V at 0.47 ± 0.25 ng/parasite; $P<0.001$, n=3) was also significantly higher than during early gametocyte

development, although the yields for these two stages (IV and V) were not statistically different from each other (*P*>0.05).

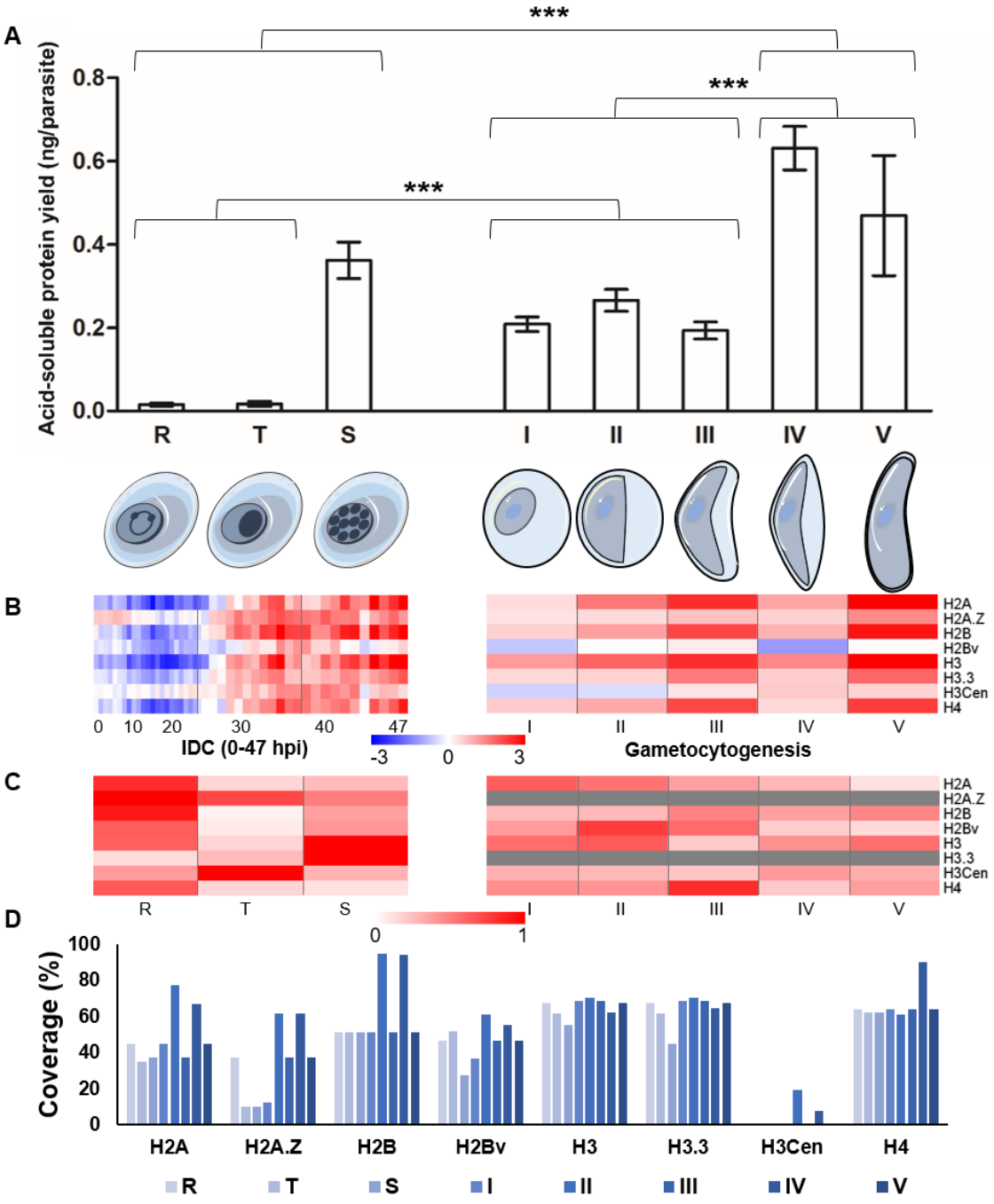

Figure 2.2: *P. falciparum* histone prevalence during development. Eight *P. falciparum* life cycle stages, including rings, trophozoites, schizonts and stage I, II, III, IV and V gametocytes were isolated and the histones were acid-extracted. **(A)** The yield (ng/parasite) of histone-enriched, acid-soluble protein fractions per isolated parasite for each developmental stage was determined (two-tailed equal variance t-test, ***= *P*<0.001, n=3 ±SEM). Histones refer to the isolated acid-soluble protein fraction containing the histone proteins and not to pure isolated histones. **(B)** Expression of the eight *P. falciparum* histones over asexual and sexual life cycle development. The expression values (log_2, Cy5/Cy3) of the core and variant histone transcripts are shown over the 48 h IDC (hpi) and throughout the duration of gametocytogenesis (days). **(C)** Protein abundance of the eight *P. falciparum* histones over asexual and sexual life cycle development. The relative abundance (normalised %) of the core and variant histone proteins are shown over the IDC and gametocytogenesis. The relative abundance data for H2A.Z and H3.3 was not available (indicated by grey bar). **(D)** Histone sequence coverage (%) for the eight *P. falciparum* histones are shown for each life cycle stage. H3Cen was only identified in stage II and IV gametocytes.

The yields of the histone-enriched fraction showed similar trends compared to increased gene expression levels of the histones observed during schizogony and gametocyte development (Figure 2.2B, RA van Biljon data, unpublished), clearly peaking in the mature developmental stages of *P. falciparum* parasites. The variant histones were shown to have an overall lower expression than the core histones, peaking in mature asexual development. Interrogation of the relative abundance levels of the histones showed that these proteins are present throughout asexual and sexual development, with some histones peaking in different developmental stages (Figure 2.2C). These increased expression levels of histones in mature gametocytes occur against a background of general decreased RNA and protein synthesis [78, 187, 220], with no translational repression seen for histones [72].

2.3.2 Complete quantitative histone PTM landscape of asexual and sexual *P. falciparum* parasites

We performed a quantitative assessment of histone samples using high-resolution nanoLC-MS/MS; data processing/peak area extraction was performed by using EpiProfile [243], and spectra identification was performed by using Proteome Discoverer (Thermo). This enabled confident identification and quantification of histone PTMs, as well as horizontal comparison of the histone PTM landscape during *P. falciparum* parasite development. For the quantitative chromatin proteomics study, a complete validated dataset of 125 individual peptides were confidently identified (<20% coefficient of variance between biological replicates), of which 17% constituted the unmodified proportion of the peptides (see Appendix IV: Supplementary File 1). Reproducibly high sequence coverage was obtained in all three biological replicates, particularly for the core histones at 61 ± 15% (Figure 2.2D). In total, the variant histones were associated with lower sequence coverage compared to their core partners (H2A.Z vs. H2A, P=0.84; H2Bv vs. H2B, P=0.69). As expected, due to the centromere-restricted localisation of H3Cen [250], this protein was present in low abundance with significantly lower sequence coverage (P<0.01) than any of the other histones.

The high mass accuracy (0.8 ppm), as well as manual curation, enabled confident discrimination between modifications such as acetylation (42.011 Da) and trimethylation (42.047 Da). Our in-house software EpiProfile also includes features like intelligent retention time evaluation, i.e. uses previous knowledge about the order of elution from LC of differently modified peptides, and uses MS/MS fragment profiles to discriminate the

abundance of isobaric and co-eluting histone peptides (Figure 2.3) [243]. By using this approach, we could evaluate all MS peaks and quantify the presence of specific histone PTMs.

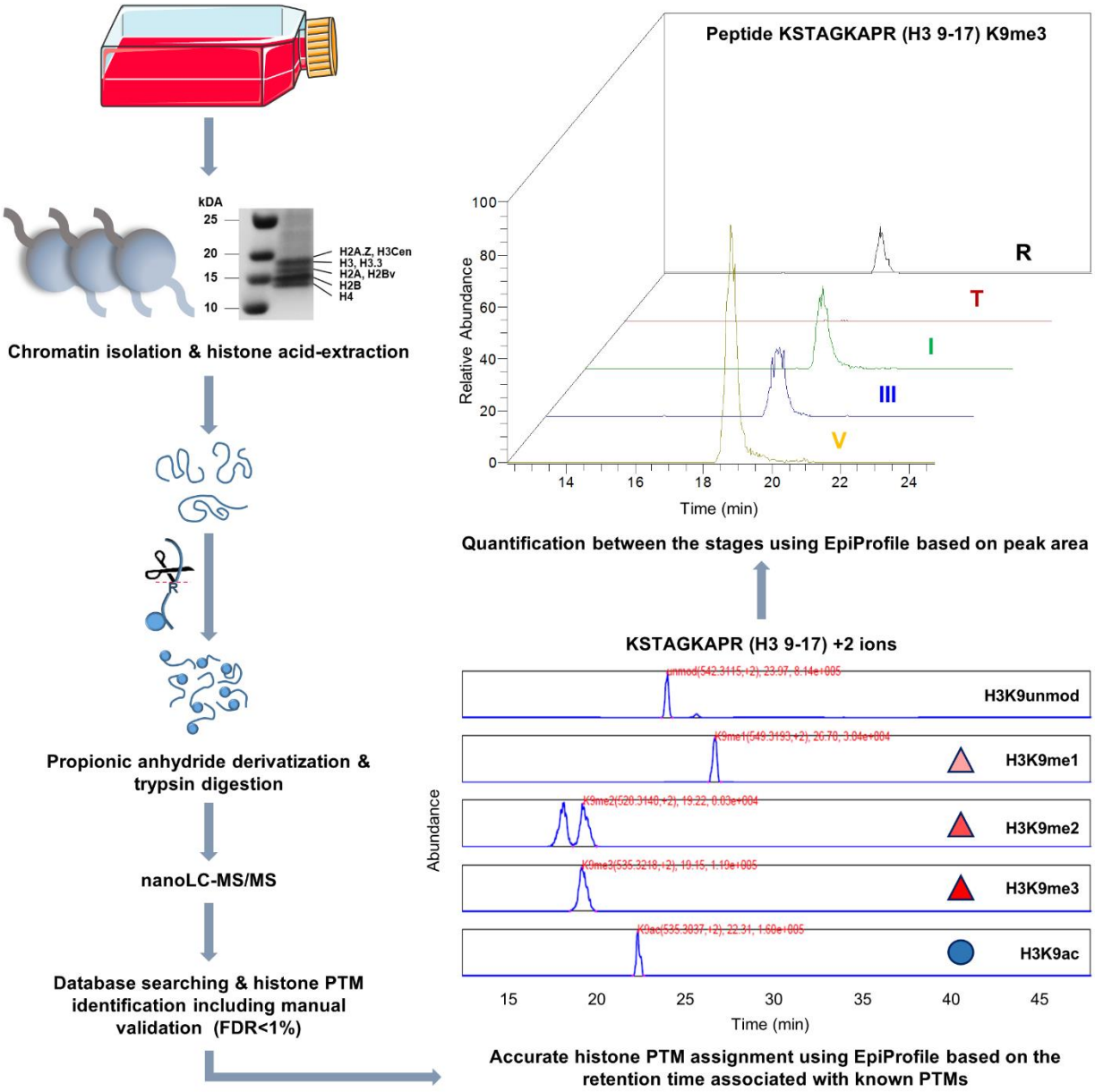

Figure 2.3: Chromatin proteomics approach for histone PTM quantification. The core and variant histones from each of the eight representative life cycle stages were acid-extracted, propionylated and trypsin digested. NanoLC-MS/MS was performed, followed by database searching and histone PTM identification including manual validation (FDR<1%). MS1 spectra of the *P. falciparum* histone H3 peptide KSTAGKAPR (aa 9-17), illustrating the discrimination between varying histone PTMs of H3K9 based on the retention time associated with known PTMs. After accurate PTM assignments, relative quantification using EpiProfile was performed, enabling accurate quantification of histone PTMs based on peak area and determination of co-existing PTMs on longer peptides. The abundance profiles during life cycle development were derived in this manner. The culture flask image was adapted from Servier Medical Art (URL link to the license: https://creativecommons.org/licenses/by/3.0/) and changes were made in terms of colour and size.

Initial analysis revealed a total of 493 histone PTMs over all the life cycle stages (Appendix IV: Supplementary File 2), after which the spectra were manually validated and the resulting semi-quantitative histone PTM landscape of *P. falciparum* parasites contained 106 individual validated histone PTMs (Figure 2.4 & Table 2.1). This included the majority of the histone PTMs that have previously been identified in *P. falciparum* but certain modifications that have been previously reported (H2AK5sumo, H2AK20sumo, H2AK36sumo, H2AS104ph, H2AS120ph, H2AK123sumo, H2AS126ph, H2BK112ub and H3K37ub) were not detected in this study [100, 136, 139]. Moreover, only qualitative identification of 19 individual phosphorylation sites was obtained. Enrichment for SUMOylation and ubiquitination was not performed to maintain the integrity of the isolated histone samples; the dataset therefore does not contain any information on these modifications.

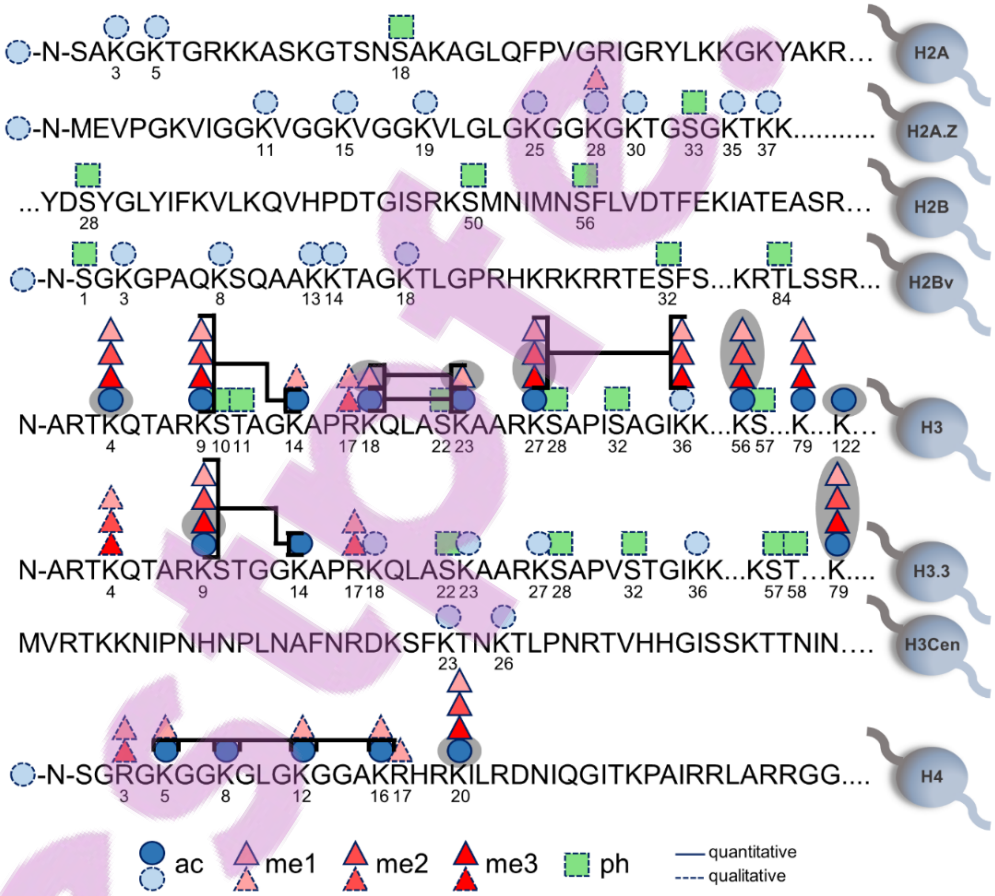

Figure 2.4: *P. falciparum* histone PTM landscape. A wide array of histone PTMs have been identified in *P. falciparum*, including 15 novel PTMs that were identified for the first time in this study (shaded grey). Five principle types of histone PTMs have previously been reported, including acetylation, methylation (mono-, di- and tri-), phosphorylation, ubiquitination and SUMOylation. In this study, 106 PTMs were identified (dashed line), but only 46 of these were quantitative in all stages over life cycle development (solid line). Co-existing histone PTMs on individual peptides were also identified (brackets).

To allow accurate and comparative data across the life cycle stages, stringent quantification and validation was performed on the 106 modifications identified. This

resulted in 55 modifications that could be accurately quantified using EpiProfile (Figure 2.4 & Table 2.1) and from these, 46 histone PTMs were validated and therefore represents the complete and comparative quantitative histone PTM landscape for *P. falciparum* parasites across its entire life cycle in human blood (Appendix IV: Supplementary File 3). These individual modifications occurred mostly on histone H3 and its variant H3.3, followed by H4 with the third most prevalent number of modifications. These histones are known to be highly susceptible to modification. Comparatively, very few modifications were observed on H2A and H2B (and their variants) as well as H3Cen, and none of these modifications could be quantified, due to their low abundance status in the total population.

Table 2.1: Histone PTMs identified in *P. falciparum* parasites.

Histone	Acetylation	Methylation			Phosphorylation
		Mono-	**Di -**	**Tri-**	
H2A	N-term, K3, K5				S18
H2A.Z	N-term, K11, K15, K19, K25, K28, K30, K35, K37	K28			S33
H2B					S28, S50, S56
H2Bv	N-term, K3, K8, K13, K14, K18				S1, S32, T84
H3	**K4**, **K9, K14**, **K18, K23**, **K27,** K36, **K56, K79**, **K122**	**K4, K9,** K14, R17, **K18, K23, K27, K36, K56, K79**	**K4, K9,** R17, **K27, K36, K56, K79**	**K4, K9, K27, K36, K56, K79**	S10, T11, S22, S28, S32, S57
H3.3	**K9**, **K14**, K18,K23, K27, K36, **K79**	K4, **K9,** R17, **K79**	K4, **K9,** R17, **K79**	K4, **K9, K79**	S22, S28, S32, S57, T58
H3Cen	K23, K26				
H4	N-term, **K5**, **K8**, **K12**, **K16**, **K20**	R3, K5, K12, K16, R17, **K20**	R3, **K20**	**K20**	

Regular font indicates qualitative PTMs identified in this study (also previously identified)
Bold indicates quantitative PTMs identified in this study (also previously identified)
Bold & underlined indicates quantitative PTMs identified in this study (novel PTMs)

The histone PTM landscape contained quantitative identification of 26 histone PTMs that have previously been only qualitatively described by MS based approaches (Figure 2.4 & Table 2.1) [100, 114, 136-143]. However, in total, 15 histone PTMs were additionally quantitatively identified for the first time in *P. falciparum* (Figure 2.4 & Table 2.1). These

novel marks included 6 modifications that are known to be involved in transcriptional activation (H3K4ac, H3K122ac) and repression (H3K27me2, H3K27me3, H3K56me3, H3.3K9me3) based on their functions in other model organisms [145, 204, 217, 251-255].

In addition to the set of unique, single histone PTMs, we also identified 39 individual peptides that contained conclusive data for the co-existence of histone PTMs on neighbouring residues (Figure 2.4, indicated by brackets, see Appendix IV: Supplementary File 4). This included 30 validated combinations of all modifications on H3K9 (ac, me1, me2 & me3) with H3K14ac, with the same combinations seen for histone H3.3 (Figure 2.5A&B). Of the co-existing marks, the majority (61%) showed increased abundance in gametocytes compared to the asexual stages (39%), suggesting a particular need for these forms of the parasite for tight regulation of histone modifications (Figure 2.5B). Additional combinations include H3K18ac/me1 & H3K23ac/me1, H3K27me1-3 & H3K36me1-3 and H4ac at K5, K8, K12 and K16.

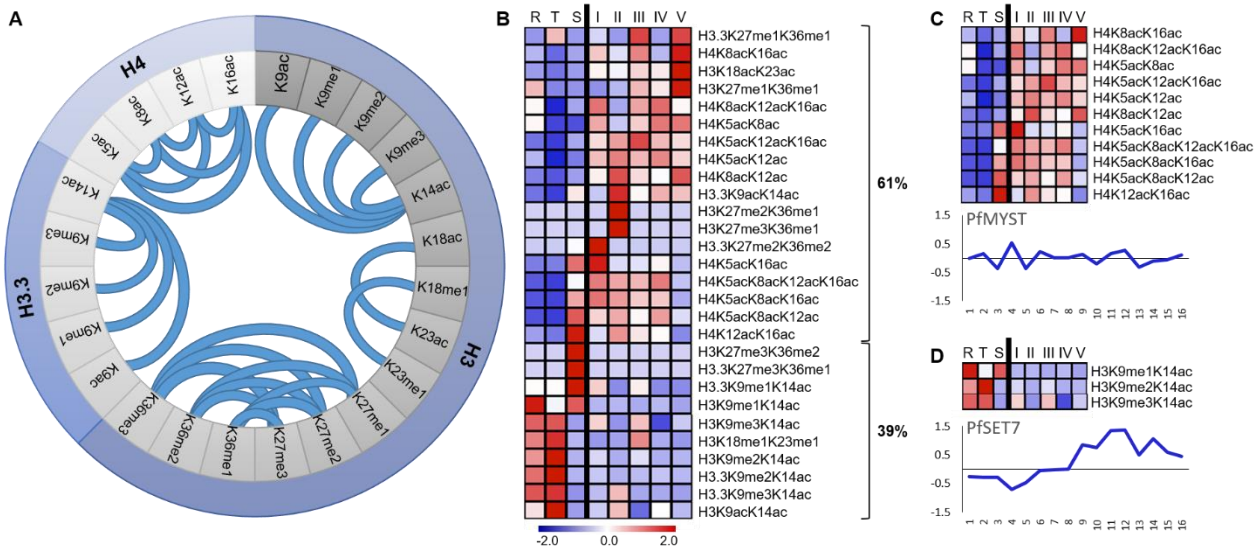

Figure 2.5: Co-existing histone PTMs found in *P. falciparum*. (A) Various co-existing histone PTMs were identified mostly on histone H3, H3.3 and H4. **(B)** The abundance of each combination was mapped across the life cycle (z-scores) and showed 61% enrichment for gametocyte stages, compared to 39% for asexual stages. **(C)** Eleven co-existing acetylation combinations are shown on the four lysines on H4, peaking in gametocytes, and PfMYST is the epigenetic writer associated with these PTMs. The PfMYST expression profile (log_2, Cy5/Cy3) during gametocytogenesis is shown (days; RA van Biljon data, unpublished). **(D)** Three combinations with H3K9me and H3K14ac are shown, peaking in asexuals, and PfSET7 is the epigenetic writer associated with these PTMs. The PfSET7 expression profile (log_2, Cy5/Cy3) during gametocytogenesis is shown (days; RA van Biljon data, unpublished).

Interestingly, we identified all possible combinations of acetylation on H4 at four different positions, showing peaked abundance during gametocytogenesis and schizonts (Figure 2.5C), the regulation of which is controlled by the histone acetyltransferase PfMYST [154]. PfMYST is produced in schizonts and is important for acetylation during cell cycle

development in asexual parasites, but during gametocytogenesis, this protein is produced, at least on a transcriptional level, and may indeed be involved in this distinct acetylation in gametocytes. We also indicate co-regulation of acetylation of H3K9ac and K14ac by the histone acetyltransferase GCN5, but could not detect this co-existence for K4. However, all methylations at H3K9 was quantitatively associated with H3K14ac, with increased abundance in asexual parasites (Figure 2.5D). This confirms the previously identified co-existence of H3K9me3 with pre-existing H3K14ac by the histone methyltransferase PfSET7 [150]. PfSET7 shows increase transcript abundance during gametocytogenesis, but forms part of the previously identified translationally repressed set of proteins that are only translated upon gametogenesis in the mosquito [72]. This correlates to the lowered abundance of these co-existing marks during gametocyte development.

2.3.3 Dynamic histone PTM profiles between asexual and sexual development

The most significant observation in this study is the dynamics and plasticity of histone PTMs as the parasite differentiates during asexual and sexual development. The quantitative dataset allowed head-to-head comparison of the changes in the histone PTMs across all stages (ring, trophozoite and schizont) of the *P. falciparum* parasite's asexual developmental cycle, as well as all five distinct morphological stages (stage I-V) of sexual gametocytogenesis. A close positive correlation (r^2=0.44, Figure 2.6A) was observed between early asexual stages (ring and trophozoites). However, the transcriptionally active and differentiating schizont stage was diverged from early asexual development, as expected. Gametocyte histone PTMs is in totality divergent from that found in asexual parasites, with certain gametocyte stages showing closer total correlation (e.g. stage III & V: r^2=0.43, Figure 2.6A). Within these gametocyte stages, a subset of 13 conserved modifications (H3K4ac, H3K9me1, H3.3K9me2, H3K18me1, H3K23me1, H3K27me2&me3, H3K36me2&me3, H3K56me1&me2, H3K79me3 and H3.3K79me3) was highly correlated between stage I & III (r^2 = 0.78), I & V (r^2 = 0.70) and III & V (r^2 = 0.83) gametocytes (Figure 2.6A). Such a pattern of highly correlated and conserved modifications within the subset of 13 modifications was only observed in certain sexual stages but not in asexual parasites or stage II/IV gametocytes (Figure 2.7).

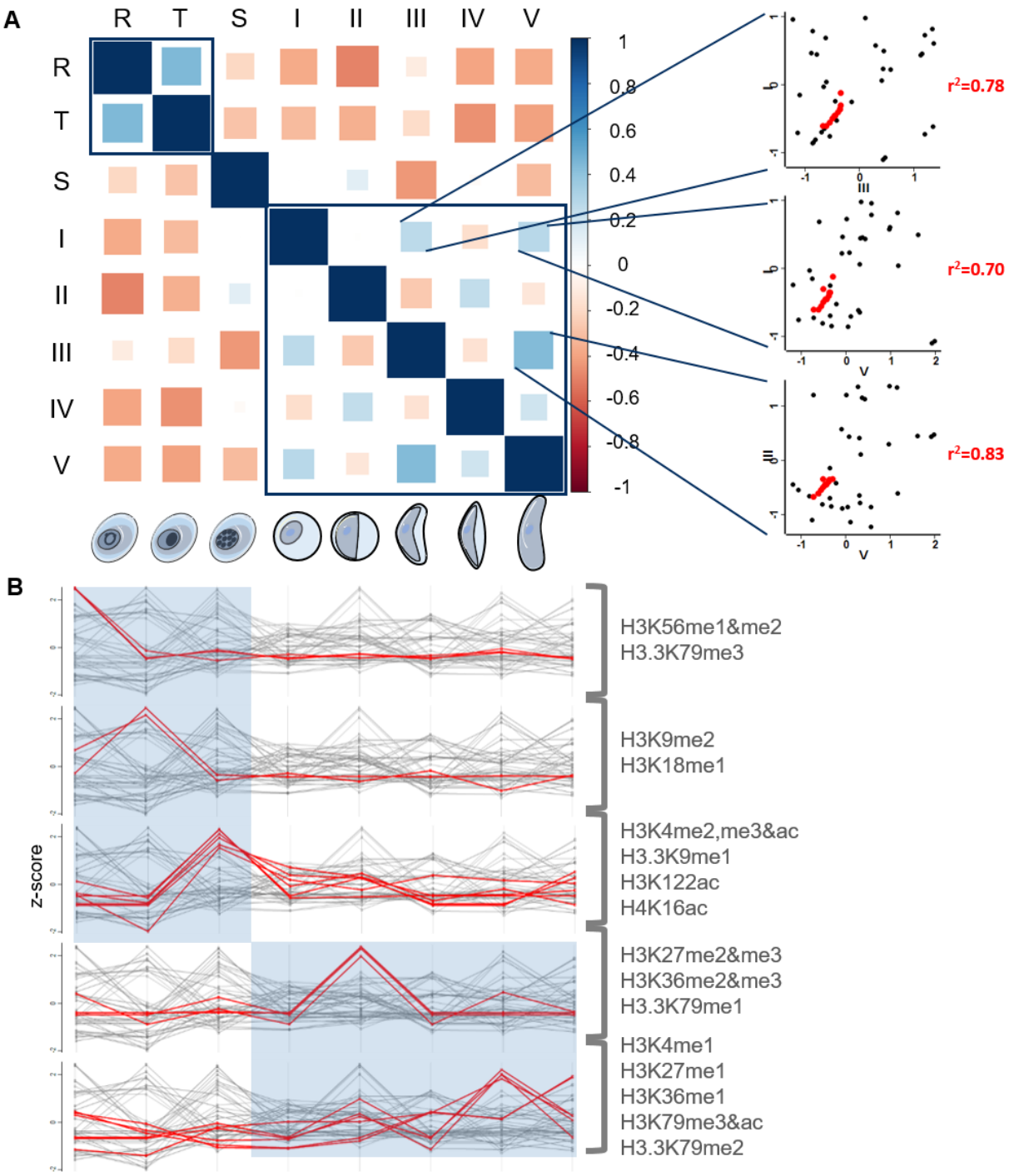

Figure 2.6: Dynamic patterns of histone PTMs between asexual and sexual development. (A) Correlation of the overall histone PTM landscape between the eight *P. falciparum* life cycle stages shows an early asexual cluster and a gametocyte cluster of correlating PTM landscapes (Pearson correlation). Correlation of a subset of 13 conserved residues (H3K4ac, H3K9me1, H3.3K9me2, H3K18me1, H3K23me1, H3K27me2&me3, H3K36me2&me3, H3K56me1&me2, H3K79me3 and H3.3K79me3) between stage I & III (r^2 = 0.78), I & V (r^2 = 0.70) and III & V (r^2 = 0.83) gametocytes are shown in red. **(B)** Stage-specific trends based on z-score distribution are shown for rings (H3K56me1&me2; H3.3K79me3), trophozoites (H3K9me2; H3K18me1), schizonts (H3K4me2, me3 & ac; H3.3K9me1; H3K122ac; H4K16ac) early gametocytes (H3K27me2 & me3; H3K36me2 & me3; H3.3K79me1) and late gametocytes (H3K4me1; H3K27me1; H3K36me1; H3K79ac & me3; H3.3K79me2).

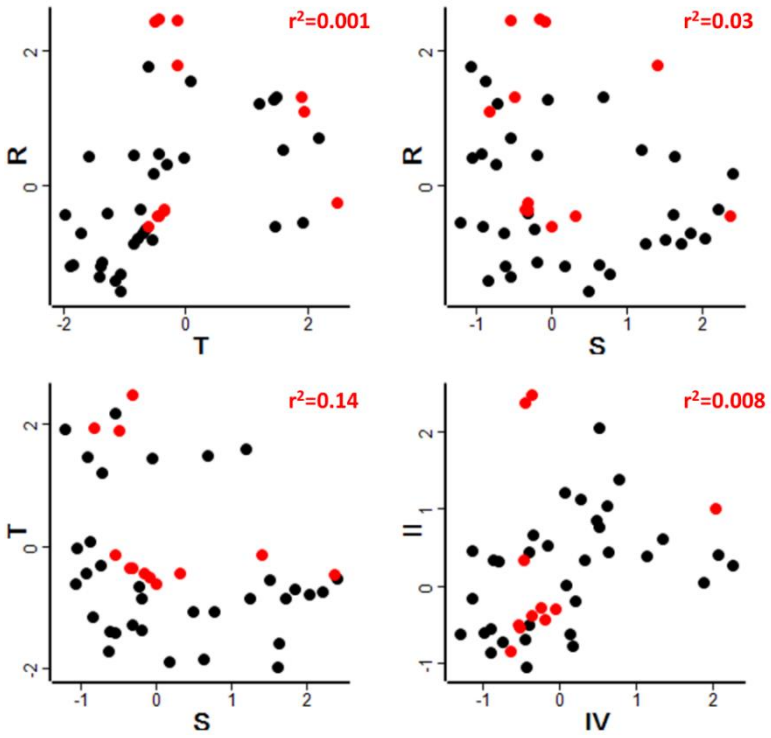

Figure 2.7: Anti-correlation of conserved histone PTMs compared to stage I, III & V gametocytes. Correlation of a set of conserved residues (H3K4ac, H3K9me1, H3.3K9me2, H3K18me1, H3K23me1, H3K27me2 & me3, H3K36me2 & me3, H3K56me1 & me2, H3K79me3 and H3.3K79me3) between rings, trophozoites, schizonts and stage II & IV gametocytes are shown (r^2 values are indicated as 0.001, 0.03, 0.14 and 0.008).

Further delineation of this stage divergence indicated subsets of modifications that have increased abundance in specific life cycle compartments (Figure 2.6B). Of these, H3K56me1&me2 and H3.3K79me3 showed peak abundance in transcriptionally inactive ring stage parasites, while transcriptional activation is associated with the presence of H3K9me2 and H3K18me1 in trophozoites. The number of stage-specific modifications increases 3-fold in schizont development, including H3K4me2, me3&ac, H3.3K9me1, H3K122ac and H4K16ac. By contrast, gametocytes are associated with a set of modifications that are quite distinct from those observed in asexual parasites, indicating diverging functionality. These PTMs include H3K27me2&me3, H3K36me2&me3 and H3.3K79me1 that peak in early stage gametocytes whilst H3K4me1, H3K27me1, H3K36me1, H3K79me3&ac and H3.3K79me2 abundance are exclusively increased in late stage gametocytes.

We subsequently interrogated the stage-specific distribution of the individual histone PTMs to the life cycle compartments. Global analysis of the dynamic nature of the histone PTM landscape indicated a phase-like distribution via hierarchical clustering (Figure 2.8A), reminiscent of differential transcriptional expression during asexual development [66]. Histone PTMs are therefore not equally distributed across the entire asexual and

sexual development, but stage-specific histone PTM abundance profiles were observed. However, the stage-specific distribution of the known histone PTMs for euchromatin (activation modifications H3K4me1/2/3, H3K9ac, H3K14ac, H3K27ac & H4ac) and heterochromatin (repressive modifications H3K9me3, H3K79me3, H4K20me3, H3K27me3) [114, 140, 143, 145, 151-154, 217, 241, 250, 252-255], showed that, even though the relative abundance of these marks may vary, all of these modifications are present in all the life cycle stages, confirming their importance and involvement in chromatin conformation during development of both asexual and sexual forms of the parasite (Figure 2.8A).

Notably, modifications associated with gene activation cluster together and correlate clearly with the transcriptionally active schizonts during asexual development, including the novel modifications H3K4ac and H3K122ac. However, once the parasite is committed to gametocytogenesis, early stage I-III gametocytes are characterised by abundant repressive modifications including H4K20me3 and H3K36me2. For the first time, we also observe the repressive modification H3K27me3 in Plasmodia, particularly abundant in stage II gametocytes [251]. This modification has previously been thought to be absent in Plasmodia, but in those studies only asexual forms of the parasite were investigated [100, 144]. Additionally, the repressive modification H3K9me3, show a marked increase in abundance throughout gametocytogenesis, but particularly so in early gametocytes. When the parasites then enter the mature stages of gametocytogenesis, abundant activation marks such as H3K4me1 (regulatory element modification), H3K18ac, H3K27me1 and H3K36me1 arise, and limited repression modifications such as H3K79me3 (elongation modification) and H3K79me1 are present. These stage-specific trends were statistically confirmed, with H3K4me1 modifications significantly (P<0.001, n=3) abundant in schizonts and gametocytes compared to other life cycle stages; H3K9me1 (P<0.01, n=3) and me2 (P<0.001, n=3) were present at significantly increased abundance in asexual stages compared to gametocytes (Figure 2.8B). Histone PTM-specific Western blotting was performed over the eight harvested life cycle stages for histone H3K9ac and H4ac (K5+K8+K12+K16) to determine the distribution during life cycle development. H4 acetylation is significantly (P<0.001, n=3) more abundant in gametocyte stages than asexual stages, with the exception of H4K16ac, which is highly abundant in all stages, but peaking in transcriptionally active schizonts. This data correlates with the Western blot results, validating this peaking trend in schizonts and gametocytogenesis.

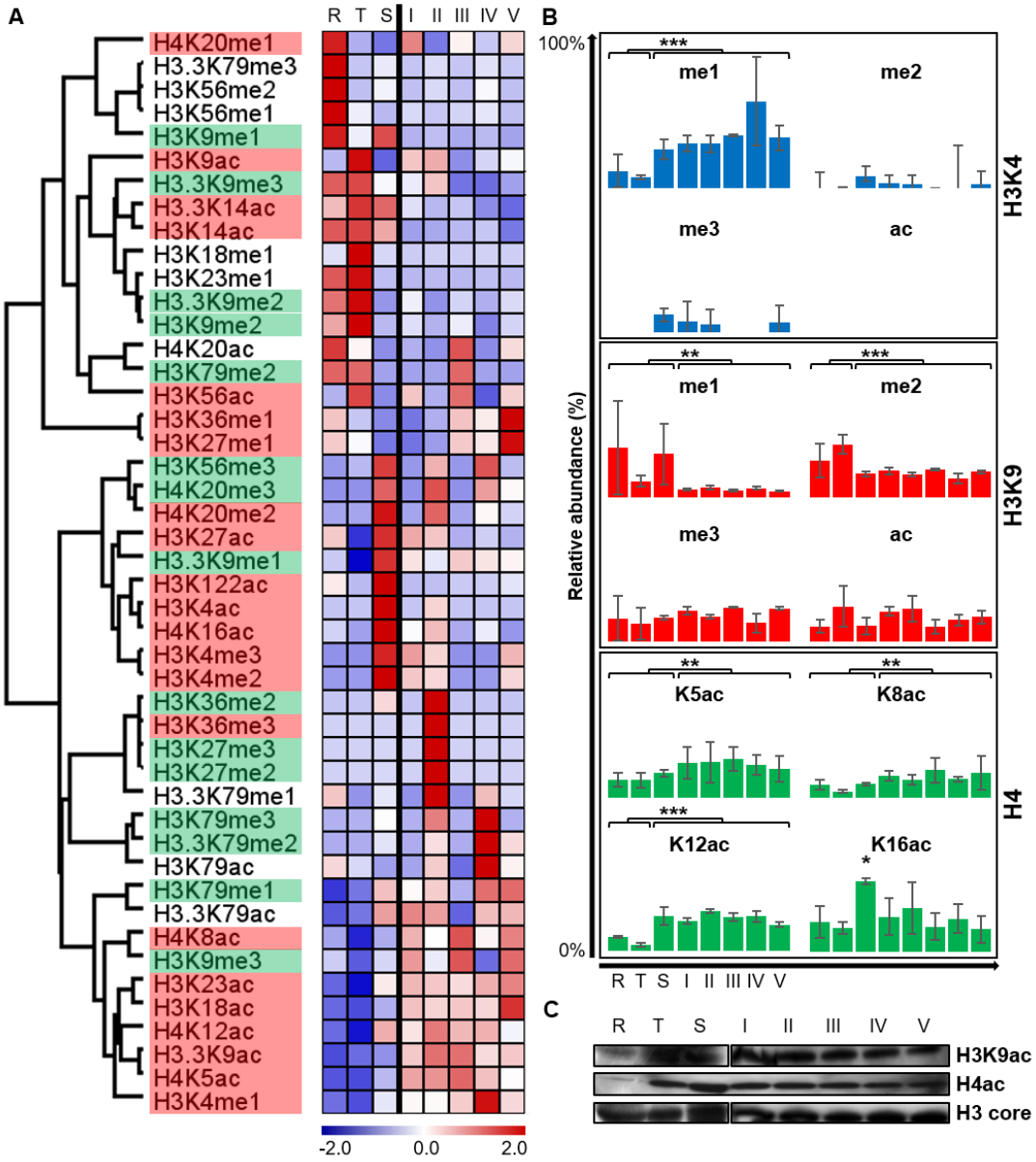

Figure 2.8: Patterns of gene activation and silencing during life cycle development. (A) The histone PTM relative abundance (z-score) over the life cycle is shown (ranging from R, T, S, I, II, III, IV and V from left to right). Z-scores were clustered hierarchically, uncentered (similar results obtained with K-means) with Pearson Correlation on average linkages, and subsequently phase ordered. Euchromatin (red) or heterochromatin (green) status for certain histone PTMs are shown where the information has previously been confirmed in *P. falciparum* or based on involvement in other model organisms [251, 256-262]. (**B)** The me1, me2, me3 and ac relative abundance levels (%) over life cycle development is shown for histone H3K4, H3K9 and H4 (***= *P*<0.001; **= *P*<0.01; *= *P*<0.05; n=3±SEM). **(C)** Histone H3K9ac, H4ac (K5+K8+K12+K16) and histone H3 (core) levels were independently investigated using immunoblotting over the eight harvested life cycle stages, validating overall lowered levels during rings (except for H3 core) and higher levels from trophozoites and schizonts through gametocytogenesis. Blots were cropped for this image (full-length blots are presented in Appendix I: Figure A1). All samples were derived from the same experiments and gels/blots were processed in parallel.

Taken together, we show confirmation of the presence and abundance of stage-specific histone PTMs across both asexual and sexual *P. falciparum* life cycle development by confident spectral histone PTM assignments. This study confirms that the histone PTM landscape in *P. falciparum* is highly dynamic with clear stage-specific developmental trends associated with either asexual or sexual development.

2.4 Discussion

With this large-scale chromatin proteomics study, we quantitatively identified a set of PTMs on histones in all life cycle forms of *P. falciparum* parasites, during both asexual proliferation and sexual differentiation. We confirmed the presence of several previously described modifications but also identified a set of completely new modifications. Moreover, we showed that histone PTMs have dynamic profiles associated with life cycle progression in malaria parasites and that there is a clear distinction between modifications employed during asexual proliferation and sexual differentiation.

Our strategy was based on stringent quantification of histone PTMs, to enable the horizontal comparison between datasets and allow extensive high-resolution dynamic analyses of the histone PTM landscape. Using three independent biological replicates, quantitative MS profiling and strict evaluation of individual PTMs, inaccurate assignments were avoided and assisted in the quantification of isobaric histone peptides [243]. Through this sensitive and stringent profiling, we were able to prove that only a proportion (20%) of 232 recently identified histone PTMs in *Plasmodium* [77] was biologically associated with life cycle progression. However, we cannot exclude the possibility that other types and positions of histone PTMs may still exist in *Plasmodium* in addition to those described in this study.

The global histone PTM landscape was shown to be highly dynamic and adaptable across the entire life cycle of the parasite, for all 46 marks quantified. Such a dynamic nature was previously eluded, but limited to only eight histone PTMs described in the parasite during asexual proliferation (H3K4me3, H3K9ac, H3K14ac, H3K56ac, H4K8ac, H4K16ac, H4ac4 and H4K20me1) [141]. These modifications were shown to be involved in euchromatin formation and are directly linked to transcriptional regulation during the IDC [141] in support of our study showing distinct stage-specific dynamics. However, the dynamics in the histone PTMs are not limited to these eight modifications but are a more global phenomenon. An additional 18 modifications were shown to increase during asexual development. Association of these marks with genome occupancy [141] and transcript expression would reveal their involvement and importance to global transcriptional regulation in the parasite.

The dynamic distribution of histone PTMs over the parasite's life cycle therefore suggests a distinct mode of transcriptional regulation in the parasite and reveals an interesting association with transcriptional activation/silencing during life cycle progression. A high

level of acetylation and mono-methylation is observed in our dataset (61% of all quantified, validated modifications), particularly associated with the asexual stages. These marks correlate to the transcriptionally permissive, euchromatic state of chromatin in the parasite's asexual IDC [77, 100, 204] and confirms that *P. falciparum* histones contain more euchromatic than heterochromatic modifications [114, 140, 143, 145, 151-154, 217, 241, 250, 252-255], a phenomenon observed in most eukaryotes. Known activation marks (H3K4me2, H3K4me3, H3K9ac, H3K14ac and H4ac) increase in abundance as the parasite progresses from trophozoites to schizonts. This can be associated with increased transcriptional activity of the parasite of a previously suggested 76% of the *P. falciparum* genome during the IDC [141]. Previous reports showed peak occupancy of H3K4me3 during trophozoite development that strongly correlates with transcriptional expression evenly distributed along the IDC [141]. Here we show increased abundance for H3K4me3 in schizont stages, previously associated with promoters of active metabolism and invasion related genes [176, 203].

In contrast to the transcriptionally permissive state associated with high levels of histone acetylation and mono-methylation marks of asexual stages, an increased abundance of di- and tri-methylation marks is observed during gametocytogenesis. These methylations are typically associated with the core histones, particularly H3 and are generally indicative of heterochromatic nuclei in a transcriptionally repressive state [140, 143, 145, 241, 250]. Their presence in gametocytes (particularly early gametocyte development) could indicate an associated heterochromatic status in these parasites, which we are currently investigating. Histone PTMs that have previously been shown to be associated with transcriptional silencing were confirmed in our study to be more abundant in earlier asexual stages. H3K9me3, the well-known PTM marking heterochromatic islands in clonally variant gene families involved in immune evasion [141, 145, 176, 217], had an increased abundance during gametocytogenesis, particularly during early gametocyte development. Likewise, the recently identified global repressive mark H3K36me2 [144] was also shown here to have a higher abundance in early stage gametocytes. Another repressive mark, H3K27me3, was abundantly present in early stage II gametocytes but was not previously detected in studies using only asexual forms of the parasite [77, 144]. In model eukaryotes, H3K27me3 is catalysed by the polycomb group proteins [263], a family of proteins responsible for cellular differentiation during development via facultative heterochromatin formation [264]. These polycomb group proteins form a polycomb-repressive complex and co-localise with H3K27me3 at specific repressed genes that are

involved in cellular fate decisions [263]. The polycomb-repressive complex and the associated polycomb group protein homologues have not been identified to date in *P. falciparum*, although a large subset of *P. falciparum* proteins have not been annotated (~60%). This implies that H3K27me3 is either not functional in *P. falciparum* or its functionality is regulated by another protein family that takes over this classical regulatory aspect. This opens up avenues toward the implication of these polycomb group proteins and H3K27me3 in the establishment of pre-programmed epigenetic memory marking specific genes as repressive during cellular differentiation.

Stage II gametocytes also showed peak abundance of H3K36me3, a known *var* gene silencing mark in *P. falciparum* parasites [138]. An active *var* gene is characterised by, amongst other PTMs, H3K4me2 that is shown here to be highly abundant in schizonts [151]. This might suggest an inactive *var* gene expression state in the early stages of gametocyte development, strongly correlating to recent work showing downregulated *var* genes found in stage II gametocytes [265]. Various known euchromatin-associated modifications (e.g. H3K9ac, H3K14ac and H4ac) that are involved in parasite growth, metabolism and host-parasite interactions [84, 90, 93, 100], were shown here to be present in the sexual developmental stages as well. A number of modifications (H4K20me3, H3K27ac and H3K4me1) with increased abundance during early gametocyte development were also associated with genes in a prepared state for transcription, but not yet fully transcribed [144]. Taken together, early gametocyte development show histone PTMs indicative of a G_0 cellular stage [15], similar to ring stage asexual parasites. This early gametocyte-specific histone PTM profile allows us to distinguish these stages from their asexual counterparts and is likely to be involved in a subset of essential gametocyte genes, which can further be clarified by chromatin immunoprecipitation sequencing strategies.

Another interesting stage-specific observation was the abundance of euchromatic histone PTMs in the mature stages (stage IV/V) of gametocytogenesis. Schizogony is known to involve high levels of transcription, however, a decreasing transcriptional activity was previously indicated as gametocytes progress to maturity [54]. Additionally, translational repression has been linked to the regulation of gene expression in gametocytogenesis, where the ‘quiescent’ mature gametocytes are said to store translationally repressed mRNAs to be used for subsequent developmental changes upon activation i.e. the onset of gametogenesis [224, 266]. The presence of activation modifications like H3K27me1 and H4K36me1 might be associated with a poised instead of a repressed transcriptional

state, where stage IV/V gametocytes contain activation PTMs but show a lack of transcription, awaiting activation in the mosquito midgut. This would correlate to the activity of these marks found in other model organisms [256, 262]. H4ac (K5, K8, K12 & K16), a set of activation marks that has also been linked to the poised state of *var* genes in combination with H3K9me3 [144], was found to be more abundant during gametocytogenesis compared to asexual proliferation, further inferring toward a poised transcriptional state.

In totality, the comprehensive PTM landscape included 15 novel histone PTMs in Plasmodia. The schizont-associated novel PTMs, H3K4ac and H3K122ac, have been described in mammalian cells and *Saccharomyces* to define genetic elements involved in active transcription [258, 260], suggesting this association can be extrapolated to this transcriptionally active stage of Plasmodia. Transcriptional poised states of stage V gametocytes are again linked to H3K27me1 & H3K36me1 [256, 262]. Novel repressive marks have a wide distribution over the life cycle, including H3K27me2&3 (stage II gametocytes), H3K56me3 (schizonts, stage II & IV gametocytes) and H3.3K9me3 (rings & trophozoites) [251, 256, 257, 259, 261].

Although this data links the presence of individual histone PTMs to specific life cycle compartments, the occurrence of co-existing PTMs is of particular interest. In eukarya, histone PTMs have been hypothesised to form a 'histone code', implying that dynamic patterns of combinations of histone PTMs correlate with specific chromosomal states and binding of regulatory proteins [116, 267], thereby coordinating epigenetic gene regulation and development [125]. We accurately quantified 30 co-existing histone PTMs over the parasite's life cycle, including acetylation of histone H4 at four different lysine residues (K5, K8, K12 and K16) on a single peptide, resultant of simultaneous acetylation by the HAT PfMYST [154]. This co-occurrence of H4ac is particularly evident in gametocyte stages, and corresponds to the increased expression of PfMYST during gametocytogenesis (results not shown). The co-occurrence of H3K9me3 and H3K14ac also confirms previous findings that the newly characterised HKMT (PfSET7) methylates H3K9 with pre-existing H3K14ac [150]. The co-occupancy of genomic loci for H3K4me3 and H3K9ac [144] is also justified by the presence of both PTMs during life cycle development. Various other combinations were also identified, including combinations of novel *P. falciparum* histone PTMs e.g. H3K18me1 & H3K23me1, H3K27me1-3 & known H3K36me1-3 and H3.3K9me1-3 & H3.3K14ac. Of the co-existing marks, the majority could be assigned with increased abundance in gametocytes, suggesting a particular

need for these forms of the parasite for tight regulation of histone modifications. The functional significance of these co-occurrences is currently under investigation.

Our study reveals unique plasticity and dynamics in the histone PTM landscape of *P. falciparum* parasites, which is associated with life cycle progression and differentiation. This first description of the extensive, quantitative histone PTM landscape of *P. falciparum* parasites and the wide array of histone PTMs found in the various life cycle stages supports the notion that the epigenome of the *P. falciparum* parasite is complex and adaptive during development, and might be the parasite's Achilles heel [93, 102, 103, 115, 130]. Epigenetic regulatory machinery is deemed an essential target for chemotherapy, as cancer development has been widely linked to epigenetic regulation by histone PTMs, their regulating enzymes and histone-binding proteins [268, 269]. For *Plasmodium*, we need to reach a similar level of understanding concerning the epigenetic regulatory processes of parasite development on a molecular level, in order to enhance diagnosis and treatment strategies.

Chapter 3

Stage-specific protein abundance drives gametocytogenesis of *Plasmodium falciparum* parasites

3.1 Introduction

The life cycle of *P. falciparum* involves stage-specific development, invasion of various cell types and host immune evasion, which all requires tight gene regulation and specialised protein expression at specific time points [68]. The activation or silencing of certain genes and their related products are tightly regulated at multiple levels (transcriptional, post-transcriptional, translational and post-translational) [79-83], ultimately depicting the distinct morphology and physiology of each developmental stage [29, 270]. Adaptive transcriptional responses in the parasite follows the binary switch between continued asexual proliferation and terminal sexual differentiation. Divergence is observed between asexual blood stage parasites and gametocytes on the transcriptional level ([66, 78]; RA van Biljon, unpublished) and this is mediated by a few transcription factors [86], epigenetic regulatory mechanisms [67] and mRNA stabilisation [271]. Throughout the IDC and gametocytogenesis, post-transcriptional control has been implicated in fine-tuning protein levels and regulating mRNA dynamics in response to environmental and developmental transitions, supported by the extensive repertoire of RNA-binding proteins compared to specific transcription factors [70, 85, 87, 88]. This accentuates the value of proteomic evaluation of the fundamental biology of organisms as it allows an unbiased study of the cellular composition and protein interactions under changing conditions and reflects the ultimate product of gene regulatory events.

Currently, the *P. falciparum* proteome of ~3000 proteins is unique for every stage investigated thus far (sporozoites, merozoites, rings, trophozoites, schizonts, stage I/II gametocytes, stage IV/V gametocytes, male and female stage V gametocytes, gametes, oocysts, ookinetes and hepatic schizonts), although ~50% conserved proteins are shared during development [68, 69, 71-73, 75, 76, 224-228]. This supports the model of “just-in-time” translation that was proposed for the IDC, suggesting that a specific proteomic signature can be associated with any given stage during parasite development to respond to a variety of environmental signals [73]. Protein expression during the IDC is mostly periodic and closely correlated to transcription [69, 75], with an 11-18 h delay in peak mRNA and protein levels observed for ~30% of the IDC genes that is suggestive of post-

transcriptional control mechanisms in this subset [73]. The timing of mRNA translation during the IDC has been linked to ribosomal association [272, 273], with specific decay rates associated with mRNAs of proteins that belong to the same biological pathways [274]. Recent evidence supports the involvement of post-transcriptional and translational regulatory processes in sexual reproduction of *P. falciparum* parasites. A subset of female-specific gametocyte transcripts are translationally repressed; these transcripts are therefore not needed for gametocytogenesis but are stored and rapidly translated into proteins in gametes in the mosquito midgut in preparation for fertilisation. In the rodent malaria species *P. berghei*, this involves regulation via the RNA helicase DOZI and CITH protein [225, 266, 275, 276]. In *P. falciparum* the Puf-family of RNA-binding proteins are involved [91, 92], with a subset of ~500 putative translationally repressed transcripts identified to date [72].

Collectively, this data associates importance to post-transcriptional level regulation of gene expression in gametocytes. However, the importance of gene regulation leading to dynamics in the proteome and contributing to stage-specific transitions during gametocytogenesis (stage I-V) of *P. falciparum* parasites has not been described. Therefore, we need clear quantitative evidence for stage-specific protein sets involved in key cellular processes to understand the unique regulation of *P. falciparum* gametocyte differentiation.

In this study, we quantitatively characterised the complete proteome across stage I-V of *P. falciparum* gametocyte development, compared to the asexual IDC with comprehensive, high-resolution nanoLC-MS/MS. Functional stage-specific gametocyte protein differences were revealed, identifying key biological processes involved in gametocyte differentiation. Furthermore, a cluster of previously identified translationally repressed proteins were quantified in this study throughout gametocytogenesis, implying that these proteins are not repressed. A set of gametocyte sex-specific proteins were also found to be present very early during gametocyte differentiation, suggesting that molecular players involved in sex differentiation might play essential roles as early as stage I. Finally, epigenome, transcriptome and proteome contributions to gametocyte development were mapped, and the interplay between these were identified as possible regulatory mechanisms involved in gametocytogenesis.

3.2 Materials & Methods

3.2.1 Parasite production and isolation

Parasite cultures and samples were identical to those in Section 2.2.1, Chapter 2. The same experimental procedure was followed for parasite production and isolation.

3.2.2 Cell lysis & total proteome isolation

Total protein content was isolated as described previously by Nirmalan *et al*. (2004) [75]. Briefly, isolated parasites were lysed (8 M urea, 2 M thiourea, 2% w/v CHAPS, 0.5% w/v DTT) and pulse sonicated (Sonifier® Cell Disruptor B-30, Branson Sonic Power Co.) for 20 s (alternating pulsing of 1 s; 3 W output; 1 min cooling in-between; repeated x6). This was followed by separation using ultracentrifugation for 1 h at 16000*g* at 4ºC (Optima™ L-80 XP Ultracentrifuge, Beckman Coulter). The protein-containing supernatant was used for all downstream analysis (soluble protein fraction). Protein concentration was determined using the 2-D Quant kit (GE Healthcare, Sigma-Aldrich), reading absorbance at 492 nm.

3.2.3 Protein sample preparation for mass spectrometry analysis

The MS analysis was performed at the Garcia Lab at the University of Pennsylvania (Philadelphia, USA) by Dr. Katarzyna Kulej and Dr. Simone Sidoli. The ***candidate (Ms N. Coetzee)*** *was trained on the Q-Exactive mass spectrometer and* ***was able to do her own sample preparation and could observe the MS operating procedure. All data analysis was independently performed by the candidate.***

All samples were thawed at room temperature and kept on ice for the duration of the sample preparation. The protein samples were prepared by using the Wessel/Flügge method of chloroform/methanol precipitation and extraction (adapted for larger sample volumes) [277]. This method was optimised to concentrate protein samples of larger volumes and to remove unwanted contaminants such as salts, detergents, lipids and nucleic acids. Briefly, protein samples were mixed with an equal volume of methanol:chloroform (3:1 ratio), followed by a brief vortex step and centrifugation at 9,000*g* for 5 min (Eppendorf centrifuge 5415C) at 4°C. Each sample separated into an upper methanol layer containing unwanted salts and contaminants; an interphase aqueous precipitated protein layer and a bottom chloroform layer containing lipids. The top layer was removed and discarded without disturbing the interphase protein layer, and

the samples were washed twice with methanol followed by centrifugation at 17,000*g* for 3 min (AccuSpin Micro17, Fischer Scientific) and complete removal of methanol:chloroform. The resulting precipitated proteins were dried at room temperature to allow for evaporation of the resultant methanol:chloroform. All samples were dissolved in a solution containing 6 M urea, 2 M thiourea and 50 mM ammonium bicarbonate, pH 7-8.

Samples were subjected to reduction, alkylation and digestion in preparation for MS as follows. Samples were incubated at room temperature for 1 h in 100 mM DTT to reduce disulphide bonds, subjected to Lys-C (1-1.5 µg) and trypsin (10 µg) digestion at room temperature for 3 h. Lys-C digestion was used in tandem with trypsin digestion to decrease the amount of tryptic missed cleavages, as the endoproteinase Lys-C can cleave lysine residues followed by proline residues, unlike trypsin. Samples were then diluted with 50 mM ammonium bicarbonate to lower the urea and DTT concentrations in solution to prevent trypsin inactivation. The samples were sonicated (Sonic Dismembrator Model 100, Fischer Scientific) for 3 cycles of 10 s continuous sonication (output 2) followed by 10 s resting on ice to dissolve the pellets completely. Cysteine residues were alkylated by incubation with 40 mM iodoacetamide (Bio-Rad, USA) at room temperature in the dark for 1 h to prevent reformation of disulfide bonds. This was followed by overnight digestion with 10 µg trypsin at room temperature.

The pH of the trypsin digested samples were adjusted with ammonium hydroxide to ~pH 8-8.3 followed by centrifugation at 17,000*g* for 1 min. StageTip (STop And Go Extraction Tip) clean-up in combination with protein fractionation was performed for all the samples using a dual resin approach, where both Empore^{TM} C_{18} disks (3M, USA) and Oligo^{TM} R3 reversed-phase resins (Thermo Scientific, USA) were used in combination [278, 279]. This was done to remove unwanted contaminants before MS and to fractionate the samples to ensure optimal protein detection. The column was equilibrated with 1 mM ammonium bicarbonate (pH 8.0), after which the supernatant of each sample was added to the dual resin StageTip and pushed through the column using a syringe (dropwise). Nine fractions were collected for each sample using an acetonitrile (ACN) concentration gradient: 1) dH_20; 2) 10% ACN/dH_20; 3) 12.5% ACN/dH_20; 4) 15% ACN/dH_20; 5) 17.5% ACN/dH_20; 6) 20% ACN/dH_20; 7) 25% ACN/dH_20; 8) 60% ACN/dH_20; 9) 60% ACN/0.1% trifluoroacetic acid (TFA) and 10) 80% ACN/0.1% TFA (fractions 9 and 10 were combined for MS run). All samples were dried down completely under vacuum (SpeedVac concentrator).

In preparation for the MS run, 0.1% formic acid was added to the samples followed by ultrasonic bath sonication for 10 min at 4°C. The samples were centrifuged at 17,000*g* for 10 min and the supernatant was loaded onto an Easy-nLC system (Thermo Fisher Scientific, San Jose, CA, USA), coupled online with a Q-Exactive mass spectrometer (Thermo Scientific). Peptides were loaded into a picofrit 20 cm long fused silica capillary column (75 µm inner diameter) packed in-house with reversed-phase Repro-Sil Pur C_{18}-AQ 3 µm resin. A gradient of 105 min was set for peptide elution from 2-28% buffer B (100% ACN/0.1% formic acid), followed by a gradient from 28-80% buffer B in 5 min and an isocratic 80% B for 10 min. The flow rate was set at 300 nl/min. MS method was set up in a DDA mode. The full MS scan was performed at 70,000 resolution [full width at half maximum (FWHM) at 200 *m/z*] in the *m/z* range 350-1200 and an AGC target of 10^6. Tandem MS (MS/MS) was performed at a resolution of 17,500 with a Higher Energy Collision Dissociation (HCD) collision energy set to 20, an AGC target of $5x10^4$, a maximum injection time to 100 ms, a loop count of 12, an intensity threshold for signal selection at 10^4, including charge states 2-4, and a dynamic exclusion set to 45 s.

3.2.4 Data analysis

MS raw files were analysed by MaxQuant software version 1.5.2.8 [280]. MS/MS spectra were searched by the Andromeda search engine [281] against the *P. falciparum* UniProt FASTA database (version: April 2016). All parameters for the search were kept as default, including set mass accuracy at 4.5 ppm for precursor and 20 ppm for the product mass tolerance. Peptides were filtered for high confidence (FDR<1%) using Fixed Value validator. Intensity-based absolute quantification (iBAQ) was enabled for label-free quantification, where iBAQ values are calculated by a MaxQuant algorithm (sum of peak intensities of all peptides matching to a specific protein/number of theoretical peptides) [282]. These values are proportional to the molar quantities (i.e. absolute copy numbers) of the proteins and provides an estimate of the absolute abundance of proteins within each sample. Match between runs was enabled and set to a 1 min window. All samples were run in triplicate for three independent biological replicates. For data analysis, iBAQ values were $\log_2$-transformed and normalised by subtracting to each value the average value of the respective sample.

3.2.5 Transcriptomics data

Data was acquired from a parallel study done in our lab by a fellow PhD student (RA van Biljon, manuscript in preparation) that investigated the transcriptome of *P. falciparum* parasites during gametocytogenesis. The daily time course spans commitment to gametocytogenesis and the full differentiation process (days; -2 to 0 and 1 to 13).

3.3 Results

3.3.1 The *P. falciparum* proteome during gametocytogenesis

To characterise the protein abundance profiles across *Plasmodium* life cycle development, we isolated soluble protein fractions from three asexual stages (ring, trophozoite and schizont; >90% synchronised each) and five stages throughout gametocytogenesis (>60% stage I; >50% stage II; >80% stage III; >90% stage IV; and >85% stage V; see Figure 2.1 - Chapter 2). Isolated soluble protein yield varied between the different stages (Figure 3.1) with the lowest yield observed in immature parasites during asexual development (rings at 0.33 ± 0.03 ng/parasite; trophozoites at 0.76 ± 0.11 ng/parasite, n=3). Mature schizonts contained 3.2 ± 0.4 ng protein per parasite (n=3), similar to previous reports indicating peaked protein synthesis during schizogony [283]. However, a significant (P<0.001, n=3) increase in protein yield was observed in early gametocyte stages (stages I-III) compared to all stages of asexual development (stage I at 8.2 ± 0.9 ng/parasite, stage II at 11.2 ± 2.6 ng/parasite, stage III at 16 ± 10 ng/parasite). The same significant increase was seen when comparing late gametocyte development with asexual development (stage IV at 13.5 ± 1.7 ng/parasite and stage V at 30 ± 17 ng/parasite; P<0.001, n=3), although the yields between early and late gametocyte development were not statistically different from each other (P>0.05). Protein synthesis occurs during stage II-III gametocyte development, correlating to the increase in protein yield from these stages [54].

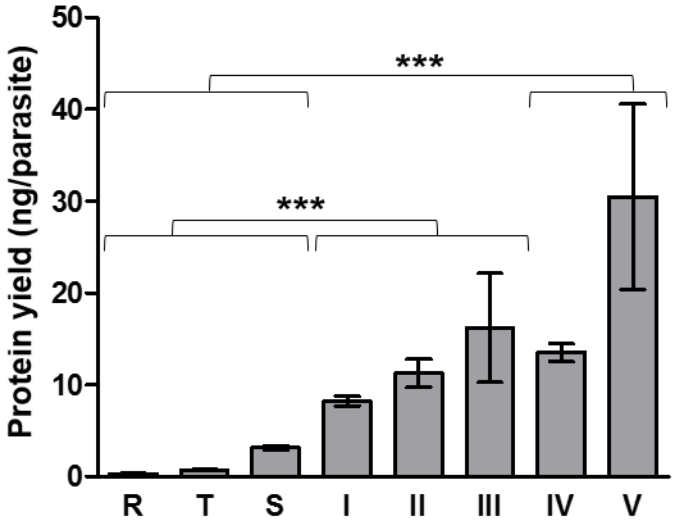

Figure 3.1: Protein yield for asexual and sexual *P. falciparum* life cycle stages. Soluble protein fractions were isolated from eight *P. falciparum* life cycle stages, including rings (R), trophozoites (T), schizonts (S) and stage I, II, III, IV and V gametocytes. The total protein yield (ng/parasite) per isolated parasite for each developmental stage was determined (two-tailed equal variance *t*-test, ***= P<0.001, n=3 ±SEM).

We performed quantitative assessment of proteins during development using high-resolution nanoLC-MS/MS (Figure 3.2). This allowed for high confidence (three independent biological replicates; FDR<1%) in protein identification and quantification using iBAQ, as well as horizontal comparison of the soluble proteome during all stages of *P. falciparum* parasite development. The proteins were not quantified based on spectral counting, but rather on peak intensities (iBAQ), lending to more accurate absolute protein quantification per stage [280, 282]. High mass accuracy (4.5 ppm for precursor and 20 ppm for product mass tolerance) and limited variance between replicates (6% average coefficient of variance between biological replicates; PCA for replicates shown in Appendix I: Figure A2) enabled high reproducibility, confident evaluation of all MS peaks and quantification of specific proteins in all samples.

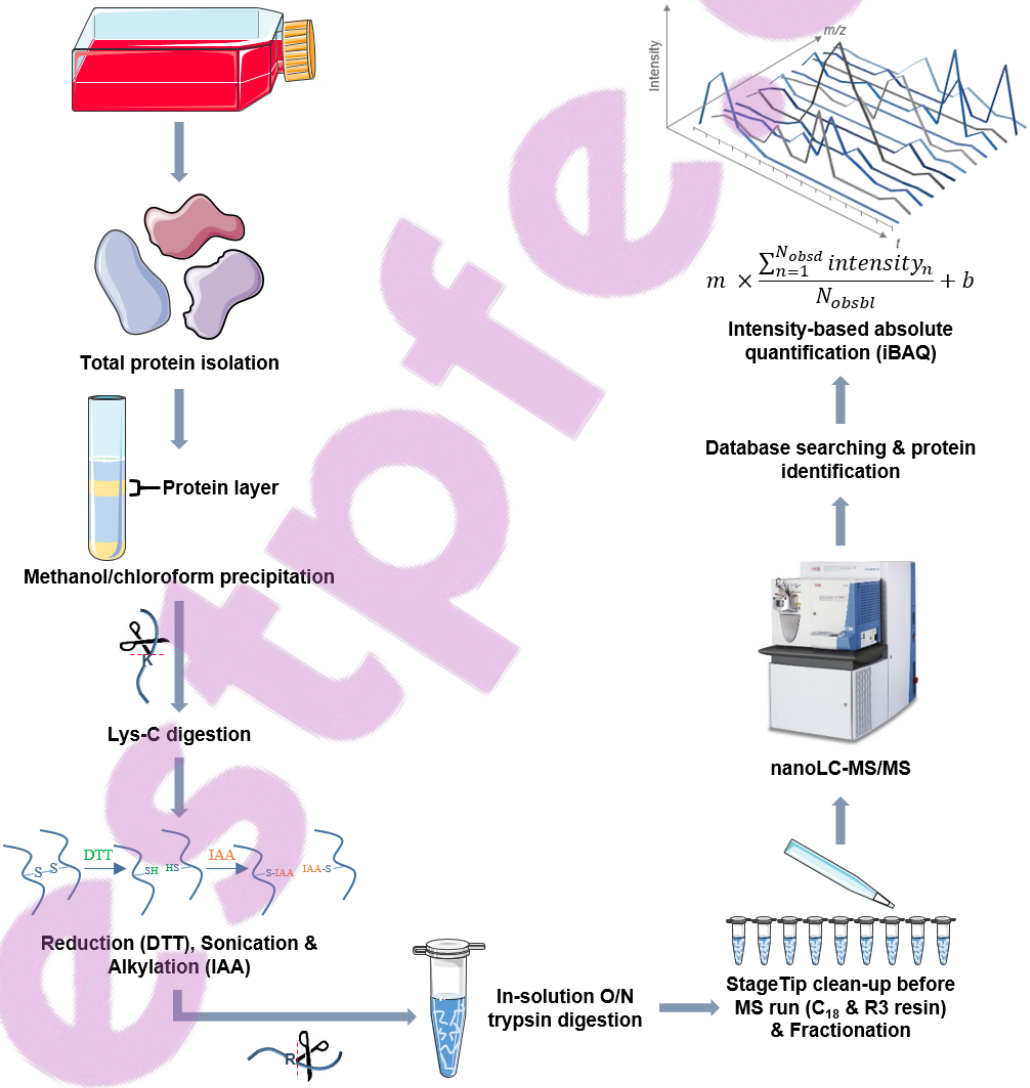

Figure 3.2: Quantitative proteomics approach. The proteins from each of the eight representative life cycle stages were isolated, precipitated, Lys-C digested, reduced (using DTT), sonicated, alkylated (using IAA), trypsin digested and finally cleaned up and fractionated for MS analysis. NanoLC-MS/MS was performed, followed by database searching and protein identification. Proteins were quantified using iBAQ. Images were adapted from Servier Medical Art (URL link to the license: https://creativecommons.org/licenses/by/3.0/) and changes were made in terms of colour and size.

A total of 997 quantitative proteins were identified across all eight life cycle stages, with the majority of proteins identified by the presence of a large number of peptides (Appendix IV: Supplementary File 5). This provides confidence in the reliability of the analysis with, on average, ~70 peptides identified per protein (Figure 3.3A). To allow comparative proteomics, only proteins with a quantitative profile in all eight life cycle stages were evaluated further in this study.

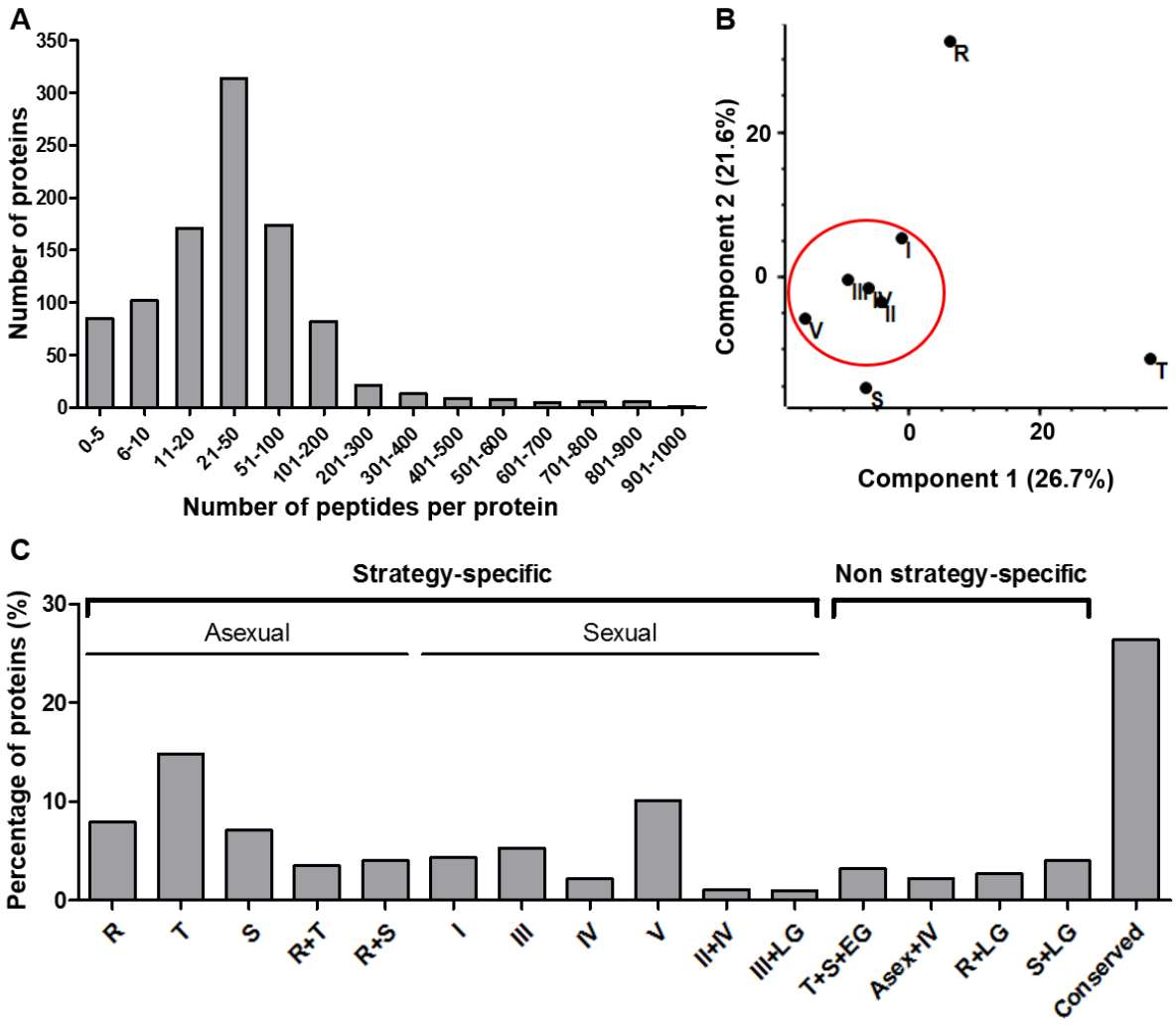

Figure 3.3: Proteome evaluation during *P. falciparum* asexual and sexual development. Eight *P. falciparum* life cycle stages, including rings (R), trophozoites (T), schizonts (S) and stage I, II, III, IV and V gametocytes were analysed. **(A)** The number of peptides used for the identification and quantification of each protein is shown. **(B)** Principle Component Analysis (PCA) showing the relationship between the quantitative proteomes of the various life cycle stages using component 1 and 2; gametocytogenesis indicated with red circle. **(C)** The percentage of proteins that showed strategy-specific or non-strategy-specific peaked abundance profiles per life cycle stage is indicated (ANOVA, $P<0.05$), as well as the conserved proteins that showed no significant stage-specific abundance ($P>0.05$) (Asex = asexual; EG = early gametocyte stage I, II & III; LG = late gametocyte stage IV & V).

The total soluble proteome was compared between all eight life cycle stages using Principle Component Analysis (PCA; Figure 3.3B). The proteome of stage I-V gametocytes (particularly stage II, III and IV) were more closely related (red circle) than

any of the asexual stages were to each other. Rings and trophozoites showed proteomes completely divergent from the other stages, which is expected due to the early asexual development occurring during these stages. The 997 quantified proteins were then compared across the eight life cycle stages using one-way analysis of variance (ANOVA; 0.05 cut-off *P*-value; Figure 3.3C; Appendix IV: Supplementary File 6). Of these, 263 (~26%) had no significant stage- or strategy-specific abundance profile ($P>0.05$; Figure 3.3C) and are designated as 'conserved' proteins that are constitutively expressed throughout development. The remaining 734 proteins (~74%) showed significantly ($P<0.05$) altered expression patterns between (Figure 3.3C). This includes strategy-specific protein expression (asexual preference vs. sexual preference) as well as proteins that show periodicity in expression, but where this is irrespective of a specific developmental strategy (non-strategy-specific).

Strategy-specific protein expression was observed for 37% (373 proteins) associated with asexual development compared to 24% (240 proteins) exclusively found in abundance during sexual development (Figure 3.3C). Within the asexual population, trophozoite stage parasites showed the largest abundance of stage-specific proteins (148 proteins, ~15%). Interestingly, within the sexual gametocyte population, stage V gametocytes contained 101 stage-specific proteins, indicating that these late stages of gametocytogenesis are dependent on specific proteins in preparation for gametogenesis. Stage II gametocytes showed no significant stage-specific abundant proteins.

Various non-strategy-specific proteins (121 proteins) peaked in expression in >3 stages, irrespective of a specific developmental stage (Figure 3.3C). Interestingly, trophozoites, schizonts and early gametocytes (stage I, II & III) shared 32 proteins that might be involved in asexual to sexual conversion, or early asexual and sexual parasite development. Stage III, IV and V gametocytes shared 10 proteins that may be involved in gametocyte maturation after RNA and protein synthesis that occurs early in stage II-III development. Schizonts and late stage gametocytes (stage IV & V) shared 40 proteins that may be involved in similar processes required for mature asexual and sexual parasite development.

3.3.2 Gametocytogenesis is characterised by stage-specific protein abundance profiles

The protein abundance profiles were mapped to life cycle development, indicating clear developmental preferences for certain protein sets (z-scores = hierarchical clustering

uncentered with Pearson Correlation on average linkages; Figure 3.4A). Of the 997 quantitative proteins, only 67% could be annotated using GO on biological processes, leaving 33% proteins unannotated or hypothetical. This 67% annotation outweighs the ~50% of genes from *P. falciparum* parasites for which function has yet to be ascribed [284]. Association of GO annotations to the average protein abundance per stage-specific cluster (Figure 3.4B) indicated those biological processes that were involved in each developmental stage ($P<0.05$; Figure 3.4C). As expected, immature ring stage parasites were enriched for proteins involved in host cell entry and immune regulation, whereas trophozoites and schizonts, the more metabolically active and replicating stages, showed enrichment for metabolism, cell cycle regulation and DNA processing. During entry to gametocytogenesis at stage I, fatty acid metabolism becomes increasingly essential, whereas programmed cell death is also enriched in these stages possibly due to the remaining proportion of uncommitted asexual parasites. Fatty acid metabolism and the tricarboxylic acid (TCA) cycle was prevalently enriched throughout gametocytogenesis, specifically during stage III-IV maturation, whereas haemoglobin metabolism was seemingly depleted mostly during these more mature gametocyte stages. Translational regulation showed increased abundance during stage IV gametocytes. This indicates that these more mature stages of gametocytogenesis are not metabolically inactive, but rather has altered metabolism compared to earlier stages or asexual development.

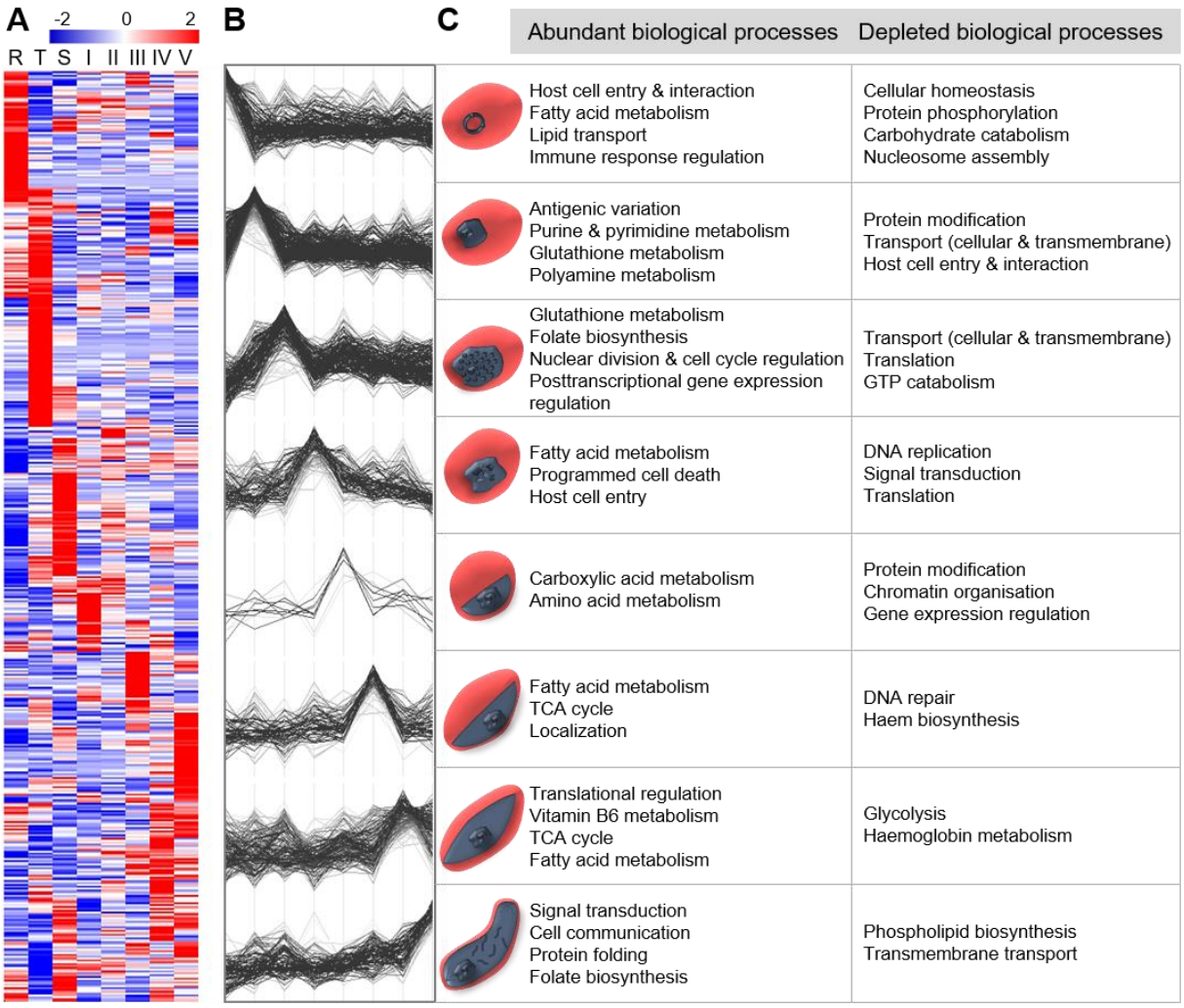

Figure 3.4: Stage-specific protein abundance profiles during *P. falciparum* life cycle development. **(A)** The relative protein abundance (z-score) of the 997 quantified proteins over the life cycle is shown (ranging from R, T, S, I, II, III, IV and V from left to right). Z-scores were clustered hierarchically, uncentered (similar results obtained with K-means) with Pearson Correlation on average linkages, and subsequently phase ordered. **(B)** Average protein abundance profiles per stage-specific cluster, based on clusters identified in A. **(C)** Abundant and depleted biological processes are shown per stage-specific cluster, based on clusters identified in A (Gene Ontology enrichment based on biological processes, $P<0.05$) and limited to proteins for which annotation exists.

The protein abundance profiles in Figure 3.3C were further probed for significantly differentially expressed proteins, resulting in identified protein sets that were highly abundant in one group and depleted in another group. Differential protein abundance profiles were identified by comparing protein abundance of those proteins that are significantly differentially expressed between asexual (rings, trophozoites and schizonts) and gametocyte stages (stage I-V gametocytes), as well as between early (stage I-III) and late (stage IV-V) stage gametocytes (z-scores; Student's *t*-test, $P<0.05$; Figure 3.5; Appendix IV: Supplementary File 7).

Comparison of asexual- vs. gametocyte-specific proteins identified 178 and 116 proteins that were differentially expressed, respectively ($P<0.05$; Figure 3.5A). These strategy-

specific differentially expressed proteins associated with asexual development were enriched for antigenic variation (*rif* family proteins), entry into host cell (PfBDP1, PfRH2, PfRhopH, etc.), immune response regulation (PfRESA, PfSERA) and haemoglobin catabolism (PfPMI, PfHDP, PfAPP, PfHlyIII, etc.) (GO enrichment based on biological processes, $P<0.05$). Comparatively, gametocytes showed enrichment for strategy-specific proteins involved in post-transcriptional and translational regulation of gene expression (PfPuf1, PfeIF4E, PfAP2-O, PfRNaseII), exit from host cell (PfMDV1, Pfg377) and pathogenesis (PfP230).

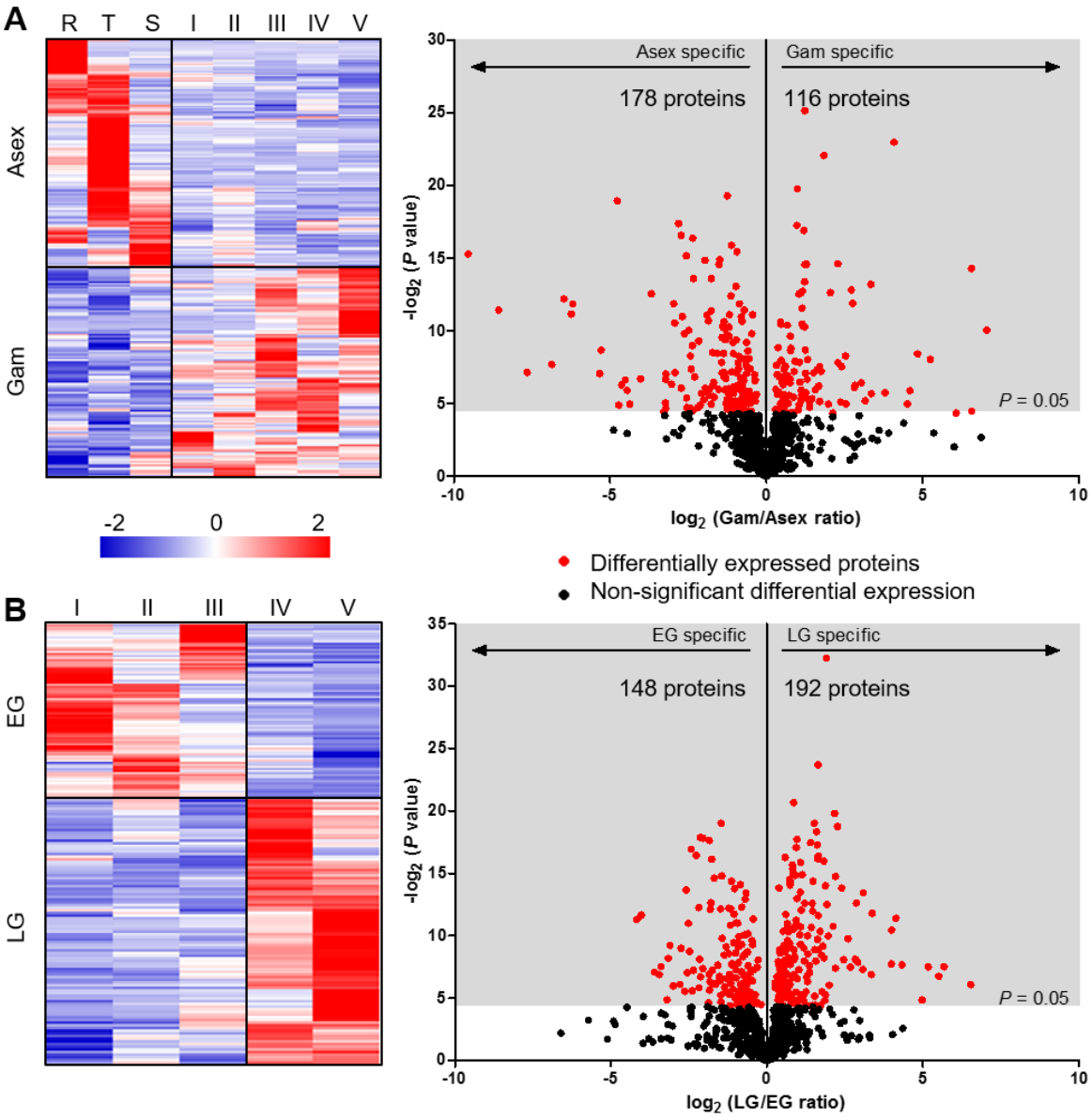

Figure 3.5: Differential protein abundance profiles between asexual, early and late gametocyte development. (A) The clusters showing differential protein abundance between the asexual stages (Asex) and gametocytogenesis (gam) (z-score; k-means clustering with Pearson Correlation on average linkages, phase ordered). The volcano plot indicates differential expression of proteins by Gam/Asex ratios versus *P*-values (Student's *t*-test, red dots indicate significantly differentially expressed proteins, $P<0.05$). **(B)** The clusters showing differential protein abundance between the early (EG) and late (LG) stage gametocytes (z-score). The volcano plot indicates differential expression of proteins by LG/EG ratios versus *P*-values (Student's *t*-test, red dots indicate significantly differentially expressed proteins, $P<0.05$).

Similar differential protein abundance profiles were observed between early and late stage gametocyte-specific proteins, where 148 and 192 proteins were significantly differentially expressed, respectively (P<0.05) (Figure 3.5B). These proteins are sexual strategy-specific proteins that could further be differentiated as either early or late gametocyte-specific, showing significantly high abundance profiles in one group and depleted abundance in the comparative group. Early gametocyte-specific proteins were involved in cellular transport (PfERC, PfRAB5, PfCRT, PfATPase), translational regulation (PfIF1, PfeIF4G, various ribosomal proteins), protein phosphorylation (PfCRK3, PfMRK, PfCDPK7, PfPP7, PfCLK1), protein modification (PfUb, PfUBC, PfDER1-1) and subcellular localisation (PfMC-2TM) (GO enrichment based on biological processes, P<0.05); whereas proteins in late gametocytes showed enrichment for protein metabolism and modification (PfSUMO, PfUFD1, PfUCH54, PfUba2, PfHRD1), protein phosphorylation (PfCDPK2, PfARK1, PfPI3K) and particularly cell cycle and translational regulation (PfeIF4A, PfPK5, PfCRK4, ribosomal proteins, etc.). This dataset was subsequently interrogated for specific biological processes known to be associated with gametocytogenesis including sex differentiation, translational repression and regulation of epigenetic modulators.

3.3.3 Sex-specific proteins peak early during gametocyte development

Certain proteins have been designated as sex-specific, associated with either mature male or female gametocytes, although the data from three different reports on such sex-specific proteomes are not consistent [72, 226, 228]. In total, 493 male-specific and 736 female-specific proteins were identified from these quantitative published datasets, with only a small number of proteins shared between the three datasets. Using this combined dataset, we interrogated our quantitative, comparative proteome data across all the stages of gametocytogenesis for these proteins (Figure 3.6; Appendix IV: Supplementary File 8). In our data, 95 male-specific proteins were quantified in all five stages of gametocyte differentiation (Figure 3.6A). A third of these male-specific proteins showed constitutive expression throughout gametocytogenesis while 64 others showed peaked abundance in either stages III, IV or V. For the female-specific proteins, 247 quantitative proteins were identified in our data (Figure 3.6B). For the first time, we showed that proteins involved in female sex-specific differentiation is evident very early on in gametocytogenesis, with 33 proteins already showing distinct increased abundance profiles as early as stage I & II of development. These genes show concomitantly decreased abundance in stage III-V. The majority of the proteins (n=158), however, only

peaked in abundance in stages III, IV and V, respectively, whilst 56 proteins showed no stage-specificity, with constitutive expression throughout gametocytogenesis. These results suggest that gametocyte sex differentiation is indeed differential and dynamic during gametocytogenesis but that these proteins are abundantly present earlier in development than only in terminal stage V gametocytes as previously described.

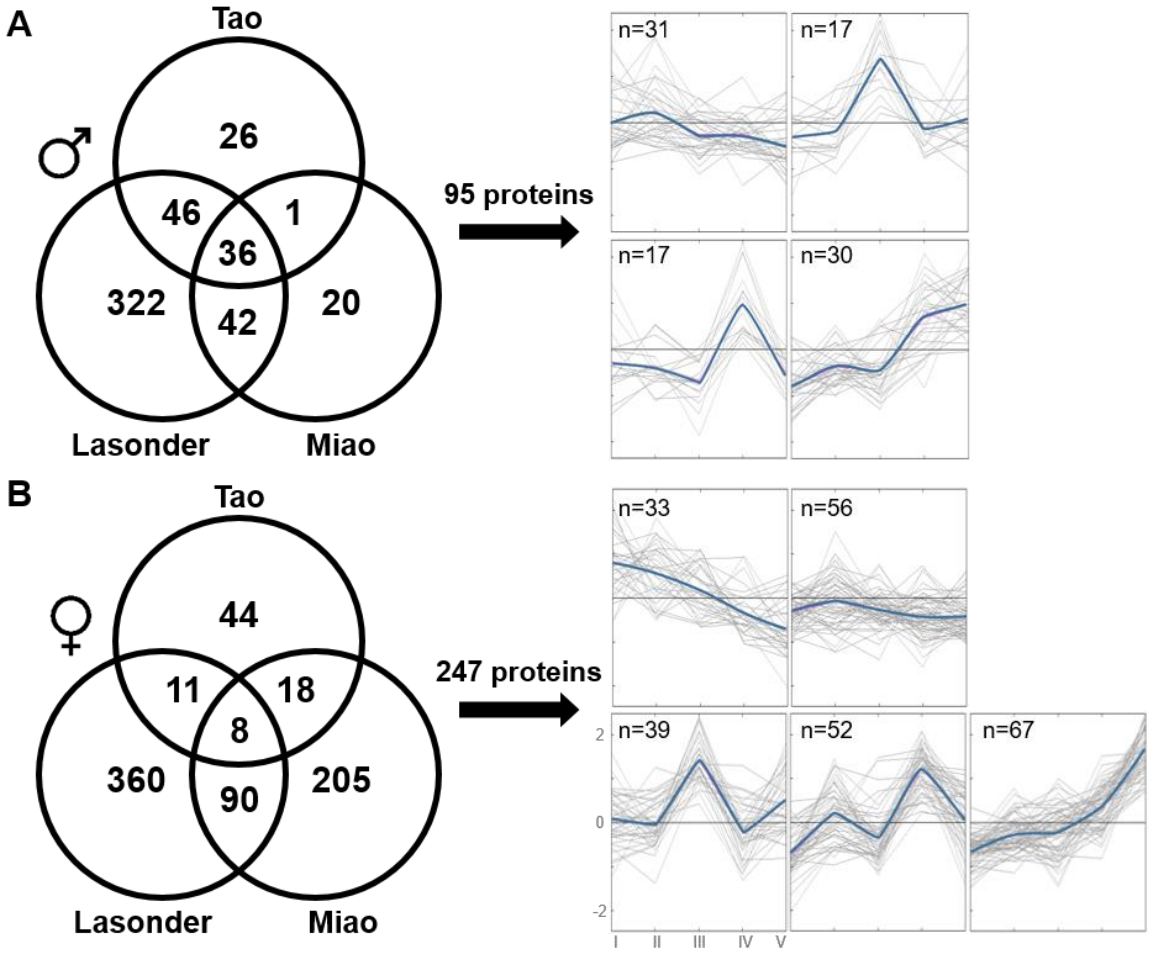

Figure 3.6: Gametocyte stage abundance profiles of sex-specific proteins. (A) Male-specific proteins from three different studies (Tao *et al.* 2014, Lasonder *et al.* 2016, Miao *et al.* 2017); 95 proteins were quantified in this study with four clusters showing varied abundance profiles (average profile indicated in solid line; protein abundance shown as z-scores from stage I-V). **(B)** Female-specific proteins from three different studies; 247 proteins were quantified in this study with five clusters showing varied abundance profiles (average profile indicated in solid lines; protein abundance indicated as z-scores from stage I-V).

3.3.4 A quantitative protein set is not translationally repressed during female gametocyte development

A putative set of 512 transcripts have recently been described as being translationally repressed during gametocytogenesis, where the transcripts are present but not translated until gametogenesis as a result of post-transcriptional regulation [72]. This observation was made based on, amongst other factors, the absence of quantitative evidence for proteins within stage V female gametocytes for which detectable transcripts were present.

We compared these transcripts with our quantitative proteome data from across gametocytogenesis and found 54 proteins for which we had quantitative data, but which were previously said not to be expressed (Figure 3.7A; Appendix IV: Supplementary File 9). Overall, these proteins were mostly (78%) present at low abundance in stage V gametocytes in our data, which might explain the lack of identification and quantification in the previous study as the MS analysis might not have been sensitive enough to quantify these proteins [72] (Figure 3.7B). However, 22% of the proteins were indeed significantly abundant. Only 5 of the 54 proteins were previously associated with *Plasmodium* gamete proteomes [71, 285] including PfNT4, PfP28, PfGDH2, PfAARP2 and PfMTIP. This suggests that the remaining 49 proteins that were not found in the *Plasmodium* gamete proteomes might be redundant during gamete production and it is therefore not rational that these proteins are translationally repressed.

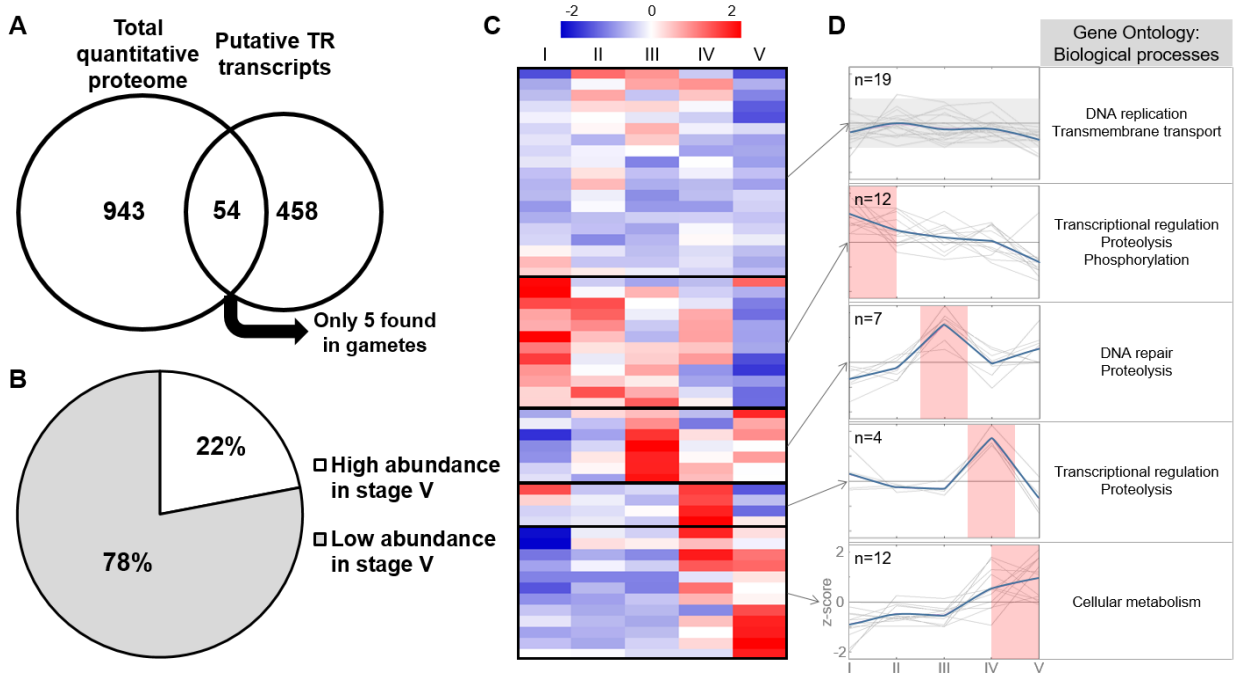

Figure 3.7: Putative translationally repressed proteins are present during gametocytogenesis. (A) Venn diagram showing the overlap of the whole quantitative proteome with the set of putative translationally repressed proteins identified in Lasonder *et al.* (2016). **(B)** Percentage of the non-translationally repressed protein set that has high/low abundance in stage V gametocytes. **(C)** The clusters of the 54 non-translationally repressed proteins that could be quantified during gametocyte development in this study (z-score; k-means clustering with Pearson Correlation on average linkages; phase ordered). **(D)** Stage-specific abundance profiles of the non-translationally repressed proteins that show steady-state abundance during gametocytogenesis (shaded grey; z-score), or increased abundance at specific stages (shaded red). Gene Ontology enrichment based on biological processes and limited to proteins for which annotation exists (P<0.05).

The set of 54 proteins that are therefore not translationally repressed were found to have varied stage-specific abundance profiles throughout gametocytogenesis (Figure 3.7C). A cluster of proteins, enriched for DNA replication and transmembrane transport (GO

enrichment based on biological processes, *P*<0.05), showed steady-state abundance throughout the five stages of gametocyte development (n=19), whereas the remaining clusters had clear stage-specific abundance in stage I, III, IV and V, in that order (Figure 3.7D). Specifically, 12 proteins peaked in abundance during stage V gametocyte development, including PfAdoMetDC/ODC, PfP28, PfMAPK1 and plasmepsin VII&VIII. Overall, these results suggest that this set of proteins previously thought to be translationally repressed are indeed expressed during gametocytogenesis in a stage-specific manner.

3.3.5 Epigenetically driven regulation of protein expression during gametocytogenesis

In an effort to observe trends associated with epigenetic regulation manifesting in differential gene expression during gametocytogenesis, and in the absence of data directly linking epigenetic marking of histones with gene expression during this development phase, the regulation of *P. falciparum* stage-specific asexual and sexual development was evaluated by integrating global datasets from the histone PTM landscape, transcriptome and proteome. These datasets were all generated in-house as either part of this study or a related PhD study by RA van Biljon (gametocytogenesis transcriptome, PhD thesis, University of Pretoria). Straightforward parallel evaluation of abundance profiles from these datasets was performed, rather than direct feature overlap (i.e. expression level associations). This objective evaluation simply relied on similar abundance profiles associated with stage-specific profiles during gametocytogenesis.

From Chapter 2, several single and co-existing histone PTMs showed exclusive increased abundance during gametocyte development. This includes the increased abundance of repressive marks (H3K36me2, H3K27me2/me3) in stage II gametocytes (Figure 3.8A). This correlated to the decreased expression of ~300 genes during early stage gametocyte development from the gametocytogenesis transcriptome (data from RA van Biljon, unpublished, Figure 3.8B). Of these, 28 showed similar low abundance protein levels throughout gametocytogenesis (Figure 3.8C). These proteins include PfETRAMP2&12, PfGAP45, PfMSP9&11, PfSERA3&5 and a PfApiAP2. The absence of these proteins during gametocytogenesis may therefore be significant in gametocyte development. This data indicate that, at least for some genes, post-transcriptional level regulation is observed during early gametocyte development and this may be directly driven by epigenetic repression of gene expression.

Once commitment to gametocytogenesis has been established, stage-specific transition and differentiation is marked by the increased abundance of several acetylation marks (H4K8ac, H3K23ac, H3K18ac, H4K12ac, H3.3K9ac, H4K5ac & H3K4me1) and the co-existing H4 acetylations (11 combinations identified, Chapter 2). This was associated with two very distinct gene clusters (360 & 209 genes, respectively) from the gametocytogenesis transcriptome data, which showed overall increased expression during gametocytogenesis (Figure 3.8B). This included well-known gametocyte-specific markers like Pfs16, PfP230, Pfs25, Pfs28 and Pfs48/45 (Figure 3.8C) [286-290]. Most of the proteins for these transcripts showed a mixed abundance profile during gametocytogenesis, with a general decreased abundance in stage I-II gametocytes and an increased abundance in stage III, IV or V gametocytes (Figure 3.8C). For these genes, there therefore seems to be epigenetically driven activation of gene expression as manifested in protein production.

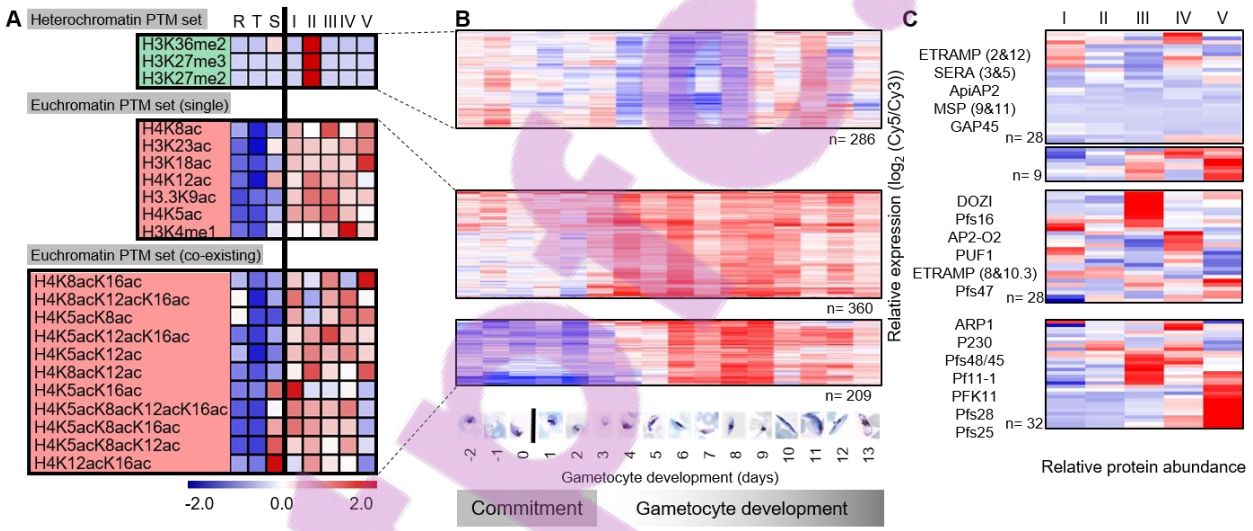

Figure 3.8: Integration of histone PTM landscape, transcriptome and proteome data to evaluate regulation of stage-specific gametocyte differentiation. (A) Single and co-existing histone PTMs associated with increased abundance during gametocyte development (z-score), that are known to be involved in euchromatin (shaded red; single & co-existing PTMs) and heterochromatin (shaded green) regulation. **(B)** Relative transcript expression levels (log_2, Cy5/Cy3) for certain gene clusters are shown throughout the duration of gametocytogenesis (days; RA van Biljon data, unpublished). The gene clusters from top to bottom correspond to the decrease in early gametocytes, and increase in gametocytogenesis overall (two bottom clusters). **(C)** Relative protein abundance during gametocytogenesis for subsets of proteins corresponding to the gene sets in B (z-score).

To provide validation for the integrative evaluation of the histone PTM landscape, transcriptome and proteome datasets, we independently analysed the correlation between certain abundance profiles with functional outcomes involved in *var* gene and epigenetic regulation during gametocytogenesis (Figure 3.9). *Var* gene expression in asexual parasites is clearly epigenetically driven (see Chapter 1 – Figure 1.10). However,

it is thought that *var* genes are not abundantly expressed in gametocytes [291]. Therefore, we mapped *var* gene expression profiles throughout gametocytogenesis from the transcriptome data, which indeed showed mostly downregulation of these genes during this process. Only two PfEMP1 genes (Pf3D7_0421300 & Pf3D7_0114400) showed marked increased expression in late stage gametocytes (Figure 3.9A). The H3K9me3 abundance profile was mapped to the average *var* gene expression profile and showed an inverse correlation, where increased H3K9me3 abundance correlated to the overall decreased *var* gene expression during gametocytogenesis, suggesting that repressed *var* genes may be marked by H3K9me3 in gametocytes (Figure 3.9B).

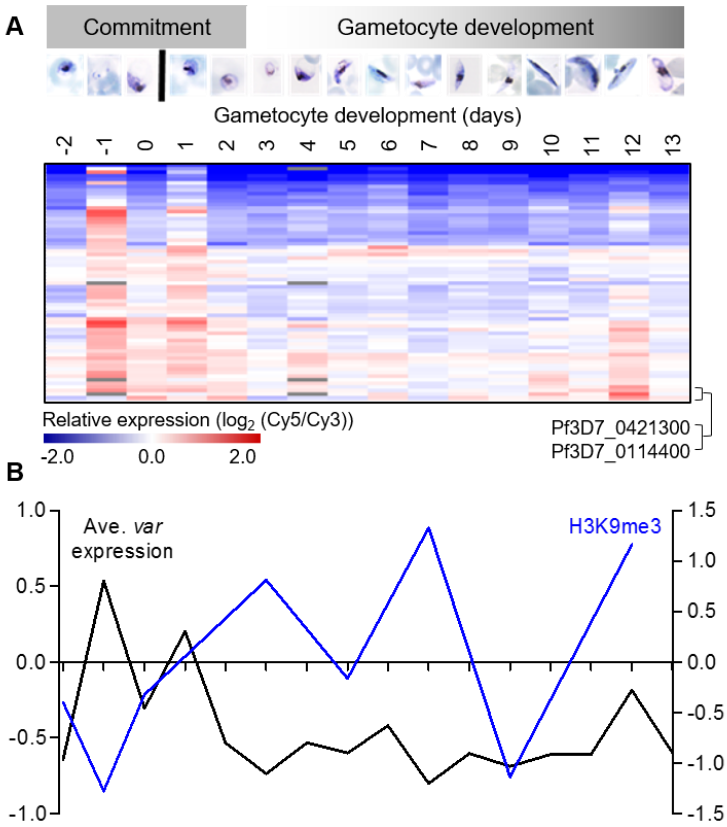

Figure 3.9: Integrated *var* gene regulation during gametocytogenesis. (A) Relative transcript expression levels (log_2, Cy5/Cy3) for the *var* gene cluster is shown throughout the duration of gametocytogenesis (days; RA van Biljon data, unpublished), with only two *var* genes showing increased expression levels as indicated. **(B)** The average *var* gene expression profile (log_2, Cy5/Cy3) was mapped together with the H3K9me3 abundance profile (z-score) to show inverse correlation.

We further evaluated the correlation between transcriptome and proteome abundance profiles of epigenetic modulators during gametocytogenesis (Figure 3.10). During gametocytogenesis, histone PTM profiles are completely divergent from asexual parasites (Chapter 2), with a subset of 13 conserved histone PTMs that was highly correlated within different gametocyte stages and associated with stage-specific transitions during the differentiation process. These unique histone PTM signatures and

combinations observed exclusively in gametocytes implies that different epigenetic regulatory mechanisms must be in play during the terminal differentiation process in gametocytogenesis. As such, we interrogated the transcriptome and proteome datasets for epigenetic modulators, including writers, erasers and readers. Although certain epigenetic modulators showed decreased transcript abundance during gametocytogenesis, the transcripts for several were constitutively expressed, with marked increased abundance in late gametocyte development. This includes the transcripts for a HDAC (PfSIR2A), four HKMTs (PfSET3,4,7&8) and two Pf14-3-3 readers (Figure 3.10A). From the quantitative proteome data, 11 modulators were detected and quantified with varying abundance profiles during gametocytogenesis (Figure 3.10B). This included PfHP1, PfHDAC1, PfSIR2A, PfJmjC1 and PfSETvs, which were differentially expressed between early and late gametocytes, showing a clear preference towards expression in late stage gametocyte development ($P<0.05$). The high proteome abundance profiles for these modulators did not correlate with the depleted transcriptome expression profile, suggesting that these transcripts might be stored from earlier developmental stages during differentiation to be abundantly expressed in late gametocytes. Pf14-3-3I showed a similar increased protein abundance profile throughout gametocytogenesis to the transcriptome level. Various epigenetic modulators, particularly, the HKMTs, could not be quantitatively identified in our proteome data, but this does not exclude their presence in gametocytes.

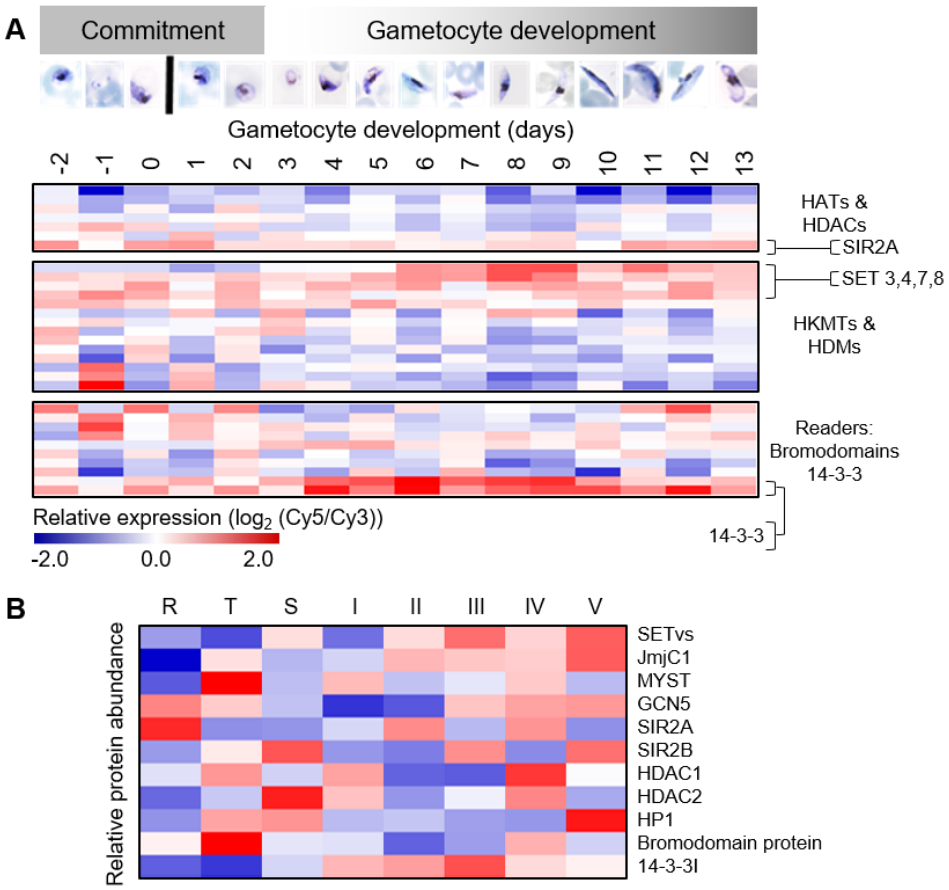

Figure 3.10: Integrated epigenetic regulation mechanisms during gametocytogenesis. (A) Relative transcript expression levels (log_2, Cy5/Cy3) for the epigenetic modulators (HATs & HDACs, HKMTs & HDMs, readers) are shown throughout the duration of gametocytogenesis (days; RA van Biljon data, unpublished), with a few genes showing increased expression levels as indicated. **(B)** Relative protein abundance during life cycle development for subsets of epigenetic proteins corresponding to the gene sets in A (z-score).

3.4 Discussion

This study provides the most comprehensive and quantitative evaluation of protein expression during *P. falciparum* gametocytogenesis. Moreover, the comparative nature of the dataset enabled quantitative evaluation of the proteomes of all the blood stages of *P. falciparum* parasites, both for asexual proliferation and sexual differentiation (stringent iBAQ quantification on three independent biological replicates). We extensively characterised gametocyte stage differentiation based on specific proteomic signatures that could be associated with prevalent biological processes required for development. We showed that certain proteins are differentially expressed during stage-specific parasite development, and that proteins involved in gametocyte sex differentiation are prevalent early on during gametocytogenesis. This work proposes that gametocytes employ a well-balanced regulatory cascade involving various facets, including post-transcriptional, translational and post-translational regulation, and that epigenetic mechanisms might drive stage-specific protein expression during gametocyte differentiation.

Through this stringent profiling, we were able to show that ~1000 proteins contribute to stage-specific development and this correlates to key biological processes required for *P. falciparum* gametocyte differentiation, and that the proteome is highly dynamic and adaptable across the entire life cycle of the parasite in human blood. A quarter of the identified proteins showed similar abundance across the eight stages, suggesting that these proteins are constitutively expressed and are required for normal cellular metabolism in all forms of the parasite. The remaining larger proportion of the quantitative proteome showed differential or strategy-specific abundance profiles between stages, indicating that the *P. falciparum* proteome undergoes significant changes during development, specifically separating the asexual and sexual life cycles. The stage-specific asexual proteomes were completely divergent from the gametocytes, showing reliance on antigenic variation, host cell entry and immune response regulation, as previously reported [68, 71, 73, 227]. The total quantitative proteome for stage II, III and IV gametocytes were closely correlated, indicating that these intermediate stages of gametocyte development share similar molecular characteristics and biological processes regulating their development, confirming previous findings that these stages exploit sexual stage-specific molecules to alter the parasitophorous vacuole and the host erythrocyte during gametocytogenesis [227]. Stage I gametocytes were characterised with various stage-specific abundant proteins, which is surprising due to the fact that

protein synthesis only occurs as the gametocytes progress to stage II-III [54]. This might suggest that the proteins required for stage I development are already present or being produced in the committed schizont population. Proteins associated with fatty acid metabolism and the TCA cycle showed increased abundance during gametocyte maturation, confirming previous findings that glucose is the preferred carbon source for TCA metabolism in mature gametocytes that require more energy-efficient metabolism and shows for the first time that stage I gametocytes share this metabolic proteome [68, 292]. Stage III gametocytes were previously thought to enter a quiescent metabolic state due to their non-proliferative nature [244], but we propose that these parasites merely enter an altered metabolic state to prepare for parasite transmission. During stage III-IV maturation haemoglobin metabolism was depleted, supporting prior knowledge that the newly invaded gametocytes increase their size by subsequent depletion of host cell haemoglobin and cytoplasm [52, 53].

The molecular players involved in gametocyte sex differentiation were expressed in sequential waves after commitment, supporting findings that the onset of sex differentiation occurs right from the beginning of gametocyte development (stage I/II for females) [34, 35]. Similar observations were found in other organisms (e.g. fission yeast), where transcription factors were implicated in the regulation of sequential transcriptional waves during sexual differentiation [293]. Previous reports showed that male and female gametocytes can be morphologically distinguished clearly from stage III-IV [42] and that various proteins are designated as either male- or female-specific in the terminally differentiated stage V gametocytes, with biased-ratios allowing for separation between these two sexes [72, 226, 228], but these molecular players might be involved earlier during the process of sex differentiation. Our data provide evidence for certain protein clusters that are abundant prior to late gametocyte development for both males and females, although these stages were not experimentally separated. Specifically, for the female-biased proteins, sequential waves of protein expression occur during sexual differentiation, reflective of the overall proteome dynamics between stages, with a large cluster showing stage-specific abundance from stage III-V. Interestingly, a set of proteins mostly enriched for translation, cell redox homeostasis, protein folding and modification (phosphorylation, etc.) is highly abundant during stage I/II gametocytes and becomes depleted later during development. This suggests that the molecular descriptors associated with female sex differentiation is already in play at early onset, correlating to the finding that gametocyte sex precedes commitment and is determined during

schizogony [34, 35]. Other reports showed that the female-biased proteins Pfg377 [60, 294] and Pfs48/45 [244, 295] are abundant in early gametocytes, therefore this study characterised additional molecular players involved in female differentiation. This additionally raises questions whether these early stage abundant proteins are involved during early female development into subsequent stages, if other proteins take over their regulatory function upon depletion, and if the proteins peaking in the later stages (e.g. stage V) are being produced in preparation for gametogenesis. For male-biased proteins, the molecular players involved in sex differentiation seem to be utilised from stage III onwards, with no significantly abundant proteins identified during early gametocyte development. These male-biased proteins are mostly enriched for protein phosphorylation, DNA replication and repair. The larger number of proteins associated with female gametocytes and the lack of identifiable male-biased proteins earlier during gametocytogenesis can possibly be attributed to the female-biased ratio of 5:1 [51] or to the fact that female gametocytes are required to be ready for mitosis upon activation of gametogenesis in the mosquito midgut [296], where the male gametocytes still need to undergo DNA replication upon exflagellation [62].

Translational repression has become a great interest in *P. falciparum*, as it provides evidence that these parasites possess the means to control its maternal mRNAs by selectively repressing these transcripts until the products are needed for gamete fertilisation as a form of post-transcriptional gene regulation. However, we provide evidence that a set of putative transcripts that have previously been identified as translationally repressed are in fact translated and quantitative throughout gametocytogenesis and display stage-specific regulatory roles during development. Gametocytes are proposed to be translationally active throughout gametocytogenesis in order to supply stage-specific proteins required for development. Stage-specific abundance was observed for this protein set, where ~65% were also associated with translational repression in two other studies [91, 275]. These proteins were mostly shown to have a functionally annotated role in gametocyte differentiation, specifically involved in transcriptional regulation. Our data only shows steady-state protein abundance, therefore the regulatory mechanisms involved here remain to be clarified e.g. degradation etc. Only 10% of this protein set was found to be present in the *Plasmodium* gamete proteome [71, 285]. This is interesting because the whole theory of translational repression is based on the need and sporadic translation of these transcripts upon gametogenesis, and if these proteins are not found in the gamete proteome, they can be seen as redundant for gamete

production. The absence of the quantitative protein data in previous studies is not necessarily proof for the repression of the transcripts. Therefore further investigation needs to be done to fully characterise the extent of translational repression in *P. falciparum* gametocytogenesis and the molecular players involved in its regulation.

Although various levels of gene regulation is employed during parasite stage transitions, some regulatory aspects during gametocyte differentiation remain unknown. Our data collectively suggests that a fine-tuned balance between post-transcriptional, translational and post-translational regulation is involved in gametocyte differentiation, with differential aspects of each regulatory level employed for early and late stage gametocytes. The lack of translational repression in this study also correlates to altered regulatory mechanisms. These claims are supported by the differential enrichment of gametocytes in post-transcriptional and translational regulatory proteins, implying that gametocytes utilise significantly altered mechanisms of gene regulation compared to the asexual IDC. This correlates to recent work illustrating the RNA transcriptional dynamics [271] and epigenetic involvement during gametocyte commitment [160, 163, 210] and differentiation [67], integrating various levels of gene regulation throughout gametocytogenesis. The cell cycle “arrest” observed during late gametocytes was previously associated with increased transcriptional control mechanisms [64, 68]. Various proteins involved in transcription, cell cycle progression, DNA processing and translational regulation were highly abundant during late gametocyte development. One such regulator, PfAlba1, has been implicated in monitoring the timing of mRNA translation in the asexual stages [297], but its role in gametocyte differentiation remains to be elucidated.

Protein phosphorylation and modification was significantly and differentially enriched in both early and late stage gametocytes, indicating that altered mechanisms and molecules are needed for protein modification in these two differential stages, although a fine-tuned balance of these processes are required for stage-specific gametocyte development. In particular, Pf14-3-3I was mostly abundant during gametocytogenesis, a protein class known to specifically bind to phosphorylated histones (H3S28ph) and are involved in the regulation of chromatin remodelling, transcription initiation and cellular differentiation [142, 298]. This suggests that gametocytes rely on histone phosphorylation mechanisms during gene expression regulation, particularly during early sexual development. 14-3-3 proteins also generally interact with protein kinases and regulate these master switches in cellular pathways [299], where differential protein phosphorylation was shown here between early and late gametocyte development. This differential kinase/phosphorylation

pattern during gametocytogenesis proposes altered cellular signalling during differentiation when compared to asexual proliferation, and the extent of the involvement of these processes in cellular divergence needs to be clarified. These findings support previous data that deemed protein phosphorylation as an essential aspect of various cellular processes such as asexual proliferation, migration, cellular homeostasis, and specifically sexual differentiation and male gametogenesis [300-303].

Finally, we investigated the integrated regulation of gametocytogenesis by linking the histone PTM landscape, transcriptome and proteome datasets to interrogate the involvement of epigenetic regulatory processes in differentiation. This direct overlapping strategy has various limitations, including biased analysis of corresponding transcripts without experimental validation of the correlation with euchromatic/heterochromatic PTMs and the failure to take complex biochemical cellular regulation into account. Various challenges remain for within and between '-omic'-dataset integration, with novel software tools available to integrate these datasets based on biochemical pathway, ontology, network or empirical correlations [304]. Other ways of integrating omics datasets are emerging to help address these challenges in realising a systems biology view of cellular processes, specifically at the level of protein interaction networks [305]. Nevertheless, this straightforward comparison was attempted to integrate three -omics datasets to possibly identify further avenues that might elucidate some answers pertaining to the involvement of key molecular players during gametocytogenesis. Overall, the distinction between histone PTM abundance profiles, transcript expression levels, protein abundance levels, epigenetic effector proteins and *var* gene expression between asexual and sexual development implies that these parasites differentiate using altered mechanisms of gene regulation than their asexual counterpart.

Epigenetic regulation plays a crucial role in various cellular aspects during parasite development, and here we suggest that strategy-specific protein expression is driven by abundant activating or repressive histone PTMs during gametocytogenesis. We additionally showed that the epigenetic regulatory mechanisms for variant gene families may indeed be conserved between asexual parasites and gametocytes and that the majority of *var* genes are repressed during gametocytogenesis and may be maintained in a silent state by H3K9me3 [145, 156, 163, 164, 175, 176]. The correlation between repressive histone PTMs and downregulated gene and protein clusters implies that these genes that are subject to epigenetic repression early in gametocytogenesis either remain repressed even though the transcripts are expressed later in development, or they are

translated in later development and seemingly utilised in gametocyte development. On the other hand, activating histone PTMs positively correlated with increased transcript levels and stage-specific protein expression. Some epigenetic proteins were abundant during late gametocyte development even though their transcriptional expression was low. This could suggest that translation is halted until the point where the proteins are needed for stage V differentiation in preparation for gametogenesis. These results collectively demonstrate that although these genes are transcribed either throughout or at specific points during gametocytogenesis, there are altered post-transcriptional, translational or post-translational regulators involved in stage-specific gametocyte development, as these proteins are only present in specific gametocyte stages where they are needed for the subsequent stage differentiation [89].

We conclude that the *P. falciparum* parasite has immense control over its gene expression and regulation of stage-specific transitions that is accompanied by a unique set of proteins to be translated at the exact developmental cues where they are needed. This corresponds with prior knowledge about the parasite's transcriptional and translational profiles during asexual and sexual development, where the genes are transcribed and subsequently translated "just-in-time" [69, 73]. This is facilitated by various integrated regulatory mechanisms that are employed after transcription to result in unique proteome signatures per associated gametocyte stage. Further investigations are required specifically focusing on characterisation of gametocyte sex differentiation from early onset, the full extent of translational repression during gametocytogenesis and how this data translates to the situation during gametogenesis.

Chapter 4

Multi-stage inhibition of *Plasmodium falciparum* by targeting the parasite's epigenetic gene regulation machinery

4.1 Introduction

It is inevitable that malaria parasites will develop resistance against any clinically used antimalarial therapies [17]. Therefore novel classes of antimalarial drugs with alternative modes of action are urgently and continuously needed [306, 307]. To adequately treat malaria, drugs must be fast-acting, highly potent against asexual blood stage infections, minimally toxic and be amenable to drug combinations to curb resistance development [13, 19]. Additionally, there is a need for antimalarials that prevent relapses of dormant forms of the parasite (hypnozoites, specifically in *P. vivax* and *P. ovale*) [306]. Future compounds must effectively suppress or block the formation of gametocytes and subsequent transmission to the mosquito vector, thereby halting the infection cycle and contributing to global malaria elimination [307, 308].

P. falciparum gametocytes are the longer-living form of the parasite, which makes transmission-blocking approaches challenging. However, these gametocytes are the only transmissible forms amenable to chemotherapy due to their pharmacological accessibility in human blood. Since *P. falciparum* gametocyte development is still rather poorly understood compared to their asexual blood stage partners, efforts to develop transmission-blocking antimalarials is only now gaining momentum [309, 310]. However, no transmission-blocking vaccine and only one licensed antimalarial that inhibits mature gametocytes is available [309]. Currently, primaquine is seen as the gold standard for antimalarials that target the non-dividing parasite stages, due to its rapid gametocytocidal capacity and successful prevention of *P. vivax* relapse [308]. The clinical use of primaquine is hindered by safety concerns in terms of haemolysis in patients with glucose-6-phosphate dehydrogenase deficiency [308]. Artemisinin combination therapies, the current first line treatment against malaria, have not shown activity against mature gametocytes (stage V), leaving the patients infective long after clinical symptoms have been relieved and the asexual parasites have been cleared [311].

Various novel chemical scaffolds with different mechanisms of action have undergone clinical development in recent years, including clinical candidates KAE609, OZ439, DSM265, KAF156, MMV390048, etc. (Figure 4.1) [312]. The majority of compounds that

are currently in clinical development originated from phenotypic screening, with the molecular targets initially unknown [312]. Phenotypic screening involves primary screening against *P. falciparum* infected erythrocytes to identify hits in a large array of compounds. The benefit of this approach is that large compound quantities can be pre-screened at a lower cost to identify compounds that decrease parasite numbers *in vitro* and additionally, specific active compound groups can be identified to define possible structure activity relationships.

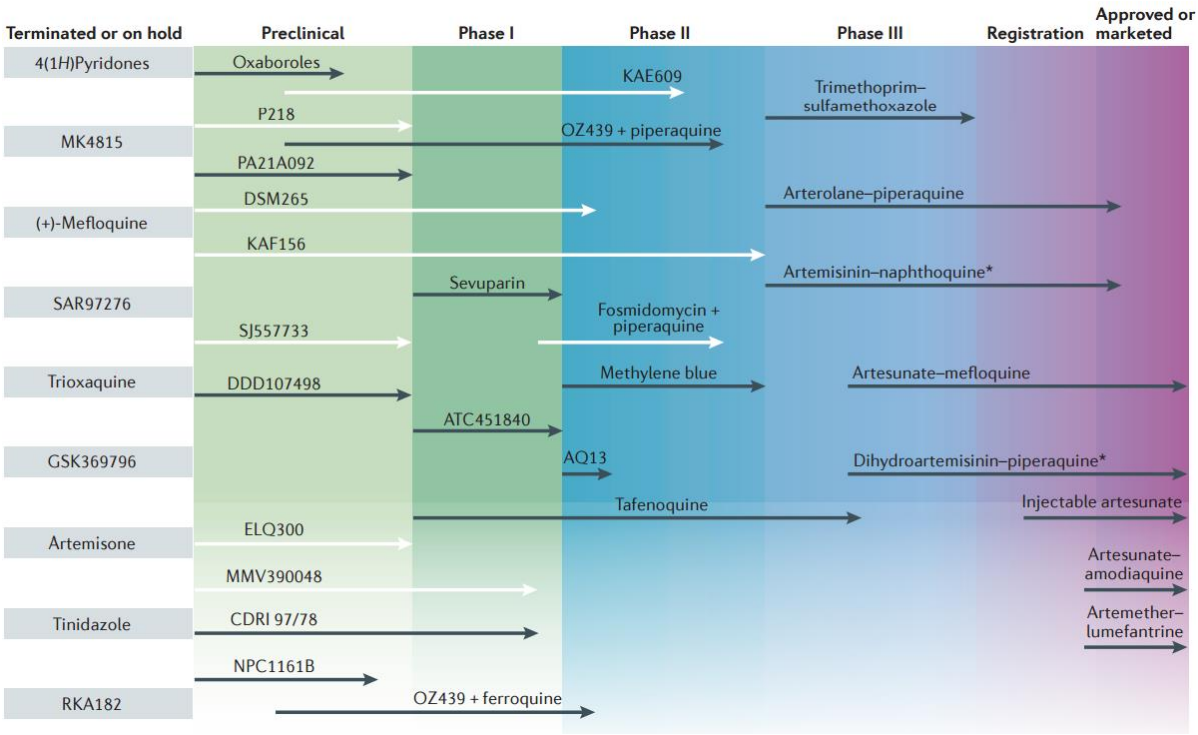

Figure 4.1: Clinical development of novel antimalarial compounds (2010-2015). Various novel candidates have entered the clinical development platform in recent years. Some compounds have been approved for public use, including a wide array of artemisinin combination therapies. Novel chemical scaffolds are also being discovered and are proving to be successful in clinical development, e.g. KAE609, OZ439, MMV390048, etc. Reprinted by permission from Macmillan Publishers Ltd: Nature Reviews Drug Discovery [312], copyright (2015).

Another approach to novel compound identification is target-based screening. The identification of a novel target, preferably in both the asexual and sexual stages, is essential [19]. Certain essential characteristics pertain to novel antimalarial targets, including essentiality in the parasite's life cycle progression, significant variation from the corresponding process in the human host, low probability for resistance, known compounds against the target must exist and the parasite must not be able to evade the target with an alternate pathway [19, 20, 313]. A combination of phenotypic screening that is focused on potential drug targets (i.e. target-focused library) e.g. kinase inhibitor screens, has also been successful in antimalarial drug discovery [314].

Drug repurposing is a third avenue to discover new antimalarials and rely on the evaluation of compounds that have previous described activity against another disease, for its activity against malaria parasites. In oncology research, epigenetic therapeutics have been a large area of focus over the past decade, as inhibition of epigenetic modulators result in epigenetic de-regulation with antitumor activity, which evidently hold great promise as targets for anticancer therapies [315]. Most 'epi-drugs' target the histone modifying enzymes and DNMTs, or facilitate reader interference by inhibiting or activating epigenetic processes, and various anticancer epi-drugs have been approved for clinical use, including Azacitidine, Decitabine, Vorinostat and Romidepsin (Figure 4.2) [316]. Azacitidine (5-azacytidine) and Decitabine (5-aza'-2-deoxycytidine) are DNMT inhibitors (DNMTi), thereby removing the methyl group from CpG islands [317]. These two DNMTi have been approved for the treatment of myelodysplastic syndrome and low-blast count acute myeloid leukemia [318]. Vorinostat (Suberoylanilide hydroxamic acid; SAHA) and Romidepsin, inhibitors of some classes of HDACs (HDACi) that result in restoration of histone acetylation patterns, have recently been approved for the treatment of progressive or recurrent cutaneous T-cell lymphoma [319]. Various other HDACi, DNMTi and other epigenetic inhibitors (e.g. GSK2879552 – LSD1 inhibitor) are currently in clinical development for the treatment of various cancers [316].

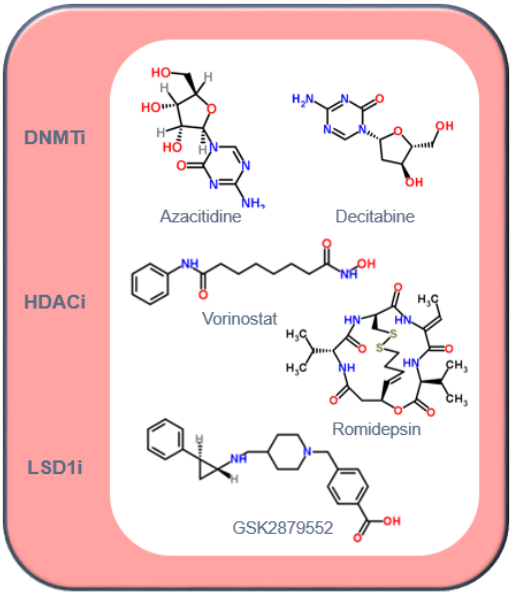

Figure 4.2: Epi-drugs approved or in clinical development in cancer. DNMTi (Azacitidine and Decitabine) and HDACi (Vorinostat and Romidepsin) have been clinically approved for use in certain cancers. LSD1i (GSK2879552) is currently in clinical development. Data obtained from [316].

Selective anticancer epi-drugs have previously been investigated for their activity against *P. falciparum* asexual and gametocyte stages as the unusual epigenome of the malaria parasite is hypothesised to be the parasite's "weak spot" (Table 4.1) [102]. Epi-drugs

disturb the parasite's gene expression, ultimately leading to cell death [320-322]. HDACs are seen as promising drug targets due to resultant hyperacetylation and ultimate cell death, and upon investigation, HDACi including SAHA, Belinostat, Romidepsin, Panobinostat and Trichostatin A (TSA), have shown selective inhibition against asexual *P. falciparum* stages [159, 322, 323]. Panobinostat was clinically approved for the treatment of multiple myeloma and shows potent inhibition against *P. falciparum* asexual stages [323] and late stage gametocytes [324]. TSA and SAHA showed potent inhibitory activity against both early and late stage gametocytes [223]. In *P. falciparum*, HKMTs are involved in both transcriptional activation (H3K4me) and repression (H3K9me), and are also hypothesised to be promising drug targets [222]. One such HKMTi, BIX01294, successfully inhibits asexual *P. falciparum* proliferation and gametocyte viability [222], and the LSD1 inhibitor Tranylcypromine also showed micromolar activity against the asexual parasites.

Table 4.1: Epi-drugs with reported activity against *P. falciparum* asexual and gametocyte stages. The compound name, together with the type of epigenetic inhibitor [histone deacetylase (HDAC); histone lysine methyltransferase (HKMT); and histone demethylase (HDM)], chemical structure, asexual IC_{50} (μM) and late stage gametocyte IC_{50} (μM) is shown.

Compound name	Type of inhibitor	Chemical structure	*P. falciparum* asexual IC_{50} (μM)	*P. falciparum* late stage gametocyte IC_{50} (μM)
Belinostat (PXD101)	HDAC	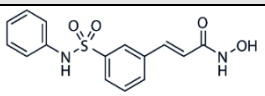	0.06	-
BIX01294	HKMT	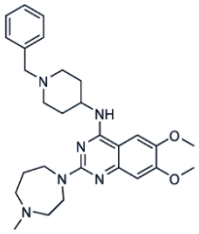	0.075	3.84 (*1.07)
Panobinostat (LBH 589)	HDAC	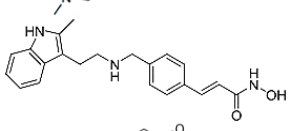	0.01	0.935
Romidepsin (FK228)	HDAC	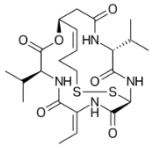	0.09	0.637
Tranylcypromine	HDM	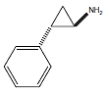	34	-
Trichostatin A (TSA)	HDAC	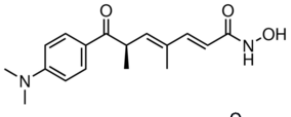	0.01	0.07 (*0.09)
Vorinostat (SAHA)	HDAC	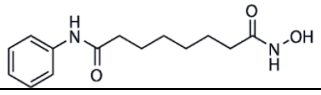	0.12	0.81 (*1.41)

*IC_{50} value against early stage gametocytes

This data support the notion that epigenetic modulators could be essential drug targets in parasite development as well as differentiation. Exploring additional chemotypes for inhibition of these epigenetic modulators is therefore needed. Various other epi-drugs, specifically developed in the cancer research field, have not yet been tested against *P. falciparum* and should be explored as potential antimalarial agents.

In this study, a library of anticancer compounds (Cayman Epigenetics Screening Library, Cayman's Chemicals, USA) with known capabilities to inhibit epigenetic modulators in these cells, were tested for their antiplasmodial activity against multiple *P. falciparum* stages, including asexual parasites, early and late stage gametocytes. Early stage gametocytes were shown to be more susceptible to epigenetic inhibition when compared to the other two stages. Epi-drugs were shown to have limited resistance potential but definite cytotoxicity concerns. We also demonstrate that HDACi and HKMTi are multi-stage potent compounds with the potential to be used as chemical starting points in the antimalarial drug discovery pipeline. This work provides the first multi-stage investigation of the antiplasmodial capabilities of epi-drugs to this scale.

4.2 Materials & Methods

4.2.1 SYBR Green I-based fluorescence assay to determine inhibition against the asexual *P. falciparum* parasite stages

P. falciparum parasites were maintained at 37˚C in human erythrocytes suspended in complete culture medium and ring-stage synchronised as described in Section 2.2.1, Chapter 2. The SYBR Green I-based fluorescence assay (as a proxy of DNA replication in viable cells) was used in this study to determine compound activity against the asexual stages of the parasite's life cycle [325-327]. *In vitro* ring-stage intra-erythrocytic *P. falciparum* 3D7 parasite cultures (genotyped drug sensitive) at 1% haematocrit and 1% parasitaemia were treated with compounds at 1 and 5 µM for dual-point primary screening of inhibitory activity. The controls for this assay included chloroquine disulphate (1 µM, positive drug control) and complete RPMI media (growth control). The treated parasites were allowed to grow for 96 h at 37˚C, where after equal volumes (100 µl each) of the *P. falciparum* parasite suspensions were incubated with SYBR Green I lysis buffer [0.2 µl/ml 10000xSYBR Green I (Invitrogen); 20 mM Tris, pH 7.5; 5 mM EDTA; 0.008% (w/v) saponin; 0.08% (v/v) Triton X-100] for 1 h at 37˚C in the dark. The fluorescence was measured using a Fluoroskan Ascent FL microplate fluorometer (Thermo Scientific, excitation at 485 nm and emission at 538 nm). The data were represented as a percentage of the treated control after background subtraction (chloroquine-treated infected RBC samples in which parasite proliferation was completely inhibited), to determine the percentage inhibition for each compound. Unless otherwise stated, each compound was screened in technical triplicates for at least three independent biological replicates (n=3). The hit compounds were selected for full dose response evaluation (IC_{50} determination) if they showed good or moderate activity based on pre-determined and standardised selection criteria (Table 4.2), or showed promising compound stability under freeze/thaw conditions.

Table 4.2: Selection criteria of primary compound screens. Compounds were selected for IC_{50} determination if they showed good activity (>70% inhibition at 5 µM and >50% inhibition at 1 µM), considered at moderate activity but not at minimal activity [247].

Good activity (IC_{50} expected to be below 1 µM)	>70% inhibition at 5 µM and >50% inhibition at 1 µM
Moderate activity (IC_{50} expected to be between 1 and 5 µM)	>70% inhibition at 5 µM and <50% inhibition at 1 µM <70% inhibition at 5 µM and >50% inhibition at 1 µM 50 to 70% inhibition at 5 µM and <50% inhibition at 1 µM
No/minimal activity (IC_{50} expected to be above 5 µM)	<50% inhibition at 5 µM and <50% inhibition at 1 µM

A full dose-response evaluation was performed for hit compounds against the *P. falciparum* drug sensitive 3D7 strain, as well as the W2 (chloroquine, quinine, pyrimethamine and cycloguanil resistant) and K1 (chloroquine, pyrimethamine, mefloquine and cycloguanil resistant) strains. A minimum of 9-point curves were evaluated using 2-fold dilution series of each drug individually. From these, the inhibitory concentration of the drug needed to affect 50% of the parasite population (IC_{50}), was determined (n=3 ± SEM). For the dose-response curves, data were represented as a percentage of untreated control to determine cell proliferation. Sigmoidal dose-response curves were plotted using GraphPad 5.0, from which the IC_{50} values could be determined. Assay performances were evaluated with average %CV at 4.47 and Z-factors at >0.6.

4.2.2 Parasite lactate dehydrogenase assay to determine inhibition against the early and late stage *P. falciparum* gametocytes

Gametocytes were induced from an asexual *P. falciparum* NF54-PfS16-GFP-Luc (early stage gametocytes) or NF54-Mal8p1.16-GFP-Luc (late stage gametocytes) culture (see Section 2.2.1, Chapter 2 [247]). To determine gametocytocidal activity of compounds against early and late stage gametocytes, the parasite lactate dehydrogenase (pLDH) assay was performed [247, 328]. This assay relies on the preference of *P. falciparum* LDH for 3-acetylpyridine adenine dinucleotide (APAD) as a coenzyme in the reaction leading to the conversion of lactate to pyruvate compared to host LDH, for the colorimetric measurement of a formazan product [329]. Early and late stage *P. falciparum* gametocyte cultures (2% haematocrit, 5% gametocytaemia) were treated with compounds at 1 and 5 µM for dual-point primary screening of inhibitory activity. The controls for this assay included Methylene blue (5 µM, positive control for inhibition) and complete RPMI media (gametocyte viability control). The treated gametocytes were allowed to mature for 72 h

at 37˚C, after which a proportion of the culture medium (70 µl) was replaced and the plates incubated for a further 72 h. This was followed by the addition of Malstat reagent [0.21 % v/v Triton-100; 222 mM L-(+)-lactic acid; 54.5 mM Tris; 0.166 mM APAD (Sigma-Aldrich); adjusted to pH 9 with 1 M NaOH] and PES/NBT [1.96 mM nitro blue tetrazoliumchloride (NBT); 0.239 mM phenazine ethosulphate (PES)]. The ratio of parasite suspension:Malstat:PES/NBT was kept consistent at 1:5:1.25. The plates were incubated for 40 min in the dark, after which the absorbance was measured with a Multiskan Ascent 354 multiplate scanner (Thermo Labsystems, Finland) at 620 nm.

The data were represented as a percentage of the treated control after background subtraction (methylene blue-treated infected RBC samples in which parasite viability was completely inhibited), to determine the percentage inhibition for each compound. Each compound was screened in triplicate for one independent biological replicate (n=1) against early and late stage gametocytes. Compounds were selected for IC_{50} determination if they showed good or moderate activity (as outlined in Table 4.2, Section 4.2.1), and showed promising compound stability under freeze/thaw conditions.

A full dose-response evaluation was performed for hit compounds against early and late stage *P. falciparum* gametocytes at predetermined concentration ranges. From these, the inhibitory concentration of the drug needed to affect 50% of the parasite population (IC_{50}), was determined (n=3 ± SEM). For the dose-response curves, data were represented as a percentage of untreated control to determine gametocyte viability. Sigmoidal dose-response curves were plotted using GraphPad 5.0, from which the IC_{50} values could be determined. Assay performances were evaluated with average %CV at 4.54 and Z-factors at >0.5.

4.3 Results

4.3.1 Antiplasmodial activity, cross-resistance and selectivity against asexual *P. falciparum* stages

All 95 compounds comprising the Cayman Epigenetics library were screened for *in vitro* activity against 3D7 *P. falciparum* asexual parasites. Each compound was screened at two concentrations (1 and 5 µM) to allow selection of the most active compounds for IC_{50} determination (data for all compounds in Appendix II: Table A1). Based on these selection criteria, we observed a 24% hit rate, with 15% of the compounds from the epi-drug library that showed good activity and 9% of compounds described as only moderately active. The majority of the compounds (76%) showed no/minimal activity against asexual stages (Figure 4.3).

Of the hits, 21 compounds met the criteria for selection for IC_{50} determination (>50% inhibition at 1 µM or >70% inhibition at 5 µM). This included 5 moderately active compounds (Ellagic acid, Tenovin-6, Oxamflatin, Suberohydroxamic acid and CBHA). SB939, HC Toxin, UNC0638, ITF2357, BIX01294, CAY10398 and TSA were shown to be highly active against the asexual stages, with 100% inhibition at 5 µM and 80-100% inhibition at 1 µM. Scriptaid and (-)-Neplanocin A were excluded from IC_{50} determination due to compound instability during consecutive freeze/thaw cycles, despite showing promising inhibition.

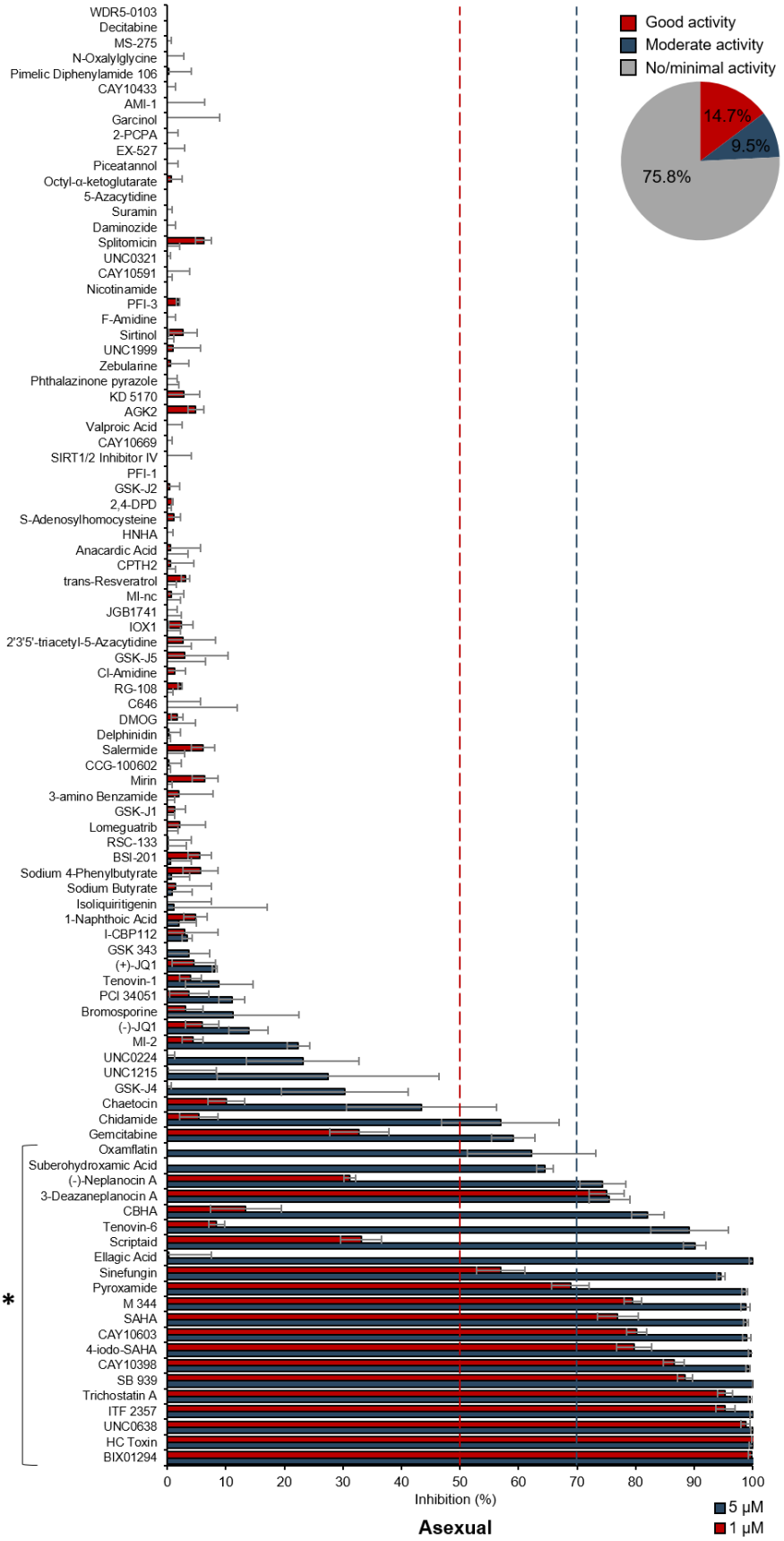

Figure 4.3: *In vitro* activity against asexual 3D7 *P. falciparum* parasites. Primary compound screening of 95 epi-drugs was performed using the SYBR Green I-based fluorescence assay at 1 µM and 5 µM, with 21 active compounds (*) selected for IC_{50} determination for asexual stages. Compounds were grouped into three categories: good activity, moderate activity or no/minimal activity based on % inhibition at 1 µM and 5 µM and selection criteria set out in Table 4.2. Results for all compounds are representative of three independent biological replicates with technical triplicates (n=3 ± SEM).

The IC_{50} of the selected active epi-drugs was determined on the asexual 3D7, drug sensitive strain of *P. falciparum* parasites. In parallel, this was also performed for K1 and W2 (both drug resistant) strains of *P. falciparum* to determine if cross-resistance is found against the active epi-drugs (Figure 4.4; see Appendix I: Figure A3 for the dose-response curves of the other compounds not shown here; IC_{50} values above 100 nM).

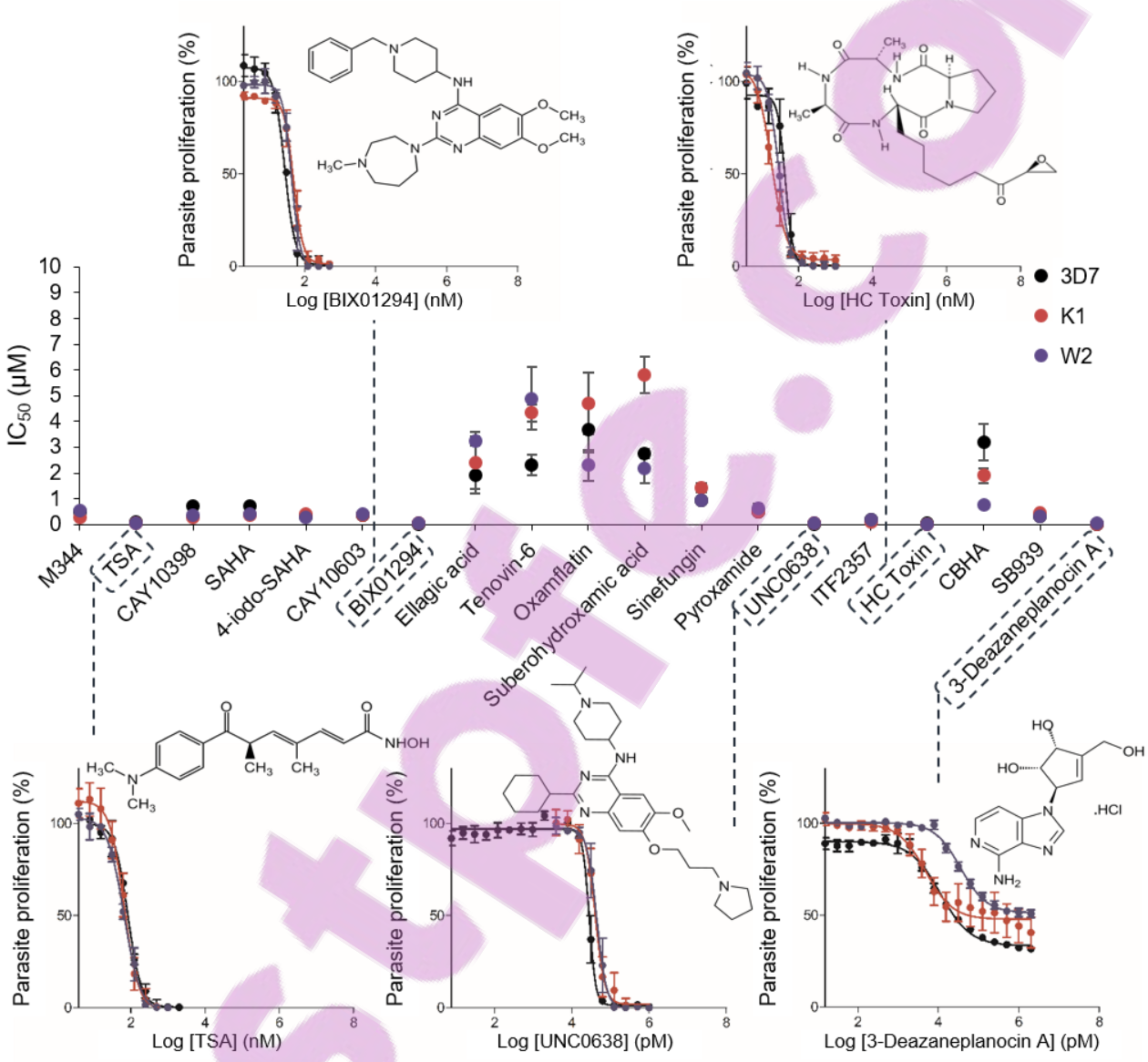

Figure 4.4: Comparative IC_{50} values for the most active epi-drugs against asexual drug sensitive and resistant *P. falciparum* strains. Compounds were screened using the SYBR Green I-based fluorescence assay to determine dose-response against 3D7 (drug sensitive, black), K1 (drug resistant, red) and W2 (drug resistant, blue). Results for all compounds are representative of three independent biological replicates (n=3 ± SEM).

Collectively, IC_{50} values were determined for 19 compounds against three asexual *P. falciparum* parasite strains, ranging between 7 nM to 6 μM. Five compounds showed IC_{50} values below 0.1 μM against asexual drug sensitive and drug resistant *P. falciparum* parasite strains, namely TSA, BIX01294, UNC0638, HC Toxin and 3-Deazaneplanocin

A, that are seen as highly active against all parasite strains (Figure 4.4 & Table 4.3). TSA, BIX01294 and SAHA showed similar IC_{50} values to those found in previous reports, validating the accuracy of our data [222, 223, 322]. 3-Deazaneplanocin A could consistently not cause complete parasite clearance irrespective of concentration up to 100 µM or of exposure time (24, 48, 72 and 96 h) (see Appendix I: Figure A4). Nine compounds (M344, CAY10398, SAHA, 4-iodo-SAHA, CAY10603, Sinefungin, Pyroxamide, ITF2357 and SB939) reported moderate activity with IC_{50} values ranging between 0.1 µM and 1 µM. This left five compounds (Ellagic acid, Tenovin-6, Oxamflatin, CBHA and Suberohydroxamic acid) that are not considered to have potent activity with IC_{50} values above 1 µM for all three parasite strains, as predicted by the primary dual-point screens (moderately active compounds).

Table 4.3: Cross-resistant dose-response for the active epi-drugs. Compounds were screened for IC_{50} against 3D7, K1 and W2 asexual parasite strains using the SYBR Green I-based fluorescence assay. The resistance index (RI; shaded grey) and selectivity index (SI) for each compound is shown. Compounds with SI>10 are shaded in blue. Results for all compounds are representative of three independent biological replicates with technical triplicates (n=3 ± SEM).

Compound name	IC_{50} value against *P. falciparum* strains								IC_{50} value against human cell line (µM) [a]	SI (based on 3D7 IC_{50})
	3D7		K1			W2				
	Value (µM)	±SEM	Value (µM)	±SEM	RI (K1/3D7)	Value (µM)	±SEM	RI (W2/3D7)		
M344	0.51	0.08	0.29	0.04	0.57	0.53	0.04	1.04	2.3	4.6
TSA	0.078	0.008	0.066	0.008	0.85	0.066	0.005	0.85	0.2	2.6
CAY10398	0.726	0.005	0.2723	0.0032	0.38	0.363	0.030	0.50	-	-
SAHA	0.71	0.12	0.37	0.04	0.52	0.43	0.06	0.61	5	7
4-iodo-SAHA	0.30	0.07	0.40	0.05	1.33	0.27	0.05	0.90	1.1	3
CAY10603	0.37	0.08	0.367	0.028	0.99	0.428	0.023	1.16	10.8	29
BIX01294	0.028	0.006	0.047	0.007	1.68	0.045	0.006	1.61	11	393
Ellagic acid	1.9	0.5	2.4	1.2	1.26	3.25	0.19	1.71	45	23.7
Tenovin-6	2.3	0.4	4.33	0.32	1.88	4.9	1.2	2.13	6.09	2.65
Oxamflatin	3.7	0.9	4.7	1.2	1.27	2.3	0.6	0.62	0.25	0.07
Suberohydroxamic acid	2.77	0.18	5.8	0.7	2.09	2.2	0.6	0.79	50	18
Sinefungin	0.94	0.04	1.43	0.16	1.52	0.949	0.032	1.01	-	-
Pyroxamide	0.51	0.14	0.50	0.07	0.98	0.64	0.15	1.25	-	-
UNC0638	0.0283	0.0032	0.039	0.005	1.38	0.05	0.01	1.77	23	812
ITF2357	0.17	0.01	0.122	0.028	0.72	0.178	0.015	1.05	0.2	1.2
HC Toxin	0.035	0.013	0.019	0.004	0.54	0.0291	0.0016	0.83	0.037	1
CBHA	3.2	0.7	1.9	0.3	0.59	0.77	0.04	0.24	1.8	0.56
SB939	0.32	0.11	0.44	0.10	1.38	0.30	0.04	0.94	1.48	5
3-Deazaneplanocin A	0.0117	0.0023	0.007	0.004	0.60	0.0358	0.0032	3.06	0.19	16

The resistance index (RI; ratio of the IC_{50} value of the resistant strain to the sensitive strain, i.e. K1/3D7 and W2/3D7) was calculated for each compound to assess the potential of resistance development (due to e.g. similar mode of action) of known resistant parasite strains to these novel epi-drugs. A maximum RI of 3 was obtained (average RI of 1.12), indicating limited cross-resistance to the K1 and W2 *P. falciparum* parasite strains that still show low µM IC_{50} values (Table 4.3).

The selective toxicity of the compounds towards *P. falciparum* parasites was also evaluated. IC_{50} values on various mammalian cell lines were collected for the compounds where the data was previously determined in other studies [159, 330-336]. The selectivity index (SI; compound IC_{50} mammalian cell/IC_{50} *P. falciparum*) for each compound was subsequently calculated based on the 3D7 IC_{50} values. CAY10603, BIX01294, Ellagic acid, Suberohydroxamic acid, UNC0638 and 3-Deazaneplanocin A (shaded in blue; Table 4.3) showed SI values >10, indicating that these compounds do not show general cytotoxicity to mammalian cells and that *P. falciparum* parasites show selective sensitivity to these compounds (as outlined by the MMV criteria for validated hits [337]). BIX01294 and UNC0638 were shown to be highly selective towards the parasite with SI>300. For most of the other active compounds against *P. falciparum* asexual stages, cytotoxicity is an apparent issue with inhibition of epigenetic modulators, with compounds such as Oxamflatin, ITF2357, HC Toxin and CBHA showing major cytotoxicity concerns where IC_{50} values are closely related between the parasite and mammalian cell lines.

4.3.2 Gametocytocidal activity & dual reactivity against early and late stage *P. falciparum* gametocytes

The 95 compounds were screened for *in vitro* activity against early and late stage *P. falciparum* gametocytes at 1 and 5 µM using the pLDH assay, after which the most active compounds were selected for IC_{50} determination (data for all compounds in Appendix II: Table A1). For the early stage gametocytes, a 30% hit rate was observed based on the selection criteria, where 13% of compounds from the epi-drug library showed good activity and 18% of compounds described as only moderately active. This differed for late stage gametocytes with an 18% hit rate, with 10% and 8% of the compounds showing good or moderate activity, respectively. The majority of the compounds showed no/minimal activity against early (69%) and late (82%) stage gametocytes (Figure 4.5).

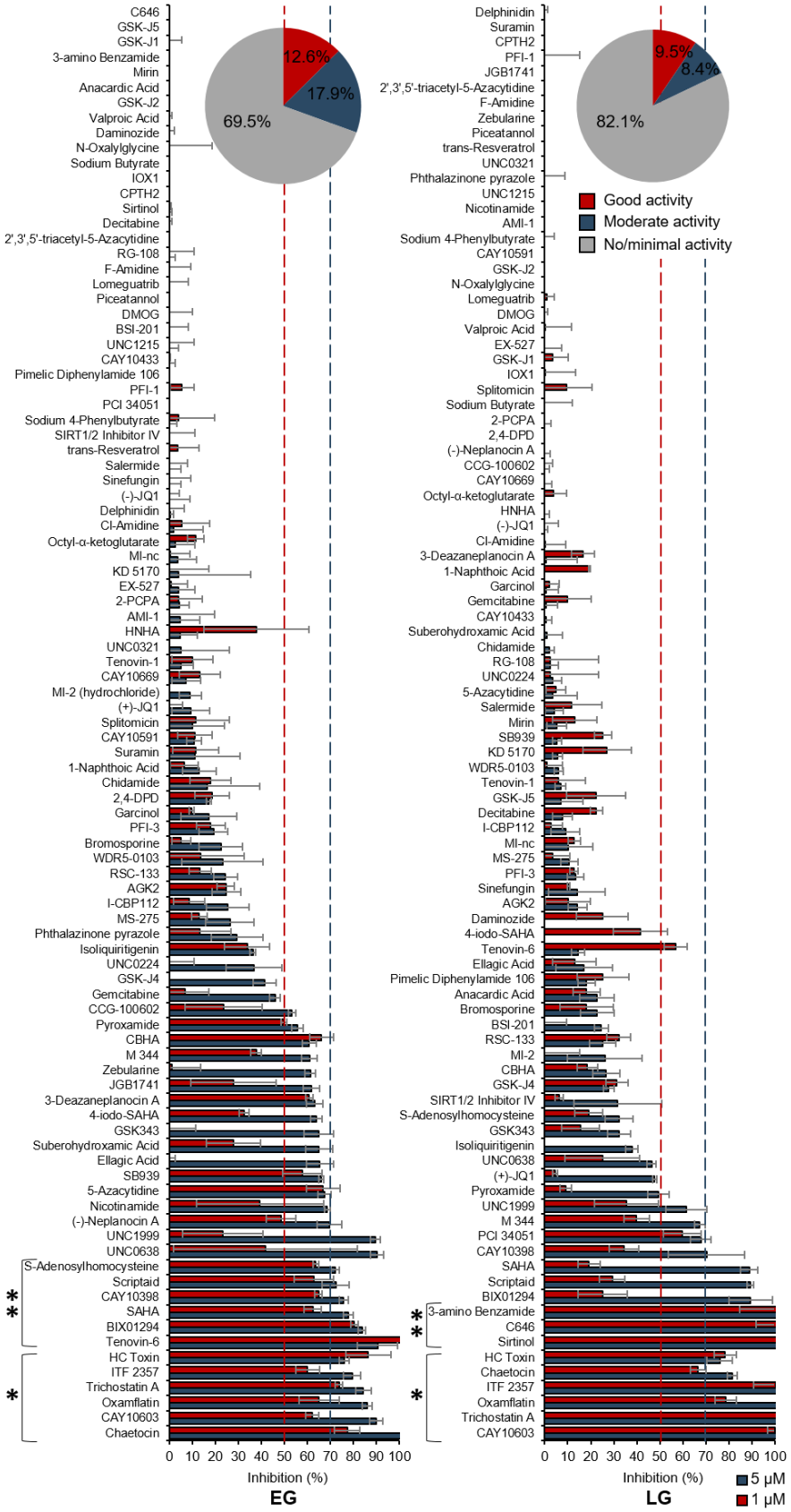

Figure 4.5: *In vitro* activity against early and late stage gametocytes. Primary compound screening of 95 epi-drugs was performed using the pLDH assay at 1 µM and 5 µM, with 6 active compounds (*) selected for IC_{50} determination for early (EG) and late stage (LG) gametocytes. Additional active compounds (**) were identified but not selected for IC_{50} due to not being active against both stages. Compounds were grouped into three categories: good activity, moderate activity or no/minimal activity based on inhibition at 1 µM and 5 µM and selection criteria set out in Table 4.2. Results for all compounds are representative of one independent biological replicate with technical triplicates (n=1 ± SD).

For early and late stage gametocytes, 12 and 9 compounds met the criteria for selection for IC_{50} determination, respectively. The compounds were further filtered based on dual reactivity and resulting compounds were selected for IC_{50} determination if they showed promising activity against both these stages, and not specificity towards either early or late stage gametocytes. This resulted in 6 compounds that were highly active against both stages, including CAY10603, Chaetocin, HC Toxin, ITF 2357, Oxamflatin and Trichostatin A. For early stage gametocytes, 6 additional compounds showed promising activity but were not selected for IC_{50} determination due to lack of late gametocyte activity (BIX01294, CAY10398, S-Adenosylhomocysteine, SAHA, Scriptaid and Tenovin-6). This differed in late gametocytes, where only 3 compounds showed additional good activity that were excluded from IC_{50} determination (3-amino Benzamide, C646 and Sirtinol).

IC_{50} values were ultimately determined for 4 compounds showing dual reactivity against early and late stage gametocytes, ranging between 1-3 µM (Figure 4.6A & B). HC Toxin was excluded from IC_{50} determination despite promising activity due to compound quantity limitations and cytotoxicity concerns based on the asexual selectivity data. Trichostatin A was also excluded from IC_{50} determination due to previous reports already showing potent activity (IC_{50} values below 100 nM) against both early and late stage gametocytes, signifying potent dual reactivity and this makes it a good epi-drug for comparative purposes [223]. Chaetocin (0.92 ± 0.29 µM early gametocyte IC_{50}; 1.34 ± 0.17 µM late gametocyte IC_{50}) and CAY10603 (1.6 ± 0.8 µM early gametocyte IC_{50}; 1.30 ± 0.29 µM late gametocyte IC_{50}) showed potent activity (i.e. low IC_{50} values) against both early and late stage gametocytes (Figure 4.6C), similar to the well-known HDACi, SAHA (1.41 ± 0.13 µM early gametocyte IC_{50}; 0.81 ± 0.21 µM late gametocyte $IC_{50;}$ [223]). Oxamflatin (1.2 ± 0.6 µM early gametocyte IC_{50}; 3.0 ± 0.4 µM late gametocyte IC_{50}) and ITF 2357 (3.0 ± 0.9 µM early gametocyte IC_{50}; 2.23 ± 0.09 µM late gametocyte IC_{50}) also showed dual reactivity, but preference toward early and late gametocytes, respectively.

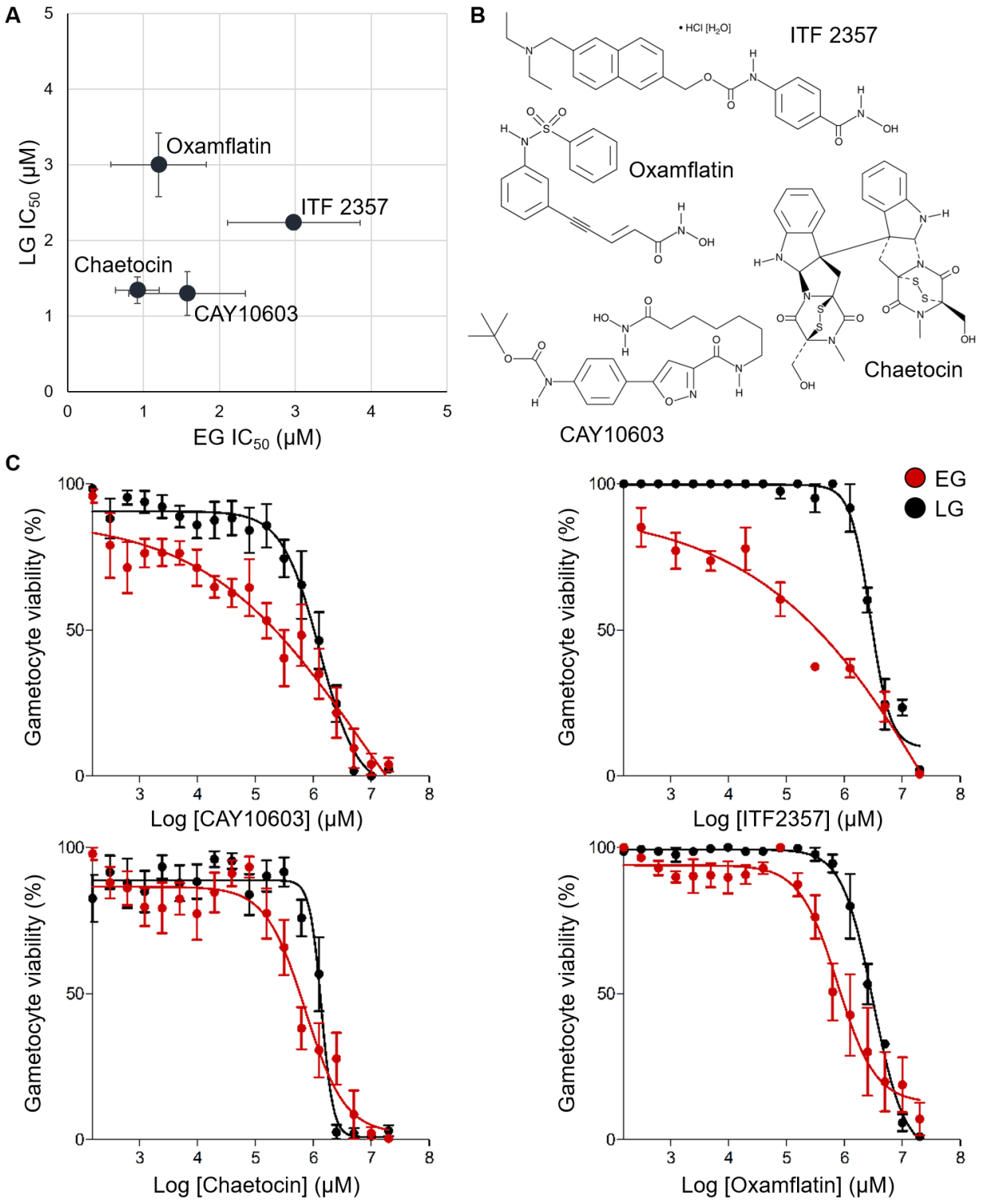

Figure 4.6: Dual reactivity against early and late stage *P. falciparum* gametocytes. (A) Compounds were screened using the pLDH assay to determine dual reactivity against early (EG) and late (LG) stage gametocytes, comparative IC_{50} values shown. **(B)** Chemical structures of the dual reactive compounds CAY10603, Chaetocin, ITF 2357 and Oxamflatin. **(C)** Full dose-response and IC_{50} values (μM) for each compound were determined against EG (red) and LG (black). Data are representative of three independent biological replicates with technical triplicates (n=3 ± SEM; n=2 for only ITF2357 against LG).

4.3.3 HDACi and HKMTi are potent multi-stage targeting epi-drugs

The multi-stage activity of the 95 compounds were investigated to identify possible inhibitor classes that show potent activity against all three parasite stages included in the primary screens (5 μM; Figure 4.7A&B; detailed in Appendix II: Table A1). Overall, correlation between the three primary screen datasets was low, with asexual stages and early gametocytes being closest related (Pearson correlation r^2 of 0.5). Asexual parasites and late gametocytes, as well as early and late stage gametocytes showed poor correlation between datasets (r^2 of 0.3 and 0.2, respectively).

The library consists of ~39% HDACi and ~15% HKMTi; with the remaining compounds divided into 11 other inhibitor types (Figure 4.7A). Inhibitor types that mostly lacked activity against all three parasite stages interrogated include HAT, DNA demethylase (DNDM), DNMT, PRMT, Protein arginine deiminase, Bromodomain, HDM, Hydroxylation, LSD, phosphorylation (Phospho) and unclassified compounds. Some compounds showed good/moderate activity against only one or two parasite stages. Within these compounds, some showed distinct dual stage-specific activity against asexual and early gametocyte stages (CBHA, Ellagic Acid, SB939, Suberohydroxamic acid, 3-Deazaneplanocin A, (-)-Neplanocin A, 4-iodo-SAHA), or both gametocyte stages (UNC1999) (Figure 4.7B&C). Additionally, some compounds showed stage-specific activity for a single parasite stage, specific for only asexual (Sinefungin, Gemcitabine), early (S-Adenosylhomocysteine, 5-Azacytidine, GSK 343, Nicotinamide, JGB1741, Zebularine, CCG-100602) or late stage gametocytes (3-amino Benzamide, C646, Sirtinol, PCI 34051).

The 26 compounds that were selected as active hits in the primary screens were further probed to identify multi-stage or stage-specific activity (Figure 4.7C). Compounds with multi-stage activity were classified as having at least 50% inhibition at 5 μM against all three parasite stages and included mostly HDACi (Scriptaid, HC Toxin, ITF 2357, Tenovin-6, CAY10603, M 344, Oxamflatin, Pyroxamide, Trichostatin A, CAY10398, SAHA, Chidamide) and some HKMTi (Chaetocin, UNC0638, BIX01294).

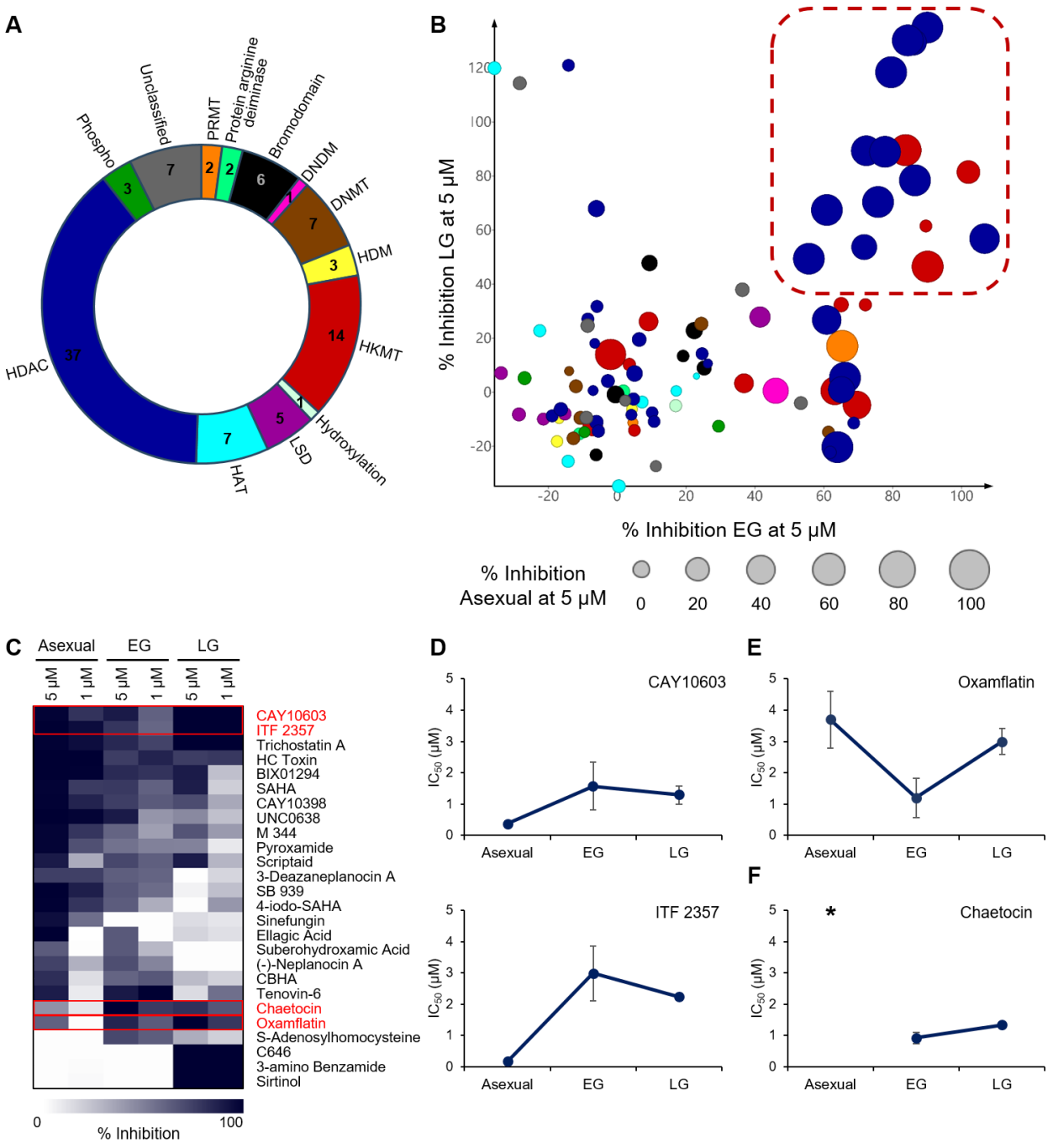

Figure 4.7: Multi-stage or stage-specific activity of different epi-drugs. (A) Epi-drug library composition based on inhibitor type; including PRMT, Protein arginine deiminase, Bromodomain, DNDM, DNMT, HDM, HKMT, Hydroxylation, LSD, HAT, HDAC, Phospho, Unclassified. **(B)** Inhibition at 5 µM (%) was compared between asexual parasites (circle size; n=3) and early (EG) & late (LG) stage gametocytes (n=1); separated based on the inhibitor type (colour scale corresponding to A). Compounds with multi-stage activity were identified (red block). **(C)** Primary screen data at 1 & 5 µM for asexual, EG and LG for the active compounds/hits from all three stages. **(D)** CAY10603 and ITF 2357 shows asexual preference with lower IC_{50} values compared to EG and LG. **(E)** Oxamflatin shows EG preference with lower IC_{50} values compared to asexual and LG. **(F)** Chaetocin shows preference for both EG and LG with lower IC_{50} values compared to the predicted asexual IC_{50} (* = IC_{50} predicted to be above 5 µM based on primary dual-point screen data). IC_{50} values (µM) for each compound are representative of three independent biological replicates with technical triplicates (n=3 ± SEM; n=2 for only ITF 2357 against LG).

Although 4 compounds were confirmed to target all the stages of parasite development, these activities are indeed not equipotent. CAY10603 and ITF 2357 showed the expected loss of activity between asexual parasites and late stage gametocytes (~10-fold for ITF 2357), as previously seen for other multi-stage compounds (Figure 4.7D) [338]. Oxamflatin shows some early gametocyte preference, with lower IC_{50} values compared to asexual parasites and late stage gametocytes (2-3 fold lower IC_{50}; Figure 4.7E) whereas Chaetocin shows preference for both gametocyte stages, with lower IC_{50} values compared to the predicted asexual IC_{50} (Figure 4.7F).

As HDACi and HKMTi show promising activity against multiple *P. falciparum* parasite stages, the structure activity relations between these two inhibitor classes were investigated (Figure 4.8; see Appendix I: Figure A5 for chemical structures of selected groups; Appendix IV: Supplementary File 10 for data & compound SMILES). For the HDACi, 5 compounds showed >80% structural similarity, including Pyroxamide, SAHA, 4-iodo-SAHA, CAY10433 and Pimelic Diphenylamide 106, with a hydroxamate-based structural similarity. Conversely, 4 HKMTi showed >80% structural similarity as 4-quinazolinamine-based structures, including BIX01294, UNC0638, UNC0224 and UNC0321. A few other structurally similar pairs were also identified, including CAY10398 and M 344 (both HDACi) that has multi-stage activity and only differs with a single backbone carbon. However, the majority (>80%) of compounds were not structurally related even though they were identified as active against multiple stages, including CAY10603, Chaetocin, HC Toxin, ITF 2357, Oxamflatin, Scriptaid and Trichostatin A (see Appendix I: Figure A6 for chemical structures of selected compounds). These compounds show promise as chemical starting points for antimalarial optimisation as they have unique chemical scaffolds compared to most compounds and have an altered molecular target.

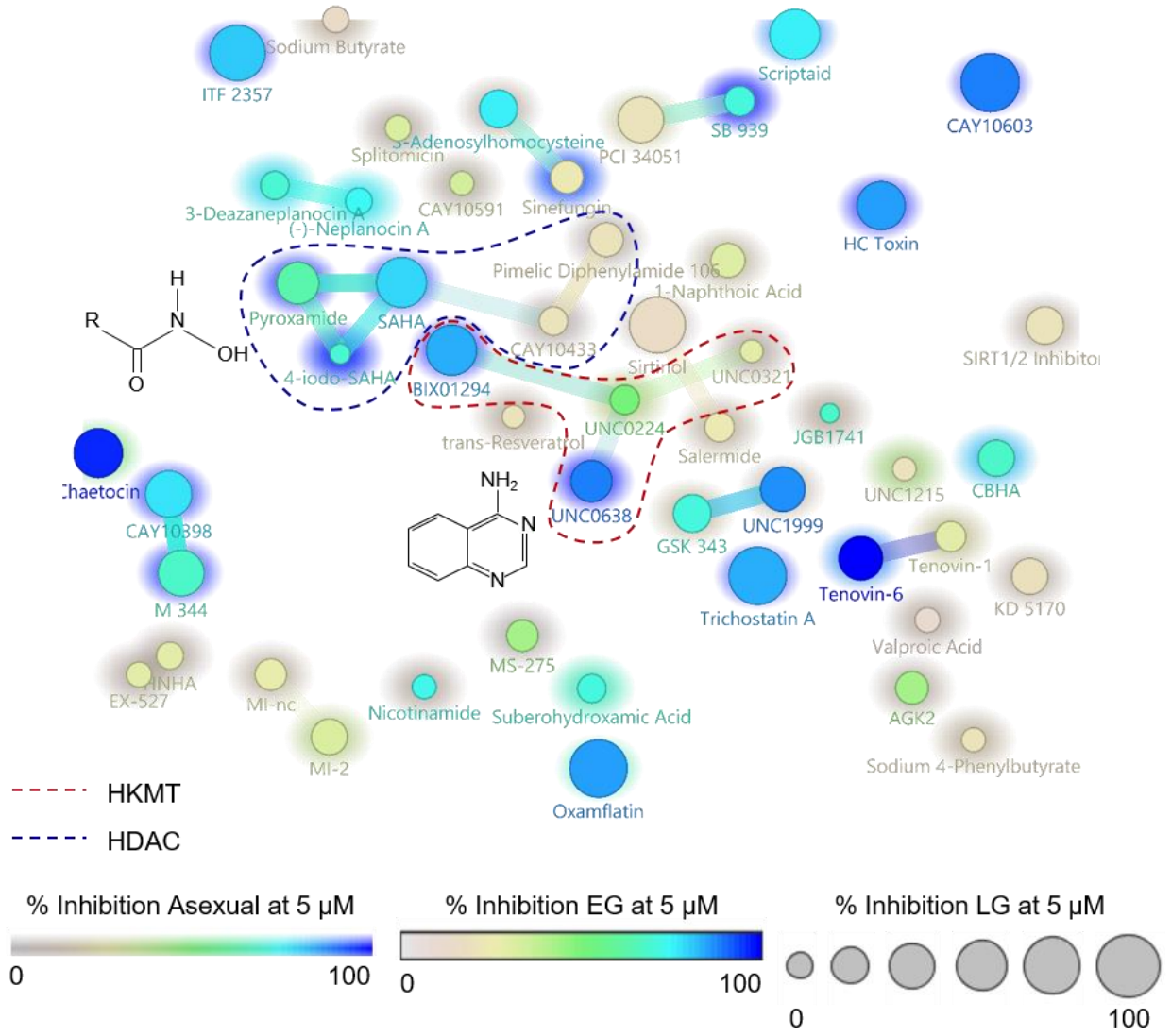

Figure 4.8: Structure activity relationship within the HDAC and HKMT inhibitor series. Structural feature (SkelSphere) analysis was performed with superimposed activity cliff analysis (Osiris DataWarrior V4.2.2) at 80% structural similarity cut-off. Compounds are limited to HDAC (blue line) and HKMT (red line) inhibitors. Inhibition at 5 µM (%) was compared between asexual parasites (background shading; n=3), early (EG; circle colour; n=1) and late (LG; circle size; n=1) stage gametocytes. The active chemical groups shared between two major inhibitor groups are shown; hydroxamate for HDAC and 4-quinazolinamine for HKMT.

4.4 Discussion

Although the understanding of the epigenetic mechanisms of gene regulation in various research areas (neurology, metabolism and infectious diseases) are only emerging [125], epi-drugs are extensively used in cancer research as lead compounds in the drug discovery pipeline due to the contribution of histone PTMs to transcriptional processes in cells, chromatin structure maintenance and DNA repair [324, 339]. The *P. falciparum* parasite's epigenetic regulatory machinery has previously been shown to be a valuable drug target given the importance of gene expression for parasite development, but remains to be exploited in full [94, 159, 222, 322, 333, 340-342]. In this study, various chemical scaffolds known to target the epigenetic gene regulatory machinery were investigated for their antiplasmodial activity against asexual parasites, early and late stage gametocytes. Overall, early stage gametocytes were particularly susceptible to epi-drug inhibition. Potent chemical scaffolds were identified with multi-stage activity, including HDACi and HKMTi with potential to be exploited as lead compounds upon further experimental validation, cytotoxicity reduction and chemical property optimisation.

Early stage gametocytes were the most susceptible to epi-drug inhibition (30% hit rate), corresponding to the unique epigenetic repertoire associated with these stages in Chapter 2, where the switch between asexual and sexual stages was accompanied by dynamic histone PTM landscape alterations [67]. Asexual stage parasites were also prone to epi-drug inhibition (24% hit rate), compared to late stage gametocytes where the least susceptibility was shown (18% hit rate). The overall low correlation between these three datasets are supported by data observed in Chapter 2 and other studies [67, 141, 144], where stage-specific histone PTM dynamics are abundant during life cycle development, with clear peaking trends for some epigenetic mechanisms in particular life cycle stages. Overall, the epi-drugs investigated in this study showed promise as antiplasmodial compounds, with high hit rates for the series compared to previous studies investigating gametocytocidal activity, ranging between 4-33% [343-347]. This can possibly be due to the epigenetic library being target-focused, where higher hit rates are expected compared to high throughput screens of diversity sets [348]. The next step for the epi-drugs would be cross-validation of primary screen data on secondary orthogonal assay platforms e.g. luciferase reporter assay [349], ATP assay [350], etc. (as outlined in [338]). This would increase the confidence of hit prediction to eliminate false positive identifications, reduce the effect of possible compound-mediated interference and investigate different metabolic parameters.

All compounds showed limited potential for cross-resistance development, but the majority were hindered with cytotoxicity concerns, and upon progression in the drug discovery pipeline, these aspects need to be optimised in order to be validated as lead compounds (as outlined by the MMV criteria for validated leads [337]). Firstly, it is inferred that the epi-drugs have altered modes of action to some of the previously known antimalarials for which resistance has developed, e.g. chloroquine, mefloquine, pyrimethamine and cycloguanil. The cross-resistance against artemisinin-resistant strains remains to be determined, as resistance to these front-line therapies are only emerging [17]. Secondly, selective *Plasmodium* inhibition was only shown for 6 compounds of the series (SI>10). This suggests that the epigenetic mechanisms targeted by these compounds (HKMT, HDAC and PRMT) are diverse between the parasite and human, as previously shown by the unique set of *Plasmodium*-specific epigenetic factors that differs vastly from those in its mammalian host [103]. This supports the proposal for the *P. falciparum* parasite's epigenetic gene regulatory machinery as a promising novel target for drug discovery efforts in the malaria field.

Certain epigenetic inhibitor classes were shown to be mostly inactive against all three stages, suggesting that these epigenetic modulators are not essential in the survival of the parasite through development, or that the homologues for these epi-drug mammalian targets are not found in *P. falciparum.* These epigenetic inhibitor classes included phosphorylation, PRMT, DNDM, DNMT, protein arginine deiminase, HDM, hydroxylation, LSD, HAT and bromodomain inhibitors. Some stage-specific compounds include the DNMTi Zebularine that selectively targets early gametocytes, whereas the DNDMi Gemcitabine only targets asexual stages, suggesting possible and antagonistic involvement of DNA methylation-linked chromatin condensation in these stages of development [134]. HATi were only moderately active against early gametocytes, including the stage-specific compound C646, but lacked activity against the other stages. PRMTi were moderately active against asexual and early gametocyte stages, specifically Ellagic Acid, suggesting a possible role of arginine methylation during these stages, but loss in activity occurred as the gametocytes matured. The stage-specific inhibition profiles observed for this wide variety of epi-drug inhibitor classes again support the findings that the parasite makes use of altered epigenetic regulatory mechanisms to differentiate itself during asexual proliferation and sexual differentiation [67, 141, 144].

Investigation of structure-related multi-stage activity for the epi-drugs identified hydroxamate-based HDACi and 4-quinazolinamine-based HKMTi as potent chemical

scaffolds that target *Plasmodium* parasite development at the symptomatic asexual and both transmissible gametocyte forms. Hydroxamate-based HDACi were previously shown to have potent antiplasmodial activity with limited cytotoxicity, and this class contains some clinically approved compounds which have been attempted in drug repurposing studies [322, 323, 334, 351-353]. These compounds lead to DNA hyper-acetylation, resulting in the de-regulation of transcription and ultimately cell cycle arrest and cell death [90]. Some HDACi were also completely pan-inactive, thereby suggesting that the parasite relies on a specific set of HDACs to regulate its chromosomal condensation via acetylation (reviewed in [354]). As an example of the importance of specific acetylation patterns in gene regulation, Apicidin, the class I and II HDAC inhibitor, has been shown to lead to de-regulation of transcription, 60% alternative gene expression and changes in *P. falciparum* parasite growth [96]. The hit compounds selected in this study includes mostly compounds with unique chemical scaffolds that showed activity against all stages, but with stage-specific preferences (CAY10603, Chaetocin, ITF 2357 and Oxamflatin). Stage-specific preference implicated HDACi as showing asexual and early gametocyte preference, whereas HKMTi showed overall gametocyte preference. 4-Quinazolinamine-based HKMTi showed promising potential as antiplasmodial and gametocytocidal compounds in previous reports [222, 333], suggesting that these chemical groups are worth investigating further for antimalarial drug discovery efforts. Selective inhibition of HKMT activity can either lead to an increase or decrease in transcription, depending on the position and degree of methylation and ultimately contributes to transcriptional de-regulation and cell death [222]. One such HKMTi, 3-Deazaneplanocin A, that selectively inhibits H3K27me3 and H4K20me3, was recently shown to reactivate silenced developmental genes in cancer cells that are not silenced by DNA methylation [355]. Unfortunately, this compound was only active against the asexual stages of *P. falciparum*. Collectively, the data implies that the epigenetic modulators affected by these compounds are essential for parasite development throughout its asexual and sexual life cycle. On an epigenetic regulatory level, these compounds directly or indirectly affect transcription based on the tightening or loosening of the chromatin structure, or via the interference of effector protein recruitment.

Our study reveals that certain chemical scaffolds shared between multi-stage active compounds hold potential as chemical starting points in the antimalarial drug discovery pipeline, whereas other unique chemical structures can also be further exploited. We showed that the *P. falciparum* parasite is differentially susceptible to epigenetic

perturbation during asexual and sexual development, contributing to the hypothesis of altered epigenetic regulation during stage-specific parasite development (Chapter 2) [67]. The data suggests that the parasite's epigenetic gene regulation can be seen as a promising novel target class for chemotherapeutic intervention strategies in multiple parasite stages and specifically interfering with parasite transmission via altered gametocyte viability. Overall, these results warrant further examination of the potential antimalarial properties of these hit compounds and to search for or synthesise derivatives of these chemical scaffolds that might have increased potency, selectivity, or improved physico-chemical properties to be validated as a lead for further drug development.

Chapter 5

Concluding Discussion

Despite global efforts to combat malaria, complete drug resistance is an imminent threat as resistance to the current first-line treatment strategies are already emerging [17]. Furthermore, to progress from malaria control to elimination, it is pertinent to target the transmissible sexual forms of the parasite. This greatly emphasises the need to constantly populate the antimalarial drug discovery pipeline, particularly with compounds showing essential transmission blocking capabilities and novel mechanisms of action to avoid resistance [13]. Current limitations in antimalarial drug discovery arise due to our lack of understanding of the complexities associated with specific developmental transitions made by the parasite to ensure its own survival. This typically involves tightly controlled stage-specific *P. falciparum* development through the asexual IDC and the process of gametocyte differentiation, employing a wide array of gene regulatory mechanisms during these processes [66, 68-74, 78, 84-89, 91, 93, 141, 144, 154, 271]. These regulatory mechanisms have, to a large extent, been elucidated in the asexual IDC; however, the full extent and fine-combed functional outcome of stage-specific gene expression and regulation has not been described during gametocytogenesis to date. This process is characterised by essential morphological and molecular adaptations of the parasite to differentiate in preparation for transmission, illuminating various exploitable aspects for drug discovery efforts.

This study particularly aimed to investigate the contribution of epigenetic regulatory mechanisms and protein expression as the result of regulation during stage-specific parasite development, with the focus on gametocyte differentiation. A high-resolution nanoLC-MS/MS approach was selected to quantitatively evaluate the comparative histone PTM landscape and associated proteome between stage-specific gametocyte development. Collectively, this thesis provides extensive evidence of an epigenetic regulatory cascade and how this manifests functionally in altered protein abundance during life cycle development. These findings were extrapolated to antimalarial development, where the unique epigenetic repertoire was chemically targeted, resulting in these aspects being shown as essential for parasite survival and allows for potential novel avenues in antimalarial drug development.

For both the chromatin proteomic and proteomic investigations, the data are comparative between stages following stringent relative and absolute quantification, respectively. This is the first study to quantitatively evaluate the histone PTM landscape and steady-state proteome throughout the five gametocyte stages, with clear stage-specific dynamics indicated for both datasets. In parallel, advanced computational quantification techniques were implemented to allow accurate and consistent analysis of the large amounts of mass spectra generated in this study [243, 280, 282]. Multiple previous reports for both datasets were either limited to the asexual IDC or mosquito stages, or merely reported qualitative data for either early or late gametocyte populations, without stage profiling [68, 69, 71-73, 75-77, 93, 100, 103, 114, 115, 130, 136-143, 224-228].

P. falciparum life cycle progression is inarguably affected by a variety of highly connected epigenetic mechanisms [103] that have been implicated in the regulation of key developmental decisions such as erythrocyte invasion, nutrient uptake, CVGE, stage-specific life cycle development and sexual commitment [115]. Recent findings revealing epigenetic involvement in gametocytogenesis gave rise to various aspects during these developmental stages for which the epigenetic involvement remains unknown [97, 160, 162, 163, 217, 222, 223, 356]. In an attempt to rectify this, we showed that the histone PTM landscape is highly dynamic and adaptable during stage-specific progression, and that specific combinations of activating/repressive epigenetic signals alternate between stages where tight control of specific gene sets are needed. Our data, together with findings showing epigenetically-driven sexual commitment [160, 162, 163, 217], imply that these parasites are able to use particular combinations of histone PTMs and associated effector proteins to differentiate themselves between life cycle stages once the binary commitment decision has been made. Our ability to distinguish between different modified states and to identify unique PTM combinations using quantitative mass spectrometry adds a level of depth to previous reports and can also aid in the design of novel chemotherapeutic interventions [268].

Although we did not functionally characterise our data to identify genomic occupation (e.g. ChIP-on-chip), we extrapolated previous findings to our data to show that euchromatic/heterochromatic transcriptional states could be associated during life cycle progression [141, 144]. Particularly, gametocytogenesis was associated with a fine-tuned balance of activating/repressive histone PTMs, inferring a poised transcriptional state. This is reminiscent of stem cells where genes are switched on or off as cell differentiation is required, also involving a balanced combination of activating/repressive histone PTMs

[251, 357, 358]. As previously suggested, *P. falciparum* parasites seemingly retain genes in a repressed state, but possess the ability to rapidly switch them on when they are required to progress into the next developmental stage [291]. The data collectively suggest that these histone PTMs that are associated with specific parasite stages integrate specific environmental and developmental cues to facilitate stage-specific life cycle progression [94].

These observations support the model that the *P. falciparum* parasite employs a tightly regulated highly interconnected gene expression cascade that features distinct mechanisms as the parasite is required to alter its morphology and biology to develop into the next stage [66, 69, 73, 78, 89, 146, 179]. This is additionally complemented by the diverse RNA transcriptional dynamics [271] and epigenetic involvement during differentiation [67, 160, 163, 210], integrating various levels of gene regulation throughout gametocytogenesis. During gametocytogenesis, gene expression was shown to be specifically associated with distinctive post-transcriptional and translational regulation that differed between early and late stage gametocyte development and was not found during the asexual IDC, implying that these stages of the parasite goes about gene regulation in vastly different ways than their asexual counterpart. However, although the associated proteins appear to be present throughout development, the dynamic expression profiles suggest that key modulators are associated with certain developmental branch-points, implying that there may be more complex gaps in our current understanding of gene expression regulation in gametocytogenesis than initially assumed. This leaves room for speculation on whether epigenetic mechanisms drive sexual differentiation, or if it is the result of invaluable pre-programmed cellular events. Additionally, the stage-specific proteins involved in female development appear to be part of a sequential cascade that facilitates female gametocyte evolvement into the next stage, where different protein sets take over the regulatory role in subsequent stages. We propose that gametocytes adopt a well-balanced regulatory cascade involving various facets, including post-transcriptional, translational and post-translational regulation, and that epigenetic mechanisms might drive stage-specific protein expression during gametocyte differentiation.

Upon further investigation, these highly abundant proteins that are proposed key regulators of specific gametocyte stages might be further exploited as either diagnostic markers to detect gametocytes through highly abundant proteins, or as stage-specific markers to be utilised in drug screening platforms, as the proposed metabolic quiescence

of late stage gametocytes has restricted the development of screening assays to date [247, 338, 346]. One application of the latter could be to identify male/female-biased markers to be exploited very early on in gametocytogenesis in e.g. the dual-gamete formation assay to primarily assess the possibility of compound sex-specificity *in vitro* [359].

Based on the collective evidence for the involvement of epigenetic regulation in *P. falciparum* life cycle development [67, 77, 141] and the unique *Plasmodium*-specific epigenetic repertoire compared to model eukaryotes [131], epigenetic modulators are suggested as a novel target class for malaria control strategies. Various studies pertaining to the essentiality of the histones, histone modifying enzymes and associated effector proteins showed that a vast majority of these proteins are likely essential in *P. falciparum* development (or orthologous proteins are essential for *P. berghei*) [360-364]. Our data show that the novel epigenetic regulatory mechanisms identified in this study can be targeted with chemotherapeutic interventions and that this results in universal parasite death, whilst overcoming current resistance mechanisms. Interference with the tightly controlled epigenetic network is proposed as a strategy to prevent asexual proliferation and sexual differentiation, either by directly altering chromatin dynamics or interfering with effector protein recruitment.

Since our quantitative histone PTM landscape publication was released in April 2017, two related studies cited our work. Gupta *et al*. (2017) further characterised one of our identified histone PTMs (H4K8ac) as a potential essential regulator of chromatin-associated transcriptional changes during the asexual IDC, proving its involvement in cellular proliferation and host-pathogen interaction [356]. Another study investigating the mechanisms of translational regulation in *P. falciparum* suggested a role for H3K27me3 in global transcriptional re-programming during gametocyte differentiation (Chan *et al*. (2017); PhD thesis, Karolinska Institutet, Sweden). Both publications referred to our work as the status quo for the histone PTM landscape in the field. As epigenetic regulation of *P. falciparum* development is an expanding field in malaria biology, our work is expected to initiate various other studies in the field as key biological questions pertaining to the full extent of epigenetic mechanisms utilised by gametocytes remain unanswered.

Future studies should make use of continuously developing technologies to characterise the full extent of important biological questions that we raised in this thesis. The genome occupancy of histone PTMs and the functional significance of co-existing histone PTMs

during gametocytogenesis can further clarify the unique epigenetic cascade and how this functionally contributes to gametocyte differentiation *in vitro*. Furthermore, the implication of H3K27me3 and polycomb group proteins need to be investigated, that can elucidate their functional role in pre-programmed epigenetic memory during parasite differentiation. Extended work on the histone PTM landscape and quantitative proteome in gametes can show how our work correlates to the situation in the mosquito stages. As portrayed in our work, there is a demand to clarify the full extent of translational repression in gametocytes and to identify the key proteins involved in this type of gene regulation. Lastly, derivatisation and optimisation of chemical entities from epigenetic inhibitors (as promising multi-stage and selective antimalarials) could help populate the antimalarial drug discovery pipeline. Answering these important biological questions will further contribute to our understanding of the complex development of *P. falciparum*.

In conclusion, in this thesis we have presented the most complete and comparative chromatin proteomic and global proteomic analyses over the entire development of malaria parasites. Specific histone PTM and protein abundance trends associated with stage-specific developmental transitions provide significant implications for our understanding of Plasmodial developmental biology and gene expression regulation, specifically during gametocytogenesis. We prove that these characteristic stage-specific biochemical processes in the parasite can be targeted for chemotherapeutic intervention, supporting the proposal of epigenetic inhibitors as a viable antimalarial chemotherapeutic strategy for future investigations.

References

1. WORLD HEALTH ORGANIZATION. (2016). World malaria report. Geneva, Switzerland, World Health Organization.
2. Wellcome Trust (2004) Malaria control measures. Available at: http://malaria.wellcome.ac.uk/doc_WTD023987.html (Accessed 28 May 2014)
3. Centers for Disease Control and Prevention (2015) Malaria. Available at: https://www.cdc.gov/malaria/about/biology/mosquitoes/ [Accessed 17 May 2017].
4. Burke, A., Dandalo, L., Munhenga, G., Dahan-Moss, Y., Mbokazi, F., Ngxongo, S., Coetzee, M., Koekemoer, L.*, et al.* (2017) A new malaria vector mosquito in South Africa, Sci Rep 7, 43779.
5. Sinka, M. E., Bangs, M. J., Manguin, S., Coetzee, M., Mbogo, C. M., Hemingway, J., Patil, A. P., Temperley, W. H.*, et al.* (2010) The dominant *Anopheles* vectors of human malaria in Africa, Europe and the Middle East: occurrence data, distribution maps and bionomic precis, Parasites & vectors 3, 117.
6. Touré, Y. T., and Coluzzi, M. (2001) Malaria vector control in Africa: Strategies and Challenges, Bull. World Health Organ. 78.
7. Walker, K. (2000) Cost-comparison of DDT and alternative insecticides for malaria control, Med. Vet. Entomol. 14, 345-354.
8. Chitnis, N., Schapira, A., Smith, T., and Steketee, R. (2010) Comparing the effectiveness of malaria vector-control interventions through a mathematical model, Am. J. Trop. Med. Hyg. 83, 230-240.
9. Brooke, B., Koekemoer, L., Kruger, P., Urbach, J., Misiani, E., and Coetzee, M. (2013) Malaria vector control in South Africa, South African medical journal = Suid-Afrikaanse tydskrif vir geneeskunde 103, 784-788.
10. Crompton, P. D., Pierce, S. K., and Miller, L. H. (2010) Advances and challenges in malaria vaccine development, J. Clin. Invest. 120, 4168-4178.
11. Smith, J. D., Rowe, J. A., Higgins, M. K., and Lavstsen, T. (2013) Malaria's deadly grip: cytoadhesion of *Plasmodium falciparum*-infected erythrocytes, Cell Microbiol 15, 1976-1983.
12. White, N. J. (2011) Determinants of relapse periodicity in *Plasmodium vivax* malaria, Malar J 10, 297.
13. Burrows, J. N., Duparc, S., Gutteridge, W. E., Hooft van Huijsduijnen, R., Kaszubska, W., Macintyre, F., Mazzuri, S., Mohrle, J. J.*, et al.* (2017) New developments in anti-malarial target candidate and product profiles, Malar J 16, 26.
14. Parasites in humans (2014) *Plasmodium falciparum* – Malaria. Available at: http://www.parasitesinhumans.org/plasmodium-falciparum-malaria.html (Accessed 20 January 2017)
15. Leete, T. H., and Rubin, H. (1996) Malaria and the cell cycle, Parasitol. Today 12, 442-444.
16. Barnwell, J. W. (2001) Hepatic Kupffer cells: the portal that permits infection of hepatocytes by malarial sporozoites?, Hepatology 33, 1331-1333.
17. Blasco, B., Leroy, D., and Fidock, D. A. (2017) Antimalarial drug resistance: linking *Plasmodium falciparum* parasite biology to the clinic, Nat Med 23, 917-928.
18. Rosenthal, P. J. (2003) Antimalarial drug discovery: old and new approaches, J. Exp. Biol. 206, 3735-3744.
19. Burrows, J. N., Burlot, E., Campo, B., Cherbuin, S., Jeanneret, S., Leroy, D., Spangenberg, T., Waterson, D.*, et al.* (2014) Antimalarial drug discovery - the path towards eradication, Parasitology 141, 128-139.
20. malERA Consultative Group on Drugs (2011) A research agenda for malaria eradication: drugs, PLoS Med. 8, e1000402.
21. Yamauchi, L. M., Coppi, A., Snounou, G., and Sinnis, P. (2007) *Plasmodium* sporozoites trickle out of the injection site, Cell Microbiol 9, 1215-1222.
22. Hafalla, J. C., Silvie, O., and Matuschewski, K. (2011) Cell biology and immunology of malaria, Immunological reviews 240, 297-316.
23. Mota, M. M., and Rodriguez, A. (2002) Invasion of mammalian host cells by *Plasmodium* sporozoites, Bioessays 24, 149-156.
24. Prudencio, M., Rodriguez, A., and Mota, M. M. (2006) The silent path to thousands of merozoites: the *Plasmodium* liver stage, Nat Rev Microbiol 4, 849-856.
25. Bannister, L., and Mitchell, G. (2003) The ins, outs and roundabouts of malaria, Trends Parasitol 19, 209-213.
26. Silvie, O., Mota, M. M., Matuschewski, K., and Prudencio, M. (2008) Interactions of the malaria parasite and its mammalian host, Curr Opin Microbiol 11, 352-359.
27. Arnot, D. E., and Gull, K. (1998) The *Plasmodium* cell-cycle: facts and questions, Annals of tropical medicine and parasitology 92, 361-365.

28. Doerig, C., Chakrabarti, D., Kappes, B., and Matthews, K. (2000) The cell cycle in protozoan parasites, Progress in cell cycle research 4, 163-183.
29. Hakimi, M. A., and Deitsch, K. W. (2007) Epigenetics in Apicomplexa: control of gene expression during cell cycle progression, differentiation and antigenic variation, Curr. Opin. Microbiol. 10, 357-362.
30. Arnot, D. E., Ronander, E., and Bengtsson, D. C. (2011) The progression of the intra-erythrocytic cell cycle of *Plasmodium falciparum* and the role of the centriolar plaques in asynchronous mitotic division during schizogony, Int. J. Parasitol. 41, 71-80.
31. Naughton, J. A., and Bell, A. (2007) Studies on cell-cycle synchronization in the asexual erythrocytic stages of *Plasmodium falciparum*, Parasitology 134, 331-337.
32. Dixon, M. W., Dearnley, M. K., Hanssen, E., Gilberger, T., and Tilley, L. (2012) Shape-shifting gametocytes: how and why does *P. falciparum* go banana-shaped?, Trends Parasitol. 28, 471-478.
33. Bruce, M. C., Alano, P., Duthie, S., and Carter, R. (1990) Commitment of the malaria parasite *Plasmodium falciparum* to sexual and asexual development, Parasitology 100, Pt 2:191-200.
34. Smith, T. G., Lourenco, P., Carter, R., Walliker, D., and Ranford-Cartwright, L. C. (2000) Commitment to sexual differentiation in the human malaria parasite, *Plasmodium falciparum*, Parasitology 121, (Pt 2):127-133.
35. Silvestrini, F., Alano, P., and Williams, J. L. (2000) Commitment to the production of male and female gametocytes in the human malaria parasite *Plasmodium falciparum*, Parasitology 121, Pt 5:465-471.
36. Buckling, A., Ranford-Cartwright, L. C., Miles, A., and Read, A. F. (1999) Chloroquine increases *Plasmodium falciparum* gametocytogenesis *in vitro*, Parasitology 118 (Pt 4), 339-346.
37. Carter, R., and Miller, L. H. (1979) Evidence for environmental modulation of gametocytogenesis in *Plasmodium falciparum* in continuous culture, Bull. World Health Organ. 57 Suppl 1, 37-52.
38. Dyer, M., and Day, K. P. (2003) Regulation of the rate of asexual growth and commitment to sexual development by diffusible factors from *in vitro* cultures of *Plasmodium falciparum*, Am J Trop Med Hyg 68, 403-409.
39. Mantel, P. Y., Hoang, A. N., Goldowitz, I., Potashnikova, D., Hamza, B., Vorobjev, I., Ghiran, I., Toner, M.*, et al.* (2013) Malaria-infected erythrocyte-derived microvesicles mediate cellular communication within the parasite population and with the host immune system, Cell Host Microbe 13, 521-534.
40. Regev-Rudzki, N., Wilson, D. W., Carvalho, T. G., Sisquella, X., Coleman, B. M., Rug, M., Bursac, D., Angrisano, F.*, et al.* (2013) Cell-cell communication between malaria-infected red blood cells via exosome-like vesicles, Cell 153, 1120-1133.
41. Williams, J. L. (1999) Stimulation of *Plasmodium falciparum* gametocytogenesis by conditioned medium from parasite cultures, Am J Trop Med Hyg 60, 7-13.
42. Josling, G. A., and Llinas, M. (2015) Sexual development in *Plasmodium* parasites: knowing when it's time to commit, Nat Rev Microbiol 13, 573-587.
43. Alano, P. (2014) The sound of sexual commitment breaks the silencing of malaria parasites, Trends Parasitol 30, 509-510.
44. Dixon, M. W., Thompson, J., Gardiner, D. L., and Trenholme, K. R. (2008) Sex in *Plasmodium*: a sign of commitment, Trends Parasitol 24, 168-175.
45. Hawking, F., Wilson, M. E., and Gammage, K. (1971) Evidence for cyclic development and short-lived maturity in the gametocytes of *Plasmodium falciparum*, Transactions of the Royal Society of Tropical Medicine and Hygiene 65, 549-559.
46. Sinden, R. E., Canning, E. U., Bray, R. S., and Smalley, M. E. (1978) Gametocyte and gamete development in *Plasmodium falciparum*, Proceedings of the Royal Society of London. Series B, Biological sciences 201, 375-399.
47. Smalley, M. E., and Sinden, R. E. (1977) *Plasmodium falciparum* gametocytes: their longevity and infectivity, Parasitology 74, 1-8.
48. Bray, R. S., and Garnham, P. C. (1982) The life-cycle of primate malaria parasites, British medical bulletin 38, 117-122.
49. Gautret, P., Miltgen, F., Chabaud, A. G., and Landau, I. (1996) Synchronized *Plasmodium yoelii yoelii*: pattern of gametocyte production, sequestration and infectivity, Parassitologia 38, 575-577.
50. Mons, B., Janse, C. J., Boorsma, E. G., and Van der Kaay, H. J. (1985) Synchronized erythrocytic schizogony and gametocytogenesis of *Plasmodium berghei in vivo* and *in vitro*, Parasitology 91 (Pt 3), 423-430.
51. Kuehn, A., and Pradel, G. (2010) The coming-out of malaria gametocytes, J. Biomed. Biotechnol. 2010, 976827.
52. Aingaran, M., Zhang, R., Law, S. K., Peng, Z., Undisz, A., Meyer, E., Diez-Silva, M., Burke, T. A.*, et al.* (2012) Host cell deformability is linked to transmission in the human malaria parasite *Plasmodium falciparum*, Cell Microbiol 14, 983-993.

53. Hanssen, E., Knoechel, C., Dearnley, M., Dixon, M. W., Le Gros, M., Larabell, C., and Tilley, L. (2012) Soft X-ray microscopy analysis of cell volume and hemoglobin content in erythrocytes infected with asexual and sexual stages of *Plasmodium falciparum*, Journal of structural biology 177, 224-232.
54. Sinden, R. E., and Smalley, M. E. (1979) Gametocytogenesis of *Plasmodium falciparum in vitro*: the cell-cycle, Parasitology 79, 277-296.
55. Aguilar, R., Magallon-Tejada, A., Achtman, A. H., Moraleda, C., Joice, R., Cistero, P., Li Wai Suen, C. S., Nhabomba, A.*, et al.* (2014) Molecular evidence for the localization of *Plasmodium falciparum* immature gametocytes in bone marrow, Blood 123, 959-966.
56. Farfour, E., Charlotte, F., Settegrana, C., Miyara, M., and Buffet, P. (2012) The extravascular compartment of the bone marrow: a niche for *Plasmodium falciparum* gametocyte maturation?, Malar J 11, 285.
57. Joice, R., Nilsson, S. K., Montgomery, J., Dankwa, S., Egan, E., Morahan, B., Seydel, K. B., Bertuccini, L.*, et al.* (2014) *Plasmodium falciparum* transmission stages accumulate in the human bone marrow, Science translational medicine 6, 244re245.
58. Billker, O., Lindo, V., Panico, M., Etienne, A. E., Paxton, T., Dell, A., Rogers, M., Sinden, R. E.*, et al.* (1998) Identification of xanthurenic acid as the putative inducer of malaria development in the mosquito, Nature 392, 289-292.
59. Billker, O., Miller, A. J., and Sinden, R. E. (2000) Determination of mosquito bloodmeal pH *in situ* by ion-selective microelectrode measurement: implications for the regulation of malarial gametogenesis, Parasitology 120 (Pt 6), 547-551.
60. de Koning-Ward, T. F., Olivieri, A., Bertuccini, L., Hood, A., Silvestrini, F., Charvalias, K., Berzosa Diaz, P., Camarda, G.*, et al.* (2008) The role of osmiophilic bodies and *Pf*g377 expression in female gametocyte emergence and mosquito infectivity in the human malaria parasite *Plasmodium falciparum*, Mol Microbiol 67, 278-290.
61. Ponzi, M., Siden-Kiamos, I., Bertuccini, L., Curra, C., Kroeze, H., Camarda, G., Pace, T., Franke-Fayard, B.*, et al.* (2009) Egress of *Plasmodium berghei* gametes from their host erythrocyte is mediated by the MDV-1/PEG3 protein, Cell Microbiol 11, 1272-1288.
62. Janse, C. J., Ponnudurai, T., Lensen, A. H., Meuwissen, J. H., Ramesar, J., Van der Ploeg, M., and Overdulve, J. P. (1988) DNA synthesis in gametocytes of *Plasmodium falciparum*, Parasitology 96 (Pt 1), 1-7.
63. Pradel, G. (2007) Proteins of the malaria parasite sexual stages: expression, function and potential for transmission blocking strategies, Parasitology 134, 1911-1929.
64. Sinden, R. E. (1983) The cell biology of sexual development in *Plasmodium*, Parasitology 86, 7-28.
65. Sinden, R. E. (1999) *Plasmodium* differentiation in the mosquito, Parassitologia 41, 139-148.
66. Bozdech, Z., Llinas, M., Pulliam, B. L., Wong, E. D., Zhu, J., and DeRisi, J. L. (2003) The transcriptome of the intraerythrocytic developmental cycle of *Plasmodium falciparum*, PLoS Biol. 1, E5.
67. Coetzee, N., Sidoli, S., van Biljon, R., Painter, H., Llinas, M., Garcia, B. A., and Birkholtz, L. M. (2017) Quantitative chromatin proteomics reveals a dynamic histone post-translational modification landscape that defines asexual and sexual *Plasmodium falciparum* parasites, Sci Rep 7, 607.
68. Florens, L., Washburn, M. P., Raine, J. D., Anthony, R. M., Grainger, M., Haynes, J. D., Moch, J. K., Muster, N.*, et al.* (2002) A proteomic view of the *Plasmodium falciparum* life cycle, Nature 419, 520-526.
69. Foth, B. J., Zhang, N., Chaal, B. K., Sze, S. K., Preiser, P. R., and Bozdech, Z. (2011) Quantitative time-course profiling of parasite and host cell proteins in the human malaria parasite *Plasmodium falciparum*, Mol Cell Proteomics 10, M110 006411.
70. Gardner, M. J., Hall, N., Fung, E., White, O., Berriman, M., Hyman, R. W., Carlton, J. M., Pain, A.*, et al.* (2002) Genome sequence of the human malaria parasite *Plasmodium falciparum*, Nature 3, 498-511.
71. Lasonder, E., Ishihama, Y., Vermunt, A. M., Pain, A., Sauerwein, R. W., Eling, W. M., Hall, N., Waters, A. P.*, et al.* (2002) Analysis of the *Plasmodium falciparum* proteome by high-accuracy mass spectrometry, Nature 3, 537-542.
72. Lasonder, E., Rijpma, S. R., van Schaijk, B. C., Hoeijmakers, W. A., Kensche, P. R., Gresnigt, M. S., Italiaander, A., Vos, M. W.*, et al.* (2016) Integrated transcriptomic and proteomic analyses of *P. falciparum* gametocytes: molecular insight into sex-specific processes and translational repression, Nucleic acids research 44, 6087-6101.
73. Le Roch, K. G., Johnson, J. R., Florens, L., Zhou, Y., Santrosyan, A., Grainger, M., Yan, S. F., Williamson, K. C.*, et al.* (2004) Global analysis of transcript and protein levels across the *Plasmodium falciparum* life cycle, Genome Res 14, 2308-2318.

74. Le Roch, K. G., Zhou, Y., Blair, P. L., Grainger, M., Moch, J. K., Haynes, J. D., De La Vega, P., Holder, A. A.*, et al.* (2003) Discovery of gene function by expression profiling of the malaria parasite life cycle, Science 301, 1503-1508.
75. Nirmalan, N., Sims, P. F., and Hyde, J. E. (2004) Quantitative proteomics of the human malaria parasite Plasmodium falciparum and its application to studies of development and inhibition, Mol Microbiol 52, 1187-1199.
76. Pease, B. N., Huttlin, E. L., Jedrychowski, M. P., Talevich, E., Harmon, J., Dillman, T., Kannan, N., Doerig, C.*, et al.* (2013) Global analysis of protein expression and phosphorylation of three stages of *Plasmodium falciparum* intraerythrocytic development., J. Proteome Res 12(9).
77. Saraf, A., Cervantes, S., Bunnik, E. M., Ponts, N. P., Sardiu, M. E., Chung, D. D., Prudhomme, J., Varberg, J.*, et al.* (2016) Dynamic and combinatorial landscape of histone modifications during the intra-erythrocytic developmental cycle of the malaria parasite, J Proteome Res 15, 2787-2801.
78. Young, J. A., Fivelman, Q. L., Blair, P. L., de la Vega, P., Le Roch, K. G., Zhou, Y., Carucci, D. J., Baker, D. A.*, et al.* (2005) The *Plasmodium falciparum* sexual development transcriptome: a microarray analysis using ontology-based pattern identification, Mol Biochem Parasitol 143, 67-79.
79. Cui, L., Lindner, S., and Miao, J. (2015) Translational regulation during stage transitions in malaria parasites, Ann N Y Acad Sci 1342, 1-9.
80. Doerig, C., Rayner, J. C., Scherf, A., and Tobin, A. B. (2015) Post-translational protein modifications in malaria parasites, Nat Rev Microbiol 13, 160-172.
81. Hughes, K. R., Philip, N., Starnes, G. L., Taylor, S., and Waters, A. P. (2010) From cradle to grave: RNA biology in malaria parasites, Wiley interdisciplinary reviews. RNA 1, 287-303.
82. Voss, T. S., Bozdech, Z., and Bartfai, R. (2014) Epigenetic memory takes center stage in the survival strategy of malaria parasites, Curr. Opin. Microbiol. 20C, 88-95.
83. Zhang, M., Joyce, B. R., Sullivan, W. J., Jr., and Nussenzweig, V. (2013) Translational control in *Plasmodium* and *toxoplasma* parasites, Eukaryot Cell 12, 161-167.
84. Cui, L., and Miao, J. (2010) Chromatin-mediated epigenetic regulation in the malaria parasite *Plasmodium falciparum*, Eukaryot. Cell 9, 1138-1149.
85. Coulson, R. M., Hall, N., and Ouzounis, C. A. (2004) Comparative genomics of transcriptional control in the human malaria parasite *Plasmodium falciparum*, Genome Res 14, 1548-1554.
86. Painter, H. J., Campbell, T. L., and Llinas, M. (2011) The Apicomplexan AP2 family: integral factors regulating *Plasmodium* development, Mol Biochem Parasitol 176, 1-7.
87. Bunnik, E. M., Batugedara, G., Saraf, A., Prudhomme, J., Florens, L., and Le Roch, K. G. (2016) The mRNA-bound proteome of the human malaria parasite *Plasmodium falciparum*, Genome biology 17, 147.
88. Reddy, B. P., Shrestha, S., Hart, K. J., Liang, X., Kemirembe, K., Cui, L., and Lindner, S. E. (2015) A bioinformatic survey of RNA-binding proteins in *Plasmodium*, BMC Genomics 16, 890.
89. Vembar, S. S., Droll, D., and Scherf, A. (2016) Translational regulation in blood stages of the malaria parasite *Plasmodium spp.*: systems-wide studies pave the way, Wiley interdisciplinary reviews. RNA 7, 772-792.
90. Horrocks, P., Wong, E., Russell, K., and Emes, R. D. (2009) Control of gene expression in *Plasmodium falciparum* - ten years on, Mol. Biochem. Parasitol. 164, 9-25.
91. Miao, J., Fan, Q., Parker, D., Li, X., Li, J., and Cui, L. (2013) Puf mediates translation repression of transmission-blocking vaccine candidates in malaria parasites, PLoS Pathog 9, e1003268.
92. Miao, J., Li, J., Fan, Q., Li, X., Li, X., and Cui, L. (2010) The Puf-family RNA-binding protein PfPuf2 regulates sexual development and sex differentiation in the malaria parasite *Plasmodium falciparum*, Journal of cell science 123, 1039-1049.
93. Duffy, M. F., Selvarajah, S. A., Josling, G. A., and Petter, M. (2012) The role of chromatin in *Plasmodium* gene expression, Cell Microbiol. 14, 819-828.
94. Duffy, M. F., Selvarajah, S. A., Josling, G. A., and Petter, M. (2014) Epigenetic regulation of the *Plasmodium falciparum* genome, Briefings in functional genomics 13, 203-216.
95. Saksouk, N., Bhatti, M. M., Kieffer, S., Smith, A. T., Musset, K., Garin, J., Sullivan, W. J., Jr., Cesbron-Delauw, M. F.*, et al.* (2005) Histone-modifying complexes regulate gene expression pertinent to the differentiation of the protozoan parasite *Toxoplasma gondii*, Mol Cell Biol 25, 10301-10314.
96. Chaal, B. K., Gupta, A. P., Wastuwidyaningtyas, B. D., Luah, Y. H., and Bozdech, Z. (2010) Histone deacetylases play a major role in the transcriptional regulation of the *Plasmodium falciparum* life cycle, PLoS Pathog. 6, e1000737.
97. Ngwa, C. J., Kiesow, M. J., Papst, O., Orchard, L. M., Filarsky, M., Rosinski, A. N., Voss, T. S., Llinas, M.*, et al.* (2017) Transcriptional Profiling Defines Histone Acetylation as a Regulator of Gene Expression during Human-to-Mosquito Transmission of the Malaria Parasite *Plasmodium falciparum*, Frontiers in cellular and infection microbiology 7, 320.

98. Gupta, A. P., and Bozdech, Z. (2017) Epigenetic landscapes underlining global patterns of gene expression in the human malaria parasite, *Plasmodium falciparum*, Int J Parasitol 47, 399-407.
99. Holliday, R. (1987) The inheritance of epigenetic defects, Science 238, 163-170.
100. Trelle, M. B., Salcedo-Amaya, A. M., Cohen, A. M., Stunnenberg, H. G., and Jensen, O. N. (2009) Global histone analysis by mass spectrometry reveals a high content of acetylated lysine residues in the malaria parasite *Plasmodium falciparum*, J Proteome Res 8, 3439-3450.
101. Willbanks, A., Leary, M., Greenshields, M., Tyminski, C., Heerboth, S., Lapinska, K., Haskins, K., and Sarkar, S. (2016) The Evolution of Epigenetics: From Prokaryotes to Humans and Its Biological Consequences, Genetics & epigenetics 8, 25-36.
102. Salcedo-Amaya, A. M., Hoeijmakers, W. A., Bartfai, R., and Stunnenberg, H. G. (2010) Malaria: could its unusual epigenome be the weak spot?, Int. J. Biochem. Cell Biol. 42, 781-784.
103. Hoeijmakers, W. A., Stunnenberg, H. G., and Bartfai, R. (2012) Placing the *Plasmodium falciparum* epigenome on the map, Trends Parasitol. 28, 486-495.
104. Annunziato, A. (2008) DNA packaging: Nucleosomes and chromatin., Nature Education 1.
105. Wang, Z., and Patel, D. J. (2011) Combinatorial readout of dual histone modifications by paired chromatin-associated modules, J. Biol. Chem. 286, 18363-18368.
106. Sandman, K., and Reeve, J. N. (2000) Structure and functional relationships of archaeal and eukaryal histones and nucleosomes, Archives of microbiology 173, 165-169.
107. White, M. F., and Bell, S. D. (2002) Holding it together: chromatin in the Archaea, Trends Genet 18, 621-626.
108. Blow, M. J., Clark, T. A., Daum, C. G., Deutschbauer, A. M., Fomenkov, A., Fries, R., Froula, J., Kang, D. D.*, et al.* (2016) The Epigenomic Landscape of Prokaryotes, PLoS Genet 12, e1005854.
109. Cedar, H., and Bergman, Y. (2009) Linking DNA methylation and histone modification: patterns and paradigms, Nat Rev Genet 10, 295-304.
110. Sippl, W., and Jung, M. (2009) Epigenetic targets in drug discovery, Vol. 42, Wiley, Germany.
111. Daura-Oller, E., Cabre, M., Montero, M. A., Paternain, J. L., and Romeu, A. (2009) Specific gene hypomethylation and cancer: new insights into coding region feature trends, Bioinformation 3, 340-343.
112. Mercer, T. R., and Mattick, J. S. (2013) Structure and function of long noncoding RNAs in epigenetic regulation, Nature structural & molecular biology 20, 300-307.
113. Buschbeck, M., and Hake, S. B. (2017) Variants of core histones and their roles in cell fate decisions, development and cancer, Nat Rev Mol Cell Biol 18, 299-314.
114. Miao, J., Fan, Q., Cui, L., and Li, J. (2006) The malaria parasite *Plasmodium falciparum* histones: organization, expression, and acetylation, Gene 369, 53-65.
115. Merrick, C. J., and Duraisingh, M. T. (2010) Epigenetics in *Plasmodium*: what do we really know?, Eukaryot. Cell 9, 1150-1158.
116. Strahl, B. D., and Allis, C. D. (2000) The language of covalent histone modifications, Nature 403, 41-45.
117. ATDBio (2014) Epigenetics. Available at: http://www.atdbio.com/content/56/Epigenetics (Accessed 6 April 2013)
118. Minucci, S., and Pelicci, P. G. (2006) Histone deacetylase inhibitors and the promise of epigenetic (and more) treatments for cancer, Nat. Rev. Cancer 6, 38-51.
119. Martin, C., and Zhang, Y. (2005) The diverse functions of histone lysine methylation, Nat. Rev. Mol. Cell Biol. 6, 838-849.
120. Farley, A. R., and Link, A. J. (2009) Identification and quantification of protein posttranslational modifications, Methods Enzymol. 463, 725-763.
121. Cao, J., and Yan, Q. (2012) Histone ubiquitination and deubiquitination in transcription, DNA damage response, and cancer, Front Oncol. 2, 26.
122. Shiio, Y., and Eisenman, R. N. (2003) Histone sumoylation is associated with transcriptional repression, Proc. Natl. Acad. Sci. U.S.A. 100, 13225-13230.
123. Iniguez-Lluhi, J. A. (2006) For a healthy histone code, a little SUMO in the tail keeps the acetyl away, ACS Chem. Biol. 1, 204-206.
124. Cosgrove, M. S., and Wolberger, C. (2005) How does the histone code work?, Biochem. Cell Biol. 83, 468-476.
125. Burridge, S. (2013) Target watch: Drugging the epigenome, Nat. Rev. Drug Discov. 12, 92-93.
126. Wang, Z., Zang, C., Rosenfeld, J. A., Schones, D. E., Barski, A., Cuddapah, S., Cui, K., Roh, T. Y.*, et al.* (2008) Combinatorial patterns of histone acetylations and methylations in the human genome, Nat Genet 40, 897-903.
127. Fischle, W., Tseng, B. S., Dormann, H. L., Ueberheide, B. M., Garcia, B. A., Shabanowitz, J., Hunt, D. F., Funabiki, H.*, et al.* (2005) Regulation of HP1-chromatin binding by histone H3 methylation and phosphorylation, Nature 438, 1116-1122.

128. Hirota, T., Lipp, J. J., Toh, B. H., and Peters, J. M. (2005) Histone H3 serine 10 phosphorylation by Aurora B causes HP1 dissociation from heterochromatin, Nature 438, 1176-1180.
129. Trojer, P., and Reinberg, D. (2006) Histone lysine demethylases and their impact on epigenetics, Cell 125, 213-217.
130. Cortes, A., Crowley, V. M., Vaquero, A., and Voss, T. S. (2012) A view on the role of epigenetics in the biology of malaria parasites, PLoS Pathog. 8, e1002943.
131. Le Roch, K. G., Chung, D. W., and Ponts, N. (2012) Genomics and integrated systems biology in *Plasmodium falciparum*: a path to malaria control and eradication, Parasite Immunol. 34, 50-60.
132. Baum, J., Papenfuss, A. T., Mair, G. R., Janse, C. J., Vlachou, D., Waters, A. P., Cowman, A. F., Crabb, B. S*., et al.* (2009) Molecular genetics and comparative genomics reveal RNAi is not functional in malaria parasites, Nucleic Acids Res. 37, 3788-3798.
133. McInroy, G. R., Beraldi, D., Raiber, E. A., Modrzynska, K., van Delft, P., Billker, O., and Balasubramanian, S. (2016) Enhanced Methylation Analysis by Recovery of Unsequenceable Fragments, PLoS One 11, e0152322.
134. Ponts, N., Fu, L., Harris, E. Y., Zhang, J., Chung, D. W., Cervantes, M. C., Prudhomme, J., Atanasova-Penichon, V*., et al.* (2013) Genome-wide mapping of DNA methylation in the human malaria parasite *Plasmodium falciparum*, Cell Host Microbe 14, 696-706.
135. Choi, S. W., Keyes, M. K., and Horrocks, P. (2006) LC/ESI-MS demonstrates the absence of 5-methyl-2'-deoxycytosine in *Plasmodium falciparum* genomic DNA, Mol. Biochem. Parasitol. 150, 350-352.
136. Treeck, M., Sanders, J. L., Elias, J. E., and Boothroyd, J. C. (2011) The phosphoproteomes of *Plasmodium falciparum* and *Toxoplasma gondii* reveal unusual adaptations within and beyond the parasites' boundaries, Cell Host Microbe 10, 410-419.
137. Miao, J., Lawrence, M., Jeffers, V., Zhao, F., Parker, D., Ge, Y., William J., J., Sullivan, W. J. J*., et al.* (2013) Extensive lysine acetylation occurs in evolutionarily conserved metabolic pathways and parasite-specific functions during *Plasmodium falciparum* intraerythrocytic development, Mol. Microbiol. 89, 660-675.
138. Jiang, L., Mu, J., Zhang, Q., Ni, T., Srinivasan, P., Rayavara, K., Yang, W., Turner, L*., et al.* (2013) PfSETvs methylation of histone H3K36 represses virulence genes in Plasmodium falciparum, Nature 499, 223-227.
139. Issar, N., Roux, E., Mattei, D., and Scherf, A. (2008) Identification of a novel post-translational modification in *Plasmodium falciparum*: protein sumoylation in different cellular compartments, Cell Microbiol. 10, 1999-2011.
140. Issar, N., Ralph, S. A., Mancio-Silva, L., Keeling, C., and Scherf, A. (2009) Differential sub-nuclear localisation of repressive and activating histone methyl modifications in *P. falciparum*, Microbes Infect. 11, 403-407.
141. Gupta, A. P., Chin, W. H., Zhu, L., Mok, S., Luah, Y. H., Lim, E. H., and Bozdech, Z. (2013) Dynamic epigenetic regulation of gene expression during the life cycle of malaria parasite *Plasmodium falciparum*, PLoS Pathog. 9, e1003170.
142. Dastidar, E. G., Dzeyk, K., Krijgsveld, J., Malmquist, N. A., Doerig, C., Scherf, A., and Lopez-Rubio, J. J. (2013) Comprehensive histone phosphorylation analysis and identification of Pf14-3-3 protein as a histone H3 phosphorylation reader in malaria parasites, PLoS One 8, e53179.
143. Cui, L., Fan, Q., and Miao, J. (2008) Histone lysine methyltransferases and demethylases in *Plasmodium falciparum*, Int. J. Parasitol. 38, 1083-1097.
144. Karmodiya, K., Pradhan, S. J., Joshi, B., Jangid, R., Reddy, P. C., and Galande, S. (2015) A comprehensive epigenome map of *Plasmodium falciparum* reveals unique mechanisms of transcriptional regulation and identifies H3K36me2 as a global mark of gene suppression, Epigenetics Chromatin 8, 32.
145. Lopez-Rubio, J. J., Mancio-Silva, L., and Scherf, A. (2009) Genome-wide analysis of heterochromatin associates clonally variant gene regulation with perinuclear repressive centers in malaria parasites, Cell Host Microbe 5, 179-190.
146. Cortes, A., and Deitsch, K. W. (2017) Malaria Epigenetics, Cold Spring Harbor perspectives in medicine.
147. Kishore, S. P., Stiller, J. W., and Deitsch, K. W. (2013) Horizontal gene transfer of epigenetic machinery and evolution of parasitism in the malaria parasite *Plasmodium falciparum* and other apicomplexans, BMC evolutionary biology 13, 37.
148. Ukaegbu, U. E., Kishore, S. P., Kwiatkowski, D. L., Pandarinath, C., Dahan-Pasternak, N., Dzikowski, R., and Deitsch, K. W. (2014) Recruitment of PfSET2 by RNA polymerase II to variant antigen encoding loci contributes to antigenic variation in P. falciparum, PLoS Pathog 10, e1003854.

149. Volz, J., Carvalho, T. G., Ralph, S. A., Gilson, P., Thompson, J., Tonkin, C. J., Langer, C., Crabb, B. S.*, et al.* (2010) Potential epigenetic regulatory proteins localise to distinct nuclear sub-compartments in Plasmodium falciparum, Int J Parasitol 40, 109-121.
150. Chen, P. B., Ding, S., Zanghi, G., Soulard, V., DiMaggio, P. A., Fuchter, M. J., Mecheri, S., Mazier, D.*, et al.* (2016) *Plasmodium falciparum* PfSET7: enzymatic characterization and cellular localization of a novel protein methyltransferase in sporozoite, liver and erythrocytic stage parasites, Sci Rep 6, 21802.
151. Volz, J. C., Bartfai, R., Petter, M., Langer, C., Josling, G. A., Tsuboi, T., Schwach, F., Baum, J.*, et al.* (2012) PfSET10, a *Plasmodium falciparum* methyltransferase, maintains the active var gene in a poised state during parasite division, Cell Host Microbe 11, 7-18.
152. Cui, L., Miao, J., Furuya, T., Li, X., Su, X. Z., and Cui, L. (2007) PfGCN5-mediated histone H3 acetylation plays a key role in gene expression in *Plasmodium falciparum*, Eukaryot Cell 6, 1219-1227.
153. Fan, Q., An, L., and Cui, L. (2004) *Plasmodium falciparum* histone acetyltransferase, a yeast GCN5 homologue involved in chromatin remodeling, Eukaryot Cell 3, 264-276.
154. Miao, J., Fan, Q., Cui, L., Li, X., Wang, H., Ning, G., Reese, J. C., and Cui, L. (2010) The MYST family histone acetyltransferase regulates gene expression and cell cycle in malaria parasite *Plasmodium falciparum*, Mol Microbiol 78, 883-902.
155. Duraisingh, M. T., Voss, T. S., Marty, A. J., Duffy, M. F., Good, R. T., Thompson, J. K., Freitas-Junior, L. H., Scherf, A.*, et al.* (2005) Heterochromatin silencing and locus repositioning linked to regulation of virulence genes in Plasmodium falciparum, Cell 121, 13-24.
156. Freitas-Junior, L. H., Hernandez-Rivas, R., Ralph, S. A., Montiel-Condado, D., Ruvalcaba-Salazar, O. K., Rojas-Meza, A. P., Mancio-Silva, L., Leal-Silvestre, R. J.*, et al.* (2005) Telomeric heterochromatin propagation and histone acetylation control mutually exclusive expression of antigenic variation genes in malaria parasites, Cell 121, 25-36.
157. Merrick, C. J., Jiang, R. H., Skillman, K. M., Samarakoon, U., Moore, R. M., Dzikowski, R., Ferdig, M. T., and Duraisingh, M. T. (2015) Functional analysis of sirtuin genes in multiple *Plasmodium falciparum* strains, PLoS One 10, e0118865.
158. Tonkin, C. J., Carret, C. K., Duraisingh, M. T., Voss, T. S., Ralph, S. A., Hommel, M., Duffy, M. F., Silva, L. M.*, et al.* (2009) Sir2 paralogues cooperate to regulate virulence genes and antigenic variation in *Plasmodium falciparum*, PLoS Biol 7, e84.
159. Andrews, K. T., Haque, A., and Jones, M. K. (2012) HDAC inhibitors in parasitic diseases, Immunol Cell Biol 90, 66-77.
160. Coleman, B. I., Skillman, K. M., Jiang, R. H., Childs, L. M., Altenhofen, L. M., Ganter, M., Leung, Y., Goldowitz, I.*, et al.* (2014) A *Plasmodium falciparum* histone deacetylase regulates antigenic variation and gametocyte conversion, Cell Host Microbe 16, 177-186.
161. Josling, G. A., Petter, M., Oehring, S. C., Gupta, A. P., Dietz, O., Wilson, D. W., Schubert, T., Langst, G.*, et al.* (2015) A Plasmodium Falciparum Bromodomain Protein Regulates Invasion Gene Expression, Cell Host Microbe 17, 741-751.
162. Brancucci, N. M., Bertschi, N. L., Zhu, L., Niederwieser, I., Chin, W. H., Wampfler, R., Freymond, C., Rottmann, M.*, et al.* (2014) Heterochromatin protein 1 secures survival and transmission of malaria parasites, Cell Host Microbe 16, 165-176.
163. Flueck, C., Bartfai, R., Volz, J., Niederwieser, I., Salcedo-Amaya, A. M., Alako, B. T., Ehlgen, F., Ralph, S. A.*, et al.* (2009) Plasmodium falciparum heterochromatin protein 1 marks genomic loci linked to phenotypic variation of exported virulence factors, PLoS Pathog 5, e1000569.
164. Perez-Toledo, K., Rojas-Meza, A. P., Mancio-Silva, L., Hernandez-Cuevas, N. A., Delgadillo, D. M., Vargas, M., Martinez-Calvillo, S., Scherf, A.*, et al.* (2009) Plasmodium falciparum heterochromatin protein 1 binds to tri-methylated histone 3 lysine 9 and is linked to mutually exclusive expression of var genes, Nucleic acids research 37, 2596-2606.
165. Chandra, B. R., Olivieri, A., Silvestrini, F., Alano, P., and Sharma, A. (2005) Biochemical characterization of the two nucleosome assembly proteins from *Plasmodium falciparum*, Mol Biochem Parasitol 142, 237-247.
166. Gill, J., Kumar, A., Yogavel, M., Belrhali, H., Jain, S. K., Rug, M., Brown, M., Maier, A. G.*, et al.* (2010) Structure, localization and histone binding properties of nuclear-associated nucleosome assembly protein from *Plasmodium falciparum*, Malar J 9, 90.
167. Waters, A. P. (2016) Epigenetic Roulette in Blood Stream *Plasmodium*: Gambling on Sex, PLoS Pathog 12, e1005353.
168. Lavazec, C., Sanyal, S., and Templeton, T. J. (2007) Expression switching in the *stevor* and *Pfmc-2TM* superfamilies in *Plasmodium falciparum*, Mol Microbiol 64, 1621-1634.
169. Petter, M., Haeggstrom, M., Khattab, A., Fernandez, V., Klinkert, M. Q., and Wahlgren, M. (2007) Variant proteins of the *Plasmodium falciparum* RIFIN family show distinct subcellular localization and developmental expression patterns, Mol Biochem Parasitol 156, 51-61.

170. Rovira-Graells, N., Gupta, A. P., Planet, E., Crowley, V. M., Mok, S., Ribas de Pouplana, L., Preiser, P. R., Bozdech, Z.*, et al.* (2012) Transcriptional variation in the malaria parasite *Plasmodium falciparum*, Genome Res 22, 925-938.
171. Scherf, A., Lopez-Rubio, J. J., and Riviere, L. (2008) Antigenic variation in *Plasmodium falciparum*, Annual review of microbiology 62, 445-470.
172. Baruch, D. I., Pasloske, B. L., Singh, H. B., Bi, X., Ma, X. C., Feldman, M., Taraschi, T. F., and Howard, R. J. (1995) Cloning the *P. falciparum* gene encoding PfEMP1, a malarial variant antigen and adherence receptor on the surface of parasitized human erythrocytes, Cell 82, 77-87.
173. Smith, J. D., Chitnis, C. E., Craig, A. G., Roberts, D. J., Hudson-Taylor, D. E., Peterson, D. S., Pinches, R., Newbold, C. I.*, et al.* (1995) Switches in expression of *Plasmodium falciparum var* genes correlate with changes in antigenic and cytoadherent phenotypes of infected erythrocytes, Cell 82, 101-110.
174. Su, X. Z., Heatwole, V. M., Wertheimer, S. P., Guinet, F., Herrfeldt, J. A., Peterson, D. S., Ravetch, J. A., and Wellems, T. E. (1995) The large diverse gene family *var* encodes proteins involved in cytoadherence and antigenic variation of *Plasmodium falciparum*-infected erythrocytes, Cell 82, 89-100.
175. Crowley, V. M., Rovira-Graells, N., Ribas de Pouplana, L., and Cortes, A. (2011) Heterochromatin formation in bistable chromatin domains controls the epigenetic repression of clonally variant Plasmodium falciparum genes linked to erythrocyte invasion, Mol Microbiol 80, 391-406.
176. Salcedo-Amaya, A. M., van Driel, M. A., Alako, B. T., Trelle, M. B., van den Elzen, A. M., Cohen, A. M., Janssen-Megens, E. M., van de Vegte-Bolmer, M.*, et al.* (2009) Dynamic histone H3 epigenome marking during the intraerythrocytic cycle of *Plasmodium falciparum*, Proc. Natl. Acad. Sci. U.S.A. 106, 9655-9660.
177. Schotta, G., Ebert, A., Krauss, V., Fischer, A., Hoffmann, J., Rea, S., Jenuwein, T., Dorn, R.*, et al.* (2002) Central role of Drosophila SU(VAR)3-9 in histone H3-K9 methylation and heterochromatic gene silencing, EMBO J 21, 1121-1131.
178. Zhang, C. L., McKinsey, T. A., and Olson, E. N. (2002) Association of class II histone deacetylases with heterochromatin protein 1: potential role for histone methylation in control of muscle differentiation, Mol Cell Biol 22, 7302-7312.
179. Batugedara, G., Lu, X. M., Bunnik, E. M., and Le Roch, K. G. (2017) The Role of Chromatin Structure in Gene Regulation of the Human Malaria Parasite, Trends Parasitol 33, 364-377.
180. Lopez-Rubio, J. J., Gontijo, A. M., Nunes, M. C., Issar, N., Hernandez Rivas, R., and Scherf, A. (2007) 5' flanking region of *var* genes nucleate histone modification patterns linked to phenotypic inheritance of virulence traits in malaria parasites, Mol Microbiol 66, 1296-1305.
181. Hoeijmakers, W. A., Salcedo-Amaya, A. M., Smits, A. H., Francoijs, K. J., Treeck, M., Gilberger, T. W., Stunnenberg, H. G., and Bartfai, R. (2013) H2A.Z/H2B.Z double-variant nucleosomes inhabit the AT-rich promoter regions of the *Plasmodium falciparum* genome, Mol. Microbiol. 87, 1061-1073.
182. Petter, M., Lee, C. C., Byrne, T. J., Boysen, K. E., Volz, J., Ralph, S. A., Cowman, A. F., Brown, G. V.*, et al.* (2011) Expression of *P. falciparum var* genes involves exchange of the histone variant H2A.Z at the promoter, PLoS Pathog 7, e1001292.
183. Petter, M., Selvarajah, S. A., Lee, C. C., Chin, W. H., Gupta, A. P., Bozdech, Z., Brown, G. V., and Duffy, M. F. (2013) H2A.Z and H2B.Z double-variant nucleosomes define intergenic regions and dynamically occupy *var* gene promoters in the malaria parasite *Plasmodium falciparum*, Mol Microbiol 87, 1167-1182.
184. Broadbent, K. M., Park, D., Wolf, A. R., Van Tyne, D., Sims, J. S., Ribacke, U., Volkman, S., Duraisingh, M.*, et al.* (2011) A global transcriptional analysis of *Plasmodium falciparum* malaria reveals a novel family of telomere-associated lncRNAs, Genome biology 12, R56.
185. Chakrabarti, K., Pearson, M., Grate, L., Sterne-Weiler, T., Deans, J., Donohue, J. P., and Ares, M., Jr. (2007) Structural RNAs of known and unknown function identified in malaria parasites by comparative genomics and RNA analysis, Rna 13, 1923-1939.
186. Gunasekera, A. M., Patankar, S., Schug, J., Eisen, G., Kissinger, J., Roos, D., and Wirth, D. F. (2004) Widespread distribution of antisense transcripts in the *Plasmodium falciparum* genome, Mol Biochem Parasitol 136, 35-42.
187. Lopez-Barragan, M. J., Lemieux, J., Quinones, M., Williamson, K. C., Molina-Cruz, A., Cui, K., Barillas-Mury, C., Zhao, K.*, et al.* (2011) Directional gene expression and antisense transcripts in sexual and asexual stages of *Plasmodium falciparum*, BMC Genomics 12, 587.
188. Mourier, T., Carret, C., Kyes, S., Christodoulou, Z., Gardner, P. P., Jeffares, D. C., Pinches, R., Barrell, B.*, et al.* (2008) Genome-wide discovery and verification of novel structured RNAs in *Plasmodium falciparum*, Genome Res 18, 281-292.
189. Patankar, S., Munasinghe, A., Shoaibi, A., Cummings, L. M., and Wirth, D. F. (2001) Serial analysis of gene expression in *Plasmodium falciparum* reveals the global expression profile of erythrocytic

stages and the presence of anti-sense transcripts in the malarial parasite, Molecular biology of the cell 12, 3114-3125.
190. Raabe, C. A., Sanchez, C. P., Randau, G., Robeck, T., Skryabin, B. V., Chinni, S. V., Kube, M., Reinhardt, R.*, et al.* (2010) A global view of the nonprotein-coding transcriptome in *Plasmodium falciparum*, Nucleic acids research 38, 608-617.
191. Siegel, T. N., Hon, C. C., Zhang, Q., Lopez-Rubio, J. J., Scheidig-Benatar, C., Martins, R. M., Sismeiro, O., Coppee, J. Y.*, et al.* (2014) Strand-specific RNA-Seq reveals widespread and developmentally regulated transcription of natural antisense transcripts in *Plasmodium falciparum*, BMC Genomics 15, 150.
192. Sierra-Miranda, M., Delgadillo, D. M., Mancio-Silva, L., Vargas, M., Villegas-Sepulveda, N., Martinez-Calvillo, S., Scherf, A., and Hernandez-Rivas, R. (2012) Two long non-coding RNAs generated from subtelomeric regions accumulate in a novel perinuclear compartment in *Plasmodium falciparum*, Mol Biochem Parasitol 185, 36-47.
193. Upadhyay, R., Bawankar, P., Malhotra, D., and Patankar, S. (2005) A screen for conserved sequences with biased base composition identifies noncoding RNAs in the A-T rich genome of *Plasmodium falciparum*, Mol Biochem Parasitol 144, 149-158.
194. Wei, C., Xiao, T., Zhang, P., Wang, Z., Chen, X., Zhang, L., Yao, M., Chen, R.*, et al.* (2014) Deep profiling of the novel intermediate-size noncoding RNAs in intraerythrocytic *Plasmodium falciparum*, PLoS One 9, e92946.
195. Amit-Avraham, I., Pozner, G., Eshar, S., Fastman, Y., Kolevzon, N., Yavin, E., and Dzikowski, R. (2015) Antisense long noncoding RNAs regulate *var* gene activation in the malaria parasite *Plasmodium falciparum*, Proc Natl Acad Sci U S A 112, E982-991.
196. Epp, C., Li, F., Howitt, C. A., Chookajorn, T., and Deitsch, K. W. (2009) Chromatin associated sense and antisense noncoding RNAs are transcribed from the *var* gene family of virulence genes of the malaria parasite *Plasmodium falciparum*, Rna 15, 116-127.
197. Guizetti, J., Barcons-Simon, A., and Scherf, A. (2016) Trans-acting GC-rich non-coding RNA at *var* expression site modulates gene counting in malaria parasite, Nucleic acids research 44, 9710-9718.
198. Wright, G. J., and Rayner, J. C. (2014) *Plasmodium falciparum* erythrocyte invasion: combining function with immune evasion, PLoS Pathog 10, e1003943.
199. Cortes, A., Carret, C., Kaneko, O., Yim Lim, B. Y., Ivens, A., and Holder, A. A. (2007) Epigenetic silencing of Plasmodium falciparum genes linked to erythrocyte invasion, PLoS Pathog 3, e107.
200. Comeaux, C. A., Coleman, B. I., Bei, A. K., Whitehurst, N., and Duraisingh, M. T. (2011) Functional analysis of epigenetic regulation of tandem RhopH1/clag genes reveals a role in *Plasmodium falciparum* growth, Mol Microbiol 80, 378-390.
201. Mira-Martinez, S., Rovira-Graells, N., Crowley, V. M., Altenhofen, L. M., Llinas, M., and Cortes, A. (2013) Epigenetic switches in *clag3* genes mediate blasticidin S resistance in malaria parasites, Cell Microbiol 15, 1913-1923.
202. Nguitragool, W., Bokhari, A. A., Pillai, A. D., Rayavara, K., Sharma, P., Turpin, B., Aravind, L., and Desai, S. A. (2011) Malaria parasite *clag3* genes determine channel-mediated nutrient uptake by infected red blood cells, Cell 145, 665-677.
203. Bartfai, R., Hoeijmakers, W. A., Salcedo-Amaya, A. M., Smits, A. H., Janssen-Megens, E., Kaan, A., Treeck, M., Gilberger, T. W.*, et al.* (2010) H2A.Z demarcates intergenic regions of the *Plasmodium falciparum* epigenome that are dynamically marked by H3K9ac and H3K4me3, PLoS Pathog 6, e1001223.
204. Ponts, N., Harris, E. Y., Prudhomme, J., Wick, I., Eckhardt-Ludka, C., Hicks, G. R., Hardiman, G., Lonardi, S.*, et al.* (2010) Nucleosome landscape and control of transcription in the human malaria parasite, Genome Res 20, 228-238.
205. Westenberger, S. J., Cui, L., Dharia, N., Winzeler, E., and Cui, L. (2009) Genome-wide nucleosome mapping of *Plasmodium falciparum* reveals histone-rich coding and histone-poor intergenic regions and chromatin remodeling of core and subtelomeric genes, BMC Genomics 10, 610.
206. Kensche, P. R., Hoeijmakers, W. A., Toenhake, C. G., Bras, M., Chappell, L., Berriman, M., and Bartfai, R. (2016) The nucleosome landscape of *Plasmodium falciparum* reveals chromatin architecture and dynamics of regulatory sequences, Nucleic acids research 44, 2110-2124.
207. Bunnik, E. M., Polishko, A., Prudhomme, J., Ponts, N., Gill, S. S., Lonardi, S., and Le Roch, K. G. (2014) DNA-encoded nucleosome occupancy is associated with transcription levels in the human malaria parasite *Plasmodium falciparum*, BMC Genomics 15, 347.
208. Hoeijmakers, W. A., Flueck, C., Francoijs, K. J., Smits, A. H., Wetzel, J., Volz, J. C., Cowman, A. F., Voss, T.*, et al.* (2012) *Plasmodium falciparum* centromeres display a unique epigenetic makeup and cluster prior to and during schizogony, Cell Microbiol 14, 1391-1401.

209. Kelly, J. M., McRobert, L., and Baker, D. A. (2006) Evidence on the chromosomal location of centromeric DNA in *Plasmodium falciparum* from etoposide-mediated topoisomerase-II cleavage, Proc Natl Acad Sci U S A 103, 6706-6711.
210. Kafsack, B. F., Rovira-Graells, N., Clark, T. G., Bancells, C., Crowley, V. M., Campino, S. G., Williams, A. E., Drought, L. G.*, et al.* (2014) A transcriptional switch underlies commitment to sexual development in malaria parasites, Nature 507, 248-252.
211. Sinha, A., Hughes, K. R., Modrzynska, K. K., Otto, T. D., Pfander, C., Dickens, N. J., Religa, A. A., Bushell, E.*, et al.* (2014) A cascade of DNA-binding proteins for sexual commitment and development in *Plasmodium*, Nature 507, 253-257.
212. Iwanaga, S., Kaneko, I., Kato, T., and Yuda, M. (2012) Identification of an AP2-family protein that is critical for malaria liver stage development, PLoS One 7, e47557.
213. Kaneko, I., Iwanaga, S., Kato, T., Kobayashi, I., and Yuda, M. (2015) Genome-Wide Identification of the Target Genes of AP2-O, a *Plasmodium* AP2-Family Transcription Factor, PLoS Pathog 11, e1004905.
214. Santos, J. M., Josling, G., Ross, P., Joshi, P., Orchard, L., Campbell, T., Schieler, A., Cristea, I. M.*, et al.* (2017) Red Blood Cell Invasion by the Malaria Parasite Is Coordinated by the PfAP2-I Transcription Factor, Cell Host Microbe 21, 731-741 e710.
215. Yuda, M., Iwanaga, S., Shigenobu, S., Kato, T., and Kaneko, I. (2010) Transcription factor AP2-Sp and its target genes in malarial sporozoites, Mol Microbiol 75, 854-863.
216. Yuda, M., Iwanaga, S., Shigenobu, S., Mair, G. R., Janse, C. J., Waters, A. P., Kato, T., and Kaneko, I. (2009) Identification of a transcription factor in the mosquito-invasive stage of malaria parasites, Mol Microbiol 71, 1402-1414.
217. Flueck, C., Bartfai, R., Volz, J., Niederwieser, I., Salcedo-Amaya, A. M., Alako, B. T. F., Ehlgen, F., Ralph, S. A.*, et al.* (2009) *Plasmodium falciparum* heterochromatin protein 1 marks genomic loci linked to phenotypic variation of exported virulence factors, PLoS Pathog 5, e1000569.
218. Guizetti, J., and Scherf, A. (2013) Silence, activate, poise and switch! Mechanisms of antigenic variation in *Plasmodium falciparum*, Cell Microbiol 15, 718-726.
219. Bechtsi, D. P., and Waters, A. P. (2017) Genomics and epigenetics of sexual commitment in *Plasmodium*, Int J Parasitol.
220. Cui, L., Rzomp, K. A., Fan, Q., Martin, S. K., and Williams, J. (2001) *Plasmodium falciparum*: differential display analysis of gene expression during gametocytogenesis, Exp Parasitol 99, 244-254.
221. Navadgi, V. M., Chandra, B. R., Mishra, P. C., and Sharma, A. (2006) The two *Plasmodium falciparum* nucleosome assembly proteins play distinct roles in histone transport and chromatin assembly, J Biol Chem 281, 16978-16984.
222. Malmquist, N. A., Sundriyal, S., Caron, J., Chen, P., Witkowski, B., Menard, D., Suwanarusk, R., Renia, L.*, et al.* (2015) Histone Methyltransferase Inhibitors Are Orally Bioavailable, Fast-Acting Molecules with Activity against Different Species Causing Malaria in Humans, Antimicrob Agents Chemother 59, 950-959.
223. Trenholme, K., Marek, L., Duffy, S., Pradel, G., Fisher, G., Hansen, F. K., Skinner-Adams, T. S., Butterworth, A.*, et al.* (2014) Lysine acetylation in sexual stage malaria parasites is a target for antimalarial small molecules, Antimicrob. Agents. Chemother. 57, 3666-3678.
224. Hall, N., Karras, M., Raine, J. D., Carlton, J. M., Kooij, T. W., Berriman, M., Florens, L., Janssen, C. S.*, et al.* (2005) A comprehensive survey of the *Plasmodium* life cycle by genomic, transcriptomic, and proteomic analyses, Science 7, 82-86.
225. Khan, S. M., Franke-Fayard, B., Mair, G. R., Lasonder, E., Janse, C. J., Mann, M., and Waters, A. P. (2005) Proteome analysis of separated male and female gametocytes reveals novel sex-specific *Plasmodium* biology, Cell 121, 675-687.
226. Miao, J., Chen, Z., Wang, Z., Shrestha, S., Li, X., Li, R., and Cui, L. (2017) Sex-Specific Biology of the Human Malaria Parasite Revealed from the Proteomes of Mature Male and Female Gametocytes, Mol Cell Proteomics 16, 537-551.
227. Silvestrini, F., Lasonder, E., Olivieri, A., Camarda, G., van Schaijk, B., Sanchez, M., Younis Younis, S., Sauerwein, R.*, et al.* (2010) Protein export marks the early phase of gametocytogenesis of the human malaria parasite *Plasmodium falciparum*, Mol Cell Proteomics 9(7), 1437-1448.
228. Tao, D., Ubaida-Mohien, C., Mathias, D. K., King, J. G., Pastrana-Mena, R., Tripathi, A., Goldowitz, I., Graham, D. R.*, et al.* (2014) Sex-partitioning of the *Plasmodium falciparum* stage V gametocyte proteome provides insight into *falciparum*-specific cell biology, Mol Cell Proteomics 13, 2705-2724.
229. Olszewski, K. L., Morrisey, J. M., Wilinski, D., Burns, J. M., Vaidya, A. B., Rabinowitz, J. D., and Llinas, M. (2009) Host-parasite interactions revealed by *Plasmodium falciparum* metabolomics, Cell Host Microbe 5, 191-199.

230. Park, Y. H., Shi, Y. P., Liang, B., Medriano, C. A., Jeon, Y. H., Torres, E., Uppal, K., Slutsker, L., *et al.* (2015) High-resolution metabolomics to discover potential parasite-specific biomarkers in a *Plasmodium falciparum* erythrocytic stage culture system, Malar J 14, 122.
231. Sana, T. R., Gordon, D. B., Fischer, S. M., Tichy, S. E., Kitagawa, N., Lai, C., Gosnell, W. L., and Chang, S. P. (2013) Global mass spectrometry based metabolomics profiling of erythrocytes infected with *Plasmodium falciparum*, PLoS One 8, e60840.
232. Li, B., Carey, M., and Workman, J. L. (2007) The role of chromatin during transcription, Cell 128, 707-719.
233. de Jesus, T. C., Nunes, V. S., Lopes Mde, C., Martil, D. E., Iwai, L. K., Moretti, N. S., Machado, F. C., de Lima-Stein, M. L., *et al.* (2016) Chromatin Proteomics Reveals Variable Histone Modifications during the Life Cycle of *Trypanosoma cruzi*, J Proteome Res 15, 2039-2051.
234. Nardelli, S. C., Che, F. Y., Silmon de Monerri, N. C., Xiao, H., Nieves, E., Madrid-Aliste, C., Angel, S. O., Sullivan, W. J., Jr.;, *et al.* (2013) The histone code of *Toxoplasma gondii* comprises conserved and unique posttranslational modifications, MBio 4, e00922-00913.
235. World Health Organization. World malaria report http://www.who.int/malaria/publications/world-malaria-report-2015/report/en/ (2016).
236. Baker, D. A. (2010) Malaria gametocytogenesis, Mol Biochem Parasitol 172, 57-65.
237. Lamour, S. D., Straschil, U., Saric, J., and Delves, M. J. (2014) Changes in metabolic phenotypes of *Plasmodium falciparum in vitro* cultures during gametocyte development, Malar J 1, 468.
238. Croken, M. M., Nardelli, S. C., and Kim, K. (2012) Chromatin modifications, epigenetics, and how protozoan parasites regulate their lives, Trends Parasitol 28, 202-213.
239. Ay, F., Bunnik, E. M., Varoquaux, N., Vert, J. P., Noble, W. S., and Le Roch, K. G. (2015) Multiple dimensions of epigenetic gene regulation in the malaria parasite *Plasmodium falciparum*: gene regulation via histone modifications, nucleosome positioning and nuclear architecture in *P. falciparum*, Bioessays 37, 182-194.
240. Garcia, B. A., Hake, S. B., Diaz, R. L., Kauer, M., Morris, S. A., Recht, J., Shabanowitz, J., Mishra, N., *et al.* (2007) Organismal differences in post-translational modifications in histones H3 and H4, J Biol Chem 282, 7641-7655.
241. Sautel, C. F., Cannella, D., Bastien, O., Kieffer, S., Aldebert, D., Garin, J., Tardieux, I., Belrhali, H., *et al.* (2007) SET8-mediated methylations of histone H4 lysine 20 mark silent heterochromatic domains in apicomplexan genomes, Mol Cell Biol 27, 5711-5724.
242. Huang, H., Lin, S., Garcia, B. A., and Zhao, Y. (2015) Quantitative proteomic analysis of histone modifications, Chem Rev 115, 2376-2418.
243. Yuan, Z. F., Lin, S., Molden, R. C., Cao, X. J., Bhanu, N. V., Wang, X., Sidoli, S., Liu, S., *et al.* (2015) EpiProfile Quantifies Histone Peptides With Modifications by Extracting Retention Time and Intensity in High-resolution Mass Spectra, Mol Cell Proteomics 14, 1696-1707.
244. Adjalley, S. H., Johnston, G. L., Li, T., Eastman, R. T., Ekland, E. H., Eappen, A. G., Richman, A., Sim, B. K., *et al.* (2011) Quantitative assessment of *Plasmodium falciparum* sexual development reveals potent transmission-blocking activity by methylene blue, Proc. Natl. Acad. Sci. U.S.A. 108, E1214-1223.
245. Trager, W., and Jensen, J. B. (1976) Human malaria parasites in continuous culture, Science 193, 673-675.
246. Lambros, C., and Vanderberg, J. P. (1979) Synchronization of *Plasmodium falciparum* erythrocytic stages in culture, J. Parasitol. 65, 418-420.
247. Reader, J., Botha, M., Theron, A., Lauterbach, S. B., Rossouw, C., Engelbrecht, D., Wepener, M., Smit, A., *et al.* (2015) Nowhere to hide: interrogating different metabolic parameters of *Plasmodium falciparum* gametocytes in a transmission blocking drug discovery pipeline towards malaria elimination, Malar J 14, 213.
248. Fivelman, Q. L., McRobert, L., Sharp, S., Taylor, C. J., Saeed, M., Swales, C. A., Sutherland, C. J., and Baker, D. A. (2007) Improved synchronous production of *Plasmodium falciparum* gametocytes *in vitro*, Mol. Biochem. Parasitol. 154, 119-123.
249. Sidoli, S., Bhanu, N. V., Karch, K. R., Wang, X., and Garcia, B. A. (2016) Complete Workflow for Analysis of Histone Post-translational Modifications Using Bottom-up Mass Spectrometry: From Histone Extraction to Data Analysis, Journal of visualized experiments : JoVE (111).
250. Shi, Y., and Whetstine, J. R. (2007) Dynamic regulation of histone lysine methylation by demethylases, Mol Cell 25, 1-14.
251. Bernstein, B. E., Mikkelsen, T. S., Xie, X., Kamal, M., Huebert, D. J., Cuff, J., Fry, B., Meissner, A., *et al.* (2006) A bivalent chromatin structure marks key developmental genes in embryonic stem cells, Cell 125, 315-326.
252. Fan, Q., Miao, J., ;, Cui, L., and Cui, L. (2009) Characterization of PRMT1 from *Plasmodium falciparum*, Biochem J 421, 107-118.

253. French, J. B., Cen, Y., and Sauve, A. A. (2008) *Plasmodium falciparum* Sir2 is an NAD+-dependent deacetylase and an acetyllysine-dependent and acetyllysine-independent NAD+ glycohydrolase, Biochemistry 47, 10227-10239.
254. Hou, H., and Yu, H. (2010) Structural insights into histone lysine demethylation, Curr Opin Struct Biol 20, 739-748.
255. Rider, S. D., Jr., and Zhu, G. (2009) An apicomplexan ankyrin-repeat histone deacetylase with relatives in photosynthetic eukaryotes, Int J Parasitol 39, 747-754.
256. Barski, A., Cuddapah, S., Cui, K., Roh, T. Y., Schones, D. E., Wang, Z., Wei, G., Chepelev, I., *et al.* (2007) High-resolution profiling of histone methylations in the human genome, Cell 129, 823-837.
257. Feng, Q., Wang, H., Ng, H. H., Erdjument-Bromage, H., Tempst, P., Struhl, K., and Zhang, Y. (2002) Methylation of H3-lysine 79 is mediated by a new family of HMTases without a SET domain, Curr Biol 12, 1052-1058.
258. Guillemette, B., Drogaris, P., Lin, H. H., Armstrong, H., Hiragami-Hamada, K., Imhof, A., Bonneil, E., Thibault, P., *et al.* (2011) H3 lysine 4 is acetylated at active gene promoters and is regulated by H3 lysine 4 methylation, PLoS Genet 7, e1001354.
259. Jack, A. P., Bussemer, S., Hahn, M., Punzeler, S., Snyder, M., Wells, M., Csankovszki, G., Solovei, I., *et al.* (2013) H3K56me3 is a novel, conserved heterochromatic mark that largely but not completely overlaps with H3K9me3 in both regulation and localization, PLoS One 8, e51765.
260. Tropberger, P., Pott, S., Keller, C., Kamieniarz-Gdula, K., Caron, M., Richter, F., Li, G., Mittler, G., *et al.* (2013) Regulation of transcription through acetylation of H3K122 on the lateral surface of the histone octamer, Cell 152, 859-872.
261. Udugama, M., FT, M. C., Chan, F. L., Tang, M. C., Pickett, H. A., JD, R. M., Mayne, L., Collas, P., *et al.* (2015) Histone variant H3.3 provides the heterochromatic H3 lysine 9 tri-methylation mark at telomeres, Nucleic acids research 43, 10227-10237.
262. Wagner, E. J., and Carpenter, P. B. (2012) Understanding the language of Lys36 methylation at histone H3, Nat Rev Mol Cell Biol 13, 115-126.
263. Bracken, A. P., Dietrich, N., Pasini, D., Hansen, K. H., and Helin, K. (2006) Genome-wide mapping of Polycomb target genes unravels their roles in cell fate transitions, Genes & development 20, 1123-1136.
264. Trojer, P., and Reinberg, D. (2007) Facultative heterochromatin: is there a distinctive molecular signature?, Mol Cell 28, 1-13.
265. Tiburcio, M., Silvestrini, F., Bertuccini, L., Sander, A. F., Turner, L., Lavstsen, T., and Alano, P. (2013) Early gametocytes of the malaria parasite *Plasmodium falciparum* specifically remodel the adhesive properties of infected erythrocyte surface, Cell Microbiol 15, 647-659.
266. Mair, G. R., Braks, J. A., Garver, L. S., Wiegant, J. C., Hall, N., Dirks, R. W., Khan, S. M., Dimopoulos, G., *et al.* (2006) Regulation of sexual development of *Plasmodium* by translational repression, Science 313, 667-669.
267. Jenuwein, T., and Allis, C. D. (2001) Translating the histone code, Science 293, 1074-1080.
268. Leroy, G., Dimaggio, P. A., Chan, E. Y., Zee, B. M., Blanco, M. A., Bryant, B., Flaniken, I. Z., Liu, S., *et al.* (2013) A quantitative atlas of histone modification signatures from human cancer cells, Epigenetics Chromatin 6, 20.
269. Dawson, M. A., and Kouzarides, T. (2012) Cancer epigenetics: from mechanism to therapy, Cell 150, 12–27.
270. Gottesfeld, J. M. (2011) Introduction to the thematic minireview series on epigenetics, J. Biol. Chem. 286, 18345-18346.
271. Painter, H. J., Carrasquilla, M., and Llinas, M. (2017) Capturing *in vivo* RNA transcriptional dynamics from the malaria parasite *Plasmodium falciparum*, Genome Res 27, 1074-1086.
272. Bunnik, E. M., Chung, D. W., Hamilton, M., Ponts, N., Saraf, A., Prudhomme, J., Florens, L., and Le Roch, K. G. (2013) Polysome profiling reveals translational control of gene expression in the human malaria parasite *Plasmodium falciparum*, Genome biology 14, R128.
273. Caro, F., Ahyong, V., Betegon, M., and DeRisi, J. L. (2014) Genome-wide regulatory dynamics of translation in the *Plasmodium falciparum* asexual blood stages, eLife 3.
274. Shock, J. L., Fischer, K. F., and DeRisi, J. L. (2007) Whole-genome analysis of mRNA decay in *Plasmodium falciparum* reveals a global lengthening of mRNA half-life during the intra-erythrocytic development cycle, Genome biology 8, R134.
275. Guerreiro, A., Deligianni, E., Santos, J. M., Silva, P. A., Louis, C., Pain, A., Janse, C. J., Franke-Fayard, B., *et al.* (2014) Genome-wide RIP-Chip analysis of translational repressor-bound mRNAs in the *Plasmodium* gametocyte, Genome biology 15, 493.
276. Mair, G. R., Lasonder, E., Garver, L. S., Franke-Fayard, B. M., Carret, C. K., Wiegant, J. C., Dirks, R. W., Dimopoulos, G., *et al.* (2010) Universal features of post-transcriptional gene regulation are critical for *Plasmodium* zygote development, PLoS Pathog 6, e1000767.

277. Wessel, D., and Flügge, U. I. (1984) A method for the quantitative recovery of protein in dilute solution in the presence of detergents and lipids, Analytical biochemistry 138, 141-143.
278. Ishihama, Y., Rappsilber, J., and Mann, M. (2006) Modular stop and go extraction tips with stacked disks for parallel and multidimensional Peptide fractionation in proteomics, J Proteome Res 5, 988-994.
279. Rappsilber, J., Mann, M., and Ishihama, Y. (2007) Protocol for micro-purification, enrichment, pre-fractionation and storage of peptides for proteomics using StageTips, Nat Protoc 2, 1896-1906.
280. Cox, J., and Mann, M. (2008) MaxQuant enables high peptide identification rates, individualized p.p.b.-range mass accuracies and proteome-wide protein quantification, Nat Biotechnol 26, 1367-1372.
281. Cox, J., Neuhauser, N., Michalski, A., Scheltema, R. A., Olsen, J. V., and Mann, M. (2011) Andromeda: a peptide search engine integrated into the MaxQuant environment, J Proteome Res 10, 1794-1805.
282. Schwanhausser, B., Busse, D., Li, N., Dittmar, G., Schuchhardt, J., Wolf, J., Chen, W., and Selbach, M. (2011) Global quantification of mammalian gene expression control, Nature 473, 337-342.
283. de Rojas, M. O., and Wasserman, M. (1985) Temporal relationships on macromolecular synthesis during the asexual cell cycle of *Plasmodium falciparum*, Transactions of the Royal Society of Tropical Medicine and Hygiene 79, 792-796.
284. Webster, W. A., and McFadden, G. I. (2014) From the genome to the phenome: tools to understand the basic biology of *Plasmodium falciparum*, The Journal of eukaryotic microbiology 61, 655-671.
285. Talman, A. M., Prieto, J. H., Marques, S., Ubaida-Mohien, C., Lawniczak, M., Wass, M. N., Xu, T., Frank, R*., et al.* (2014) Proteomic analysis of the *Plasmodium* male gamete reveals the key role for glycolysis in flagellar motility, Malar J 13, 315.
286. Barr, P. J., Green, K. M., Gibson, H. L., Bathurst, I. C., Quakyi, I. A., and Kaslow, D. C. (1991) Recombinant Pfs25 protein of Plasmodium falciparum elicits malaria transmission-blocking immunity in experimental animals, The Journal of experimental medicine 174, 1203-1208.
287. Dechering, K. J., Thompson, J., Dodemont, H. J., Eling, W., and Konings, R. N. (1997) Developmentally regulated expression of pfs16, a marker for sexual differentiation of the human malaria parasite Plasmodium falciparum, Mol Biochem Parasitol 89, 235-244.
288. Duffy, P. E., and Kaslow, D. C. (1997) A novel malaria protein, Pfs28, and Pfs25 are genetically linked and synergistic as falciparum malaria transmission-blocking vaccines, Infect Immun 65, 1109-1113.
289. Kocken, C. H., Jansen, J., Kaan, A. M., Beckers, P. J., Ponnudurai, T., Kaslow, D. C., Konings, R. N., and Schoenmakers, J. G. (1993) Cloning and expression of the gene coding for the transmission blocking target antigen Pfs48/45 of Plasmodium falciparum, Mol Biochem Parasitol 61, 59-68.
290. Williamson, K. C., Fujioka, H., Aikawa, M., and Kaslow, D. C. (1996) Stage-specific processing of Pfs230, a Plasmodium falciparum transmission-blocking vaccine candidate, Mol Biochem Parasitol 78, 161-169.
291. Gomez-Diaz, E., Yerbanga, R. S., Lefevre, T., Cohuet, A., Rowley, M. J., Ouedraogo, J. B., and Corces, V. G. (2017) Epigenetic regulation of *Plasmodium falciparum* clonally variant gene expression during development in *Anopheles gambiae*, Sci Rep 7, 40655.
292. MacRae, J. I., Dixon, M. W., Dearnley, M. K., Chua, H. H., Chambers, J. M., Kenny, S., Bottova, I., Tilley, L*., et al.* (2013) Mitochondrial metabolism of sexual and asexual blood stages of the malaria parasite *Plasmodium falciparum*, BMC Biol 13;11, 67.
293. Mata, J., Wilbrey, A., and Bahler, J. (2007) Transcriptional regulatory network for sexual differentiation in fission yeast, Genome biology 8, R217.
294. Alano, P., Read, D., Bruce, M., Aikawa, M., Kaido, T., Tegoshi, T., Bhatti, S., Smith, D. K*., et al.* (1995) COS cell expression cloning of Pfg377, a *Plasmodium falciparum* gametocyte antigen associated with osmiophilic bodies, Mol Biochem Parasitol 74, 143-156.
295. van Schaijk, B. C., van Dijk, M. R., van de Vegte-Bolmer, M., van Gemert, G. J., van Dooren, M. W., Eksi, S., Roeffen, W. F., Janse, C. J*., et al.* (2006) Pfs47, paralog of the male fertility factor Pfs48/45, is a female specific surface protein in *Plasmodium falciparum*, Mol Biochem Parasitol 149, 216-222.
296. Alano, P. (2007) *Plasmodium falciparum* gametocytes: still many secrets of a hidden life, Mol Microbiol 66, 291-302.
297. Vembar, S. S., Macpherson, C. R., Sismeiro, O., Coppee, J. Y., and Scherf, A. (2015) The PfAlba1 RNA-binding protein is an important regulator of translational timing in *Plasmodium falciparum* blood stages, Genome biology 16, 212.
298. Healy, S., Khan, D. H., and Davie, J. R. (2011) Gene expression regulation through 14-3-3 interactions with histones and HDACs, Discovery medicine 11, 349-358.

299. Kleppe, R., Martinez, A., Doskeland, S. O., and Haavik, J. (2011) The 14-3-3 proteins in regulation of cellular metabolism, Seminars in cell & developmental biology 22, 713-719.
300. Billker, O., Dechamps, S., Tewari, R., Wenig, G., Franke-Fayard, B., and Brinkmann, V. (2004) Calcium and a calcium-dependent protein kinase regulate gamete formation and mosquito transmission in a malaria parasite, Cell 117, 503-514.
301. Solyakov, L., Halbert, J., Alam, M. M., Semblat, J. P., Dorin-Semblat, D., Reininger, L., Bottrill, A. R., Mistry, S.*, et al.* (2011) Global kinomic and phospho-proteomic analyses of the human malaria parasite *Plasmodium falciparum*, Nature communications 2, 565.
302. Tewari, R., Dorin, D., Moon, R., Doerig, C., and Billker, O. (2005) An atypical mitogen-activated protein kinase controls cytokinesis and flagellar motility during male gamete formation in a malaria parasite, Mol Microbiol 58, 1253-1263.
303. Tewari, R., Straschil, U., Bateman, A., Bohme, U., Cherevach, I., Gong, P., Pain, A., and Billker, O. (2010) The systematic functional analysis of *Plasmodium* protein kinases identifies essential regulators of mosquito transmission, Cell Host Microbe 8, 377-387.
304. Wanichthanarak, K., Fahrmann, J. F., and Grapov, D. (2015) Genomic, Proteomic, and Metabolomic Data Integration Strategies, Biomarker insights 10, 1-6.
305. Perco, P., Muhlberger, I., Mayer, G., Oberbauer, R., Lukas, A., and Mayer, B. (2010) Linking transcriptomic and proteomic data on the level of protein interaction networks, Electrophoresis 31, 1780-1789.
306. Burrows, J. N., Chibale, K., and Wells, T. N. (2011) The state of the art in anti-malarial drug discovery and development, Curr. Top. Med. Chem. 11, 1226-1254.
307. Miller, L. H., Ackerman, H. C., Su, X. Z., and Wellems, T. E. (2013) Malaria biology and disease pathogenesis: insights for new treatments, Nat Med 19, 156-167.
308. Burrows, J. N., van Huijsduijnen, R. H., Möhrle, J. J., Oeuvray, C., and Wells, T. N. (2013) Designing the next generation of medicines for malaria control and eradication, Malar J 6, 187.
309. Peatey, C. L., Leroy, D., Gardiner, D. L., and Trenholme, K. R. (2012) Anti-malarial drugs: how effective are they against *Plasmodium falciparum* gametocytes?, Malar. J. 11, 34.
310. Butterworth, A. S., Skinner-Adams, T. S., Gardiner, D. L., and Trenholme, K. R. (2013) *Plasmodium falciparum* gametocytes: with a view to a kill, Parasitology 140, 1718-1734.
311. Hemingway, J., Shretta, R., Wells, T. N., Bell, D., Djimde, A. A., Achee, N., and Qi, G. (2016) Tools and Strategies for Malaria Control and Elimination: What Do We Need to Achieve a Grand Convergence in Malaria?, PLoS Biol 14, e1002380.
312. Wells, T. N., Hooft van Huijsduijnen, R., and Van Voorhis, W. C. (2015) Malaria medicines: a glass half full?, Nat Rev Drug Discov 14, 424-442.
313. Olliaro, P. L., and Yuthavong, Y. (1999) An overview of chemotherapeutic targets for antimalarial drug discovery, Pharmacol. Ther. 81, 91-110.
314. Paquet, T., Le Manach, C., Cabrera, D. G., Younis, Y., Henrich, P. P., Abraham, T. S., Lee, M. C. S., Basak, R.*, et al.* (2017) Antimalarial efficacy of MMV390048, an inhibitor of *Plasmodium* phosphatidylinositol 4-kinase, Science translational medicine 9.
315. Altucci, L., and Rots, M. G. (2016) Epigenetic drugs: from chemistry via biology to medicine and back, Clinical epigenetics 8, 56.
316. Audia, J. E., and Campbell, R. M. (2016) Histone Modifications and Cancer, Cold Spring Harbor perspectives in biology 8, a019521.
317. Hatzimichael, E., and Crook, T. (2013) Cancer epigenetics: new therapies and new challenges, Journal of drug delivery 2013, 529312.
318. Fenaux, P., Mufti, G. J., Hellstrom-Lindberg, E., Santini, V., Finelli, C., Giagounidis, A., Schoch, R., Gattermann, N.*, et al.* (2009) Efficacy of azacitidine compared with that of conventional care regimens in the treatment of higher-risk myelodysplastic syndromes: a randomised, open-label, phase III study, The Lancet. Oncology 10, 223-232.
319. Khan, O., and La Thangue, N. B. (2008) Drug Insight: histone deacetylase inhibitor-based therapies for cutaneous T-cell lymphomas, Nat. Clin. Pract. Oncol. 5, 714-726.
320. Prusty, D., Mehra, P., Srivastava, S., Shivange, A. V., Gupta, A., Roy, N., and Dhar, S. K. (2008) Nicotinamide inhibits *Plasmodium falciparum* Sir2 activity in vitro and parasite growth, FEMS Microbiol. Lett. 282, 266-272.
321. Andrews, K. T., Tran, T. N., Wheatley, N. C., and Fairlie, D. P. (2009) Targeting histone deacetylase inhibitors for anti-malarial therapy, Curr. Top. Med. Chem. 9, 292-308.
322. Andrews, K. T., Gupta, A. P., Tran, T. N., Fairlie, D. P., Gobert, G. N., and Bozdech, Z. (2012) Comparative gene expression profiling of *P. falciparum* malaria parasites exposed to three different histone deacetylase inhibitors, PLoS One 7, e31847.
323. Engel, J. A., Jones, A. J., Avery, V. M., Sumanadasa, S. D., Ng, S. S., Fairlie, D. P., Adams, T. S., and Andrews, K. T. (2015) Profiling the anti-protozoal activity of anti-cancer HDAC inhibitors

against *Plasmodium* and *Trypanosoma* parasites, International journal for parasitology. Drugs and drug resistance 5, 117-126.
324. Sun, W., Tanaka, T. Q., Magle, C. T., Huang, W., Southall, N., Huang, R., Dehdashti, S. J., McKew, J. C.*, et al.* (2014) Chemical signatures and new drug targets for gametocytocidal drug development, Sci Rep 4, 3743.
325. Johnson, J. D., Dennull, R. A., Gerena, L., Lopez-Sanchez, M., Roncal, N. E., and Waters, N. C. (2007) Assessment and continued validation of the malaria SYBR green I-based fluorescence assay for use in malaria drug screening, Antimicrob Agents Chemother 51, 1926-1933.
326. Smilkstein, M., Sriwilaijaroen, N., Kelly, J. X., Wilairat, P., and Riscoe, M. (2004) Simple and inexpensive fluorescence-based technique for high-throughput antimalarial drug screening, Antimicrob Agents Chemother 48, 1803-1806.
327. Verlinden, B. K., Niemand, J., Snyman, J., Sharma, S. K., Beattie, R. J., Woster, P. M., and Birkholtz, L. M. (2011) Discovery of novel alkylated (bis)urea and (bis)thiourea polyamine analogues with potent antimalarial activities, J Med Chem 54, 6624-6633.
328. D'Alessandro, S., Silvestrini, F., Dechering, K., Corbett, Y., Parapini, S., Timmerman, M., Galastri, L., Basilico, N.*, et al.* (2013) A *Plasmodium falciparum* screening assay for anti-gametocyte drugs based on parasite lactate dehydrogenase detection, J Antimicrob Chemother 68, 2048-2058.
329. Makler, M. T., Ries, J. M., Williams, J. A., Bancroft, J. E., Piper, R. C., Gibbins, B. L., and Hinrichs, D. J. (1993) Parasite lactate dehydrogenase as an assay for *Plasmodium falciparum* drug sensitivity, Am J Trop Med Hyg 48, 739-741.
330. Hirai, S., Endo, S., Saito, R., Hirose, M., Ueno, T., Suzuki, H., Yamato, K., Abei, M.*, et al.* (2014) Antitumor effects of a sirtuin inhibitor, tenovin-6, against gastric cancer cells via death receptor 5 up-regulation, PLoS One 9, e102831.
331. Kikuchi, J., Takashina, T., Kinoshita, I., Kikuchi, E., Shimizu, Y., Sakakibara-Konishi, J., Oizumi, S., Marquez, V. E.*, et al.* (2012) Epigenetic therapy with 3-deazaneplanocin A, an inhibitor of the histone methyltransferase EZH2, inhibits growth of non-small cell lung cancer cells, Lung cancer 78, 138-143.
332. Lai, Y. S., Chen, J. Y., Tsai, H. J., Chen, T. Y., and Hung, W. C. (2015) The SUV39H1 inhibitor chaetocin induces differentiation and shows synergistic cytotoxicity with other epigenetic drugs in acute myeloid leukemia cells, Blood cancer journal 5, e313.
333. Malmquist, N. A., Moss, T. A., Mecheri, S., Scherf, A., and Fuchter, M. J. (2012) Small-molecule histone methyltransferase inhibitors display rapid antimalarial activity against all blood stage forms in Plasmodium falciparum, Proc Natl Acad Sci U S A 109, 16708-16713.
334. Sumanadasa, S. D., Goodman, C. D., Lucke, A. J., Skinner-Adams, T., Sahama, I., Haque, A., Do, T. A., McFadden, G. I.*, et al.* (2012) Antimalarial activity of the anticancer histone deacetylase inhibitor SB939, Antimicrob Agents Chemother 56, 3849-3856.
335. Takai, N., and Narahara, H. (2010) Preclinical studies of chemotherapy using histone deacetylase inhibitors in endometrial cancer, Obstetrics and gynecology international 2010, 923824.
336. Zappasodi, R., Cavane, A., Iorio, M. V., Tortoreto, M., Guarnotta, C., Ruggiero, G., Piovan, C., Magni, M.*, et al.* (2014) Pleiotropic antitumor effects of the pan-HDAC inhibitor ITF2357 against c-Myc-overexpressing human B-cell non-Hodgkin lymphomas, International journal of cancer 135, 2034-2045.
337. Medicines for Malaria Venture (2017) Information for scientists. Available at: https://www.mmv.org/research-development/information-scientists (Accessed 30 August 2017)
338. Birkholtz, L. M., Coetzer, T. L., Mancama, D., Leroy, D., and Alano, P. (2016) Discovering New Transmission-Blocking Antimalarial Compounds: Challenges and Opportunities, Trends Parasitol 32, 669-681.
339. Dhanak, D., and Jackson, P. (2014) Development and classes of epigenetic drugs for cancer, Biochem Biophys Res Commun 455(1-2), 58-69.
340. Cui, L., Miao, J., Furuya, T., Fan, Q., Li, X., Rathod, P. K., Su, X. Z., and Cui, L. (2008) Histone acetyltransferase inhibitor anacardic acid causes changes in global gene expression during *in vitro Plasmodium falciparum* development, Eukaryot Cell 7, 1200-1210.
341. Merrick, C. J., and Duraisingh, M. T. (2007) *Plasmodium falciparum* Sir2: an unusual sirtuin with dual histone deacetylase and ADP-ribosyltransferase activity, Eukaryot Cell 6, 2081-2091.
342. Ukaegbu, U. E., Zhang, X., Heinberg, A. R., Wele, M., Chen, Q., and Deitsch, K. W. (2015) A Unique Virulence Gene Occupies a Principal Position in Immune Evasion by the Malaria Parasite *Plasmodium falciparum*, PLoS Genet 11, e1005234.
343. Duffy, S., and Avery, V. M. (2013) Identification of inhibitors of *Plasmodium falciparum* gametocyte development, Malar J 11, 12:408.
344. Lucantoni, L., Duffy, S., Adjalley, S. H., Fidock, D. A., and Avery, V. M. (2013) Identification of MMV malaria box inhibitors of *plasmodium falciparum* early-stage gametocytes using a luciferase-based high-throughput assay, Antimicrob Agents Chemother 57, 6050-6062.

345. Lucantoni, L., Silvestrini, F., Signore, M., Siciliano, G., Eldering, M., Dechering, K. J., Avery, V. M., and Alano, P. (2015) A simple and predictive phenotypic High Content Imaging assay for *Plasmodium falciparum* mature gametocytes to identify malaria transmission blocking compounds, Sci Rep 5, 16414.
346. Plouffe, D. M., Wree, M., Du, A. Y., Meister, S., Li, F., Patra, K., Lubar, A., Okitsu, S. L.*, et al.* (2016) High-Throughput Assay and Discovery of Small Molecules that Interrupt Malaria Transmission, Cell Host Microbe 19, 114-126.
347. Sanders, N. G., Sullivan, D. J., Mlambo, G., Dimopoulos, G., and Tripathi, A. K. (2014) Gametocytocidal screen identifies novel chemical classes with *Plasmodium falciparum* transmission blocking activity, PLoS One 9, e105817.
348. Harris, C. J., Hill, R. D., Sheppard, D. W., Slater, M. J., and Stouten, P. F. (2011) The design and application of target-focused compound libraries, Combinatorial chemistry & high throughput screening 14, 521-531.
349. Lucantoni, L., Fidock, D. A., and Avery, V. M. (2016) Luciferase-Based, High-Throughput Assay for Screening and Profiling Transmission-Blocking Compounds against P*lasmodium falciparum* Gametocytes, Antimicrob Agents Chemother 60, 2097-2107.
350. Lelievre, J., Almela, M. J., Lozano, S., Miguel, C., Franco, V., Leroy, D., and Herreros, E. (2012) Activity of clinically relevant antimalarial drugs on *Plasmodium falciparum* mature gametocytes in an ATP bioluminescence "transmission blocking" assay, PLoS One 7, e35019.
351. Chua, M. J., Arnold, M. S., Xu, W., Lancelot, J., Lamotte, S., Spath, G. F., Prina, E., Pierce, R. J.*, et al.* (2017) Effect of clinically approved HDAC inhibitors on *Plasmodium, Leishmania* and *Schistosoma* parasite growth, International journal for parasitology. Drugs and drug resistance 7, 42-50.
352. Dow, G. S., Chen, Y., Andrews, K. T., Caridha, D., Gerena, L., Gettayacamin, M., Johnson, J., Li, Q.*, et al.* (2008) Antimalarial activity of phenylthiazolyl-bearing hydroxamate-based histone deacetylase inhibitors, Antimicrob Agents Chemother 52, 3467-3477.
353. Giannini, G., Battistuzzi, G., and Vignola, D. (2015) Hydroxamic acid based histone deacetylase inhibitors with confirmed activity against the malaria parasite, Bioorganic & medicinal chemistry letters 25, 459-461.
354. Hailu, G. S., Robaa, D., Forgione, M., Sippl, W., Rotili, D., and Mai, A. (2017) Lysine Deacetylase Inhibitors in Parasites: Past, Present, and Future Perspectives, J Med Chem 60, 4780-4804.
355. Miranda, T. B., Cortez, C. C., Yoo, C. B., Liang, G., Abe, M., Kelly, T. K., Marquez, V. E., and Jones, P. A. (2009) DZNep is a global histone methylation inhibitor that reactivates developmental genes not silenced by DNA methylation, Molecular cancer therapeutics 8, 1579-1588.
356. Gupta, A. P., Zhu, L., Tripathi, J., Kucharski, M., Patra, A., and Bozdech, Z. (2017) Histone 4 lysine 8 acetylation regulates proliferation and host-pathogen interaction in *Plasmodium falciparum*, Epigenetics Chromatin 10, 40.
357. Azuara, V., Perry, P., Sauer, S., Spivakov, M., Jorgensen, H. F., John, R. M., Gouti, M., Casanova, M.*, et al.* (2006) Chromatin signatures of pluripotent cell lines, Nature cell biology 8, 532-538.
358. Cortes, A. (2008) Switching *Plasmodium falciparum* genes on and off for erythrocyte invasion, Trends Parasitol 24, 517-524.
359. Ruecker, A., Mathias, D. K., Straschil, U., Churcher, T. S., Dinglasan, R. R., Leroy, D., Sinden, R. E., and Delves, M. J. (2014) A male and female gametocyte functional viability assay to identify biologically relevant malaria transmission-blocking drugs, Antimicrob Agents Chemother 58, 7292-7302.
360. Bushell, E., Gomes, A. R., Sanderson, T., Anar, B., Girling, G., Herd, C., Metcalf, T., Modrzynska, K.*, et al.* (2017) Functional Profiling of a *Plasmodium* Genome Reveals an Abundance of Essential Genes, Cell 170, 260-272 e268.
361. Janse, C. J., Kroeze, H., van Wigcheren, A., Mededovic, S., Fonager, J., Franke-Fayard, B., Waters, A. P., and Khan, S. M. (2011) A genotype and phenotype database of genetically modified malaria-parasites, Trends Parasitol 27, 31-39.
362. Khan, S. M., Kroeze, H., Franke-Fayard, B., and Janse, C. J. (2013) Standardization in generating and reporting genetically modified rodent malaria parasites: the RMgmDB database, Methods Mol Biol 923, 139-150.
363. Sanderson, T., and Rayner, J. C. (2017) PhenoPlasm: a database of disruption phenotypes for malaria parasite genes, Wellcome open research 2, 45.
364. Schwach, F., Bushell, E., Gomes, A. R., Anar, B., Girling, G., Herd, C., Rayner, J. C., and Billker, O. (2015) PlasmoGEM, a database supporting a community resource for large-scale experimental genetics in malaria parasites, Nucleic acids research 43, D1176-1182.

Appendices

Appendix I: Figures

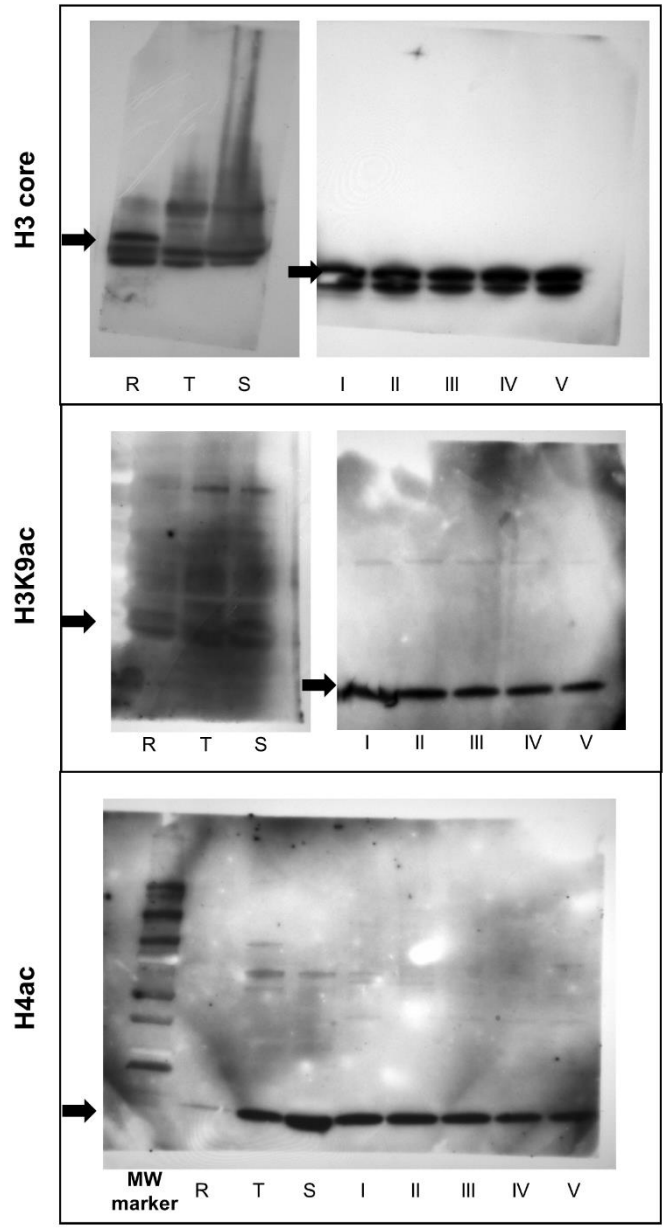

Figure A1: Full-length western blots for H3Core, H3K9ac and H4ac. The Precision Plus ProteinTM Dual Color Standard was used throughout the experiments (10-250 kDa) as molecular weight marker. Exposure times varied due to differences in antibody sensitivity. Developing and fixing times were constant at 30 s each. All samples were derived from the same experiments and gels/blots were processed in parallel.

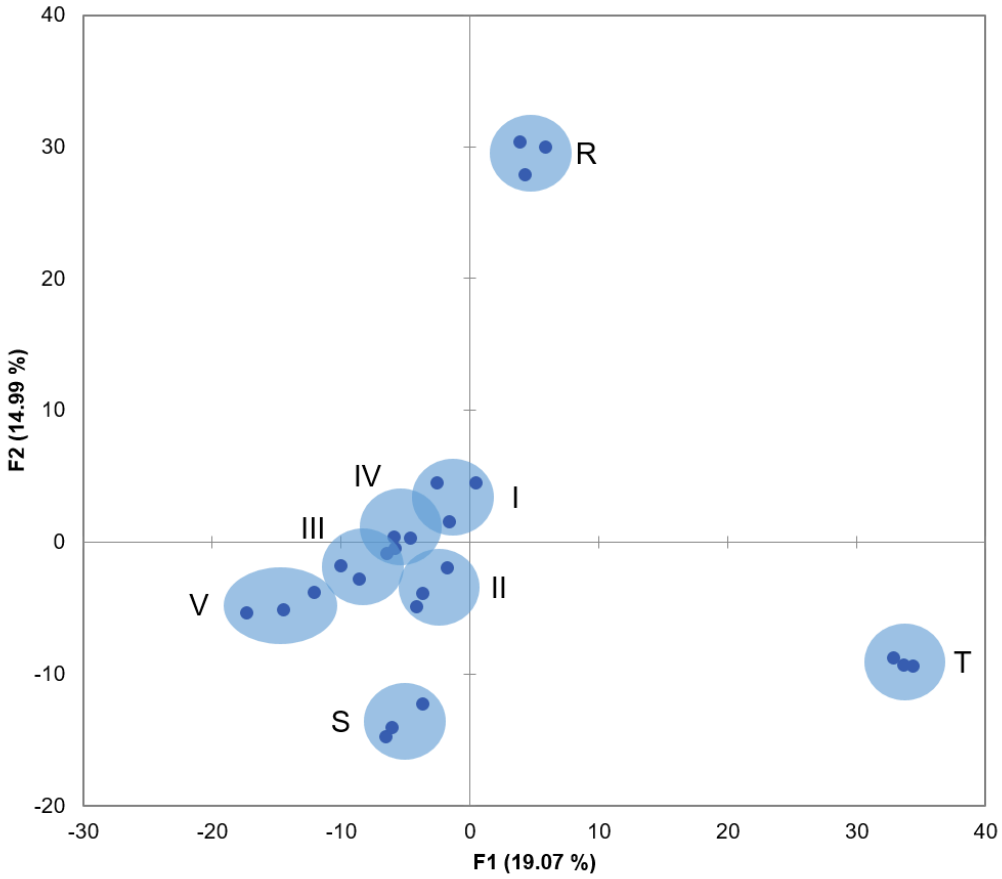

Figure A2: PCA for biological replicates for the 8 life cycle stages comparing the total quantitative proteome.

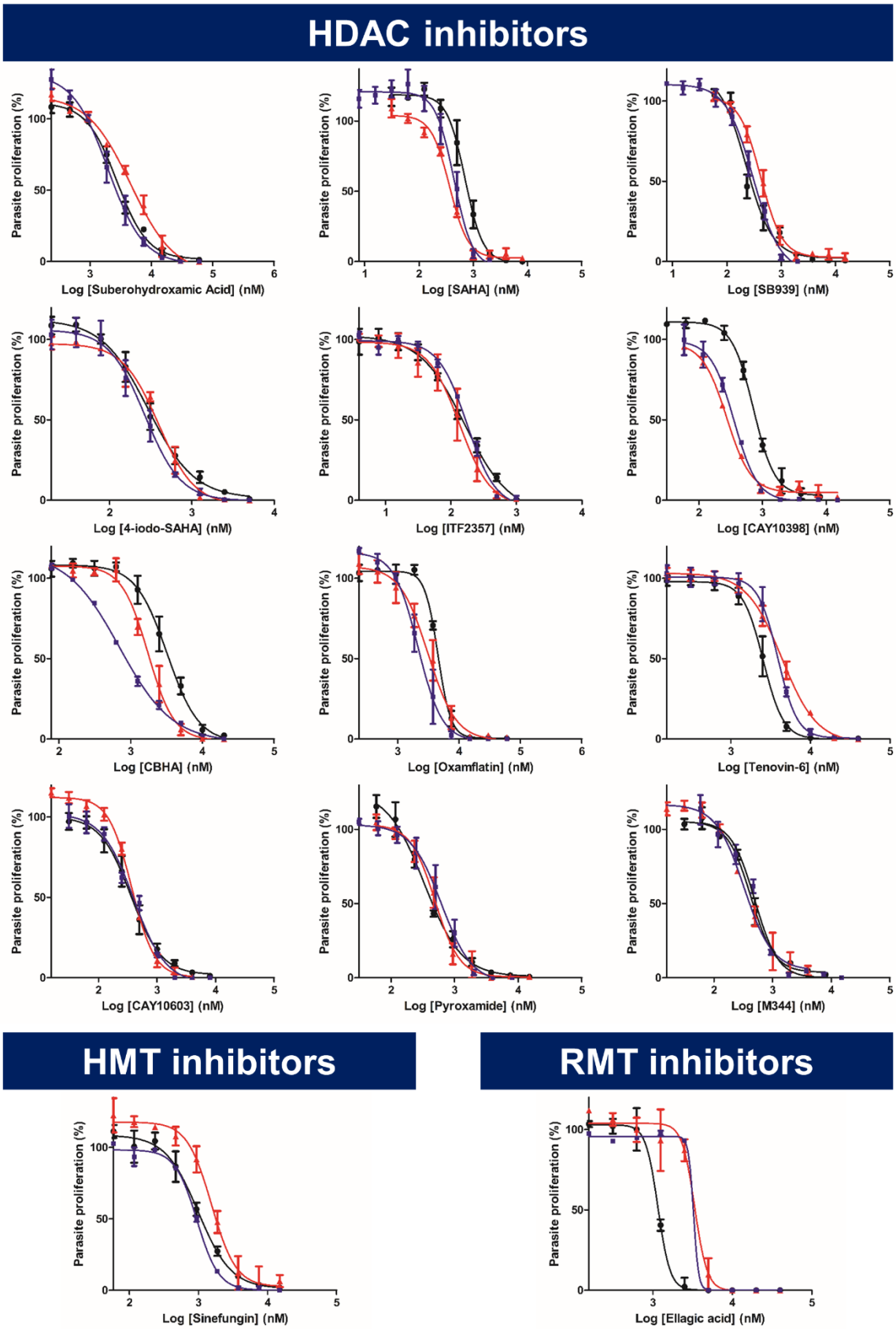

Figure A3: Dose-response curves for the active epi-drugs against asexual 3D7, K1 and W2 strains (IC_{50} values above 100 nM). Compounds were screened using the SYBR Green I-based fluorescence assay against 3D7 (black circle), K1 (red triangle) and W2 (blue square). Results for each compound are representative of three independent biological replicates (n=3 ± SEM).

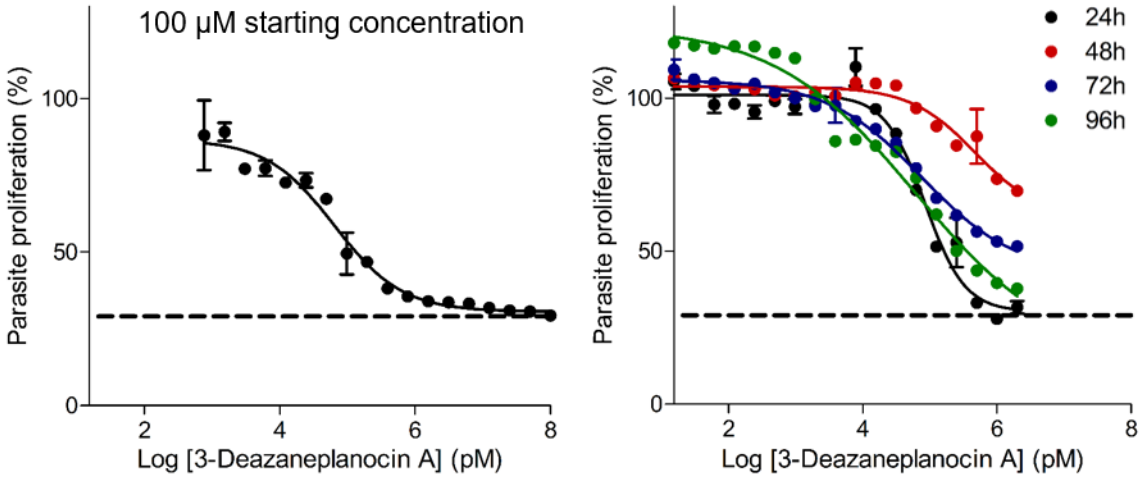

Figure A4: 3-Deazaneplanocin A does not reach 0% parasite proliferation at higher concentrations or varied incubation time. The starting concentration was increased to 100 µM, and in parallel the same concentration range was used for 24, 48, 72 and 96 h incubation time, but this effect was shown not to be concentration or time dependent.

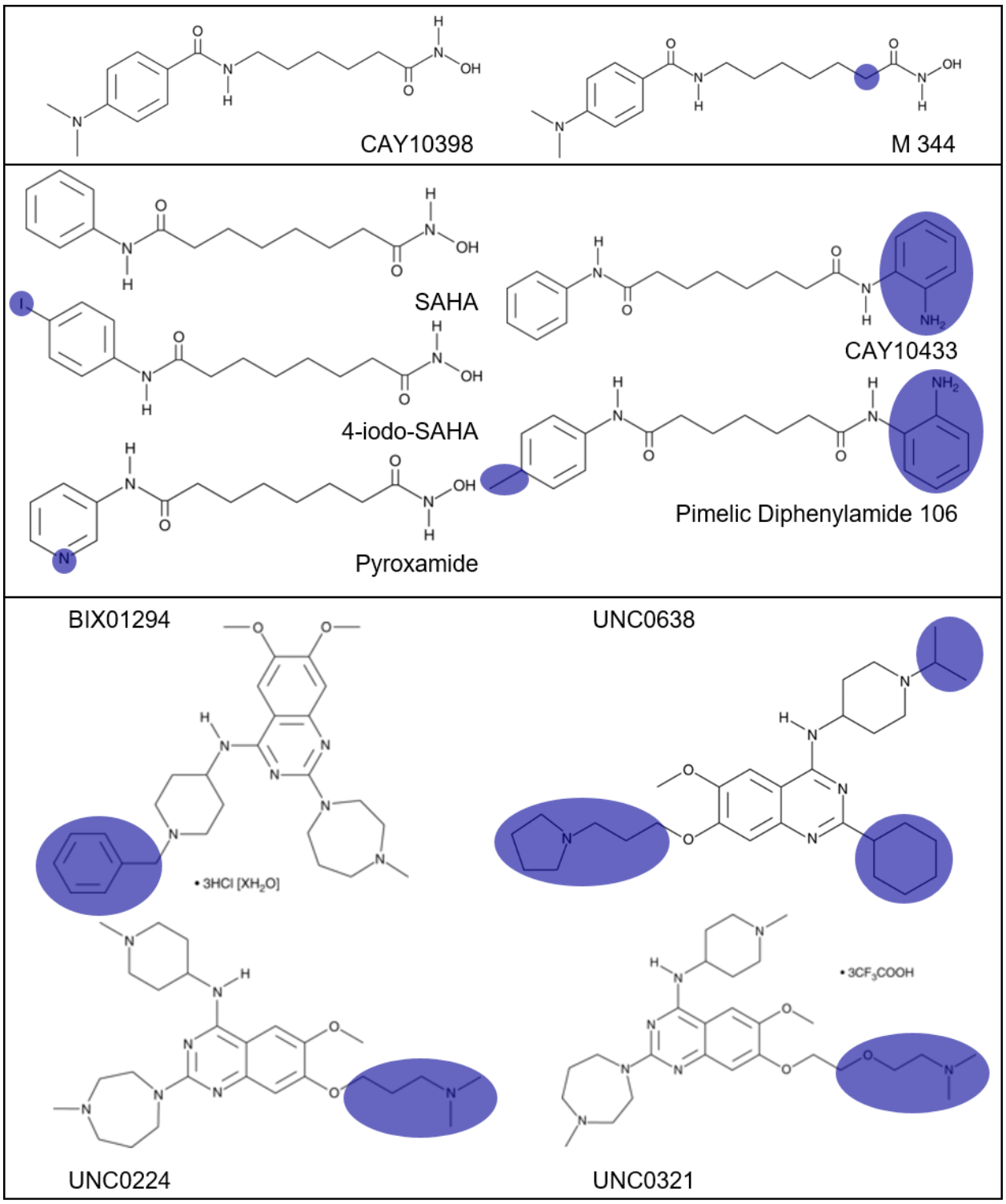

Figure A5: Chemical structures for compound groups identified in the SALI plot. Blue shading indicative of unique structural features within the groups.

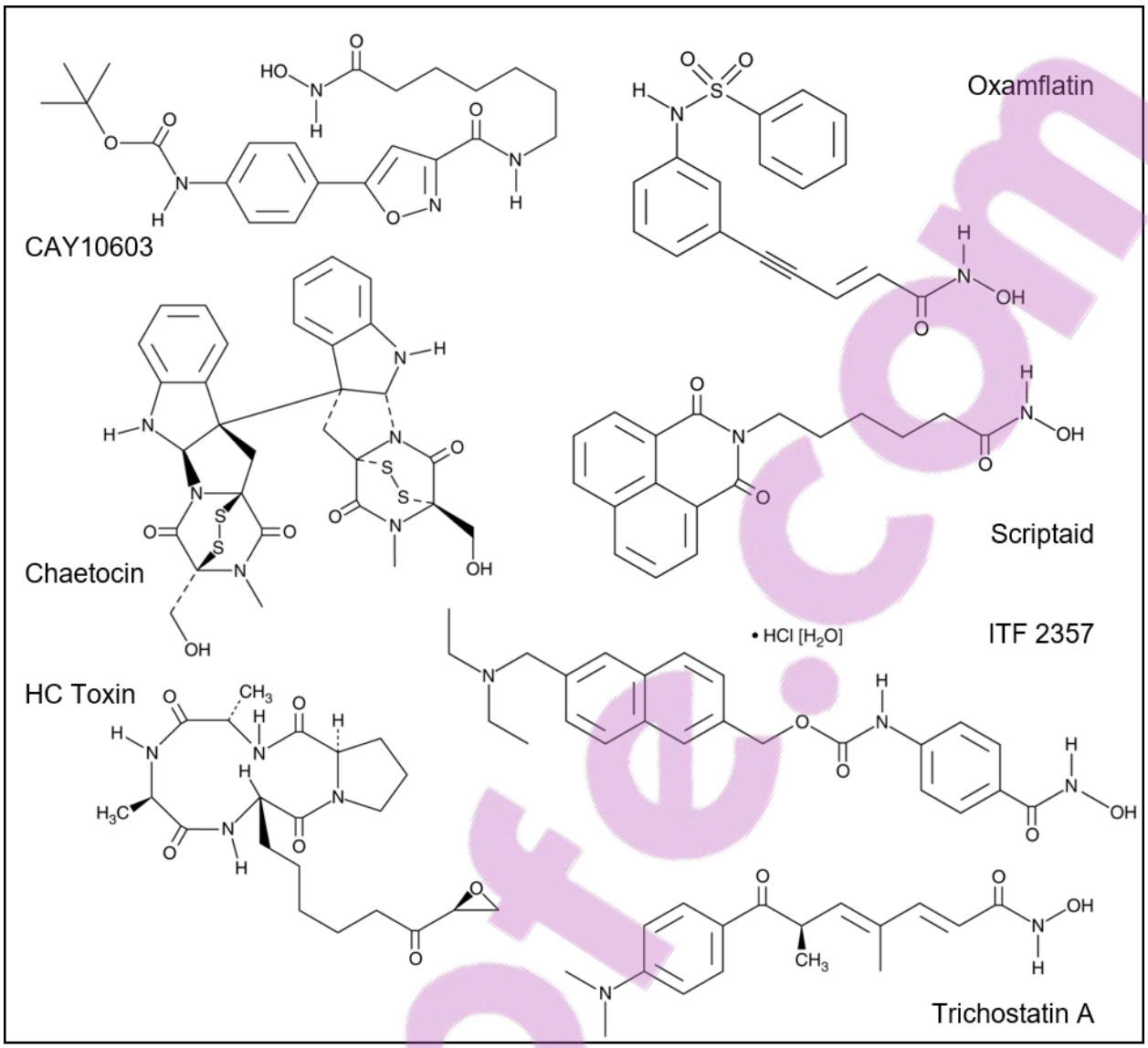

Figure A6: Chemical structures for unique structural compounds identified in the SALI plot.

Appendix II: Tables

Table A1: *In vitro* activity of the Epi-drug compounds against asexual 3D7 *P. falciparum* parasites, early and late stage gametocytes, obtained at concentrations of 5 and 1 µM (n=3). Compounds are grouped based on inhibitor class. Colour scale indicative of % inhibition (darker colour = higher % inhibition).

Compound Name	Inhibitor class	% Inhibition data					
		3D7 Asexual		Early gametocytes		Late gametocytes	
		5 µM	1 µM	5 µM	1 µM	5 µM	1 µM
Ellagic acid	PRMT	102.636	0.189	65.366	-16.802	17.085	12.899
AMI-1		-9.450	-0.107	4.570	-0.362	-11.262	-5.413
Cl-Amidine	Protein arginine deiminase	-1.440	1.289	1.794	5.476	0.355	-25.212
F-Amidine		-4.439	-1.303	-10.972	-5.761	-15.395	-22.171
PFI-1	Bromodomian	-3.929	-4.919	-6.105	5.534	-23.172	-11.517
(-)-JQ1		13.880	5.925	-0.487	-6.265	-0.809	-6.052
Bromosporine		11.178	3.076	22.370	5.101	22.827	18.208
I-CBP112		3.366	2.953	25.253	8.492	8.966	2.834
PFI-3		-4.696	1.787	19.153	17.989	13.386	12.664
(+)-JQ1		8.081	4.530	9.395	-1.671	47.804	4.612
Gemcitabine	DNDM	59.048	32.802	46.046	6.650	0.567	9.697
Zebularine	DNMT	-4.368	0.530	61.349	1.068	-14.743	-18.416
5-Azacytidine		-6.876	-6.050	67.548	66.770	3.470	4.835
Decitabine		-11.874	-8.157	-13.952	-9.983	7.831	22.469
RG-108		-1.364	2.211	-11.977	-2.333	2.187	2.288
RSC-133		0.052	0.132	24.430	13.269	25.320	32.204
Lomeguatrib		-0.331	2.097	-10.640	-1.382	-9.490	0.840
2'3'5'-triacetyl-5-Azacytidine		-1.784	2.736	-12.699	-11.844	-17.044	-21.802
Daminozide	HDM	-5.598	-0.493	-17.454	-9.863	-18.176	25.088
N-Oxalylglycine		-10.507	-0.815	-16.836	-1.147	-9.804	-8.527
2-PCPA		-7.605	-4.796	4.295	3.789	-6.250	-7.824
(-)-Neplanocin A	HKMT	74.403	31.143	69.631	48.560	-4.751	-12.782
S-Adenosylhomocysteine		-3.428	1.074	72.091	63.658	32.343	19.119
UNC1215		27.410	0.115	-7.066	-3.614	-12.489	-11.990
UNC0321		-5.136	-2.042	4.994	-12.496	-14.108	-12.995
UNC0638		100.787	98.794	90.162	41.771	46.469	25.006
MI-2		22.377	4.337	9.111	-12.663	26.171	-1.759
MI-nc		-2.727	0.660	3.552	0.116	10.244	12.833
BIX01294		100.798	99.835	83.741	80.329	89.533	25.240
Chaetocin		43.436	10.019	101.986	77.295	81.426	66.636
UNC0224		23.160	-1.532	36.836	-0.579	3.313	2.411
3-Deazaneplanocin A		75.545	75.040	63.185	60.855	0.498	16.647
Sinefungin		94.635	56.907	-1.912	-3.280	13.967	10.348
GSK 343		3.646	-2.341	65.062	-0.412	32.396	15.486
UNC1999		-4.415	0.901	89.654	23.312	61.490	35.462
2,4-DPD	Hydroxylation	-3.543	0.851	16.993	18.539	-4.959	-9.224
IOX1	LSD	-2.439	2.317	-15.197	-14.071	-7.973	0.301
GSK-J1		-0.596	1.265	-28.525	-5.302	-8.218	3.301
GSK-J2		-3.790	0.446	-21.413	-35.161	-9.945	-5.511
GSK-J4		30.306	-0.585	41.496	-15.602	27.842	31.386
GSK-J5		-1.638	2.881	-33.719	-27.965	7.080	22.219
C646	HAT	-1.269	-2.737	-35.636	-46.376	119.887	107.145
Garcinol		-8.158	-3.265	17.141	9.685	0.508	2.108
CAY10669		-4.054	-0.958	7.241	13.172	-3.646	-5.262
Delphinidin		-1.154	0.240	0.492	-5.462	-34.748	-12.361
CPTH2		-3.115	0.542	-14.260	-13.285	-25.552	-16.967
Anacardic acid		-3.250	0.527	-22.474	-18.578	22.773	18.208
WDR5-0103		-17.436	-4.458	23.048	13.424	5.952	0.991
SB 939	HDAC	100.071	88.453	66.131	57.786	5.362	25.339
PCI 34051		11.042	3.730	-6.040	-16.684	67.940	59.786
4-iodo-SAHA		99.727	79.779	63.956	32.449	-20.305	41.534

Sirtinol		-4.437	2.619	-14.143	-15.360	120.926	119.797
Scriptaid		90.100	33.110	72.338	62.821	89.327	29.291
HC Toxin		100.036	100.350	86.470	76.079	78.394	76.084
JGB1741		-2.479	-1.056	61.849	27.964	-22.225	-24.743
ITF 2357		100.135	95.336	79.550	60.123	118.375	100.295
Nicotinamide		-4.704	-4.382	68.685	39.413	-11.402	-9.186
1-Naphthoic Acid		2.006	4.796	6.407	13.030	19.505	-27.281
Sodium 4-Phenylbutyrate		0.725	5.668	-6.023	3.955	-11.043	-4.617
Valproic acid		-4.071	-1.989	-18.871	-15.205	-8.735	0.192
Tenovin-1		8.842	3.923	5.050	9.901	6.934	5.817
Tenovin-6		89.176	8.428	106.681	90.489	56.844	14.373
Sodium Butyrate		0.825	1.333	-16.342	-15.092	-6.331	-1.880
AGK2		-4.152	4.848	24.668	24.492	14.255	10.117
CAY10603		99.030	80.206	90.049	62.062	134.905	100.188
Splitomicin		-5.505	6.184	10.147	11.346	-7.504	9.513
M 344		98.805	79.529	60.888	37.679	67.416	39.844
Oxamflatin		62.239	-5.622	86.046	65.025	129.488	78.635
Salermide		-1.045	6.069	-2.688	-8.825	4.169	11.717
Pimelic Diphenylamide 106		-10.290	0.262	-6.514	-6.942	18.116	25.320
KD 5170		-4.158	2.754	-8.513	4.113	27.109	5.584
MS-275		-11.702	-1.359	26.320	12.965	10.641	3.535
HNHA		-3.333	-0.724	4.738	37.925	-2.525	-9.953
Pyroxamide		98.645	68.877	55.673	49.672	49.377	9.077
SIRT1/2 Inhibitor IV		-4.041	-0.380	-5.879	-3.748	31.749	6.334
trans-Resveratrol		-2.938	3.085	-5.465	3.743	-14.361	-15.005
CAY10398		99.222	86.565	75.767	64.801	70.353	34.370
CAY10433		-9.903	-4.614	-7.001	-7.666	0.638	-9.467
CAY10591		-4.886	-0.973	10.730	11.071	-10.854	-12.547
EX-527		-7.258	-3.661	4.123	0.740	-8.361	-9.097
SAHA		98.825	76.919	77.763	62.336	88.951	19.232
Suberohydroxamic Acid		64.498	-3.752	65.132	27.905	0.975	-6.814
CBHA		82.087	13.412	60.835	66.088	26.741	18.531
Trichostatin A		99.579	95.271	84.399	73.727	130.142	104.131
Chidamide		56.890	5.407	71.746	3.957	53.684	-16.004
Phthalazinone pyrazole	Phospho	-4.318	-5.440	29.452	13.150	-12.583	-5.414
Mirin		-0.815	6.394	-26.887	-27.779	5.214	12.967
Piceatannol		-7.119	-3.706	-9.494	-6.360	-14.726	-22.270
3-amino Benzamide	Unclassified	-0.611	1.948	-28.299	-18.236	114.304	107.246
Isoliquiritigenin		1.071	-2.282	36.348	33.793	37.935	-19.447
Suramin		-6.691	-1.472	11.264	11.338	-27.379	-20.298
BSI-201		0.506	5.446	-8.596	-3.282	24.622	-5.894
Octyl-α-ketoglutarate		-6.923	0.601	2.355	11.330	-3.100	3.913
DMOG		-1.200	1.693	-8.965	-0.203	-9.398	-12.862
CCG-100602		-0.974	0.246	53.351	23.464	-4.023	-5.601

Appendix III: Methods

Parasite production and isolation

P. falciparum NF54 (drug sensitive) parasite cultures were maintained at 5% hematocrit in O^+ human erythrocytes and RPMI-1640 cell culture medium supplemented with 24 mM sodium bicarbonate, 0.024 mg/ml gentamicin, 25 mM HEPES, 0.2% v/v glucose, 0.2 mM hypoxanthine and 0.5% w/v AlbuMAX II Lipid Rich Bovine Serum Albumin. The parasite cultures were kept at 37ºC with moderate shaking at 60 rpm and gassed with a mixture of 5% O_2, 5% CO_2 and 90% N_2. The asexual parasites were tightly synchronized with 10% w/v D-sorbitol and isolated at various time points. *P. falciparum* gametocytes were induced from a >90% synchronized asexual culture (maintained in culture medium lacking glucose) at 0.5% parasitemia (6% hematocrit) by enforcing environmental stress to asexual parasites as described previously. Gametocyte cultures were maintained for 14 days, where the early (Day 8, stage I-III) and late gametocytes (Day 14, stage IV-V) were treated with 50 mM *N*-acetyl-D-glucosamine on days 5-7 and days 9-11, respectively. The early and late gametocytes were isolated and enriched with magnetic separation (MACS® LS columns) to 90%. The asexual and sexual parasites were released from the RBCs using 0.06% w/v saponin in phosphate buffered saline (PBS), followed by several wash steps with PBS.

Histone isolation and separation

Histones were acid-extracted using a modified protocol from Trelle *et al.* (2009). All samples were kept on ice throughout the isolation protocol. The isolated *P. falciparum* parasite nuclei were released using a hypotonic buffer containing 10 mM Tris-HCl, pH 8.0, 3 mM $MgCl_2$, 0.2% v/v Nonidet P40, 0.25 M sucrose in the presence of a protease inhibitor cocktail. The mixture was centrifuged at 500*g* at 4ºC for 10 min and this hypotonic buffer wash step was repeated twice. Subsequently, the pellet was homogenized in the hypotonic buffer lacking NP-40 to obtain pelleted nuclei. To this, 10 mM Tris-HCl, pH 8.0, 0.8 M NaCl, 1 mM EDTA (including protease inhibitor cocktail) was added, followed by a 10 min ice incubation. Histones were acid extracted from the nuclei with 0.25 M HCl and rotation at 4ºC for 1 h. The histone-containing supernatant was mixed with an equal volume of 20% v/v trichloroacetic acid, incubated on ice for 15 min and pelleted. The histone-enriched pellet was washed with acetone, air-dried and resuspended in SDS sample buffer (62.5 mM Tris-HCl pH 6.8, 8.7% (v/v) glycerol, 2% (w/v) SDS, 0.2% (w/v) bromophenol blue and 0.7% (v/v) 2- β-mercaptoethanol). The samples were run on a 4-

20% separating SDS-PAGE and stained using coomassie blue R-250. Excised protein bands were destained overnight (50% (v/v) acetonitrile, 50 mM ammonium bicarbonate), after which in-gel digestion was performed overnight with 10 ng/µl trypsin at 37ºC. Peptides were extracted from the gel matrix with a 30 min incubation in 70% acetonitrile, 0.1% trifluoroacetic acid and another 30 min incubation in 100% acetonitrile, 0.1% trifluoroacetic acid. The peptides were dried and reconstituted in 5% (v/v) formic acid and cleaned using Stage Tips. The peptides were dried again and dissolved in 5% acetonitrile and 0.1% formic acid, after which 10 µl injections were made for nano-LC chromatography.

Qualitative LTQ-MS/MS histone PTM identification

All experiments were performed on a Thermo Scientific EASY-nLC II connected to a LTQ Orbitrap Velos mass spectrometer (Thermo Scientific, Bremen, Germany) equipped with a nano-electrospray source. For liquid chromatography, separation was performed on an EASY-Column (2 cm, ID 100µm, 5 µm, C18) pre-column followed by an XBridge BEH130 NanoEase column (15 cm, ID 75 µm, 3.5 µm, C18) with a flow rate of 300 nl/min. The gradient used was from 5-17% B in 5 min, 17-25% B in 90 min, 25-60% B in 10 min, 60-80% B in 5 min and kept at 80% B for 10 min. Solvent A was 100% water in 0.1 % formic acid, and solvent B was 90 % acetonitrile in 0.1% formic id. The mass spectrometer was operated in data-dependent mode to automatically switch between Orbitrap-MS and LTQ-MS/MS acquisition. Data were acquired using the Xcalibur software package. The precursor ion scan MS spectra (*m/z* 400-2000) were acquired in the Orbitrap with resolution R = 60000 with the number of cumulated ions being 1x106. The 20 most intense ions were isolated and fragmented in linear ion trap (number of cumulated ions 1.5x104) using collision-induced dissociation. The lock mass option (polydimethylcyclosiloxane; *m/z* 445.120025) enabled curate mass measurement in both the MS and MS/MS modes. In data-dependent LC-MS/MS experiments, dynamic exclusion was used with 60 s exclusion duration. Mass spectrometry conditions were 1.8 kV, capillary temperature of 250°C, with no sheath and auxiliary gas flow. The ion selection threshold was 500 counts for MS/MS. An activation Q-value of 0.25 and activation time of 10 ms were also applied for MS/MS.

Thermo Proteome Discoverer 1.3 was used to identify proteins via automated database searching of all tandem mass spectra against the PlasmoDB 7.2 database, using SEQUEST. Carbamidomethyl cysteine was set as a fixed modification, with oxidized

methionine, N-terminal acetylation, lysine acetylation, serine and threonine phosphorylation, lysine and arginine mono-, di- and trimethylation as dynamic modifications. The precursor mass tolerance and fragment mass tolerance was set to 20 ppm and 0.8 Da, respectively, with six missed tryptic cleavages allowed. Proteins were considered positively identified when they were identified with at least 1 tryptic peptide per protein, a Mascot score threshold of 20 and a SEQUEST X-score threshold of 1.5. Percolator was used for peptide validation with a maximum ΔCn of 0.5, and decoy database searches with a false discovery rate of 0.02 and 0.05, with validation based on the q-value. All the identified PTMs were manually validated against the fragment match spectrum of every identified peptide containing the PTMs of interest to establish the significance of every modification.

Appendix IV: Supplementary files provided as electronic data

Supplementary File 1 - Quantitative list of peptides.

Supplementary File 2 - All identified PTMs.

Supplementary File 3 - Quantitative histone PTM landscape.

Supplementary File 4 - Co-existing PTMs.

Supplementary File 5 - Quantitative protein list (all data processing included)

Supplementary File 6 - K-means clustering (ANOVA)

Supplementary File 7 – Volcano plot data

Supplementary File 8 - Sex-specific proteins

Supplementary File 9 - TLR protein data

Supplementary File 10 - Structure-activity analysis data